Laboratory Medicine

July 2023 Vol 54 No 4 Pgs 337–446

labmedicine.com

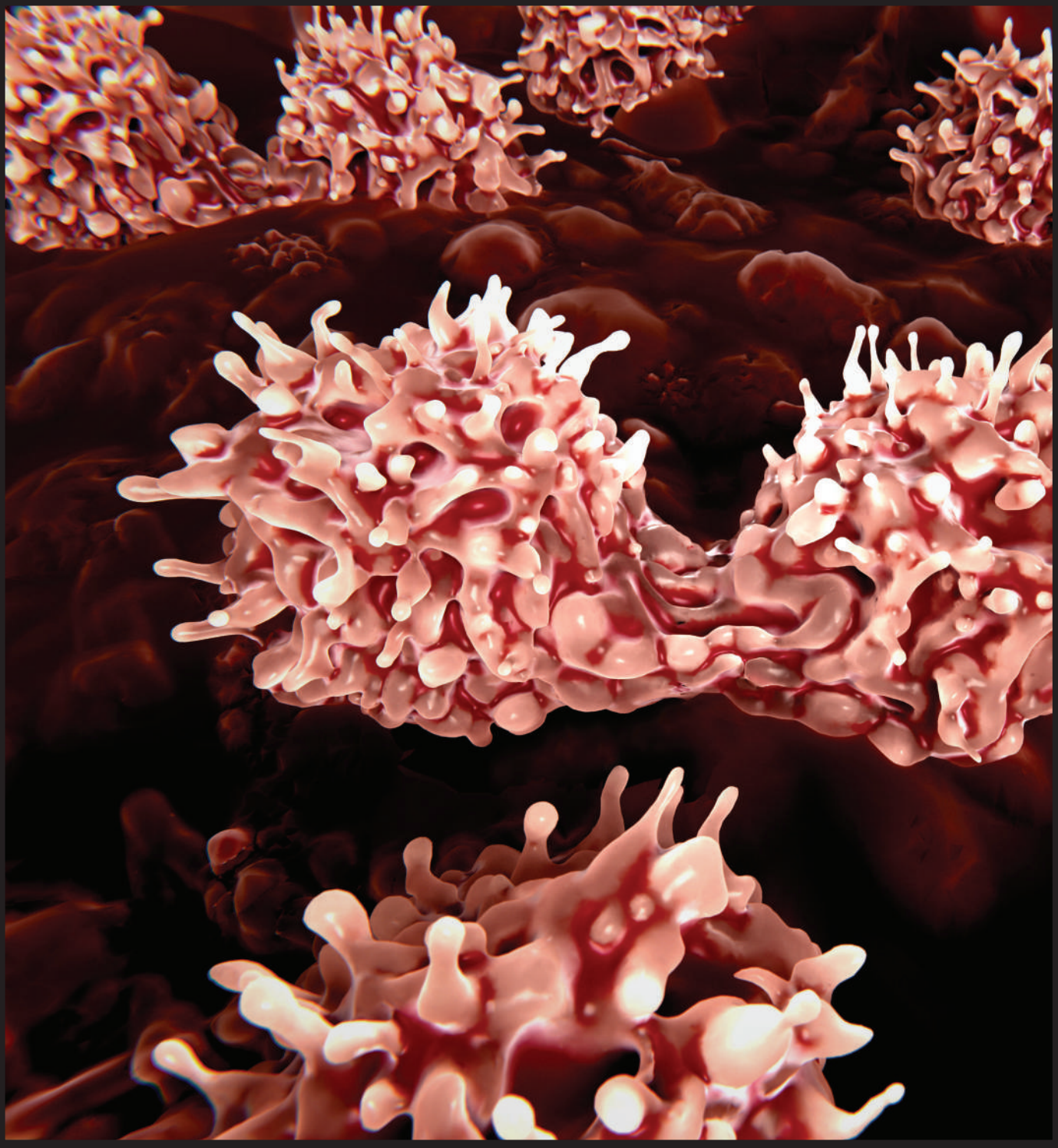

Downloaded from https://academic.oup.com/labmed/issue/54/4 by guest on 24 February 2025

BOARD OF EDITORS

Editor in Chief
Roger L. Bertholf, PhD
Houston Methodist Hospital
Weill Cornell Medicine

Reviews
ASSOCIATE EDITOR
Deniz Peker, MD
Emory University School of Medicine
ASSISTANT EDITOR
Rahul Matnani, MD, PhD
Rutgers Robert Wood Johnson Medical School

Clinical Chemistry
ASSOCIATE EDITOR
Uttam Garg, PhD
University of Missouri Kansas City School of Medicine
ASSISTANT EDITORS
David Alter, MD
Emory University School of Medicine
Hong Kee Lee, PhD
NorthShore University HealthSystem
Veronica Luzzi, PhD
Providence Regional Core Laboratory
Alejandro R. Molinelli, PhD
St Jude Children's Research Hospital

Cytology
ASSOCIATE EDITOR
Antonio Cajigas, MD
Montefiore Medical Center

Hematology
ASSOCIATE EDITOR
Shiyong Li, MD, PhD
Emory University School of Medicine
ASSISTANT EDITORS
Elizabeth Courville, MD
University of Virginia School of Medicine
Alexandra E. Kovach, MD
Children's Hospital Los Angeles
Tara N. Miller, MD
Houston Methodist Hospital

Histology
ASSOCIATE EDITOR
Carol A. Gomes, MS
Stony Brook University Hospital

Immunohematology
ASSOCIATE EDITOR
Richard Gammon, MD
OneBlood

ASSISTANT EDITORS
Phillip J. DeChristopher, MD, PhD
Loyola University Health System
Gregory Denomme, PhD
Grifols Laboratory Solutions
Amy E. Schmidt, MD, PhD
CSL Plasma

Immunology
ASSOCIATE EDITOR
Ruifeng Yang, MD, PhD
Nova Scotia Health

Laboratory Management and Administration
ASSOCIATE EDITOR
Lauren Pearson, DO, MPH
University of Utah Health
ASSISTANT EDITOR
Joseph Rudolf, MD
University of Utah

Microbiology
ASSOCIATE EDITOR
Yvette S. McCarter, PhD
University of Florida College of Medicine
ASSISTANT EDITORS
Alexander J. Fenwick, MD
University of Kentucky College of Medicine
Allison R. McMullen, PhD
Augusta University–Medical College of Georgia
Elitza S. Theel, PhD
Mayo Clinic

Molecular Pathology
ASSOCIATE EDITOR
Jude M. Abadie, PhD
Texas Tech University Health Science Center
ASSISTANT EDITORS
Holli M. Drendel, PhD
Atrium Health Molecular Pathology Laboratory
Rongjun Guo, MD, PhD
ProMedica Health System
Shuko Harada, MD
University of Alabama at Birmingham
Hongda Liu, MD, PhD
The First Affiliated Hospital of Nanjing Medical University

Pathologists' Assistant
ASSOCIATE EDITOR
Anne Walsh-Feeks, MS, PA(ASCP)
Stony Brook Medicine

STAFF

EXECUTIVE EDITOR FOR JOURNALS
Kelly Swails, MT(ASCP)
DIRECTOR OF SCIENTIFIC PUBLICATIONS
Joshua Weikersheimer, PhD
SENIOR EDITOR, JOURNALS
Philip Rogers

Laboratory Medicine (ISSN 0007-5027), is published 6 times per year (bimonthly). Periodicals Postage paid at Chicago, IL and additional mailing offices. POSTMASTER: Send address changes to *Laboratory Medicine*, Journals Customer Service Department, Oxford University Press, 2001 Evans Road, Cary, NC 27513-2009.

SUBSCRIPTION INFORMATION: Annually for North America, $182 (electronic) or $241 (electronic and print); single issues for individuals are $32 and for institutions $71. Annually for Rest of World, £118/€167 (electronic) or £154/€220 (electronic and print); single issues for individuals are £21/€30 and for institutions £44/€63. All inquiries about subscriptions should be sent to Journals Customer Service Department, Oxford Journals, Great Clarendon Street, Oxford OX2 6DP, UK, Tel: +44 (0) 1865-35-3907, e-mail: jnls.cust.serv@oup.com. In the Americas, please contact Journals Customer Service Department, Oxford Journals, 4000 CentreGreen Way, Suite 310, Cary, NC 27513, USA. Tel: 800-852-7323 (toll-free in USA/Canada) or 919-677-0977, e-mail: jnlorders@oup.com.

MEMBERSHIP INFORMATION: The ASCP membership fees for pathologists are as follows: fellow membership is $349; fellow membership plus 1-year unlimited online CE is $519; 2-year fellow membership is $675; and 2-year fellow membership plus 2-year unlimited online CE is $1,015. The ASCP membership fees for laboratory professionals are as follows: newly certified membership is $49; annual membership is $99; annual membership plus 1-year unlimited online CE is $129; 3-year membership is $349. All inquiries about membership should be sent to American Society for Clinical Pathology, 33 West Monroe Street, Suite 1600, Chicago, IL 60603, Tel: 312-541-4999, e-mail: ascp@ascp.org.

CLAIMS: Publisher must be notified of claims within four months of dispatch/ order date (whichever is later). Subscriptions in the EEC may be subject to European VAT. Claims should be made to Laboratory Medicine, Journals Customer Service Department, Oxford University Press, 4000 CentreGreen Way, Suite 310, Cary, NC 27513, USA, Tel: 800-852-7323 (toll-free in USA/Canada) or 919-677-0977, e-mail: jnlorders@oup.com.

Laboratory Medicine is published bimonthly by Oxford University Press (OUP), on behalf of the ASCP, a not-for-profit corporation organized exclusively for educational, scientific, and charitable purposes. Devoted to the continuing education of laboratory professionals, *Laboratory Medicine* features articles on the scientific, technical, managerial, and educational aspects ofthe clinical laboratory. Publication of an article, column, or other item does not constitute an endorsement by the ASCP of the thoughts expressed or the techniques, organizations, or products described therein. *Laboratory Medicine* is indexed in the following: MEDLINE/PubMed, Science Citation Index, Current Contents—Clinical Medicine, and the Cumulative Index to Nursing and Allied Health Literature.

Laboratory Medicine is a registered trademark. Authorization to photocopy items for internal and personal use, or the internal and personal use of specific clients, is granted by ASCP Press for libraries and other users registered with the Copyright Clearance Center (CCC) Transactional Reporting Service, provided that the base fee of USD 15.00 per copy is paid directly to the CCC, 222 Rosewood Drive, Danvers, MA 01923, 978.750.8400. In the United States prior to photocopying items for educational classroom use, please also contact the CCC at the address above.

Printed in the USA

© 2023 American Society for Clinical Pathology (ASCP)

Downloaded from https://academic.oup.com/labmed/issue/54/4 by guest on 24 February 2025

Advertising Sales Office Classified and Display Advertising

CORPORATE ADVERTISING
Jane Liss
732-890-9812
jliss@americanmedicalcomm.com

RECRUITMENT ADVERTISING
Lauren Morgan
267-980-6087
lmorgan@americanmedicalcomm.com

ASCP
Laboratory Medicine
33 West Monroe Street, Suite 1600
Chicago, IL 60603
T: 312-541-4999
F: 312-541-4750

Laboratory Medicine

July 2023
Vol 54, No 4
Pgs 337-446

OVERVIEW

SCIENCE

CASE STUDY

The following are online-only papers that are available as part of Issue 54(4) online.

Downloaded from https://academic.oup.com/labmed/issue/54/4 by guest on 24 February 2025

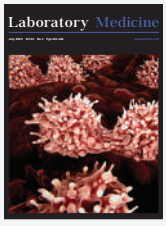

ON THE COVER: In Greek mythology, the Chimera was a terrifying lion/goat/snake hybrid, but in modern usage the term refers to a living creature that has two or more genetically distinct cell populations. Chimeras can arise naturally in utero or can be the result of hematopoietic progenitor (stem) cell transplantation. Assessment of the therapeutic success of transplantation requires distinguishing between erythrocytes that arise from engrafted cells and endogenous hematopoietic lineages. In this issue of *Laboratory Medicine*, Morris and colleagues review molecular methods applied to assess chimerism, focusing specifically on short tandem repeat analysis, which involves detection of repeated DNA motifs that are 2 to 13 nucleotides in length.

OVERVIEW

N-Terminal Prohormone Brain Natriuretic Peptide as a Prognostic Biomarker for the Risk of Complications in Type 2 Diabetes: A Systematic Review and Meta-Analysis

Zhian Salah Ramzi, PhD[1,*]

[1]Department of Family and Community Medicine, College of Medicine, University of Sulaimani, Sulaimani, Iraq. *To whom correspondence should be addressed: zhianramzi@gmail.com; zean.ramzi@univsul.edu.iq.

Keywords: natriuretic peptides, diabetes, prediction, prognosis, mortality, cardiovascular disease

Abbreviations: NT-proBNP, N-terminal prohormone brain natriuretic peptide; HR, hazard ratio; ANP, atrial natriuretic peptide; BNP, brain-type NP; PRISMA, Preferred Reporting Items for Systematic Reviews and Meta-Analyses; NHLBI, National, Heart, Lung, and Blood Institute; CI, confidence interval; MR-proANP, pro-A–type NP

Laboratory Medicine 2023;54:339-351; https://doi.org/10.1093/labmed/lmac119

ABSTRACT

Objective: This systematic review and meta-analysis aimed at summarizing the existing clinical evidence to evaluate the prognostic performance of N-terminal prohormone brain natriuretic peptide (NT-proBNP) in predicting cardiovascular events, cardiovascular-related mortality, and all-cause mortality in patients with type 2 diabetes.

Methods: Searches were performed in Medline, Embase, Scopus, and Web of Science databases before August 1, 2021. The data were recorded as adjusted hazard ratio (HR).

Results: An increase in NT-proBNP increases the risk of cardiovascular events (HR = 1.63), cardiovascular mortality (HR = 1.86) and all-cause mortality (HR = 1.54). Seemingly, the best cutoffs for predicting cardiovascular events (HR = 2.30) and cardiovascular mortality (HR = 3.77) are levels greater than 100 pg/mL. The best cutoff of NT-proBNP in predicting all-cause mortality is levels greater than 225 pg/mL (HR = 4.72).

Conclusion: A moderate level of evidence demonstrated that NT-proBNP serum levels can predict future cardiovascular events, cardiovascular mortality, and all-cause mortality. Thus, it can be used as risk stratification for type 2 diabetes.

The prevalence of type 2 diabetes has greatly increased in recent years, and the disease has been recognized as a major health problem both in developing and developed societies.[1] Type 2 diabetes is one of the leading causes of cardiovascular disease, which is one of the main causes of mortality and disease burden in many countries.[2] Statistics show that about 6.2% of the world's population have type 2 diabetes, resulting in the death of more than 1 million people annually. These numbers also show that type 2 diabetes is the ninth leading cause of death worldwide. Current estimates suggest that if the trend of type 2 diabetes prevalence continues at this rate, its prevalence will rise to 10% of the world's population in 2030.[3] Cardiovascular events and mortality are the main complications of type 2 diabetes. All of the existing interventions, including lifestyle modifications and drug treatments, are therefore aimed at preventing cardiovascular complications and death in type 2 diabetes patients.[4]

Although risk stratification of type 2 diabetes patients is based on the risk factors of cardiovascular diseases such as hypertension, there is still a need for other prognostic factors for better identifying at-risk persons.[5] Hence, researchers are investigating diagnostic tests and different biomarkers for diagnosis and prediction of the outcome in diabetes.

Natriuretic peptides are a family of 3 similar hormones: atrial natriuretic peptide (ANP), brain-type natriuretic peptide (BNP), and C-type natriuretic peptide.[6] N-terminal-prohormone BNP (NT-proBNP) is an inactive prohormone, secreted from cells along with BNP.[7] The prognostic value of these hormones and prohormones in predicting the outcome of diabetes has been evaluated in a number of studies. Occasionally, the findings of these studies are in contrast to one another, resulting in a consensus yet to be achieved. For instance, Ponikowska et al[8] report that NT-proBNP serum levels cannot predict the incidence of cardiovascular events, whereas Bidakosh et al[9] present a considerable prognostic value for this biomarker.

In addition, the optimum cutoffs of natriuretic peptides, wherein lie the best prognostic value for type 2 diabetes and the most appropriate peptide in predicting mortality and cardiovascular events, are not clear.

© The Author(s) 2022. Published by Oxford University Press on behalf of American Society for Clinical Pathology. All rights reserved. For permissions, please e-mail: journals.permissions@oup.com

Downloaded from https://academic.oup.com/labmed/article/54/4/339/6772474 by guest on 24 February 2025

To resolve these inconsistencies and respond to the uncertainties, this systematic review and meta-analysis is designed to evaluate the prognostic performance of NT-proBNP in predicting cardiovascular events, mortality rate, and all-cause mortality in type 2 diabetes patients based on the existing clinical evidence.

Materials and Methods

Study Design

The study is designed based on PRISMA (Preferred Reporting Items for Systematic Reviews and Meta-Analyses) guidelines.[10] This study is a systematic review of the existing clinical evidence regarding the prognostic value of NT-proBNP. An attempt was made to investigate the relationship between all natriuretic peptides with the outcome of type 2 diabetes. However, it was only possible to analyze the prognostic value of NT-proBNP.

Definition of PICO

Population (P) in the present study consisted of type 2 diabetes patients. Indicator (I) was determined to be the serum levels of NT-proBNP. Comparisons (C) were performed with diabetic patients not developing the defined outcome. Outcome (O) in this review included cardiovascular events, cardiovascular mortality, and all-cause mortality.

Eligibility Criteria

Clinical trials and cohort studies (retrospective and prospective) evaluating the prognostic value of NT-proBNP in type 2 diabetes patients were included in the study. Since prognostic value is time-dependent, studies that did not use survival models and did not report hazard ratios (HRs) were excluded. Studies with results published elsewhere with a higher sample size or with a longer follow-up period were also excluded (considered duplicates). Failure to assess the mentioned outcomes, selecting non-diabetes patients without reporting distinct analyses for diabetic and non-diabetic patients, studies conducted on type 1 diabetes patients, failure to adjust analyses for potential confounders, and review articles were also considered as exclusion criteria.

Search Strategy

An extensive search was performed in Medline, Embase, Scopus, and Web of Science databases for studies published before August 1, 2021. The search was performed using appropriate tags and keywords related to natriuretic peptides and diabetes. **Supplemental Table S1** depicts the search strategy in all 4 databases. In addition, a manual search in the reference lists of the relevant articles and in Google and Google Scholar search engines was performed to find possible missing articles. Consequently, 1 article was added through manual search.

Data Collection

Two reviewers independently collected the desired data. After removing duplicate articles using EndNote X8 software, title and abstract screening was performed. Next, full texts of potentially relevant articles were evaluated, and fully related articles were included in the study. The collected data included study characteristics (name of first author, date, and country of publication), study design (prospective/retrospective cohort studies or trials), condition of subjects included, sample size, mean age, sex distribution, duration of diabetes, presence of comorbidity, and outcome. Any disagreements were resolved by discussion.

Risk of Bias Assessment

Since all of the included studies were cohort or a secondary analysis on data of a clinical trial, risk of bias assessment was accomplished using the National, Heart, Lung, and Blood Institute (NHLBI) tool[11] and the Newcastle-Ottawa scale.[12] **Supplemental Table S2** shows the key questions of the NHLBI risk-of-bias tool (14 signaling questions). According to the explanation and elaboration section of the NHLBI tool, it is necessary to define fatal errors to rate an overall risk-of-bias status for each study. Therefore, a participation rate of less than 50% (item 3), assessment of exposure prior to outcome assessment (item 6), insufficient timeframe for outcome assessment (item 7), not clear and valid measurement of exposure (item 9) and outcomes (item 11), and loss to follow-up greater than 20% (item 13) were defined as fatal errors. Overall risk of bias was considered "high risk" if there was at least 1 fatal error, "some concern" if there was no fatal error, and "there was concern" (high risk, not reported or cannot determine) in at least 2 items according to a previously proposed method.[13] Overall score of bias according to Newcastle-Ottawa scale was categorized as "good," "fair," and "poor." A good-quality article was defined as (1) a score ≥3 in selection section points, (2) a score ≥1 in comparability section points, and (3) a score ≥2 of outcome points. Fair quality was defined as (1) a score of 2 points in selection, (2) a score ≥1 points in comparability, and (3) a score ≥2 points in outcome section. Poor quality was defined as (1) a selection of 0 or 1 point, (2) comparability of 0 points, or (3) an outcome of 0 or 1 point.[14]

Certainty of Evidence

Quality of evidence was rated according to the Grading of Recommendations, Assessment, Development, and Evaluations (GRADE) framework.[15]

Data Synthesis and Statistical Analysis

All analyses were performed in STATA 17.0 statistical software. Data were recorded as adjusted HR and its 95% confidence interval (CI).

The prognostic value of NT-proBNP in prediction of type 2 diabetes outcome was reported in 2 forms. One group of studies reported the prognostic performance of continuous values of NT-proBNP. In these studies, NT-proBNP level was included in the Cox model as a continuous variable. The other group of studies tried to assess the prognostic performance of NT-proBNP in different thresholds based on different cutoffs. In these situations, the serum level of NT-proBNP was included in the Cox model as categorical variable. Therefore, we stratified the analyses accordingly and provided 2 sets of meta-analysis: (1) prognostic performance of NT-proBNP as continuous values and (2) prognostic performance of NT-proBNP in different cutoffs. In addition, subgroup analyses and meta-regressions were performed to evaluate possible effects of the duration of diabetes, follow-up period, condition of diabetic patients, and sample size on prognostic value of NT-proBNP. Moreover, a sensitivity analysis was done based on the "leave one out" approach to investigate the effect of individual studies on pooled HR.

Using the "meta" command and corresponding subcommands, a pooled adjusted HR was reported. The random effect model was used to perform meta-analyses. Heterogeneity among studies was assessed using I^2 statistics and the Egger test and the funnel plot was used to recognize any possible publication bias.

Downloaded from https://academic.oup.com/labmed/article/54/4/339/6772474 by guest on 24 February 2025

Results

Study Screening

The systematic and manual search resulted in 9823 articles, from which 5590 nonduplicated articles were selected from the systematic search and 1 article from manual search. After the screening, the full texts of 93 of the studies were assessed, of which 30 articles were included in this review.[8,9,16–43] The reasons for exclusion were not reporting HR (21 studies), duplicate reporting of data (11 studies), not evaluating cardiovascular events or mortality (9 studies), reporting data of diabetic and nondiabetic patients indistinctively (7 studies), assessment of BNP (6 studies), assessment of the midregional fragment of pro-A–type natriuretic peptide (MR-proANP) (2 studies), and 1 study on type 1 diabetes patients for not reporting the required data and unadjusted analyses. **FIGURE 1** summarizes the screening process.

Characteristics of the Eligible Studies

The included 30 articles reported data of 44,889 patients, and mean age varied between 54.1 and 69.4 years. A total of 62.7% of the studied population was male, and the duration of diabetes varied between 5 and 11.3 years. In 18 articles, the research was performed on diabetic patients without considering their underlying disease. Of the rest, 6 articles focused on diabetic patients with a history of cardiovascular disease, 2 articles on nephropathic diabetic patients, 2 studies were on elderly patients, 1 study was on noncardiovascular diseases diabetic patients, and 1 study focused on hemodialysis patients. Of the included studies, 20 were prospective cohorts and 10 were secondary analyses on data of clinical trials (**TABLE 1**).

Considering outcome, cardiovascular events, cardiovascular-related death, and all-cause mortality were assessed in 22, 7, and 14 studies, respectively. There were 11 studies that assessed more than 1 outcome. The value of continuous variation of NT-proBNP in prediction of diabetes outcome was assessed in 22 studies. In addition, 24 studies investigated the value of NT-proBNP in prediction of diabetes outcome at different cutoffs. The proposed cutoffs varied between 22.5 pg/mL and 9252 pg/mL. The proposed cutoff in 19 papers was lower than 1000 pg/mL. There are 6185 (18.28%) cardiovascular events, 904 cardiovascular deaths (16.79%), and 3496 all-cause mortalities (25.76%) among included articles (**TABLE 2**).

Outcome

Relationship of NT-proBNP and Cardiovascular Events

In this section, data from 22 articles were entered. These articles compromised data of 40,055 diabetic patients. The analyses in this section showed that with an increase in the serum levels of NT-proBNP (as a continuous variable in the statistical analysis), the risk of cardiovascular events of type 2 diabetic patients over time increases significantly (HR = 1.63; 95% CI: 1.37, 1.95; I^2 = 98.47%) (**FIGURE 2**).

Assessing the optimum cutoffs of NT-proBNP serum levels for predicting cardiovascular events, it was demonstrated that the HR of their incidence in cutoffs of 0 to 100 pg/mL, 101 to 225 pg/mL, 226 to 550 pg/mL, 551 to 1100 pg/mL, and >1100 pg/mL are 3.60 (95% CI: 1.71,

FIGURE 1. PRISMA flow diagram for screening and selection process of included studies.

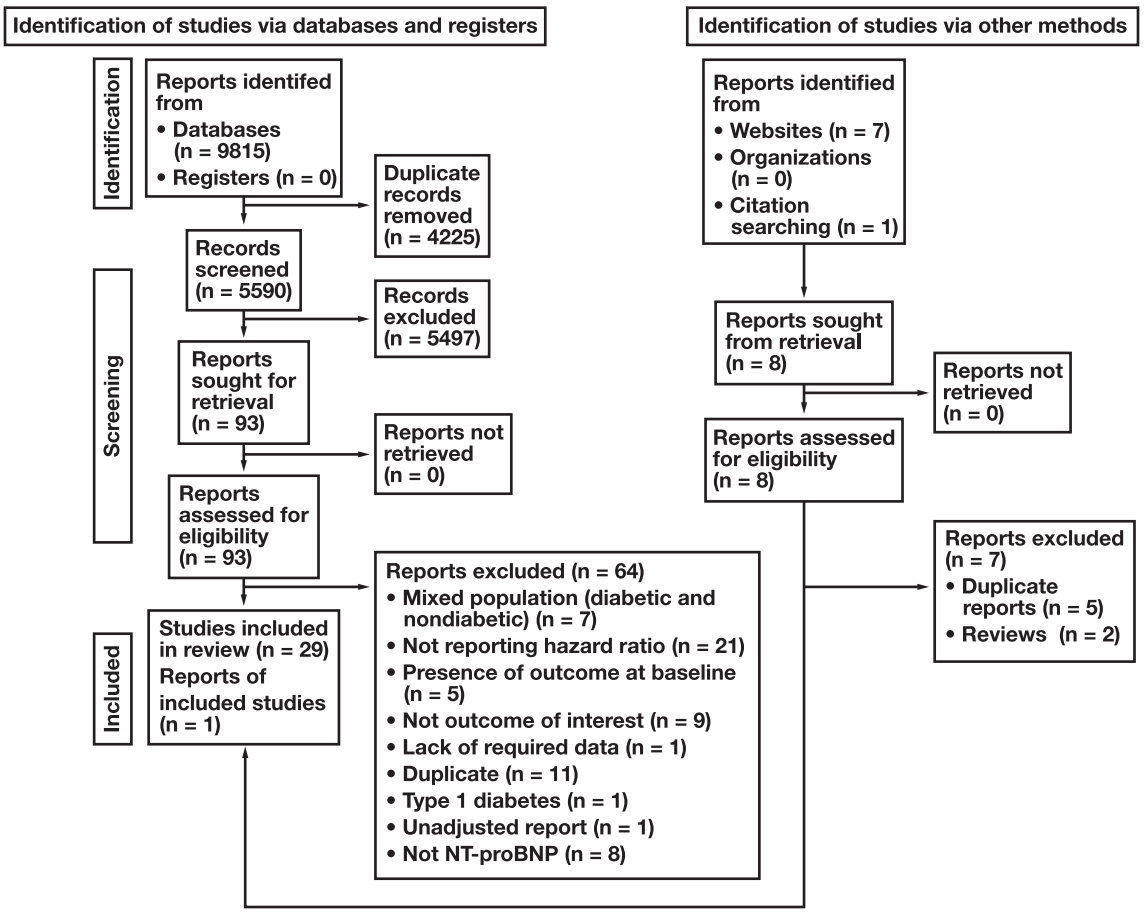

Downloaded from https://academic.oup.com/labmed/article/54/4/339/6772474 by guest on 24 February 2025

TABLE 1. Summary of Included Studies

Study	Design	Condition	Sample Size	Mean Age, y	N, Male	Duration of Diabetes	FU, y	Comorbidity (%)				
								CVD	HTN	Smoking	HLP	Albuminuria
Bidadkosh, 2017, Netherlands	RCT	Diabetic nephropathy	861	64	654	NR	0.8	NR	NR	NR	NR	NR
Birukov, 2020, Germany	PCS	General	545	NR	NR	NR	8	NR	NR	NR	NR	NR
Bruno, 2013, Italy	PCS	Elderly	1825	67.6	894	10.7	5.5	22.1	89.4	28.7	NR	25.2
Busch, 2021, Denmark	PCS	General	1030	65.2	679	11	4.7	18.6	NR	57.2	NR	22.7
Clodi, 2011, Austria	PCS	General	1071	61.5	613	15	2.75	23.7	67.5	NR	NR	23.7
Colombo, 2018, UK	RCT	Patients without history of CVD	2105	59.8	1423	6.7	5	NR	NR	65.6	NR	28.3
Czucz, 2011, Hungary	PCS	Chronic HF	192	69.4	142	NR	1.3	100	NR	NR	NR	NR
Gaede, 2005, Denmark	RCT	Diabetic nephropathy	160	55	119	NR	7.8	NR	NR	37.5	NR	NR
Gori, 2016, USA	PCS	General	1510	63	725	NR	13.1	12	60	NR	NR	NR
Gustafsson, 2010, Europe	RCT	General	389	NR	NR	NR	2.2	NR	NR	NR	NR	NR
Hillis, 2014, Australia	RCT	General	3862	66.89	2356	7.86	5	49.5	NR	15	NR	NR
Huelsmann, 2008, Austria	PCS	General	631	58.7	349	9.28	1	22.8	81.3	56.6	NR	NR
Jarolim, 2018, USA	RCT	CVD patients	5224	61	3539	9.6	1.64	96.2	83.2	13.6	NR	NR
Jhund, 2014, USA	RCT	General	8415	NR	NR	NR	NR	NR	NR	NR	NR	NR
Liu, 2021, China	PCS	General	2952	59.1	2076	NR	5	55.7	71	71	NR	NR
Malachias, 2020, 36 countries	RCT	General	5509	64.4	3811	NR	2.6	87.7	NR	50.8	NR	NR
Neuhold, 2011, Austria	PCS	General	544	60.5	299	13	3.3	38.5	65.3	55.4	NR	NR
Nguyen, 2020, USA	PCS	General	659	64.8	365	NR	12.4	NR	64.9	49.4	NR	NR
O'Donoghue, 2007, USA	PCS	General	157	68	82	NR	1	73.9	66	NR	NR	NR
Pfister, 2007, Germany	PCS	General	156	69	110	6.5	3.2	61.5	75.6	NR	NR	NR
Ponikowska, 2013, Poland	PCS	General	287	65	225	5	5	NR	NR	NR	NR	NR
Prausmüller, 2021, Austria	PCS	General	1690	62	907	11.3	10	24	67	20	68	NR
Price, 2014, UK	PCS	Elderly	1066	67.9	547	6.7	4	56.3	82.3	61.2	NR	16.5
Riphagen, 2015, Netherlands	PCS	General	1068	67	483	5	15	35.8	NR	21.6	37.2	40
Rørth, 2019, Denmark	RCT	Chronic HF	754	67	618	NR	3	100	86	12	NR	NR
Saely, 2019, Switzerland	PCS	CVD patients	317	NR	NR	NR	6.3	100	NR	NR	NR	NR
Tarnow, 2006, Denmark	PCS	General	315	54.1	194	6.8	15.5	33.2	37.6	47	NR	40.3
Trutz, 2015, Romania	PCS	CVD patients	206	62.5	108	NR	1	100	NR	NR	47.1	NR
Winkler, 2008, Germany	RCT	Hemodialysis	1255	65.6	672	NR	3.96	81.9	NR	40.2	NR	NR
Zanolin, 2018, Switzerland	PCS	PAD	134	NR	NR	NR	6	NR	NR	NR	NR	NR

BNP, B-type natriuretic peptide; CVD, cardiovascular disease; FU, follow up duration; General, all diabetic patients regardless comorbidities; HF, heart failure; HTN, hypertension; MR-ANP, midregional fragment of pro-A–type natriuretic peptide; NT-proBNP, N-terminal pro-B–type natriuretic peptide; NP, natriuretic peptide; NR, not reported; PAD, peripheral artery diseases; PCS, prospective cohort studies; RCT, randomized controlled trial.

Downloaded from https://academic.oup.com/labmed/article/54/4/339/6772474 by guest on 24 February 2025

TABLE 2. NT-proBNP Cutoffs, Assessed Outcomes, and Prevalence of Events among Included Studies

Study	Cutoff (pg/mL)	Outcome	No Event (n)	Event (n)	Prevalence
Bidadkosh, 2017, Netherlands	Continuous	MACE	754	107	12.43
Birukov, 2020, Germany	Continuous	MACE	495	50	9.17
Bruno, 2013, Italy	Continuous 41–90 91–200 >200	CVD mortality All-cause mortality	1650 1435	175 390	9.59 21.37
Busch, 2021, Denmark	>150	MACE	856	174	16.89
Clodi, 2011, Austria	Continuous	MACE	968	103	9.62
Colombo, 2018, UK	Continuous	MACE	1961	144	6.84
Czucz, 2011, Hungary	Continuous	All-cause mortality	146	46	23.96
Gaede, 2005, Denmark	>22.5	MACE	53	66	41.25
Gori, 2016, USA	>125	MACE	970	540	35.76
Gustafsson, 2010, Europe	Continuous	All-cause mortality	293	96	24.68
Hillis, 2014, Australia	Continuous	MACE All-cause mortality	3153 3156	709 706	18.36 18.28
Huelsmann, 2008, Austria	Continuous	MACE	587	44	6.97
Jarolim, 2018, USA	154.1–420.4 420.4–1084 ≥1084	MACE	4647	577	12.42
Jhund, 2014, USA	Continuous	MACE	7286	1129	13.42
Liu, 2021, China	Continuous 110.6–518.8 >518.8	MACE	2695	257	8.71
Malachias, 2020, 36 countries	Continuous	MACE All-cause mortality	4741 5040	768 469	13.94 8.51
Neuhold, 2011, Austria	Continuous	MACE All-cause mortality	481 517	63 27	11.58 4.96
Nguyen, 2020, USA	Continuous	MACE	488	171	25.95
O'Donoghue, 2007, USA	986	All-cause mortality	129	28	17.83
Pfister, 2007, Germany	518	MACE All-cause mortality	108 122	48 34	30.77 21.79
Ponikowska, 2013, Poland	Continuous	MACE All-cause mortality	227 228	60 59	20.91 20.56
Prausmüller, 2021, Austria	Continuous >122 >125 >376	MACE CVD mortality All-cause mortality	1322 1489 1242	368 201 448	21.78 11.89 26.51
Price, 2014, UK	Continuous	MACE	952	114	10.69
Riphagen, 2015, Netherlands	Continuous	CVD mortality All-cause mortality	843 549	225 519	21.07 48.60
Rørth, 2019, Denmark	Continuous 628–1342 >1342	CVD mortality All-cause mortality	NR NR	NR NR	NR NR
Saely, 2019, Switzerland	Continuous	MACE	157	160	50.47
Tarnow, 2006, Denmark	41-103 >103	CVD mortality	196 153	119 162	37.78 51.43
Trutz, 2015, Romania	400	MACE	138	68	33.01
Winkler, 2008, Germany	Continuous 1434–3361 3362–9251 9252	MACE CVD mortality All-cause mortality	790 1095 643	465 160 612	37.05 12.75 48.76
Zanolin, 2018, Switzerland	Continuous	CVD mortality All-cause mortality	110 72	24 62	17.91 46.27

CVD, cardiovascular disease; MACE, major adverse cardiovascular events.

Downloaded from https://academic.oup.com/labmed/article/54/4/339/6772474 by guest on 24 February 2025

7.56; I^2 = 0.0%), 2.30 (95% CI: 1.42, 3.71; I^2 = 86.58%), 1.67 (95% CI: 1.38, 2.04; I^2 = 0.0%), 3.09 (95% CI: 2.06, 4.63; I^2 = 78.52%), and 2.58 (95% CI: 1.40, 4.74; I^2 = 94.93%), respectively. Increased serum levels of NT-proBNP in all of the evaluated cutoffs were significantly related with the occurrence of cardiovascular events (**FIGURE 3**). Nevertheless, although the calculated HR for 550 pg/mL cutoff point is 3.09, it seems that the optimum cutoffs for predicting cardiovascular events are those greater than 100 pg/mL, because the HR of NT-proBNP serum levels in predicting cardiovascular events at this level is 2.30 and does not have a significant difference with the biomarker HR at 550 pg/mL levels (P = .110).

Subgroup analyses and meta-analysis showed that there were no significant differences in prognostic value of NT-proBNP in predicting cardiovascular events between different subgroups of diabetes duration (P = .630), follow-up duration (P > .05), different subgroups of patient conditions (P = .845), and sample size (P = .385) (**TABLE 3**).

Relationship of NT-proBNP and Cardiovascular Mortality

In this section, data from 7 articles were analyzed. These studies included data of 7041 diabetic patients. The analyses suggested that an increase in serum levels of NT-proBNP (as a continuous variable in the statistical analysis) results in an increased incidence risk of cardiovascular mortality in type 2 diabetic patents over time (HR = 1.86; 95% CI: 1.22, 2.82; I^2 = 97.48%) (**FIGURE 2**).

In evaluating the best cutoffs of NT-proBNP serum levels for predicting cardiovascular-related mortality, it was found that the HR of the cutoff points of 0 to 100 pg/mL, 101 to 225 pg/mL, 226 to 550 pg/mL, 551 to 1100 pg/mL, and >1100 pg/mL are 1.38 (95% CI: .84, 2.26; I^2 = 0.0%), 3.77 (95% CI: 2.06, 6.90; I^2 = 69.09%), 7.52 (95% CI: 2.82, 20.05; I^2 = 0.0%), 13.38 (95% CI: 6.88, 26.01; I^2 = 0.0%), and 1.92 (95% CI: 1.39, 2.64; I^2 = 54.94%), respectively. Therefore, increased serum levels of NT-proBNP above 100 pg/mL were significantly related with cardiovascular mortality of type 2 diabetic patients over time. Seemingly, the most appropriate cutoff for predicting cardiovascular mortality is levels greater than 100 pg/mL (**FIGURE 4**).

Subgroup analyses and meta-regression showed that the diversity among duration of diabetes (P = .638), follow-up duration (P = .479), type of patient condition (P = .231), and sample size (P = .771) were not sources of heterogeneity regarding the assessment of NT-proBNP's prognostic value in the prediction of cardiovascular death (**TABLE 3**).

Relationship of NT-proBNP and All-Cause Mortality

Finally, to evaluate the last outcome, the data of 18,137 diabetic patients from 15 studies were included. The results showed that the risk of all-cause mortality in diabetic patients over time increases significantly with the increase in NT-proBNP serum levels (HR = 1.54; 95% CI: 1.28, 1.85; I^2 = 98.29%) as a continuous variable in the statistical analysis (**FIGURE 2**).

Assessing the best cutoff point, it was calculated that the HR for predicting the risk of all-cause mortality in diabetic patients in cutoff points of 0 to 100 pg/mL, 101 to 225 pg/mL, 226 to 550 pg/mL, 551 to 1100 pg/mL, and >1100 pg/mL were 1.48 (95% CI: 1.08, 2.03; I^2 = 0.0%), 2.25 (95% CI: 1.65, 3.05; I^2 = 66.40%), 4.72 (95% CI: 3.22, 6.92; I^2 = 0.0%), 4.18 (95% CI: 3.08, 5.67; I^2 = 0.0%), and 1.92 (95% CI: 1.44, 2.55; I^2 = 70.55%), respectively. It can be observed that increased levels of NT-proBNP at all cutoffs are significantly related with the all-cause mortality in type 2 diabetic patients over time. Thus, it seems that the most appropriate cutoff for predicting all-cause mortality is a cutoff point of more than 225 pg/mL (**FIGURE 5**).

Subgroup analyses and meta-regression showed that the diversity among duration of diabetes (P = .750), follow-up duration (P > .05), patient condition (P = .999), and sample size (P = .815) were not sources of heterogeneity for assessment of prognostic value of NT-proBNP in prediction of all-cause mortality (**TABLE 3**).

Sensitivity Analysis

Leave one out analysis was performed to assess individual study effect on the value of NT-proBNP in prediction of diabetes outcome. The analysis showed that omitting each study does not have a significant effect on the value of NT-proBNP in prediction of cardiovascular event, cardiovascular-related death, and all-cause mortality (**Supplemental Figures S1 to S3**).

Risk of Bias

According to the researchers' judgment, items 3, 6, 7, 11, 13, and 14 of the NHLBI tool were considered fatal errors. The participation rate in 2 studies was not clear and in 1 study was less than 50% (item 3). All studies in items 6, 7, 13, and 14 were considered to be low risk.

Sample size justification (item 5) was not reported in 26 studies. A total of 17 studies did not examine different levels of exposure (NT-proBNP level) as related to the outcome (item 8). There were 29 studies that assessed the level of biomarkers 1 time (item 10). Blinding status of observers was not reported in 15 articles (item 12). Finally, overall risk of bias in 3 studies was high, in 19 studies there was some concern, and in 8 studies, risk of bias was low (**Supplemental Table S3**).

In addition, the risk of bias assessment using the Newcastle-Ottawa scale showed that all of the included studies have 3- or 4-star scores in selection of subjects. According to the reviewers' judgments, all the articles scored 2 stars in comparability section, and all scored 2 or 3 stars in outcome section. Accordingly, the overall scores of included studies based on the Newcastle-Ottawa scale were good (**Supplemental Table S4**).

Publication Bias

There was possible publication bias in the assessment of prognostic value of NT-proBNP (as a continuous variable in the statistical analysis) in the prediction of cardiovascular events (P = .025) and all-cause mortality (P = .005) (**Supplemental Figure S4**). There is no evidence of publication bias in the assessment of performance of NT-proBNP (categorical values by using different cutoffs) in prediction of a cardiovascular event (P = .193), cardiovascular mortality (P = .538), and all-cause mortality (P = .173) (**Supplemental Figure S5**).

Certainty of Evidence

The level of evidence was assessed based on the GRADE framework. There was very serious inconsistency in the assessment of the continuous value of NT-proBNP for predicting cardiovascular events, cardiovascular mortality, and all-cause mortality. Therefore, the level of evidence rated down at least 2 scores. However, a large magnitude of effect was observed, and the analyses were adjusted for residual confounders. Therefore, overall level of evidence rated up 2 scores. Finally, the overall quality of evidence

Downloaded from https://academic.oup.com/labmed/article/54/4/339/6772474 by guest on 24 February 2025

FIGURE 2. Forest plot of value of NT-proBNP (continuous values) for prognosis of cardiovascular events and morality in diabetes type 2 patients. Data were presented as adjusted hazard ratio (HR) and 95% confidence interval (95% CI).

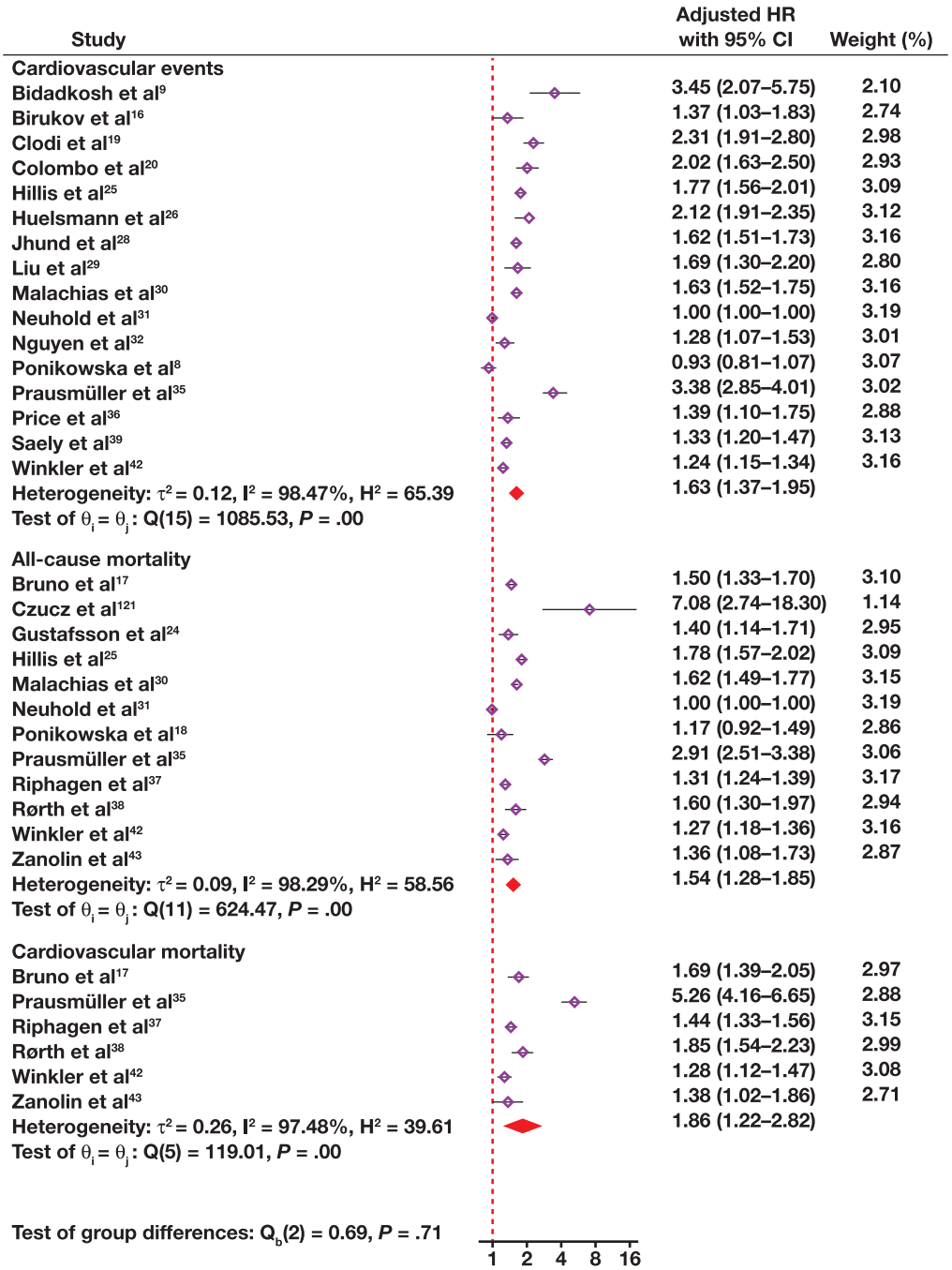

in the assessment of prognostic value of NT-proBNP (as a continuous variable) was low to very low.

There was serious risk of bias and serious inconsistency in the assessment of NT-proBNP's prognostic performance as a categorical variable. Therefore, the certainty of evidence rated down 2 scores. However, pooled analysis showed a large magnitude of effect and a possible dose-response gradient. In addition, all analyses were adjusted for potential confounders. Therefore, the level of evidence rated up 3 scores. Finally, the overall quality of evidence in assessment of prognostic value of NT-proBNP in categorical values (using different cut offs) was moderate (**Supplemental Table S5**).

Discussion

For the first time, this systematic review and meta-analysis collected the existing evidence regarding the prognostic value of natriuretic peptides among type 2 diabetes patients. A moderate level of evidence demonstrated that serum levels of NT-proBNP can predict cardiovascular events, cardiovascular mortality, and all-cause mortality among these subjects. The best cutoff points for predicting outcomes were greater than 100 pg/mL, 100 pg/mL, and 225 pg/mL, respectively.

The cutoff points of NT-proBNP reported in the studies varied between 41.0 pg/mL and 9251 pg/mL. However, few studies reported cutoff values of less than 100 pg/mL and greater than 1100 pg/mL. This

Downloaded from https://academic.oup.com/labmed/article/54/4/339/6772474 by guest on 24 February 2025

FIGURE 3. **Forest plot of value of different cutoffs of NT-proBNP for prognosis of cardiovascular events in diabetes type 2 patients. Data were presented as adjusted hazard ratio (HR) and 95% confidence interval (95% CI).**

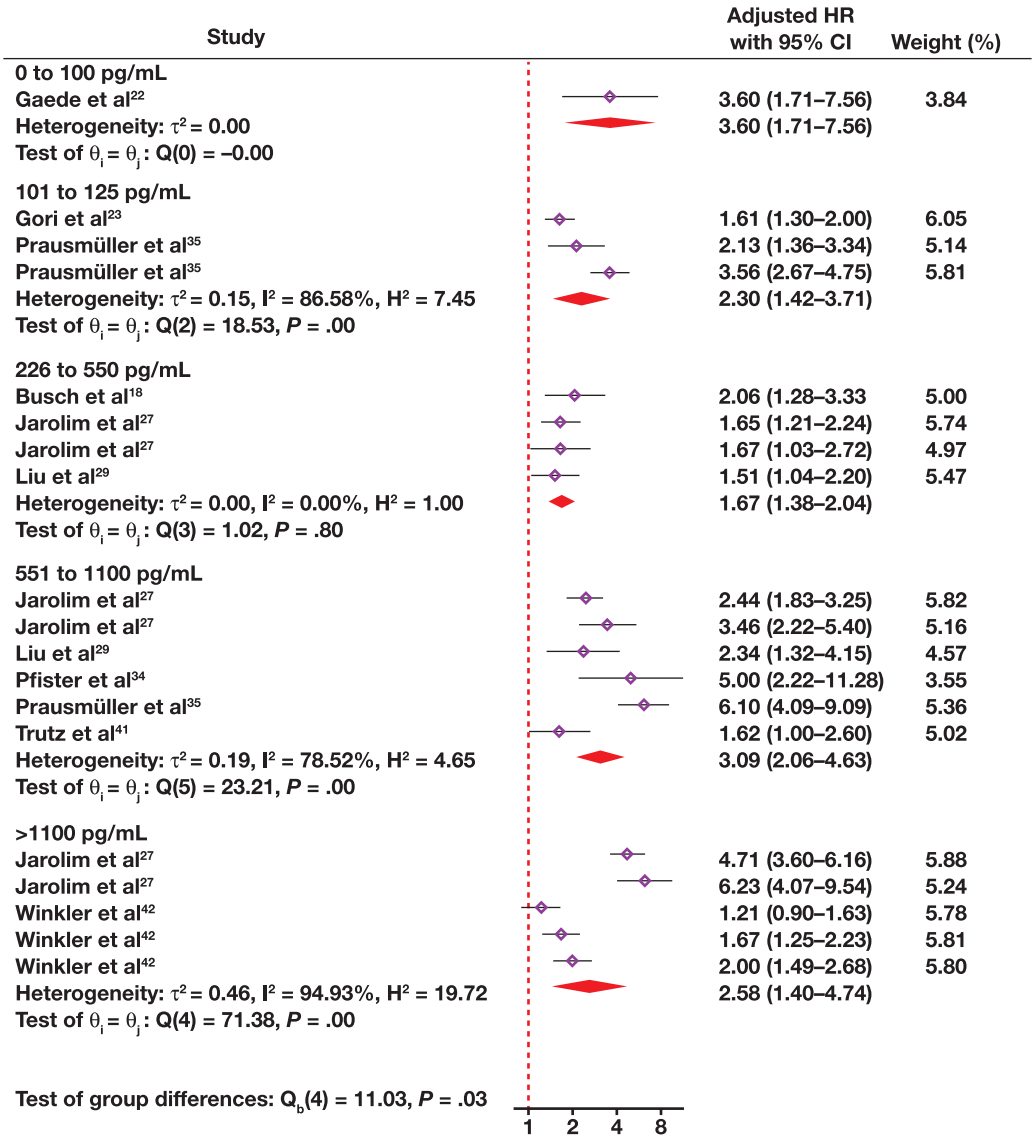

meta-analysis demonstrated that the best cutoff points for predicting cardiovascular events; its mortality lies within 100 to 225, which is in line with the findings of previous studies.[18,44–46]

The studies included in this systematic review evaluated the relationship between NT-proBNP and the outcome in type 2 diabetes patients in 2 forms. Some studies reported performance of NT-proBNP as a continuous variable and others reported categorical values based on different thresholds (cutoff points). Nevertheless, since finding a cutoff point for NT-proBNP is of utmost importance, this review mainly concentrated on studies reporting a prognosing value for NT-proBNP over a variety of cutoff points. On the other hand, the presence of publication bias in evaluating performance of the continuous value of NT-proBNP caused uncertainty in the findings in this section.

Although there exists evidence demonstrating a direct relationship between NT-proBNP serum levels and the duration of diabetes,[47] our meta-regression showed that the duration of diabetes did not change the value of NT-proBNP in predicting the outcome of diabetic patients. As a result, the prognostic value of NT-proBNP is independent from the duration of diabetes.

The follow-up period of the included studies varied between 0.8 to 11.3 years. The results indicated that the values of NT-proBNP, regardless of follow-up time, are able to predict cardiovascular events and mortality. There may be 2 reasons for this finding. First, the least follow-up period was 0.8 years, which is long enough for complications to occur. Furthermore, the minimum time of disease duration between the included studies was 5 years, indicating that an adequate time exists between diagnosis of diabetes and the incidence of complications.

Although we attempted primarily to evaluate the relationship between all natriuretic peptides and their metabolites with the outcomes of diabetes, eventually only the prognostic value of NT-proBNP was evaluated. Despite a number of articles studying the prognostic values

Downloaded from https://academic.oup.com/labmed/article/54/4/339/6772474 by guest on 24 February 2025

TABLE 3. Subgroup Analysis According to Outcome

	Effect Size		Heterogeneity		Meta-Regression	
Subgroups	Adjusted HR (95% CI)	*P* Value	I^2	*P* Value	Coefficient (95% CI)	*P* Value
Cardiovascular events						
Duration of diabetes, y						
5–10	1.71 (1.33, 2.20)	<.0001	92.29	<.0001	Reference	—
≥10	1.99 (1.18, 3.37)	.010	97.86	<.0001	0.13 (–0.39, 0.66)	.630
Follow up duration, y						
0.8–1	2.22 (1.59, 3.10)	<.0001	61.76	.095	Reference	—
1.1–5	1.69 (1.39, 2.05)	<.0001	97.76	<.0001	–0.28 (–0.75, 0.18)	.232
≥5	1.39 (1.26, 1.53)	<.0001	18.09	.049	–0.38 (–0.91, 0.16)	.168
Condition						
General diabetic	1.69 (1.43, 2.00)	<.0001	97.72	<.0001	Reference	—
Cardiovascular diabetic	1.74 (1.31, 2.31)	<.0001	91.57	<.0001	0.03 (–0.30, 0.36)	.845
Sample size						
Less than 1000	1.69 (1.23, 2.32)	.001	98.27	<.0001	Reference	—
More than 1000	1.77 (1.54, 2.04)	<.0001	91.82	<.0001	0.10 (–0.18, 0.39)	.485
Cardiovascular mortality						
Duration of diabetes, y						
5–10	1.64 (1.10, 2.45)	.015	56.58	.129	Reference	—
≥10	2.31 (1.02, 5.22)	.044	97.13	<.0001	0.27 (–0.86, 1.40)	.638
Follow-up duration, y						
0.8–1	No data		No data		No data	
1.1–5	1.53 (1.07, 2.20)	.021	89.88	.002	Reference	—
≥5	2.08 (1.26, 3.43)	<.0001	96.47	<.0001	0.30 (–0.54, 1.14)	.479
Condition						
General diabetic	2.31 (1.28, 4.16)	.005	97.12	<.0001	Reference	—
Cardiovascular diabetic	1.49 (1.17, 1.88)	.001	77.01	.007	–0.44 (–1.16. 0.28)	.231
Sample size						
Less than 1000	1.72 (1.36, 2.18)	<.0001	42.21	.174	Reference	—
More than 1000	2.00 (1.06, 3.76)	.031	98.66	<.0001	0.12 (–0.69, 0.930)	.771
All-cause mortality						
Duration of diabetes, y						
5–10	1.77 (1.21, 2.61)	.004	95.31	<.0001	Reference	—
≥10	1.63 (0.88, 3.00)	.118	99.20	<.0001	–011 (–0.82, 0.59)	.750
Follow up duration, y						
0.8–1	3.42 (1.09, 10.72)	.035	0.00	>.999	Reference	—
1.1–5	1.58 (1.23, 2.02)	<.0001	98.12	<.0001	–0.77 (–2.13. 0.59)	.267
≥5	1.78 (1.28, 2.48)	.001	96.28	<.0001	–0.65 (–2.03, 0.72)	.351
Patient condition						
General diabetic	1.69 (1.34, 2.13)	<.0001	98.48	<.0001	Reference	—
Cardiovascular diabetic	1.84 (1.01, 3.35)	.047	96.87	.001	–0.001 (–0.48, 0.48)	.999
Sample size						
Less than 1000	1.87 (1.27, 2.75)	.001	95.98	<.0001	Reference	—-
More than 1000	1.65 (1.30, 2.10)	<.0001	97.59	<.0001	–0.05 (–0.48, 0.38)	.815

CI, confidence interval; HR, hazard ratio.

of BNP[48–53] and MR-proANP,[54,55] the small number of these studies and their diverse results prevented a meta-analysis from being performed on their results.

However, as a qualitative assessment, Seki et al[51] demonstrated that with an increase in BNP serum levels, the risk of cardiovascular events (HR = 1.04; 95% CI: 1.00, 1.08) and all-cause mortality (HR = 1.05; 95% CI: 1.00, 1.10) increases. Also, Szwejkowski et al[52] and Tsuruda et al[53] reported similar results for all-cause mortality and cardiovascular events. Furthermore, Onodera et al[50] state that BNP can predict cardiovascular events at cutoff points higher than 46.5 pg/mL (HR = 4.38;

Downloaded from https://academic.oup.com/labmed/article/54/4/339/6772474 by guest on 24 February 2025

FIGURE 4. **Forest plot of value of different cutoffs of NT-proBNP for prognosis of cardiovascular mortality in diabetes type 2 patients. Data were presented as adjusted hazard ratio (HR) and 95% confidence interval (95% CI).**

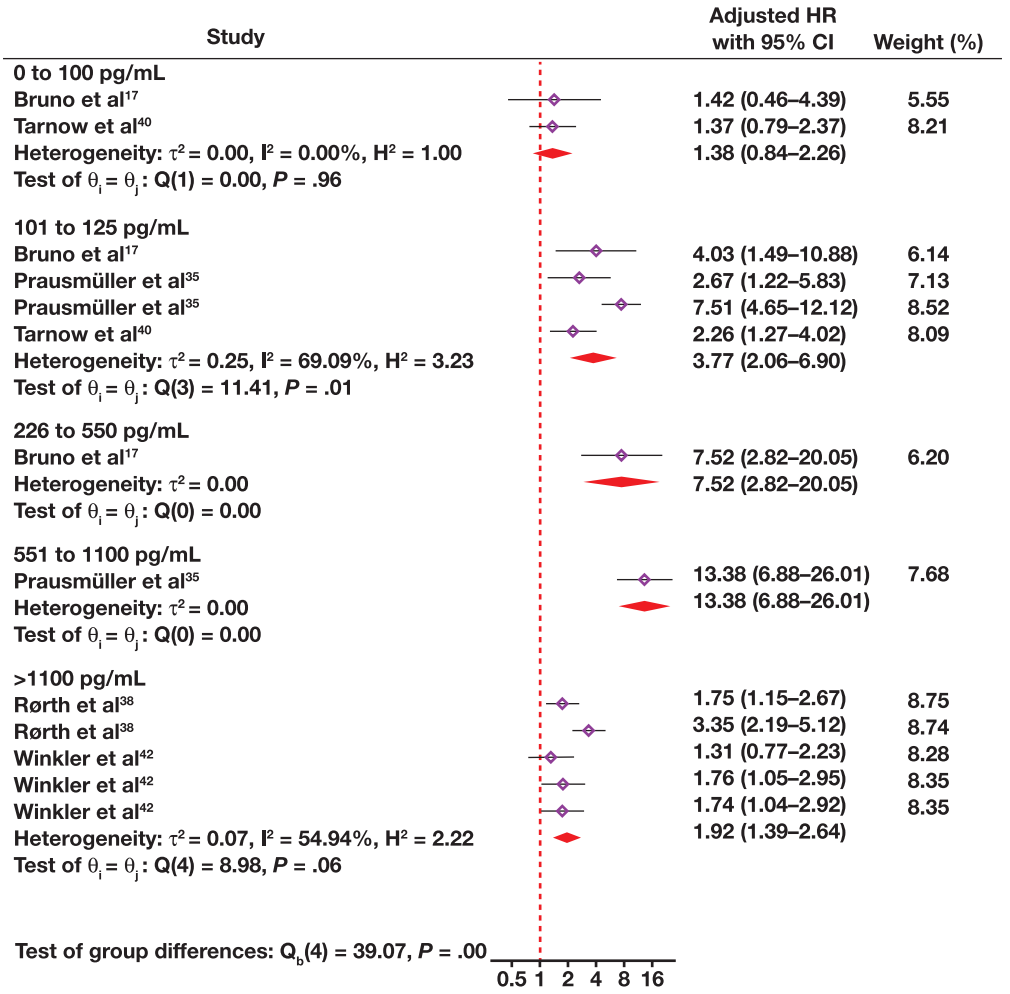

95% CI: 1.65, 11.59). However, their results indicated that in cutoff values of less than 28.3 pg/mL no relationship exists between BNP serum levels and the incidence of cardiovascular events. In addition, Ikeda et al[49] also demonstrated that BNP levels more than 28.7 may indicate a higher incidence risk of cardiovascular events.

Two studies evaluated the relationship between serum levels of MR-proANP levels with the diabetes outcomes. In the first study, Jensen et al[54] showed that the risk of cardiovascular events increases with the increase in serum levels of MR-proANP (HR = 1.71; 95% CI: 1.34, 2.18). In the second study, van Hateren et al[55] provided evidence over a significant increase in cardiovascular events (HR = 2.23; 95% CI: 1,78, 2.79) and all-cause mortality (HR = 2.42; 95% CI: 1.74, 3.37) with the increase in MR-proANP serum levels.

In comparison with previous systematic reviews, Buchan et al[56] demonstrated that the serum levels of BNP and NT-proBNP could predict all-cause mortality in heart failure patients. In addition, Shen et al[57] showed that elevated NT-proBNP is associated with the risk of post myocardial infarction death and major adverse cardiovascular events. Moreover, a recent meta-analysis showed that elevated level of NT-proBNP could predict short-term mortality following acute aortic dissection.[58] As a result, although previous systematic reviews did not assess the prognostic value of NT-proBNP in diabetic patients, their results are compatible with the current meta-analysis. It seems that NT-proBNP could be considered as an appropriate biomarker in the prognosis of cardiovascular adverse events and deaths in patients with susceptible or known cardiovascular diseases.

One of the major limitations of the present meta-analysis was disease duration reported in the included studies. The minimum duration of disease was 5 years. In other words, serum levels of NT-proBNP were eliminated at least 5 years after the diagnosis of diabetes in these patients. Hence, the prognostic value of this biomarker is rather unclear in shorter durations of the disease, and more studies are needed in this regard.

Another major limitation for the generalizability of the findings of this study is that the certainty of evidence in terms of the prognostic value of continuous level of NT-proBNP was very low. Also, the presence of an evident publication bias regarding the value of continuous level of NT-proBNP in predicting cardiovascular events and all-cause mortality is another reason to be cautious in interpreting the findings. However, this limitation did not exist regarding categorical values of NT-proBNP. Therefore, the author strongly recommends future studies to evaluate the cutoff points proposed in this study.

Downloaded from https://academic.oup.com/labmed/article/54/4/339/6772474 by guest on 24 February 2025

FIGURE 5. **Forest plot of value of different cutoffs of NT-proBNP for prognosis of all-cause mortality in diabetes type 2 patients. Data were presented as adjusted hazard ratio (HR) and 95% confidence interval (95% CI).**

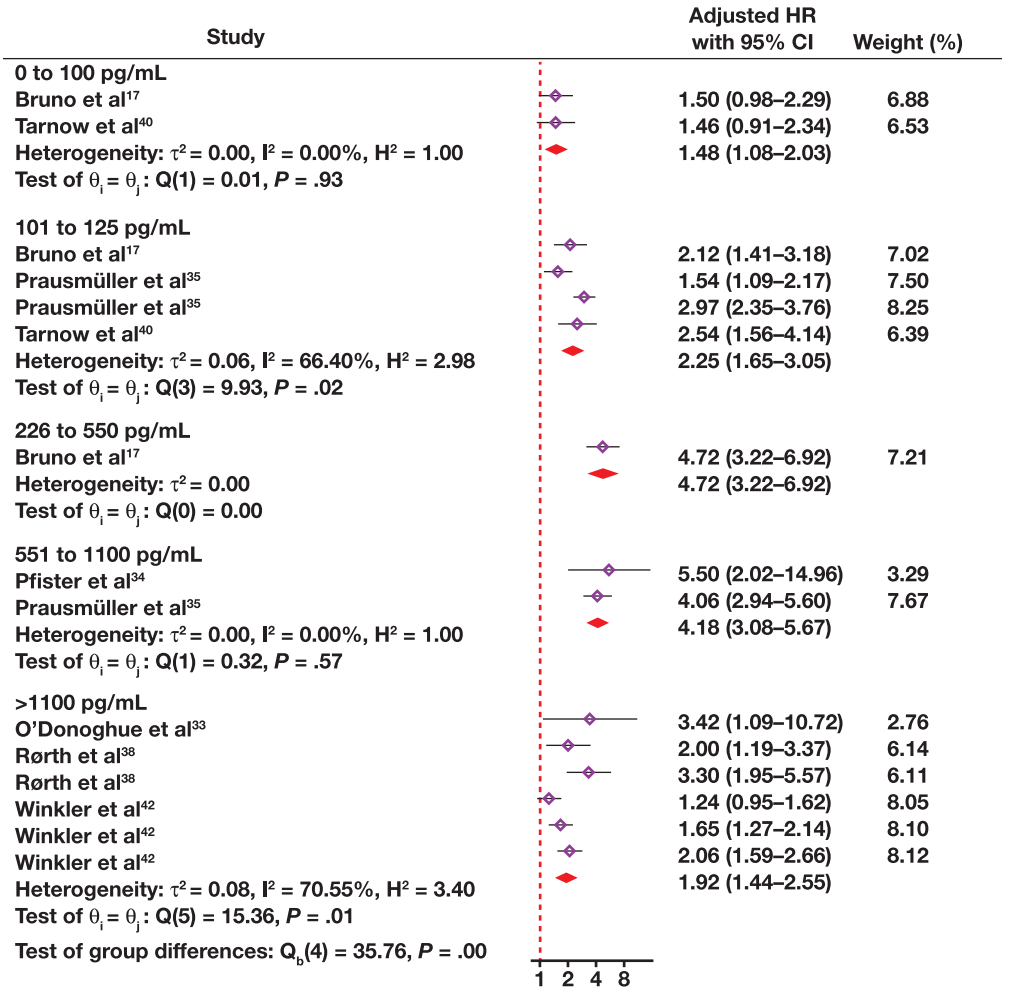

Conclusion

A moderate level of evidence indicated that serum levels of NT-proBNP can predict cardiovascular events, cardiovascular mortality, and all-cause mortality in type 2 diabetes patients. The most appropriate cutoff point for NT-proBNP in predicting cardiovascular events and cardiovascular mortality is a value greater than 100 pg/mL, and in predicting all-cause mortality a value greater than 225 pg/mL. Thus, NT-proBNP can be used as a biomarker for risk stratification of type 2 diabetes.

Supplementary Data

Supplemental figures and tables can be found in the online version of this article at www.labmedicine.com.

Acknowledgment

The author thanks Dr Muhammed IM Gubari for his invaluable contribution in collecting and summarizing the articles.

Conflict of Interest Disclosure

The author has nothing to disclose.

REFERENCES

1. Williams R, Karuranga S, Malanda B, et al. Global and regional estimates and projections of diabetes-related health expenditure: results from the International Diabetes Federation Diabetes Atlas, 9th edition. *Diabetes Res Clin Pract.* 2020;162:108072. doi:10.1016/j.diabres.2020.108072
2. Petrie JR, Guzik TJ, Touyz RM. Diabetes, hypertension, and cardiovascular disease: clinical insights and vascular mechanisms. *Can J Cardiol.* 2018;34(5):575–584.
3. Khan MAB, Hashim MJ, King JK, Govender RD, Mustafa H, Al Kaabi J. Epidemiology of type 2 diabetes - global burden of disease and forecasted trends. *J Epidemiol Glob Health.* 2020;10(1):107–111.
4. Kahn SE, Cooper ME, Del Prato S. Pathophysiology and treatment of type 2 diabetes: perspectives on the past, present, and future. *Lancet*. 2014;383(9922):1068–1083.
5. Scirica BM. Use of biomarkers in predicting the onset, monitoring the progression, and risk stratification for patients with type 2 diabetes mellitus. *Clin Chem.* 2017;63(1):186–195.
6. Pandit K, Mukhopadhyay P, Ghosh S, Chowdhury S. Natriuretic peptides: diagnostic and therapeutic use. *Indian J Endocrinol Metab.* 2011;15(suppl 4):345S345.
7. Bibbins-Domingo K, Gupta R, Na B, Wu AHB, Schiller NB, Whooley MA. N-terminal fragment of the prohormone brain-type natriuretic peptide (NT-proBNP), cardiovascular events, and mortality in patients with stable coronary heart disease. *JAMA.* 2007;297(2):169–176.

Downloaded from https://academic.oup.com/labmed/article/54/4/339/6772474 by guest on 24 February 2025

8. Ponikowska B, Suchocki T, Paleczny B, et al. Iron status and survival in diabetic patients with coronary artery disease. *Diabetes Care.* 2013;36(12):4147–4156.
9. Bidadkosh A, Lambooy SPH, Heerspink HJ, et al. Predictive properties of biomarkers GDF-15, NTproBNP, and hs-TnT for morbidity and mortality in patients with type 2 diabetes with nephropathy. *Diabetes Care.* 2017;40(6):784–792.
10. Salameh J-P, Bossuyt PM, McGrath TA, et al. Preferred reporting items for systematic review and meta-analysis of diagnostic test accuracy studies (PRISMA-DTA): explanation, elaboration, and checklist. *BMJ.* 2020;370:m2632.
11. National Heart, Lung, and Blood Institute. *National Heart, Lung, and Blood Institute Quality Assessment Tool for Observational Cohort and Cross-Sectional Studies*. Bethesda, MD: National Heart, Lung, and Blood Institute; Available from: https://www.nhlbi.nih.gov/health-topics/study-quality-assessment-tools.
12. Stang A. Critical evaluation of the Newcastle-Ottawa scale for the assessment of the quality of nonrandomized studies in meta-analyses. *Eur J Epidemiol.* 2010;25(9):603–605.
13. Yousefifard M, Toloui A, Ahmadzadeh K, et al. Risk factors for road traffic injury-related mortality in Iran; a systematic review and meta-analysis. *Arch Acad Emerg Med.* 2021;9(1):e61.
14. Yousefifard M, Ramezani F, Faridaalaee G, et al. Prevalence of posttraumatic stress disorder symptoms following traumatic spinal cord injury: a systematic review and meta-analysis. *Harv Rev Psychiatry.* 2022;30(5):1097.
15. Balshem H, Helfand M, Schünemann HJ, et al. GRADE guidelines: 3. Rating the quality of evidence. *J Clin Epidemiol.* 2011;64(4):401–406.
16. Birukov A, Eichelmann F, Kuxhaus O, et al. Opposing associations of NT-proBNP with risks of diabetes and diabetes-related complications. *Diabetes Care.* 2020;43(12):2930–2937.
17. Bruno G, Landi A, Barutta F, et al. N-terminal probrain natriuretic peptide is a stronger predictor of cardiovascular mortality than C-reactive protein and albumin excretion rate in elderly patients with type 2 diabetes: the Casale Monferrato population-based study. *Diabetes Care.* 2013;36(9):2677–2682.
18. Busch N, Jensen MT, Goetze JP, et al. Prognostic performance of echocardiography, electrocardiogram, albuminuria, plasma proBNP and hs-TnI in patients with type 2 diabetes. *Eur Heart J.* 2019;40(suppl 1):2047.
19. Clodi M, Resl M, Neuhold S, et al. A comparison of NT-proBNP and albuminuria for predicting cardiac events in patients with diabetes mellitus. *Eur J Prev Cardiol.* 2012;19(5):944–951.
20. Colombo M, Looker HC, Farran B, et al. Apolipoprotein CIII and N-terminal prohormone b-type natriuretic peptide as independent predictors for cardiovascular disease in type 2 diabetes. *Atherosclerosis.* 2018;274:182–190. doi:10.1016/j.atherosclerosis.2018.05.014
21. Czúcz J, Cervenak L, Förhécz Z, et al. Serum soluble E-selectin and NT-proBNP levels additively predict mortality in diabetic patients with chronic heart failure. *Clin Res Cardiol.* 2011;100(7):587–594.
22. Gaede P, Hildebrandt P, Hess G, Parving HH, Pedersen O. Plasma N-terminal pro-brain natriuretic peptide as a major risk marker for cardiovascular disease in patients with type 2 diabetes and microalbuminuria. *Diabetologia*. 2005;48(1):156–163.
23. Gori M, Gupta DK, Claggett B, et al. Natriuretic peptide and high-sensitivity troponin for cardiovascular risk prediction in diabetes: the atherosclerosis risk in communities (ARIC) study. *Diabetes Care.* 2016;39(5):677–685.
24. Gustafsson I, Mellbin L, Dickstein K, et al. NT-proBNP is a potent prognostic marker in patients with type 2 diabetes hospitalized for acute coronary syndrome—a DIGAMI 2 sub study. *Eur Heart J.* 2010;31(suppl 1):514–515.
25. Hillis GS, Welsh P, Chalmers J, et al. The relative and combined ability of high-sensitivity cardiac troponin T and N-terminal pro-B-type natriuretic peptide to predict cardiovascular events and death in patients with type 2 diabetes. *Diabetes Care.* 2014;37(1):295–303.
26. Huelsmann M, Neuhold S, Strunk G, et al. NT-proBNP has a high negative predictive value to rule-out short-term cardiovascular events in patients with diabetes mellitus. *Eur Heart J.* 2008;29(18):2259–2264.
27. Jarolim P, White WB, Cannon CP, Gao Q, Morrow DA. Serial measurement of natriuretic peptides and cardiovascular outcomes in patients with type 2 diabetes in the EXAMINE trial. *Diabetes Care.* 2018;41(7):1510–1515.
28. Jhund P, Claggett B, Pfeffer M, et al. NT-proBNP and hsTNT improve cardiovascular risk prediction in patients with type 2 diabetes mellitus, chronic kidney or cardiovascular disease or both. *J Am Coll Cardiol*. 2014;63(12S):A1279-A.
29. Liu HH, Cao YX, Jin JL, et al. Prognostic value of NT-proBNP in patients with chronic coronary syndrome and normal left ventricular systolic function according to glucose status: a prospective cohort study. *Cardiovasc Diabetol.* 2021;20(1):84.
30. Malachias MVB, Jhund PS, Claggett BL, et al. NT-proBNP by itself predicts death and cardiovascular events in high-risk patients with type 2 diabetes mellitus. *J Am Heart Assoc.* 2020;9(19):e017462.
31. Neuhold S, Resl M, Huelsmann M, et al. Repeat measurements of glycated haemoglobin A(1c) and N-terminal pro-B-type natriuretic peptide: divergent behaviour in diabetes mellitus. *Eur J Clin Invest.* 2011;41(12):1292–1298.
32. Nguyen K, Fan W, Bertoni A, et al. N-terminal Pro B-type natriuretic peptide and high-sensitivity cardiac troponin as markers for heart failure and cardiovascular disease risks according to glucose status (from the Multi-Ethnic Study of Atherosclerosis [MESA]). *Am J Cardiol.* 2020;125(8):1194–1201.
33. O'Donoghue M, Kenney P, Oestreicher E, et al. Usefulness of aminoterminal pro-brain natriuretic peptide testing for the diagnostic and prognostic evaluation of dyspneic patients with diabetes mellitus seen in the emergency department (from the PRIDE study). *Am J Cardiol.* 2007;100(9):1336–1340.
34. Pfister R, Tan D, Thekkanal J, Hellmich M, Erdmann E, Schneider CA. NT-pro-BNP measured at discharge predicts outcome in multimorbid diabetic inpatients with a broad spectrum of cardiovascular disease. *Acta Diabetol.* 2007;44(2):91–97.
35. Prausmüller S, Resl M, Arfsten H, et al. Performance of the recommended ESC/EASD cardiovascular risk stratification model in comparison to SCORE and NT-proBNP as a single biomarker for risk prediction in type 2 diabetes mellitus. *Cardiovasc Diabetol.* 2021;20(1):34.
36. Price AH, Welsh P, Weir CJ, et al. N-terminal pro-brain natriuretic peptide and risk of cardiovascular events in older patients with type 2 diabetes: the Edinburgh Type 2 Diabetes study. *Diabetologia.* 2014;57(12):2505–2512.
37. Riphagen IJ, Logtenberg SJ, Groenier KH, et al. Is the association of serum sodium with mortality in patients with type 2 diabetes explained by copeptin or NT-proBNP? (ZODIAC-46). *Atherosclerosis.* 2015;242(1):179–185.
38. Rørth R, Jhund PS, Kristensen SL, et al. The prognostic value of troponin T and N-terminal pro B-type natriuretic peptide, alone and in combination, in heart failure patients with and without diabetes. *Eur J Heart Fail.* 2019;21(1):40–49.
39. Saely CH, Vonbank A, Heinzle C, et al. Pro-B-type natriuretic peptide strongly predicts future cardiovascular events in cardiovascular disease patients with type 2 diabetes as well as in those without type 2 diabetes. *Atherosclerosis.* 2019;287:e189. doi:10.1016/j.atherosclerosis.2019.06.571
40. Tarnow L, Gall MA, Hansen BV, Hovind P, Parving HH. Plasma N-terminal pro-B-type natriuretic peptide and mortality in type 2 diabetes. *Diabetologia.* 2006;49(10):2256–2262.
41. Trutz J, Babeş A, Babeş K. The role of elevated Nt-proBNP and albuminuria as cardio-vascular risk factors in type 2 diabetes mellitus patients after acute coronary syndrome. *Rom J Diabetes Nutr Metab Dis*. 2015;22(2):141–149.

Downloaded from https://academic.oup.com/labmed/article/54/4/339/6772474 by guest on 24 February 2025

42. Winkler K, Wanner C, Drechsler C, Lilienthal J, März W, Krane V. Change in N-terminal-pro-B-type-natriuretic-peptide and the risk of sudden death, stroke, myocardial infarction, and all-cause mortality in diabetic dialysis patients. *Eur Heart J.* 2008;29(17):2092–2099.
43. bus D, Rein P, Saely CH, et al. Pro-B-type natriuretic peptide strongly predicts all cause and cardiovascular mortality in peripheral arterial disease patients with as well as in those without type 2 diabetes. *Diabetes.* 2017;66(suppl 1):A403–A4A4.
44. Taylor C, Roalfe A, Iles R, Hobbs F. The potential role of NT-proBNP in screening for and predicting prognosis in heart failure: a survival analysis. *BMJ Open.* 2014;4(4):e004675.
45. Rehman SU, Januzzi JL Jr. Natriuretic peptide testing in clinical medicine. *Cardiol Rev.* 2008;16(5):240–249.
46. Ballo P, Betti I, Barchielli A, et al. Prognostic role of N-terminal pro-brain natriuretic peptide in asymptomatic hypertensive and diabetic patients in primary care: impact of age and gender: results from the PROBE-HF study. *Clin Res Cardiol.* 2016;105(5):421–431.
47. Taner B, Abdulkadir U. Plasma NT-pro BNP concentrations in patients with hypertensive chronic kidney disease. *Nephro-Urol Mon.* 2010;2(4):537–542.
48. Faglia E, Clerici G, Caminiti M, et al. B-type natriuretic peptide predict mortality in diabetic patients with foot ulcer. *J Res Diabetes.* 2013; doi: 10.5171/2013.388970.
49. Ikeda S, Shinohara K, Enzan N, et al. Plasma B-type natriuretic peptide levels are associated with future cardiovascular events in patients with type 2 diabetes mellitus without known cardiovascular disease. *Circulation*. 2020;142(suppl 3):A14866.
50. Onodera M, Nakamura M, Tanaka F, et al. Plasma B-type natriuretic peptide is useful for cardiovascular risk assessment in community-based diabetes subjects: comparison with albuminuria. *Int Heart J.* 2012;53(3):176–181.
51. Seki N, Matsumoto T, Fukazawa M. Relationship between the brain natriuretic peptide (BNP) level and remission of diabetic nephropathy with microalbuminuria: a 3-year follow-up study. *Horm Metab Res.* 2015;47(2):138–144.
52. Szwejkowski BR, Elder DHJ, Dawson A, Struthers AD. Brain natriuretic peptide predicts all cause mortality in patients with type 2 diabetes and normal ejection fractions. *Heart.* 2011;97(suppl 1):A34.
53. Tsuruda T, Kato J, Sumi T, et al. Combined use of brain natriuretic peptide and C-reactive protein for predicting cardiovascular risk in outpatients with type 2 diabetes mellitus. *Vasc Health Risk Manag.* 2007;3(4):417–423.
54. Jensen J, Schou M, Kistorp C, et al. MR-proANP effectively risk stratifies patients with type 2 diabetes regardless of presence of heart failure. *Eur J Heart Fail.* 2019;21(S1):223–224.
55. van Hateren KJ, Landman GW, Kleefstra N, et al. The midregional fragment of pro-A-type natriuretic peptide, blood pressure, and mortality in a prospective cohort study of patients with type 2 diabetes (ZODIAC-25). *Diabetes Care.* 2013;36(5):1347–1352.
56. Buchan TA, Ching C, Foroutan F, et al. Prognostic value of natriuretic peptides in heart failure: systematic review and meta-analysis. *Heart Fail Rev.* 2022;27(2):645–654.
57. Shen S, Ye J, Wu X, Li X. Association of N-terminal pro-brain natriuretic peptide level with adverse outcomes in patients with acute myocardial infarction: a meta-analysis. *Heart Lung.* 2021;50(6):863–869.
58. Vrsalovic M, Vrsalovic Presecki A, Aboyans V. N-terminal pro-brain natriuretic peptide and short-term mortality in acute aortic dissection: a meta-analysis. *Clin Cardiol.* 2020;43(11):1255–1259.

Downloaded from https://academic.oup.com/labmed/article/54/4/339/6772474 by guest on 24 February 2025

A Primer on Chimerism Analysis: A Straightforward, Thorough Review

Anna B. Morris, PhD,[1] Robert Bray, PhD,[1] Howard M. Gebel, PhD,[1] H. Cliff Sullivan, MD, PhD,[1,]*

[1]Department of Pathology and Laboratory Medicine, Emory University School of Medicine, Atlanta, GA, USA. *To whom correspondence should be addressed: hcsulli@emory.edu.

Keywords: chimerism, transplant, stem cell transplant, STR, short tandem repeat, NGS, engraftment, rejection, relapse, GVHD

Abbreviations: STR, short tandem repeat; HPCT, hematopoietic progenitor cell transplantation; PCR, polymerase chain reaction; GVHD, graft-versus-host disease; RBC, red blood cell; FISH, fluorescence in situ hybridization; qPCR, quantitative PCR; NGS, next-generation sequencing; D:R, donor:recipient; CIBMTR, Center for International Blood and Marrow Transplant Research; VNTR, variable nucleotide tandem repeat; SD, standard deviation, CV, coefficient of variation; LOH, loss of heterozygosity, GvL, graft vs leukemia; MRD, minimal residual disease; TA-GVHD, transfusion-associated GVHD; indel, insertion and deletion

Laboratory Medicine 2023;54:352-362; https://doi.org/10.1093/labmed/lmac132

ABSTRACT

Short tandem repeat (STR) analysis to assess chimerism is a critical aspect of routine care particularly in patients facing stem cell transplants but is also relevant in other clinical scenarios. STR analysis provides a means to assess donor and recipient cellular origins in a patient, and, as such, can inform engraftment, rejection, and relapse status in stem cell transplant recipients. In this review of STR testing, the most commonly used method to assess chimerism, its background, procedural details, and clinical utility are discussed.

With roots imbedded in Greek mythology, Chimera, once depicted as a lion-goat-snake hybrid monster (The Chimera of Arezzo),[1] now refers to an individual composed of at least 2 genetically distinct cell populations.[2] As such, chimerism is embodied in both nature (reviewed in Madan[3]) and medicine. In nature, studies in the 1940s described erythrocyte mosaicism (chimerism) in calves, likely the phenomenon of anastomoses between twin calves in utero.[4] Similar cases have since been reported in humans.[5] The term "chimera" followed shortly thereafter, when, in the 1950s, Billingham and colleagues[6] reported that inoculation of donor cells in utero resulted in actively acquired tolerance to the same donor later in life, suggesting a role for chimerism in mediating allograft tolerance.

The 1980s saw an emergence of hematopoietic progenitor cell transplantation (HPCT) for the treatment of certain malignant and nonmalignant diseases. Establishment of hematopoiesis by donor stem cells is critical for therapeutic benefit, making analysis of the donor and recipient cellular populations following transplant important in understanding success of the therapy. Chimeric assessment of donor and recipient populations results in understanding whether the patient exhibits full chimerism (>95% cells of donor origin) or mixed chimerism (between 0% and 95% cells of donor origin), which is further classified as transient (percent recipient cells is high, but is decreasing), stable (percent recipient cells is stable overtime), progressive (percent recipient cells increases to >10%), or increasing (percent recipient increases >5% from last sample tested).[2] Other states of chimerism include split chimerism, in which 2 cellular populations (ie, T cells and myeloid cells) represent 2 different chimerism statuses in an individual, and microchimerism, in which the percent recipient is between 0% and 1%.

Early techniques to monitor chimerism included Southern blotting, restriction fragment length polymorphism, and polymerase chain reaction (PCR).[7] The prominent use of chimerism testing led to the ability to associate mixed chimerism with disease state (ie, relapse and graft rejection), and testing became a routine part of clinical practice for HPCT recipients to monitor initial engraftment, rejection, and disease relapse.[2,8,9] Today, the utility of chimerism testing is multifaceted. Although initially used to document HPCT engraftment or failure, chimerism testing is now used to monitor risk of relapse, graft-versus-host disease (GVHD), minimal residual disease, GVHD following solid organ transplantation, and transfusion-associated GVHD. These tools to assess 2 or more distinct sources of DNA have found uses in other fields outside of transplant, including forensic testing, twin zygosity, parentage/kinship testing, and specimen identification.

As technology improved, so too did chimerism testing techniques. Earlier methodologies included red blood cell (RBC) phenotyping, XY cytogenics, and fluorescence in situ hybridization (FISH), whereas modern methodologies include molecular microsatellite testing (ie, short tandem repeat [STR] assessment), quantitative polymerase chain reaction (qPCR) assays, and next-generation sequencing (NGS) assays.

Methods of Old

RBC phenotyping arose in the 1980s[10] and was shown to be a sensitive method to measure the proportion of donor and recipient populations following allogeneic HPCT by assessing the RBC phenotype.[11,12] To do this, a complete RBC phenotype was performed (including A, B, C, c, E, D, K, Fy^a, Fy^b, Jk^a, Jk^b, M, N, S, and s antigens) and mismatched antigens between the donor and recipient were identified and thereafter monitored for chimerism status. This chimerism assay was found to be useful for patients presenting with or being treated for chronic myeloid leukemia, as relapse of disease is typically associated with host

© The Author(s) 2022. Published by Oxford University Press on behalf of American Society for Clinical Pathology. All rights reserved. For permissions, please e-mail: journals.permissions@oup.com

Downloaded from https://academic.oup.com/labmed/article/54/4/352/6827470 by guest on 24 February 2025

erythrocyte expansion and easily detected with this assay.[10,11,13,14] RBC phenotyping, although fast, simple, and sensitive, only detects chimerism in the RBC compartment,[15] and due to the slow turnover rate of RBCs (>120 days), an accurate determination of chimerism could be delayed.[16]

Chromosomal assessment was another earlier method used to detect mixed chimerism. Sex-mismatched donor:recipient (D:R) pairs were assessed using XY cytogenics or with polymorphic satellites that differ between sex-matched donors and recipients.[9] Fluorescent in situ hybridization was an improvement on XY cytogenetics that allowed for the more rapid assessment of many cells with high sensitivity using fluorescent probes.[9,17] Use of these techniques was labor intensive and limited by sex-mismatched D:R pairs. A recent survey of laboratories within the Center for International Blood and Marrow Transplant Research (CIBMTR) performing chimerism testing showed that of 108 responding laboratories, none reported using RBC phenotyping and only 3 reported using FISH.[18] The vast majority (82%) reported use of the STR assay for chimeric assessment. This review will cover STR analysis in depth—from cell isolation and DNA extraction to test interpretation—as it is the most prevalent test used for chimerism analysis, with the goal to provide an all-encompassing didactic resource for those entering the field or beginning STR testing.

Microsatellite Testing: The Method of the Present

Following analysis of the whole genome, mini- and micro-satellite regions of repetitious genomic material were identified as they produced a different frequency of the 4 nucleotide bases than other areas of DNA, resulting in the separation of these regions from others in chromatography or density gradient centrifugation.[19,20] These repetitious regions include 2 major types: variable nucleotide tandem repeats (VNTR), often with the repeating sequence made of 14 to 500 base pairs (bp) in length, and STR, typically made of 1 to 6 bp in length[21,22] but also associated with lengths of up to 13 bp[23] (**FIGURE 1**). Although STRs are present in coding regions, the vast majority are in noncoding regions.[24] The amount present in the genome associates with genome size,[25] making up as much as 3% of the human genome.[23]

The discovery and implementation of PCR led to the ability to genotype individuals at these regions and rapidly revolutionized chimerism testing.[26,27] The number of times the simple STR sequence is repeated varies quite highly among individuals due to the high probability of polymerase slippage during DNA replication,[28] resulting in many different alleles. Genotyping several repeat regions can identify alleles that distinguish DNA isolated from donor vs recipient cells. The VNTRs were initially assessed for their ability to distinguish donor vs recipient, but their lower degree of polymorphism and large base pair length typically results in fewer alleles than STRs. Consequently, STR analysis has become the preferred method.[29] In addition to the 82% of responding laboratories in the CIBMTR above using STR analysis, another recent survey of accredited American Society of Histocompatibility and Immunogenetics or European Federation for Immunogenetics laboratories identified that 87% of responding laboratories (of 54 total) within these agencies used STR analysis for chimerism, making it the most common method for assessing chimerism within both groups surveyed.[30] As STR testing developed, older methods, including cytogenetic analysis and RBC phenotyping, fell out of favor for many laboratories because of their limitations and lack of sensitivity.

FIGURE 1. Visual representation of short tandem repeat (STR) and variable nucleotide tandem repeat (VNTR) differences. A, A paternal and maternal chromosome set is depicted with microsatellite regions in red. B, Depiction of a STR microsatellite locus in which 1 chromosome has 6 repeats of a 1 to 6 bp segment of DNA (Allele A6), and the other has 8 repeats (Allele A8). C, Depiction of a VNTR microsatellite locus in which one chromosome has 4 repeats of a 14 to 500 bp segment of DNA (Allele A4), and the other has 3 repeats (Allele A3).

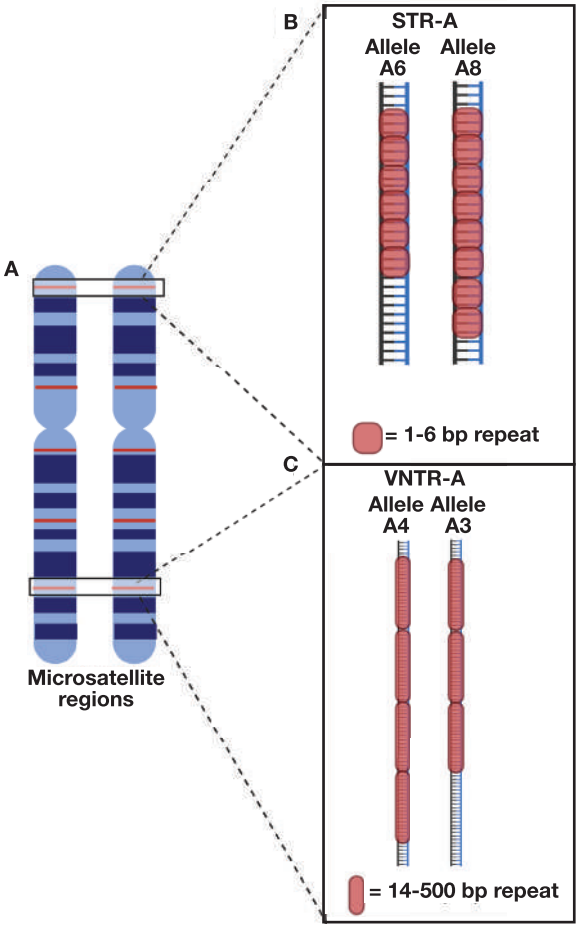

STRs can be named after the gene in which they are located in (ie, TPOX is located in the human thyroid peroxidase gene, intron 10), or with a D#S## nomenclature (eg, D2S1338) if located outside of a gene, wherein D = DNA, the number after the D refers to the chromosome in which it resides, S = STR, and the numbers after the S are its specific identifier.[21] Classification of STRs is by the length of repeating base pairs; that is, di-, tri-, tetra-, penta-, and hexa-nucleotide repeats, and then by the types of repeats: simple, compound, and complex.[31] Simple STRs are made of a single 1 to 6 bp repeating sequence (eg, $[AATG]_4$). A variation of a simple STR with 1 of the repeats containing a missing nucleotide is called a variant allele or "simple with non-consensus allele" (eg, $[TCTA]_3TCA[TCTA]_8$).[32] Compound STRs are made of multiple sets of repeats of the same bp length (eg, $[TGCC]_4[TTCC]_6$). Complex STRs are made of multiple sets of repeats of differing bp lengths, which could include nonrepeating or constant segments dispersed be-

Downloaded from https://academic.oup.com/labmed/article/54/4/352/6827470 by guest on 24 February 2025

tween (eg, $[TCTA]_4$ $[TCTG]_6$ $[TCTA]_3$ TA $[TCTA]_3$ TCA $[TCTA]_2$ TCCATA $[TCTA]_6$). Alleles of STRs are typically designated by the number of repeat sequences present[33]; this includes repeats of the same or differing sequences in simple and compound/complex STRs (eg, $[AATG]_4$ is allele 4 of TPOX and $[TGCC]_4[TTCC]_6$ is allele 10 of D2S1338). For designating alleles with incomplete repeats in compound/complex STRs, the total repeat number separated by a decimal point followed by the number of base pairs in the incomplete repeat is used (eg, $[TCTA]_3$ TCA $[TCTA]_8$ is designated as allele 11.3 of D2S441). Occasionally, there are exceptions to these guidelines from historic use, such as Penta D and E. These 2 penta-nucleotide repeats were found by the Promega Corporation in a shotgun method to identify penta-nucleotide repeats in the human genome (Promega). These 2 loci, because of their high power of discrimination, few microvariants, and low level of stutter, were singled out as useful loci in STR analysis and have kept their historical name.

Assessment of several STR loci as a panel can identify individuals forensically, as a 13-locus STR assessment can lead to nearly 10^{21} possible profiles, making any individual's profile extremely rare.[34] To this end, STR testing is a valuable tool in chimerism testing, as the possibility of 2 individuals exhibiting the same exact STR profile is also rare (except identical twins) and has been estimated to be 1 in 575 trillion for unrelated White persons for a 13-locus panel.[35] This allows STR analysis to identify unique alleles between D:R pairs to monitor chimerism following HPCT. Several commercial panels are now available for testing in chimerism laboratories.

STR Testing

Because the rate of immune cell reconstitution varies between different white blood cell types,[36] chimerism testing is typically performed on enriched populations of various cells. The recent survey of chimerism testing laboratories indicated that 74% of laboratories perform chimerism testing on cell subsets, with 68% looking at T cells (CD3+) and 52% also testing myeloid/granulocyte populations of cells (CD33+).[30] Other subsets often tested include B cells (CD19/20+), NK cells (CD56+), and CD34+ cells. The high prevalence of T-cell–enriched testing can likely be attributed to their biological relevance—T-cell mixed chimerism has been associated with relapse in several types of disease—and technological ease of enrichment; T cells typically exist in high frequency in peripheral blood, leading to high purity and yield.[18] Positive magnetic enrichment is most frequently used to separate different populations, although cell sorting via flow cytometry is another (although expensive) technique that can be used.

Following enrichment, DNA is extracted and the STR loci of interest are amplified via PCR using fluorescent primers to quantify the PCR product. These products are then subjected to capillary electrophoresis, a method that shuttles each PCR product into a capillary that separates products according to their size. Because several STR loci have overlapping size, different fluorescent labels are used in the generation of the PCR products, allowing similar size products to be easily distinguished from one another based on their fluorescence emission spectra. This approach allows multiple similar-sized STR loci to be assessed simultaneously and supports higher-throughput typing.[37] The PCR products are then outputted on an electropherogram, where the PCR products are converted into peaks of fluorescent units (which are mainly influenced by the abundance of PCR product, but can also be affected by input DNA concentration, amplification efficiency, and allele size). The position of the peak is a function of the time it took to migrate through the detector, which is then converted to base pair size according to a standard curve. Finally, the peak is associated with its particular STR locus via which fluorescent probe was used. The area under the peak, or height of the peak, is used to determine the level of chimerism in the transplant recipient (see below).

Chimerism Analysis

To perform chimerism testing, a donor sample and pretransplant recipient sample are used to determine which STR probes distinguish donor from recipient and will thus be informative to determine the degree of chimerism. Each STR locus has 2 alleles, 1 maternally inherited and 1 paternally inherited (there are some exceptions, noted in the "Limitations of the STR Assay" section). An individual can be homozygous or heterozygous for each STR locus, with homozygous alleles presenting as 1 peak and heterozygous alleles presenting as 2 peaks. Assessment of each locus can be classified as informative, noninformative, or partially informative.

To be fully informative, there must be at least 1 unique donor allele and 1 unique recipient allele, so that when chimerism analysis is performed posttransplant, the locus can be assessed for the proportion of donor allele in the DNA isolated from the posttransplant recipient (**FIGURE 2A**). When both alleles for 1 locus are shared between donor and recipient, that locus is noninformative due to the inability to distinguish donor from recipient (**FIGURE 2B**). Loci that have a unique allele only in the recipient and not in the donor or vice versa are considered partially informative. Such loci are more challenging to calculate the degree of chimerism (**FIGURE 2C**). As such, partially informative loci are generally not recommended for chimerism testing. As expected, the number of informative STR loci is lower among related donors than unrelated donors.[38] After identifying informative loci, each locus is used to calculate the percent donor chimerism. The height (or area under the peak) of the unique peaks at the informative locus is proportional to the amount of the PCR product at that locus. Therefore, the percent donor chimerism at each locus can be calculated by

$$\frac{D1 + D2}{D1 + D2 + R1 + R2} \times 100$$

where D1 and D2 represent the height or area under the peak of the donor peaks and R1 and R2 represent the height or area of the recipient peaks[39–41] (**FIGURE 3**). If the donor and/or the recipient is homozygous at the locus, then D2 and/or R2 is 0, and the peak height should be approximately double that of a heterozygous allele (**FIGURE 4**). Shared peaks between the donor and recipient can be excluded. Calculated percent donor chimerism should be similar for all informative loci, and the average of all the loci is reported as the final percent donor chimerism. It is recommended that at least 3 fully informative loci be used to calculate the average percent donor chimerism. If the chimerism calculation for an individual locus differs by >10% from other loci, it should be removed.[38,42] Also, because standard deviation (SD) measures deviation from a mean (therefore, 5% SD is worse in a recipient who is 20% chimeric than 90% chimeric), the coefficient of variation (CV), which measures the ratio of the SD to the mean, should be reported and at or below 5.[41,43] If the CV is >5, identification of the locus/loci that are causing the skew should be removed and new loci chosen that result in a CV <5.

Sensitivity of the STR assay in the detection of minor genotypes is between 0.4% and 5%.[26,44] Because of this relatively low sensitivity, many laboratories consider fully engrafted as >95% donor chimerism,

Downloaded from https://academic.oup.com/labmed/article/54/4/352/6827470 by guest on 24 February 2025

FIGURE 2. Schematic of informative (A), noninformative (B), and partially informative (C) alleles in short tandem repeat (STR) analysis. A, Electropherograms of 2 STR loci are shown in which the donor and pretransplant (pre-Tx) recipient have no shared (or nonoverlapping) alleles and are therefore informative. B, A locus in which the donor and pre-Tx recipient have all shared alleles and cannot inform chimerism analysis. C, A locus in which the donor and pre-Tx recipient have 1 shared allele and 1 nonoverlapping allele, indicating the nonoverlapping allele alone is informative, making this locus partially informative. post-Tx, posttransplant.

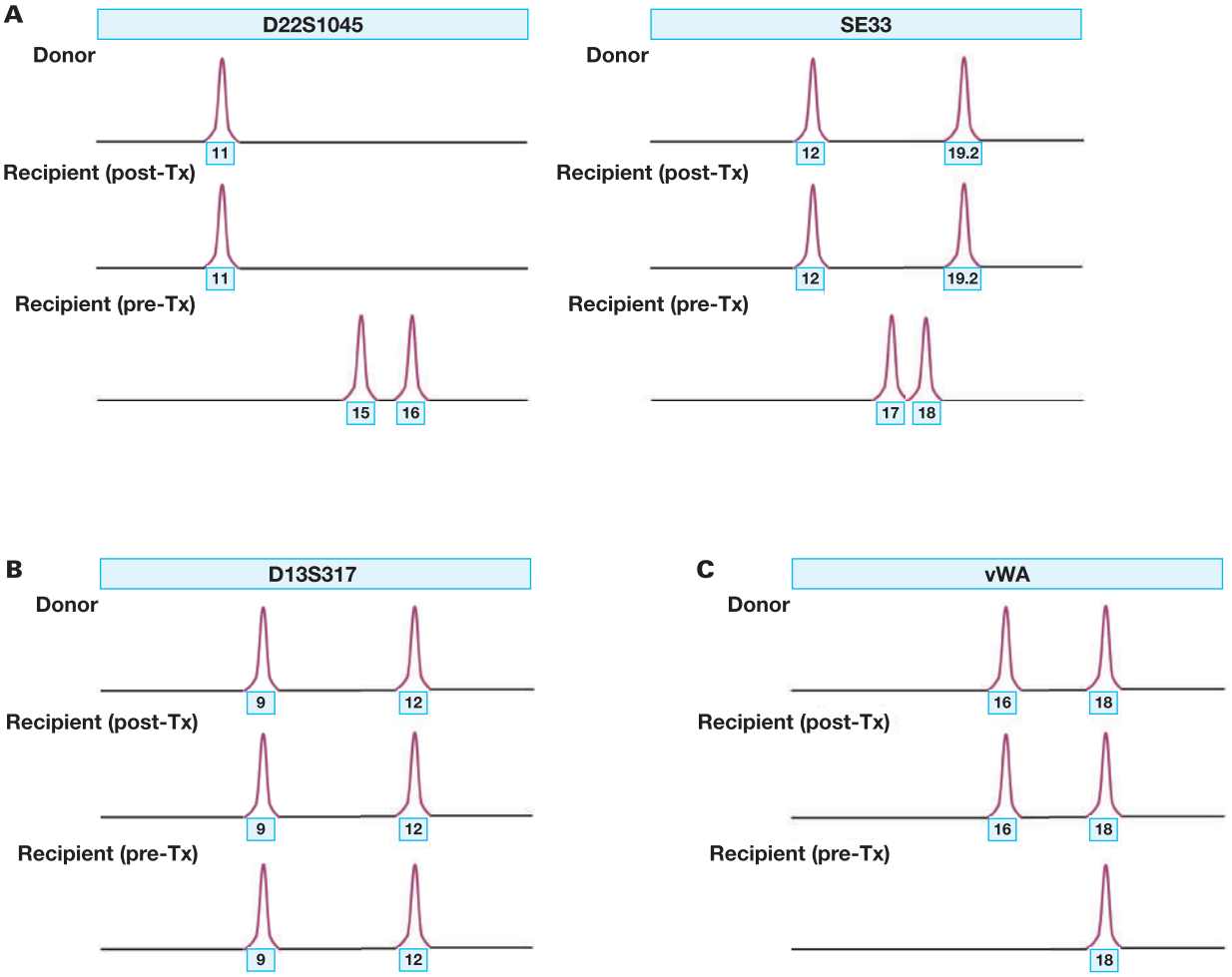

as this technique cannot accurately discern 95% from 100%. Newer methods discussed below have higher sensitivities (NGS 0.01%–1%, qPCR 0.01%–0.1%), and can provide an advantage over STR, although higher sensitivity in these assays can precipitate worse precision.[44]

Limitations of the STR Assay

As different fluorescent molecules are used to distinguish similar-sized PCR products, occasionally the emission spectrums of the fluorophore overlap and cause leakage into other channels.[45,46] This can be interpreted as a peak of the same size in 2 different fluorescent channels, known as a "pull up," and could be misinterpreted for 2 PCR products of the same size with different fluorophores, when in actuality there is only 1 true peak and the other is due to emission wavelength overlap (**FIGURE 5A**). Pull-up peaks can be identified as "extra" peaks that are in the posttransplant recipient sample that are not in the donor or pretransplant recipient sample, and they can be avoided by reducing the amount of PCR product that goes into the capillary, either by diluting the product or reducing the injection time.[47] Use of fluorochromes with little spectral overlap can also aid in prevention of pull-up peaks. Careful analysis of each loci should be performed to correctly identify pull-up peaks and the actual PCR product.

Furthermore, as patients requiring an HPCT present with a hematological malignancy, additional genetic alterations/abnormalities of the malignancy (termed loss of heterozygosity [LOH]) can disrupt the graft vs leukemia (GvL) response in haploidentical HPCT and cause relapse.[48–50] This circumstance is rather rare, but can comprise human leukocyte antigen (HLA) loss and instability at the STR loci (length variation or loss of locus), not only resulting in loss of heterozygous alleles required for GvL and subsequent relapse, but also potentially confounding HLA typing or chimerism analysis.[30,49] A recent survey of clinical practice included questions concerning this confounding phenomenon, and the response to these questions were under-answered and varied, likely indicating both the rarity of the event and unclear clinical guidelines about the management of such events.[18] LOH provides an infrequent situation in which relapse can be detected not only by reemergence of recipient peaks, but also might be evidenced by increasing donor chimer-

Downloaded from https://academic.oup.com/labmed/article/54/4/352/6827470 by guest on 24 February 2025

FIGURE 3. **Chimerism analysis when both the donor (D) and recipient (R) are heterozygous. A, Electropherograms of 2 examples in which the donor and recipient are heterozygous, the left in which no alleles are shared, and the right in which 1 allele is shared. The calculation for chimerism is shown below, with D1 the furthest left donor allele, D2 being the furthest right, R1 the furthest left recipient allele, and R2 the furthest right. B, An electropherogram in which chimerism cannot be calculated because, despite being heterozygous in the donor and recipient, they share the same alleles, rendering this locus noninformative. Note that it is not recommended to use this locus for chimerism analysis. pre-Tx, pretransplant; post-Tx, posttransplant.**

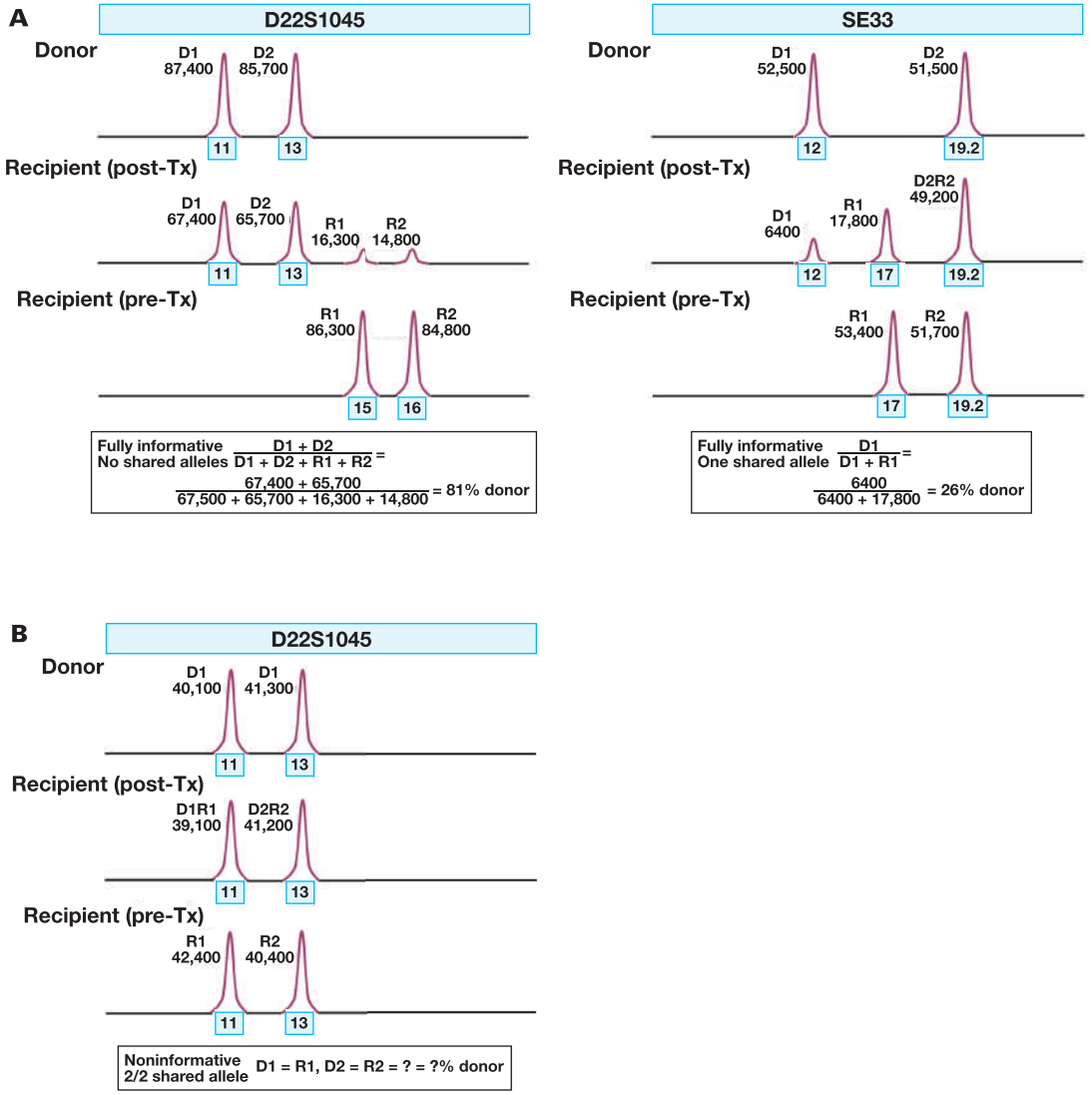

ism due to lack of the recipient allele being detected (because it was lost) despite maintaining a resurgence of recipient cells. In haploidentical settings, judicious care should be taken with patients with increasing chimerism, as there could be an underlying instable or lost STR that indicates relapse and is not truly identifying a chimeric status.

In a similar vein, chimerism analysis only determines percent DNA from recipient and donor and does not indicate whether recipient DNA is specifically derived from malignant cells. As such, the clinical significance of chimerism status indicating recurrence or relapse of disease remains debated, with the need for highly sensitive measurements of chimerism to indicate early detection and intervention.[51] In return for this ultra-high sensitivity, however, there is an enhanced likelihood for detection of contamination as false-positive (eg, skin, stroma from needle puncture[52,53]), lowering the precision of the assay and therefore resulting in a conundrum between sensitivity, precision, and the ability to detect minimal residual disease (MRD) early. Although chimerism analysis via STR can provide evidence for risk of relapse,[54] flow cytometry can specifically identify MRD via assessing aberrant cell populations, with appropriate sensitivity, and represents a better test utilization for relapse identification than chimerism assays.[55]

Often, so-called stutter peaks can occur in the amplification of STRs due to polymerase slippage on the repeat units, causing a repeat to be looped out and the PCR product to become shorter.[26] Stutter peaks exhibit low peak heights due to the infrequent nature of the slippage and are typically around 5% to 10% of the original peak height (**FIGURE 5B**). The STR loci that differ in the donor and recipient only by 1 repeat unit are not recommended for chimerism analysis because these stutter peaks could distort the percent donor chimerism.[40,42,56] If no other

Downloaded from https://academic.oup.com/labmed/article/54/4/352/6827470 by guest on 24 February 2025

FIGURE 4. Chimerism analysis when either or both the donor (D) and recipient (R) are homozygous. A, Electropherograms of 2 examples in which either the donor and recipient are homozygous, the left showing the donor homozygous and the subsequent calculation for chimerism, and the right showing the recipient homozygous and the inability to calculate chimerism. D1 is the furthest left donor allele, D2 the furthest right, R1 the furthest left recipient allele, and R2 the furthest right. Note that it is not recommended to use the SE33 locus for chimerism analysis. B, Electropherograms in which both the donor and recipient are homozygous, the right representing homozygosity at different alleles in the donor and recipient and the subsequent calculation for chimerism, and the left representing homozygosity for the same allele in the donor and recipient, rendering this locus noninformative. Note that it is not recommended to use the SE33 locus for chimerism analysis. pre-Tx, pretransplant, post-Tx, posttransplant.

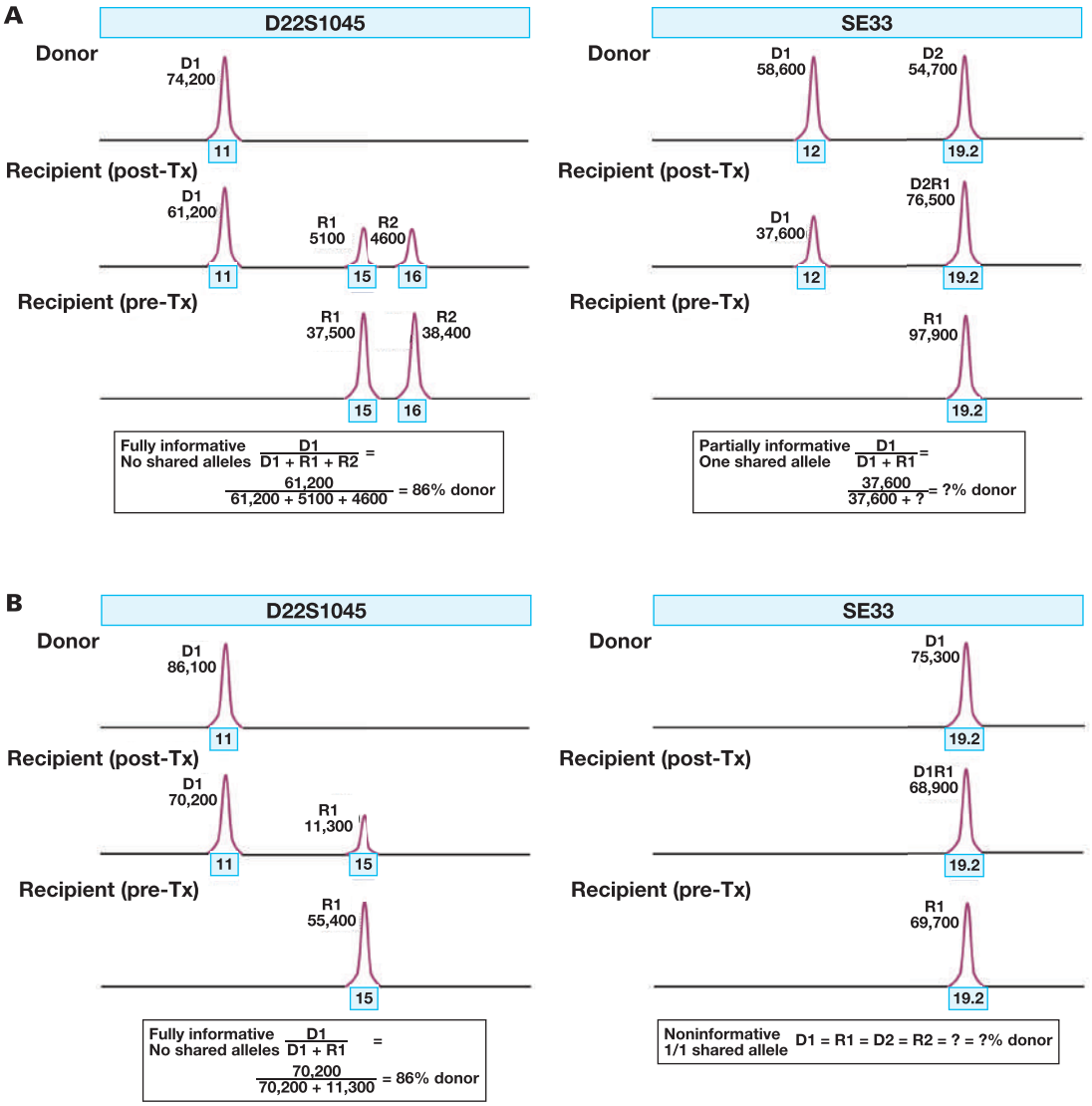

valid loci are available for chimerism analysis, a correction can be made in the chimerism analysis by accounting for the stutter height that is present in the pretransplant sample, which is then subtracted from the posttransplant sample. This assumes that the level of stutter pretransplant remains the same posttransplant.

Another phenomenon that can hinder accurate result interpretation is the occurrence of a 3' addition of adenosine at the end of the PCR-amplified products.[46,57,58] When this occurs, the PCR product appears as a double peak and can cause difficulty in interpretation (**FIGURE 5C**). These nontemplated additions arise due to the extendase activity of Taq polymerase and can occur differentially depending on the terminal amino acid.[58] Because different STR kits contain unique primers for each locus, it would stand to reason that each kit can vary in its capability to induce adenylated sequences. Early research indicated that the addition of a single terminal sequence to the primer more uniformly resulted in adenosine addition, whereas finding a sequence to prevent the addition of adenosine was more complex and usually primer specific.[58] These results indicated that it is potentially more useful to adenylate all products rather than trying to prevent the adenylation of some. Further, inclusion of a final extension step can promote adenylation across all products and is another method to prevent double peaks.[57] It is therefore prudent to identify whether this occurs in the commercial kits used by each laboratory, and if so, to either prevent the double peak occurrence by

Downloaded from https://academic.oup.com/labmed/article/54/4/352/6827470 by guest on 24 February 2025

FIGURE 5. Artifacts and rare findings in short tandem repeat analysis. A, A depiction of a pull up peak from Locus A appearing in Locus B. Two electropherograms (stacked on top of each other) from separate loci within an individual. Locus A shows 2 peaks at full-strength peak heights at its two allele sizes (10, 12). Locus B in another fluorescent channel shows a full-strength peak height at its allele size (18), but also shows 2 pull-up peaks as indicated by the weak smaller peaks in green, that appear as a 14 allele and 16 allele in Locus B but is a true 10 allele and 12 allele from Locus A that is pulling up in the bins of alleles 14 and 16 in Locus B. B, A depiction of a locus with stutter peak interference. Allele 17 should indicate percent recipient following transplantation, but because of stutter from allele 18 in the donor, the small peak posttransplant (post-Tx) could either be stutter from allele 18 or rebound of recipient cells. It is recommended that loci in which the stutter co-localizes with recipient and/or donor alleles not be used as informative. C, A locus in which a double-peak (nontemplated nucleotide addition) is shown in the recipient post-Tx at alleles 12 and 16. This example of a double peak would not interfere greatly with informativity. D, A locus in which the donor is tri-allelic, type 2, meaning the individual has 3 alleles at equal height. This tri-allelic locus would be excluded in chimerism calculation. pre-Tx, pretransplant.

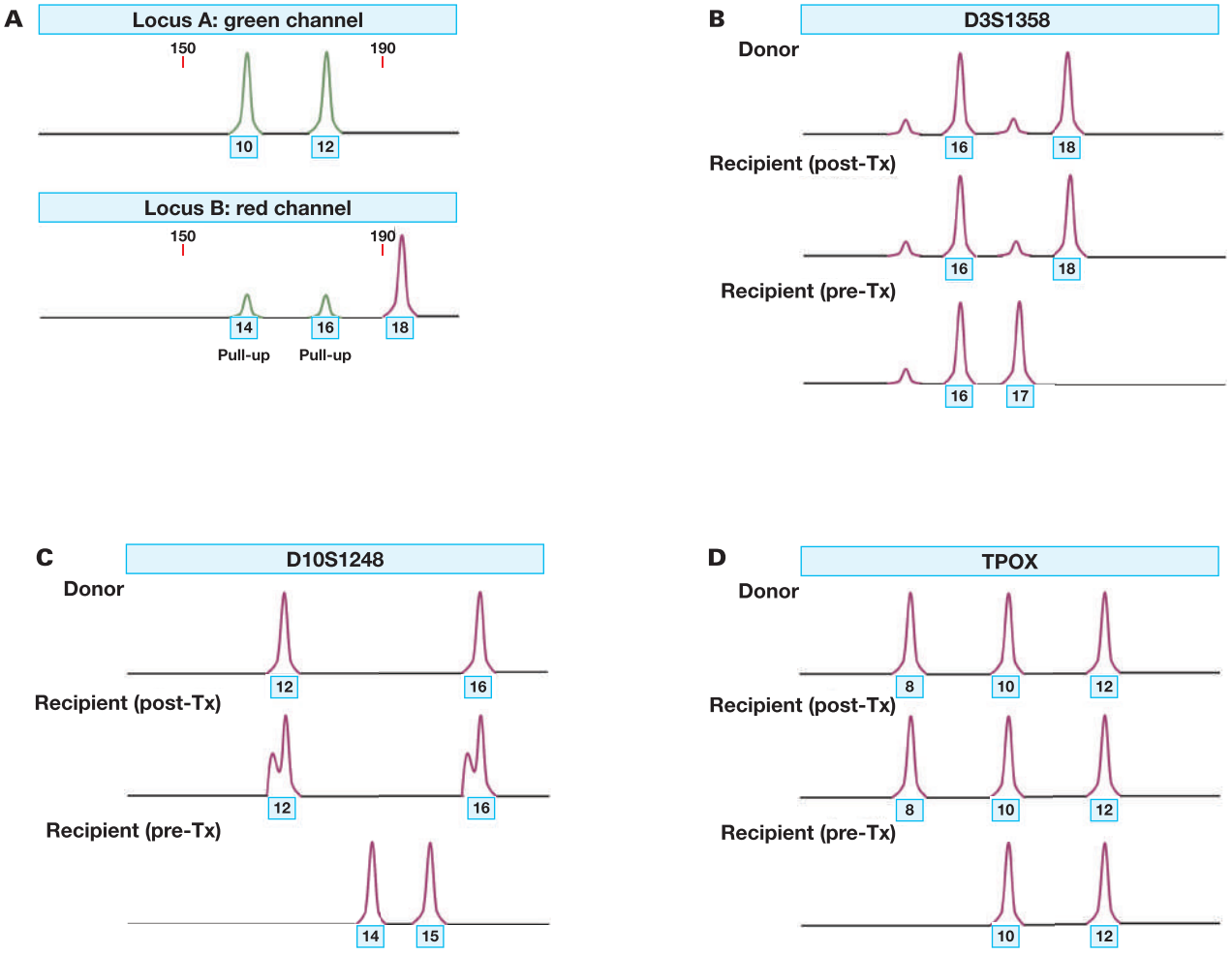

including a final extension step or excluding those loci from chimerism analysis.

In addition to double peaks, another phenomenon can occur in STR analysis in which a single locus has 3 alleles, called a tri-allelic pattern.[59] These patterns are mainly categorized into two types: type 1, in which the 3 alleles differ in allele height, and type 2, in which the 3 alleles have equal height (**FIGURE 5D**).[60] Type 1 alleles typically occur from a somatic recombination event of a heterozygous allele, resulting in 3 alleles but of unequal intensities, wherein the 2 alleles with a smaller peak value sum up to be the approximate height of the tallest peak.[61] Type 2 alleles typically arise from chromosomal duplication, triploidy, or other rearrangement events in the germline that result in 3 peaks of balanced height, representing the 3 alleles.[62,63] Identification of triallelic patterns is important to prevent the misinterpretation of the allele as chimeric. To rule out contamination and confirm the tri-allelic locus, ensure that it is present in more than 1 sample from the individual (ie, present in both CD3 and CD33 enriched populations or from separate samples). These loci can be used as informative if no peaks overlap between the donor and recipient, but if 3 other informative loci exist, use of those would be preferred.

STR Testing Utility

STR analysis can be used in chimerism analysis, relapse assessment, and GVHD monitoring in HPCT patients. Monitoring posttransplantation begins within months of transplant to inform engraftment status, with

Downloaded from https://academic.oup.com/labmed/article/54/4/352/6827470 by guest on 24 February 2025

the majority of laboratories beginning at 1 month posttransplant.[18] Continued monitoring assesses changes in chimerism status that can then be associated with rejection of the graft or disease relapse and the information can be used to inform treatment and other clinical decisions.[64–66] STR analysis can also be used in other clinical settings, such as transfusion-associated GVHD (TA-GVHD), solid organ transplant-associated GVHD, twin zygosity, parentage/kinship testing, and specimen identification.

TA-GVHD is a rare but 90% fatal condition following transfusion.[67] Because of the difficulty in diagnosis, most cases are diagnosed postmortem. TA-GVHD occurs when lymphocytes from the transfusion, instead of being eliminated by the host immune response, engraft and proliferate.[68] Risk factors include an immunocompromised recipient, shared HLA alleles between the donor and recipient, intrauterine and exchange transfusions, congenital immunodeficiency, stem cell transplantation, and lymphomas. To maintain vigilance in the detection and prevention of TA-GVHD, the National Healthcare Safety Network Biovigilance Component Hemovigilance Module Surveillance Protocol v2.6 of the Centers for Disease Control and Prevention was developed for centers that perform transfusions to judiciously monitor transfusion-associated adverse events. In this protocol, white blood cell STR analysis is used to define chimerism and diagnose TA-GVHD.

Solid organ transplant can also lead to the development of GVHD, particularly in lymphocyte-dense organs such as the small bowel[69] and liver[70] (although there have been reports of other organs inducing GVHD[71–74]), which can maintain reservoirs of lymphoid tissue. In these scenarios, lymphocytes from the graft infiltrate and engraft into the recipient and cause GVHD. Mortality is high—between 30% and 75%.[75] Detection of donor chimerism using STR analysis can aid in diagnosis of transplant-associated GVHD, as well as to monitor the efficacy of treatment regimens.[76]

Although all efforts are made to prevent mislabeling of specimens in the laboratory, it is not unusual to encounter an incorrectly labeled specimen, which can impact clinical care. In cases of suspected specimen mix-up, STR analysis can aid in the correct identification of the samples. In our laboratory, 2 colon biopsies came in from a single individual with 2 requisition forms. Later, it was determined that an individual with a specimen collected on the same day had yet to receive their results. It was hypothesized that 1 of the 2 colon biopsies and 1 of the accompanying requisition forms were incorrectly labeled and were from the individual with the missing sample. An STR analysis was performed on the biopsies and showed genetically distinct specimens. A third sample from the individual with the missing specimen was then used to confirm identity of the original "duplicate" sample. In this way, STR analysis can be used to deconvolute specimen mix-ups.

Outside clinical use, STR testing is heavily used in forensics for specimen identification.[77,78] The Combined DNA Index System is the database used by the Federal Bureau of Investigation to document and search DNA profiles collected from convicted offenders and arrestees, potential suspects, evidence from crime scenes, family members of missing persons, and unidentified specimens (www.fbi.gov). Twenty STR loci are used to create these profiles. Similar analyses are performed for forensic STR assessment as clinical STR assessment; however, the likelihood of partial or mixed profiles can be high due to DNA degradation in the forensic sample and/or contaminated samples.

Methods of the Future

New strategies for chimerism analysis, including qPCR and next-generation sequencing (NGS), are beginning to be implemented in some laboratories.[18] qPCR was first suggested as an alternative method to STR-PCR in the early 2000s as a faster and more sensitive method to detect the first sign of relapse or rejection.[44] The method detects single nucleotide polymorphisms and/or insertion and deletion (indel) polymorphisms within the genome. However, its use, although a log-fold increase in sensitivity, is not as accurate in detection of major markers due to variation in the quantification of PCR products in high concentration.[44] Because of this issue, qPCR is not routinely relied upon for chimeric analyses, and only a minority of laboratories in the CIBMTR (23%) report using it.[18]

NGS is rapidly gaining momentum as another avenue to assess chimerism due to its uptake in many immunogenetics laboratories for HLA typing of donors and recipients. Prior to its use for typing, the benefit of increased sensitivity of NGS (0.1%–1%)[79] compared to STR (0.4%–5%) for chimerism analysis was outweighed by the massive cost of its implementation. Now, as laboratories are implementing NGS to produce high-resolution donor and recipient HLA typing, ~7% of reporting laboratories are also using NGS for chimerism analysis.[18] Likely, as NGS for typing becomes the standard, more laboratories will use NGS for chimerism analysis to take advantage of the increased accuracy of the assay compared with STR. In a comparable manner to STR, cell subsets are isolated and DNA is extracted. Two PCR reactions are then used to amplify and barcode a set of indels from the genome prior to running sequencing on a NGS instrument.[79] The deep sequencing of NGS allows millions of fragments to be analyzed, contributing to its high sensitivity.[80] Typing of so many markers prevents the need for pretyping of the donor and recipient as the sophisticated bioinformatic platforms can readily distinguish 2 genomes.[81] This method can also be used to assess cell-free donor-derived DNA in solid organ transplants with high accuracy.[82,83] The NGS is not without its disadvantages, however, which mainly center on implementation and reagent cost, required bioinformatics expertise, and standardization.

Conclusions

STR analysis remains the gold standard of laboratories testing chimerism due to its high sensitivity and accuracy. Judicious care should be taken to interpret STR data and avoid making incorrect calculations of chimerism due to stutter peaks, pull-up peaks, double peaks, tri-allelic peaks, and malignant loss of alleles. Careful assessment of STR data ensures accurate percent chimerism calculations, thereby enabling accurate assessment of engraftment, rejection, and relapse in HPCT patients to guide clinical care. As NGS systems are incorporated into more laboratories for typing, it will likely become more commonly used in chimerism testing due its higher sensitivity. Transition to this technology will require standardization and bioinformatic expertise to correctly interpret data.

Acknowledgments

Figures were created with biorender.com.

Conflict of Interest Disclosure

The authors have nothing to disclose.

Downloaded from https://academic.oup.com/labmed/article/54/4/352/6827470 by guest on 24 February 2025

REFERENCES

1. Yunis EJ, Zuniga J, Romero V, Yunis EJ. Chimerism and tetragametic chimerism in humans: implications in autoimmunity, allorecognition and tolerance. *Immunol Res.* 2007;38:213–236. doi:10.1007/s12026-007-0013-3.
2. Sullivan HC, Fang DC & Zhang JQ. Bone marrow engraftment analysis. In: Ding Y, Zhang L, eds. *Practical Oncologic Molecular Pathology: Frequently Asked Questions*. Cham, Switzerland: Springer International Publishing; 2021:421–438.
3. Madan K. Natural human chimeras: a review. *Eur J Med Genet.* 2020;63:103971. doi:10.1016/j.ejmg.2020.103971.
4. Owen RD, Davis HP, Morgan RF. Quintuplet calves and erythrocyte mosaicism. *J Hered.* 1946;37:290–297.
5. Lo YM, Patel P, Sampietro M, Gillmer MD, Fleming KA, Wainscoat JS. Detection of single-copy fetal DNA sequence from maternal blood. *Lancet.* 1990;335:1463–1464. doi:10.1016/0140-6736(90)91491-r.
6. Billingham RE, Brent L, Medawar PB. Actively acquired tolerance of foreign cells. *Nature.* 1953;172:603–606. doi:10.1038/172603a0.
7. Lawler M, McCann SR, Conneally E, Humphries P. Chimaerism following allogeneic bone marrow transplantation: detection of residual host cells using the polymerase chain reaction. *Br J Haematol.* 1989;73:205–210. doi:10.1111/j.1365-2141.1989.tb00253.x.
8. Antin JH, Childs R, Filipovich AH, et al. Establishment of complete and mixed donor chimerism after allogeneic lymphohematopoietic transplantation: recommendations from a workshop at the 2001 tandem meetings of the International Bone Marrow Transplant Registry and the American Society of Blood and Marrow Transplantation. *Biol Blood Marrow Transplant.* 2001;7:473–485. doi:10.1053/bbmt.2001.v7.pm11669214.
9. Khan F, Agarwal A, Agrawal S. Significance of chimerism in hematopoietic stem cell transplantation: new variations on an old theme. *Bone Marrow Transplant.* 2004;34:1–12. doi:10.1038/sj.bmt.1704525.
10. Bar BM, Schattenberg A, Van Dijk BA, De Man AJ, Kunst VA, De Witte T. Host and donor erythrocyte repopulation patterns after allogeneic bone marrow transplantation analysed with antibody-coated fluorescent microspheres. *Br J Haematol.* 1989;72:239–245. doi:10.1111/j.1365-2141.1989.tb07689.x.
11. Schaap N, Schattenberg A, Bar B, et al. Red blood cell phenotyping is a sensitive technique for monitoring chronic myeloid leukaemia patients after T-cell-depleted bone marrow transplantation and after donor leucocyte infusion. *Br J Haematol.* 2000;108:116–125. doi:10.1046/j.1365-2141.2000.01803.x.
12. Vives J, Casademont-Roca A, Martorell L, Nogués N. Beyond chimerism analysis: methods for tracking a new generation of cell-based medicines. *Bone Marrow Transplant.* 2020;55:1229–1239. doi:10.1038/s41409-020-0822-8.
13. van Dijk BA, Drenthe-Schonk AM, Bloo A, Kunst VA, Janssen JT, de Witte TJ. Erythrocyte repopulation after allogeneic bone marrow transplantation: analysis using erythrocyte antigens. *Transplantation.* 1987;44:650–654. doi:10.1097/00007890-198711000-00011.
14. Roux E, Abdi K, Speiser D, et al. Characterization of mixed chimerism in patients with chronic myeloid leukemia transplanted with T-cell-depleted bone marrow: involvement of different hematologic lineages before and after relapse. *Blood.* 1993;81:243–248.
15. Schattenberg A, Bar B, Vet J, Van Dijk B, Smeets D, De Witte T. Comparison of chimerism of red cells with that of granulocytes, T-lymphocytes, and bone marrow cells in recipients of bone marrow grafts depleted of lymphocytes using counterflow centrifugation. *Leuk Lymphoma.* 1991;5:171–177. doi:10.3109/10428199109068122.
16. Schattenberg A, De Witte T, Salden M, et al. Mixed hematopoietic chimerism after allogeneic transplantation with lymphocyte-depleted bone marrow is not associated with a higher incidence of relapse. *Blood.* 1989;73:1367–1372.
17. Hibi S, Tsunamoto K, Todo S, et al. Chimerism analysis on mononuclear cells in the CSF after allogeneic bone marrow transplantation. *Bone Marrow Transplant.* 1997;20:503–506. doi:10.1038/sj.bmt.1700918.
18. Blouin AG, Askar M. Chimerism analysis for clinicians: a review of the literature and worldwide practices. *Bone Marrow Transplant.* 2022;57:347–359. doi:10.1038/s41409-022-01579-9.
19. Southern EM. Base sequence and evolution of guinea-pig alpha-satellite DNA. *Nature.* 1970;227:794–798. doi:10.1038/227794a0.
20. Satellite DNA sequence. *Nature.* 1970;227(5260):775. doi:10.1038/227775a0.
21. Fan H, Chu JY. A brief review of short tandem repeat mutation. *Genomics Proteomics Bioinform.* 2007;5:7–14. doi:10.1016/S1672-0229(07)60009-6.
22. Tang H, Kirkness EF, Lippert C, et al. Profiling of short-tandem-repeat disease alleles in 12,632 human whole genomes. *Am J Hum Genet.* 2017;101:700–715. doi:10.1016/j.ajhg.2017.09.013.
23. Lander ES, Linton LM, Birren B, et al. Initial sequencing and analysis of the human genome. *Nature*. 2001;409:860–921. doi:10.1038/35057062.
24. Hancock JM. The contribution of slippage-like processes to genome evolution. *J Mol Evol.* 1995;41:1038–1047. doi:10.1007/BF00173185.
25. Hancock JM. Simple sequences and the expanding genome. *Bioessays.* 1996;18:421–425. doi:10.1002/bies.950180512.
26. Kreyenberg H, Holle W, Mohrle S, Niethammer D, Bader P. Quantitative analysis of chimerism after allogeneic stem cell transplantation by PCR amplification of microsatellite markers and capillary electrophoresis with fluorescence detection: the Tuebingen experience. *Leukemia.* 2003;17:237–240. doi:10.1038/sj.leu.2402761.
27. Thiede C, Bornhauser M, Ehninger G. Strategies and clinical implications of chimerism diagnostics after allogeneic hematopoietic stem cell transplantation. *Acta Haematol.* 2004;112:16–23. doi:10.1159/000077555.
28. Ellegren H. Microsatellites: simple sequences with complex evolution. *Nat Rev Genet.* 2004;5:435–445. doi:10.1038/nrg1348.
29. Schichman SA, Suess P, Vertino AM, Gray PS. Comparison of short tandem repeat and variable number tandem repeat genetic markers for quantitative determination of allogeneic bone marrow transplant engraftment. *Bone Marrow Transplant.* 2002;29:243–248. doi:10.1038/sj.bmt.1703360.
30. Blouin AG, Ye F, Williams J, Askar M. A practical guide to chimerism analysis: review of the literature and testing practices worldwide. *Hum Immunol.* 2021;82:838–849. doi:10.1016/j.humimm.2021.07.013.
31. Tilanus MG. Short tandem repeat markers in diagnostics: what's in a repeat? *Leukemia.* 2006;20:1353–1355. doi:10.1038/sj.leu.2404273.
32. Urquhart A, Kimpton CP, Downes TJ, Gill P. Variation in short tandem repeat sequences—a survey of twelve microsatellite loci for use as forensic identification markers. *Int J Legal Med.* 1994;107:13–20. doi:10.1007/BF01247268.
33. Bar W, Brinkmann B, Budowle B, et al. DNA recommendations. Further report of the DNA Commission of the ISFH regarding the use of short tandem repeat systems. International Society for Forensic Haemogenetics. *Int J Legal Med.* 1997;110:175–176. doi:10.1007/s004140050061.
34. Weir BS. The rarity of DNA profiles. *Ann Appl Stat*. 2007;1:358–370. doi:10.1214/07-AOAS128.
35. Reilly P. Legal and public policy issues in DNA forensics. *Nat Rev Genet.* 2001;2:313–317. doi:10.1038/35066091.
36. Ogonek J, Kralj Juric M, Ghimire S, et al. Immune reconstitution after allogeneic hematopoietic stem cell transplantation. *Front Immunol.* 2016;7:507. doi:10.3389/fimmu.2016.00507.
37. Butler JM. *Advanced topics in forensic DNA typing: interpretation*. Oxford, UK: Academic Press; 2015.
38. Han E, Kim M, Kim Y, et al. Practical informativeness of short tandem repeat loci for chimerism analysis in hematopoietic stem cell transplantation. *Clin Chim Acta.* 2017;468:51–59. doi:10.1016/j.cca.2017.02.004.

Downloaded from https://academic.oup.com/labmed/article/54/4/352/6827470 by guest on 24 February 2025

39. Fernandez-Aviles F, Urbano-Ispizua A, Aymerich M, et al. Serial quantification of lymphoid and myeloid mixed chimerism using multiplex PCR amplification of short tandem repeat-markers predicts graft rejection and relapse, respectively, after allogeneic transplantation of CD34+ selected cells from peripheral blood. *Leukemia.* 2003;17:613–620. doi:10.1038/sj.leu.2402854.
40. Hancock JP, Goulden NJ, Oakhill A, Steward CG. Quantitative analysis of chimerism after allogeneic bone marrow transplantation using immunomagnetic selection and fluorescent microsatellite PCR. *Leukemia.* 2003;17:247–251. doi:10.1038/sj.leu.2402759.
41. Kristt D, Israeli M, Narinski R, et al. Hematopoietic chimerism monitoring based on STRs: quantitative platform performance on sequential samples. *J Biomol Tech.* 2005;16:380–391.
42. Murphy KM. Chimerism analysis following hematopoietic stem cell transplantation. *Methods Mol Biol.* 2013;999:137–149. doi:10.1007/978-1-62703-357-2_9.
43. Clark JR, Scott SD, Jack AL, et al. Monitoring of chimerism following allogeneic haematopoietic stem cell transplantation (HSCT): technical recommendations for the use of short tandem repeat (STR) based techniques, on behalf of the United Kingdom National External Quality Assessment Service for Leucocyte Immunophenotyping Chimerism Working Group. *Br J Haematol.* 2015;168:26–37. doi:10.1111/bjh.13073.
44. Alizadeh M, Bernard M, Danic B, et al. Quantitative assessment of hematopoietic chimerism after bone marrow transplantation by real-time quantitative polymerase chain reaction. *Blood.* 2002;99:4618–4625. doi:10.1182/blood.v99.12.4618.
45. Volgin L, Taylor D, Bright JA, Lin M-H. Validation of a neural network approach for STR typing to replace human reading. *Forensic Sci Int Genet.* 2021;55:102591. doi:10.1016/j.fsigen.2021.102591.
46. Moretti TR, Baumstark AL, Defenbaugh DA, Keys KM, Brown AL, Budowle B. Validation of STR typing by capillary electrophoresis. *J Forensic Sci.* 2001;46:661–676.
47. Schraml E, Lion T. Interference of dye-associated fluorescence signals with quantitative analysis of chimerism by capillary electrophoresis. *Leukemia.* 2003;17:221–223. doi:10.1038/sj.leu.2402755.
48. Vago L, Perna SK, Zanussi M, et al. Loss of mismatched HLA in leukemia after stem-cell transplantation. *N Engl J Med.* 2009;361:478–488. doi:10.1056/NEJMoa0811036.
49. Pereira S, Vayntrub T, Hiraki DD, et al. Short tandem repeat and human leukocyte antigen mutations or losses confound engraftment and typing analysis in hematopoietic stem cell transplants. *Hum Immunol.* 2011;72:503–509. doi:10.1016/j.humimm.2011.03.003.
50. Thiede C, Bornhauser M, Oelschlagel U, et al. Sequential monitoring of chimerism and detection of minimal residual disease after allogeneic blood stem cell transplantation (BSCT) using multiplex PCR amplification of short tandem repeat-markers. *Leukemia.* 2001;15:293–302. doi:10.1038/sj.leu.2401953.
51. Tozzo P, Delicati A, Zambello R, et al. Chimerism monitoring techniques after hematopoietic stem cell transplantation: an overview of the last 15 years of innovations. *Diagnostics (Basel).* 2021;11(4):621. doi: 10.3390/diagnostics11040621.
52. Willasch AM, Kreyenberg H, Shayegi N, et al. Monitoring of hematopoietic chimerism after transplantation for pediatric myelodysplastic syndrome: real-time or conventional short tandem repeat PCR in peripheral blood or bone marrow? *Biol Blood Marrow Transplant.* 2014;20:1918–1925. doi:10.1016/j.bbmt.2014.07.030.
53. Stahl T, Rothe C, Bohme MU, et al. Digital PCR panel for sensitive hematopoietic chimerism quantification after allogeneic stem cell transplantation. *Int J Mol Sci* . 2016;17(9):1515. doi: 10.3390/ijms17091515.
54. Lindahl H, Vonlanthen S, Valentini D, et al. Lineage-specific early complete donor chimerism and risk of relapse after allogeneic hematopoietic stem cell transplantation for acute myeloid leukemia. *Bone Marrow Transplant.* 2022;57(5):753–759. doi: 10.1038/s41409-022-01615-8.
55. Mo XD, Lv M, Huang XJ. Preventing relapse after haematopoietic stem cell transplantation for acute leukaemia: the role of post-transplantation minimal residual disease (MRD) monitoring and MRD-directed intervention. *Br J Haematol.* 2017;179:184–197. doi:10.1111/bjh.14778.
56. Lion T. Summary: reports on quantitative analysis of chimerism after allogeneic stem cell transplantation by PCR amplification of microsatellite markers and capillary electrophoresis with fluorescence detection. *Leukemia* 2003;17:252–254. doi:10.1038/sj.leu.2402753.
57. Moretti TR, Baumstark AL, Defenbaugh DA, Keys KM, Smerick JB, Budowle B. Validation of short tandem repeats (STRs) for forensic usage: performance testing of fluorescent multiplex STR systems and analysis of authentic and simulated forensic samples. *J Forensic Sci.* 2001;46:647–660.
58. Brownstein MJ, Carpten JD, Smith JR. Modulation of non-templated nucleotide addition by Taq DNA polymerase: primer modifications that facilitate genotyping. *Biotechniques.* 1996;20:1004–1006, 1008. doi:10.2144/96206st01.
59. Crouse CA, Rogers S, Amiott E, Gibson S, Masibay A. Analysis and interpretation of short tandem repeat microvariants and three-banded allele patterns using multiple allele detection systems. *J Forensic Sci.* 1999;44:87–94.
60. Clayton TM, Guest JL, Urquhart AJ, Gill PD. A genetic basis for anomalous band patterns encountered during DNA STR profiling. *J Forensic Sci.* 2004;49:1207–1214.
61. Yang Q, Shen Y, Shao C, et al. Genetic analysis of tri-allelic patterns at the CODIS STR loci. *Mol Genet Genomics.* 2020;295:1263–1268. doi:10.1007/s00438-020-01701-w.
62. Findlay I, Toth T, Matthews P, Marton T, Quirke P, Papp Z. Rapid trisomy diagnosis (21, 18, and 13) using fluorescent PCR and short tandem repeats: applications for prenatal diagnosis and preimplantation genetic diagnosis. *J Assist Reprod Genet.* 1998;15:266–275. doi: 10.1023/a:1022536309381.
63. Gu W, Zhang F, Lupski JR. Mechanisms for human genomic rearrangements. *Pathogenetics.* 2008;1:4. doi:10.1186/1755-8417-1-4.
64. Bader P, Beck J, Frey A, et al. Serial and quantitative analysis of mixed hematopoietic chimerism by PCR in patients with acute leukemias allows the prediction of relapse after allogeneic BMT. *Bone Marrow Transplant.* 1998;21:487–495. doi:10.1038/sj.bmt.1701119.
65. Horn B, Soni S, Khan S, et al. Feasibility study of preemptive withdrawal of immunosuppression based on chimerism testing in children undergoing myeloablative allogeneic transplantation for hematologic malignancies. *Bone Marrow Transplant.* 2009;43:469–476. doi:10.1038/bmt.2008.339.
66. Barrios M, Jimenez-Velasco A, Roman-Gomez J, et al. Chimerism status is a useful predictor of relapse after allogeneic stem cell transplantation for acute leukemia. *Haematologica.* 2003;88:801–810.
67. Raina A, Chaudhary G, Dogra TD, et al. Benefit of STR-based chimerism analysis to identify TA-GVHD as a cause of death: utility of various biological specimens. *Med Sci Law.* 2016;56:142–146. doi:10.1177/0025802415577457.
68. Ruhl H, Bein G, Sachs UJ. Transfusion-associated graft-versus-host disease. *Transfus Med Rev.* 2009;23:62–71. doi:10.1016/j.tmrv.2008.09.006.
69. Mazariegos GV, Abu-Elmagd K, Jaffe R, et al. Graft versus host disease in intestinal transplantation. *Am J Transplant.* 2004;4:1459–1465. doi:10.1111/j.1600-6143.2004.00524.x.
70. Taylor AL, Gibbs P, Bradley JA. Acute graft versus host disease following liver transplantation: the enemy within. *Am J Transplant.* 2004;4:466–474. doi:10.1111/j.1600-6143.2004.00406.x.
71. Luckraz H, Zagolin M, McNeil K, Wallwork J. Graft-versus-host disease in lung transplantation: 4 case reports and literature review. *J Heart Lung Transplant.* 2003;22:691–697. doi:10.1016/s1053-2498(02)00811-2.
72. Weinstein A, Dexter D, KuKuruga DL, Philosophe B, Hess J, Klassen D. Acute graft-versus-host disease in pancreas

Downloaded from https://academic.oup.com/labmed/article/54/4/352/6827470 by guest on 24 February 2025

transplantation: a comparison of two case presentations and a review of the literature. *Transplantation.* 2006;82:127–131. doi:10.1097/01.tp.0000225832.47130.10.

73. Worel N, Bojic A, Binder M, et al. Catastrophic graft-versus-host disease after lung transplantation proven by PCR-based chimerism analysis. *Transpl Int.* 2008;21:1098–1101. doi:10.1111/j.1432-2277.2008.00754.x.
74. Assi MA, Pulido JS, Peters SG, McCannel CA, Razonable RR. Graft-vs.-host disease in lung and other solid organ transplant recipients. *Clin Transplant.* 2007;21:1–6. doi:10.1111/j.1399-0012.2006.00573.x.
75. Zhang Y, Ruiz P. Solid organ transplant-associated acute graft-versus-host disease. *Arch Pathol Lab Med.* 2010;134:1220–1224. doi:10.5858/2008-0679-RS.1.
76. Rai V, Dietz NE, Agrawal DK. Immunological basis for treatment of graft versus host disease after liver transplant. *Expert Rev Clin Immunol.* 2016;12:583–593. doi:10.1586/1744666X.2016.1145056.
77. Butler JM, Hill CR. Biology and genetics of new autosomal STR loci useful for forensic DNA analysis. *Forensic Sci Rev.* 2012;24:15–26.
78. Butler JM. Genetics and genomics of core short tandem repeat loci used in human identity testing. *J Forensic Sci.* 2006;51:253–265. doi:10.1111/j.1556-4029.2006.00046.x.
79. Pettersson L, Vezzi F, Vonlanthen S, Alwegren K, Hedrum A, Hauzenberger D. Development and performance of a next generation sequencing (NGS) assay for monitoring of mixed chimerism. *Clin Chim Acta.* 2021;512:40–48. doi:10.1016/j.cca.2020.10.034.
80. Andrikovics H, Orfi Z, Meggyesi N, et al. Current trends in applications of circulatory microchimerism detection in transplantation. *Int J Mol Sci .* 2019;20(18);4450. doi: 10.3390/ijms20184450.
81. Sharon E, Shi H, Kharbanda S, et al. Quantification of transplant-derived circulating cell-free DNA in absence of a donor genotype. *PLoS Comput Biol.* 2017;13:e1005629. doi:10.1371/journal.pcbi.1005629.
82. Gordon PM, Khan A, Sajid U, et al. An algorithm measuring donor cell-free DNA in plasma of cellular and solid organ transplant recipients that does not require donor or recipient genotyping. *Front Cardiovasc Med.* 2016;3:33. doi:10.3389/fcvm.2016.00033.
83. Grskovic M, Hiller DJ, Eubank LA, et al. Validation of a clinical-grade assay to measure donor-derived cell-free DNA in solid organ transplant recipients. *J Mol Diagn.* 2016;18:890–902. doi:10.1016/j.jmoldx.2016.07.003.

Downloaded from https://academic.oup.com/labmed/article/54/4/352/6827470 by guest on 24 February 2025

Review of the Clinical Presentation, Pathology, Diagnosis, and Treatment of Leishmaniasis

Blaine A. Mathison, BS, M(ASCP),[1,] and Benjamin T. Bradley, MD, PhD[1,2]*

[1]Insitute for Clinical and Experimental Pathology, ARUP Laboratories, Salt Lake City, UT, USA, [2]Department of Pathology, University of Utah, Salt Lake City, UT, USA. *To whom correspondence should be addressed: blaine.mathison@aruplab.com.

Keywords: *Leishmania*, *Endotrypanum*, leishmaniasis, diagnostics, molecular testing, parasitology, pathology, treatment

Abbreviations: VL, visceral leishmaniasis**;** CL, cutaneous leishmaniasis; ML, mucocutaneous leishmaniasis; Th1, T helper type 1; IL, interleukin; LRV1, *Leishmania* RNA virus-1; FDA, Food and Drug Administration; WHO, World Health Organization; SbV, pentavalent antimony; CDC, Centers for Disease Control and Prevention; IFA, immunofluorescent assay; EIA, enzyme immunoassay; DAT, direct agglutination test; ICT, immunochromatographic strip test; hsp, heat shock protein; kDNA, kinetoplast DNA; qPCR, quantitative polymerase chain reaction; MLEE, multilocus enzyme electrophoresis; kb, kilobase

Laboratory Medicine 2023;54:363-371; https://doi.org/10.1093/labmed/lmac134

ABSTRACT

Leishmaniasis is a vector-borne infection caused by kinetoplastid protozoans in the genera *Leishmania* and *Endotrypanum*. The disease occurs worldwide in the tropics and subtropics and can be particularly burdensome in resource-limited settings. Diseases caused by leishmaniasis range in severity from mild cutaneous lesions to life-threatening visceral and disfiguring mucocutaneous illnesses. Rapid and accurate diagnosis is needed to ensure proper clinical management of patients afflicted with this disease. Complicating matters of diagnosis and treatment are the diversity of species within these 2 genera and the variable specificity of diagnostic assays. This mini-review provides laboratory professionals with an overview of *Leishmania* epidemiology, biology, pathogenesis, clinical presentations, and treatments with additional emphasis placed on the nuances involved in diagnosis.

Leishmaniasis is a parasitic infection caused by kinetoplastid protozoans in the genera *Leishmania* and *Endotrypanum*. The parasites are transmitted through the bite of sand flies (Diptera: Psychodidae). Leishmaniasis is a severe and, in cases of visceral leishmaniasis, potentially fatal disease that affects more than 12 million people globally with an annual case fatality rate of 20,000 to 40,000.[1] The disease is often linked to poverty, immunosuppression, malnutrition, poor housing, and a lack of adequate medical resources, with about 350 million people at risk for infection.[1]

There are 3 main clinical presentations of leishmaniasis: visceral leishmaniasis (VL), cutaneous leishmaniasis (CL), and mucocutaneous leishmaniasis (ML). Most cases of VL occur in rural and suburban areas of low socioeconomic status in Bangladesh, Ethiopia, Brazil, India, Sudan, and South Sudan.[2] Cutaneous leishmaniasis is more widespread, with nearly 75% of the cases occurring in Afghanistan, Algeria, Brazil, Ethiopia, Iran, Peru, Sudan, Costa Rica, Colombia, and Syria.[2] Mucocutaneous leishmaniasis is most commonly seen in Bolivia, Brazil, Peru, and Ethiopia, as well as Thailand.[3]

Successful patient management is linked to the ability to provide a rapid and accurate diagnosis. It is crucial to perform species-level identification on isolates from patients infected in areas with cocirculating *Leishmania* species or when the epidemiological investigation is unable to isolate the infectious event to a single region. Historically, identification of *Leishmania* species was a laborious task, ultimately achieved by isoenzyme analysis following weeks of culture. Immunologic methods and molecular tools, the latter of which are still not commonplace in many clinical laboratories, are allowing for more rapid identification, which in turn can provide for proper chemotherapy earlier in the course of infection.

The topics presented in this mini-review are targeted towards providing clinical and diagnostic context to medical laboratory and allied health professionals whose responsibilities may include appropriate stewardship of diagnostic methods.

Causal Agents

Leishmania are kinetoplastid protozoans related to the trypanosomes. Depending on taxonomic and nomenclatural systems applied, there are at least 20 species of *Leishmania* implicated in human disease divided among 4 subgenera: *Leishmania*, *Mundinia*, *Sauroleishmania*, and *Viannia*, with the most common and clinically important species belonging to the subgenera *Leishmania* and *Viannia*.[4] In 2018, *Leishmania colombiensis* and *L equatoriensis* were transferred to the genus *Endotrypanum*[5]; they are included herein because they clinically present as CL. For a complete list of species, their geographic distribution, natural hosts, and clinical presentation, please refer to **TABLE 1**.

© The Author(s) 2022. Published by Oxford University Press on behalf of American Society for Clinical Pathology. All rights reserved. For permissions, please e-mail: journals.permissions@oup.com

Downloaded from https://academic.oup.com/labmed/article/54/4/363/6873137 by guest on 24 February 2025

TABLE 1. Species of *Leishmania* and *Endotrypanum* Implicated in Human Disease[a]

Species	Geographic Distribution	Natural Host(s); Vector(s)	Clinical Presentation
Genus: *Endotrypanum*			
Endotrypanum colombiensis	Colombia	Sloths; *Lutzomyia* spp	CL
Endotrypanum equatoriensis	Colombia, Ecuador	Sloths, squirrels; *Lutzomyia* spp	CL
Genus: *Leishmania*			
Subgenus: *Leishmania*			
Leishmania (*L*) *aethiopica*	Africa (Ethiopia, Kenya, Uganda), Yemen	Mammals, including humans and rock hyraxes; *Phlebotomus* spp	CL
Leishmania (*L*) *amazonensis* (syn *L garnhami*)	Amazonian South America	Several mammals and birds, including humans; *Lutzomyia* spp	CL, ML
Leishmania (*L*) *donovani* (syn *L archibaldi*)	Indian subcontinent, China, Central Africa	Several mammals, including humans; *Phlebotomus* spp	CL, VL
Leishmania (*L*) *infantum* (syn *L chagasi*)	Mediterranean Europe and Africa, SE Europe, Central Asia, Central and South America	Many mammals, including humans; *Phlebotomus* spp (Old World), *Lutzomyia* spp (New World)	CL, VL
Leishmania (*L*) *major*	Northern and Central Africa, Middle East, India, China	Humans, gerbils, birds; *Phlebotomus* spp	CL
Leishmania (*L*) *mexicana* (syn *L pifanoi*)	Southern United States (Texas) to South America	Mammals, including humans and dogs; *Lutzomyia* spp	CL
Leishmania (*L*) *tropica*	North and Central Africa, Middle East, Central Asia, India	Mammals, including humans; *Phlebotomus* spp	CL
Leishmania (*L*) *venezuelensis*	Northern South America	Humans, cats; *Lutzomyia* spp	CL
Leishmania (*L*) *waltoni*	Dominican Republic	Mammals, possibly rats; *Lutzomyia* spp	CL
Subgenus: *Mundinia*			
Leishmania (*M*) *martiniquensis*	Martinique, Thailand	Mammals, including humans and possibly rats; vectors unknown, possibly *Sergentomyia* spp (Old World), *Lutzomyia* (New World), or *Culicoides* (Old World)	CL, ML
Leishmania (*M*) *orientalis* (syn *L siamensis*)	Thailand	Humans; vectors unknown	CL
Subgenus: *Sauroleishmania*			
Leishmania (*S*) *tarentolae*	North Africa, southern Europe, Middle East	Lizards; *Sergentomyia* spp	Unknown[b]
Subgenus: *Viannia*			
Leishmania (*V*) *braziliensis*	Amazonian South America	Dogs, rodents, marsupials, humans; *Lutzomyia* spp	CL, ML
Leishmania (*V*) *guyanensis*	Northern South America	Sloths, anteaters, rodents, marsupials, humans; *Lutzomyia* spp	CL, ML
Leishmania (*V*) *lainsoni*	South America	Lowland paca; *Lutzomyia* spp	CL
Leishmania (*V*) *lindbergi*	Brazil	Unknown, presumed zoonotic in humans; *Lutzomyia* spp	CL
Leishmania (*V*) *naiffi*	Brazil, Bolivia, Peru	Armadillos; *Lutzomyia* spp	CL
Leishmania (*V*) *panamensis*	Central and South America	Mammals, including humans; *Lutzomyia* spp	CL, ML
Leishmania (*V*) *peruvinana*	Peru, Bolivia	Humans, rodents, marsupials, dogs; *Lutzomyia* spp	CL, ML
Leishmania (*V*) *shawi*	Brazil	Nonhuman primates, sloths, coati; *Lutzomyia* spp	CL

CL, cutaneous leishmaniasis; ML, mucocutaneous leishmaniasis; VL, visceral leishmaniasis.
[a]*Adapted from Mathison and Sapp.*[4]
[b]*Cases of human infection with* L larentolae *were diagnosed by molecular testing of blood specimens.*

Biology and Life Cycle

Infection of the vertebrate host is initiated when a female phlebotomine sand fly injects the metacyclic promastigote stage of *Leishmania* while taking a blood meal. The most common vectors of agents of human leishmaniasis are members of the genus *Phlebotomus* in the Old World and *Lutzomyia* in the New World. Promastigotes are phagocytized by mononuclear lymphocytes, such as macrophages, where they mature to amastigotes within the phagosome and replicate by binary fission. Phagocytized amastigotes then travel via the blood and lymphatics, which may result in visceral or mucosal disease, depending on the species. A sand fly becomes infected after ingesting amastigotes in macrophages while taking a blood meal. Amastigotes are liberated in the gut of the fly and transform into procyclic promastigotes. The procyclic promastigotes transform into nectomonad trypomastigotes and then leptomonad promastigotes. Leptomonads migrate to the proboscis and become infectious metacyclic trypomastigotes, completing the cycle[6] (**FIGURE 1**).

Downloaded from https://academic.oup.com/labmed/article/54/4/363/6873137 by guest on 24 February 2025

FIGURE 1. Life cycle of *Leishmania* species. *Leishmania* is transmitted by the bite of infected female phlebotomine sand flies. The sand flies release the infective stage (i) (metacyclic promastigotes) during blood meals (1). Promastigotes that reach the puncture wound are phagocytized by macrophages (2) and other types of mononuclear phagocytic cells. Promastigotes transform into amastigotes, the tissue stage of the parasite (3), which multiply by binary division and proceed to infect other mononuclear phagocytic cells (4). The parasites are carried to other body sites in the infected monocytes. Sand flies become infected by ingesting infected cells during blood meals (5, 6). In the gut of the sand flies, amastigotes transform into procyclic promastigotes. The procyclic promastigotes transform into nectomonad trypomastigotes and then leptomonad promastigotes (7). The leptomonad promastigotes replicate by binary fission in the gut of the fly (8). Leptomonad promastigotes migrate to the proboscis of the fly and transform into infective metacyclic promastigotes. The cycle continues when the fly takes a blood meal. d, diagnostic stage. Image courtesy of the Centers for Disease Control and Prevention.

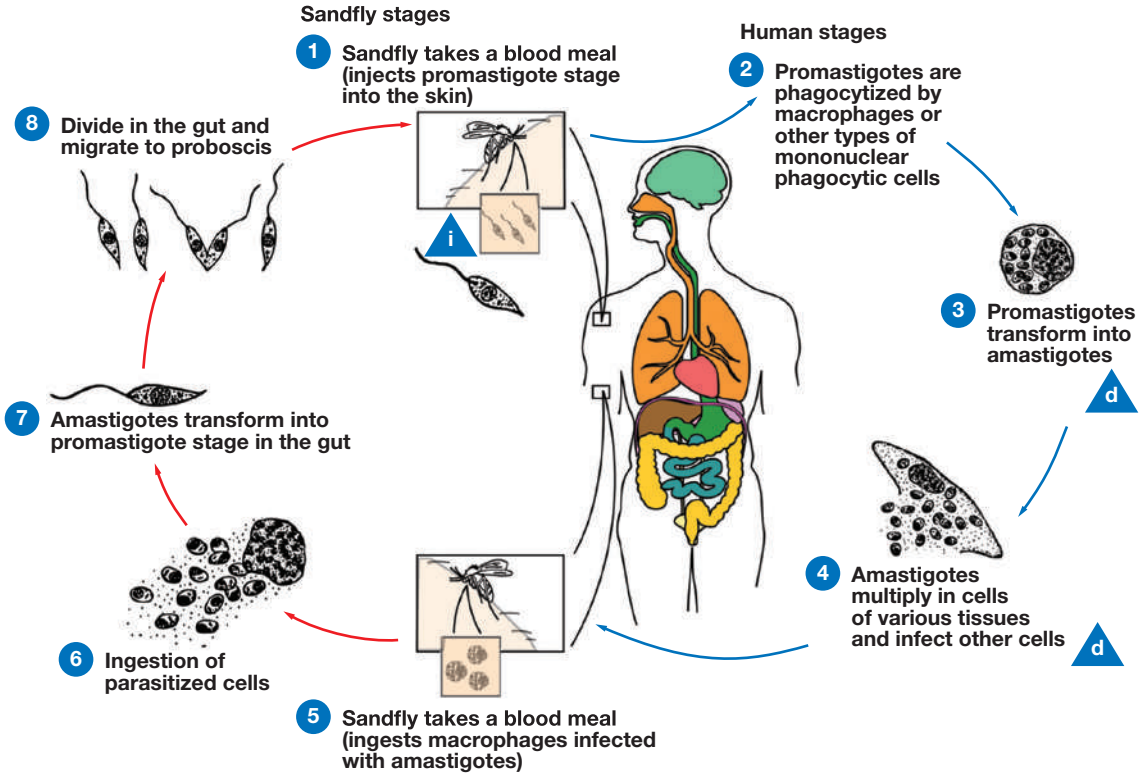

Other less common routes of *Leishmania* infection have been documented, including congenital transmission from mother to fetus and via solid organ transplant.[7]

Pathogenesis

Leishmania infections may take on several different clinical presentations even within the same species. The host immune response, specifically type 1 (Th1) and type 2 (Th2) helper T cells have been identified as critical mediators affecting disease progression. In cases of visceral *Leishmania* infections, the host immune response is skewed towards an anti-inflammatory Th2 phenotype with reduced production of interferon γ and increased interleukin (IL)4 and IL10. Conversely in individuals with cutaneous leishmaniasis, the proinflammatory Th1 response predominates systemically whereas the Th2 response remains localized to the lesion.[8] Recent data have helped expand the classic Th1/Th2 paradigm in *Leishmania* pathogenesis to include responses mediated by Th17 cells and the inflammasome.[9] The humoral immune response plays a less significant role in control of *Leishmania*. Individuals with visceral disease may have detectable antibodies to *Leishmania*; however, these are insufficient to clear the infection.[10]

Clinical Presentation

Visceral Leishmaniasis

Visceral leishmaniasis, known as kala-azar in some regions, is the most lethal manifestation of *Leishmania* disease. It is most often associated with *L donovani* (East Africa, India) and *L infantum* (Mediterranean, Middle East, and the Americas), although other species more prone to cutaneous disease have caused VL in immunosuppressed individuals.[11,12] The typical pentad of VL findings include prolonged fever, weight loss, pancytopenia, hypergammaglobulinemia, and hepatosplenomegaly.[13] In the approximately 5% of infected individuals who develop clinical disease, symptom onset is insidious, often occurring months to years following infection. If left untreated, VL may progress to bone marrow failure, cachexia, and hemorrhage.[14] Individuals with immunocompromise (eg, HIV or therapy-related immunosuppression) may be at higher risk for mortality from VL.[15] Given the low prevalence in the United States, current Infectious Diseases Society of America guidelines do not recommend universal screening.[16] Depending on the region, patients who experience VL are also at risk for the development of post-kala-azar dermal leishmaniasis. The risk is highest in areas of Africa and lower in India and the Americas.[17,18]

Downloaded from https://academic.oup.com/labmed/article/54/4/363/6873137 by guest on 24 February 2025

Clinically, these individuals present with multiple small papules with pigmentation changes distributed over much of their body.

Cutaneous Leishmaniasis

Cutaneous leishmaniasis occurs globally in regions where leishmaniasis is endemic and is divided into Old World and New World disease. Old World cutaneous leishmaniasis is most commonly associated with *L major*, *L tropica*, and *L aethiopica*; however, *L donovani* and *L infantum*, although more frequently associated with VL, can also result in solitary cutaneous lesions.[19] In the Americas, New World cutaneous leishmaniasis is caused by *Leishmania* species of the subgenera *Vianna* (most frequently *L braziliensis*) and *Leishmania* (including *L mexicana*)[20] as well as members of the genus *Endotrypanum*.[5] Following a phlebotomine sand fly blood meal, a painless papule or dermal nodule will develop 2 weeks to several months following the initial bite.[21] In its most common form, the nodule slowly expands in a concentric fashion leaving a central, ulcerated crater. Although visually striking, the ulcer is often painless. A variety of colloquial terms have been used to describe the lesions of CL, including "pizza-like" referring to the raised outer rim of epithelium and the central ulcerated area containing granulation tissue and fibrin (**FIGURE 2A**). Individuals who recover from CL are frequently left with a characteristic scar demonstrating pigment changes and a recessed central area relative to the surrounding tissue.[21] Recovery is associated with a reduced likelihood of reinfection by the same *Leishmania* species, but individuals remain at risk of relapse or reinfection. Among 3 cohorts of patients followed in Brazil, Colombia, and Peru, the rate of recurrence was 2.7% of 369 cases, 2.0 per 100 person-years, and 2.9 per 100 person-years, respectively.[22–24] Variation in cutaneous manifestations are affected in part by the infecting species. In a study of New World cutaneous leishmaniasis, *L braziliensis* demonstrated a larger lesion size, more incomplete reepithelization, and prolonged time to recovery than *L mexicana*.[25]

Mucocutaneous Leishmaniasis

Mucocutaneous manifestation of *Leishmania* are classically seen in association with the New World *Vianna* subgenus (*L braziliensis, L panamensis*, and *L guyanensis*), and less frequently observed with Old World species (*L tropica*, *L major*, and *L donovani*).[26–28] Several case reports have documented Old World MLs to be less severe than New World MLs. Specifically, Old World MLs may have a lower rate of nasal cavity involvement compared to New World MLs (15% and 90%, respectively) and better treatment prognosis (82%). The prototypical lesions of ML develop in 1% to 5% of infected individuals in regions endemic for the *Vianna* subgenus and follow resolution of the cutaneous lesions. In a minority of cases (10%–20%) mucosal lesions develop without prior or concurrent skin lesions.[26,29] Mucosal lesions most often present as destructive ulceration or inflammatory hypertrophy of the nasal cavity. At its most severe, ML may result in permanent disfigurement or airway obstruction via pharyngeal involvement.[30] Because mucosal lesions can occur months to years following treatment and resolution of cutaneous disease, close clinical follow-up is warranted in patients with confirmed or epidemiologically suspect *Vianna* subgenus infections.[16] There is emerging evidence of the potential role *Leishmania* RNA virus-1 (LRV1) plays in mediating severity of mucocutaneous disease. Initially documented in *L guyanensis*, LRV1 demonstrated increased toll-like receptor 3 (TRL3)-mediated cytokine production and elevated parasitemia in an animal model.[31] Subsequently, this virus has been detected in other *Leishmania* species, although the clinical significance of LRV1 detection remains to be determined.[32]

Treatment

Currently, the United States Food and Drug Administration (FDA) has approved 2 anti-leishmanial therapies, miltefosine (Impavido) and Amphotericin B (Fungizone; Mysteclin-F; AmBisome). Other treatment options include pentavalent antimony, paromomycin, azole compounds, and pentamidine. These treatments have demonstrated variable levels of clinical success depending on the site of infection, *Leishmania* species, and timeframe used to monitor for relapse. When evaluating treatment response, it is important to note that even if there is evidence of clinical cure (eg, wound healing, improving blood counts, or resolution of splenomegaly) this does not guarantee parasitological cure. Scar tissue from cutaneous lesions and lymph nodes have demonstrated viable organisms when cultured following clinical remission.[33,34]

Originally designed as an antineoplastic drug, miltefosine received FDA approval for the treatment of VL caused by *L donovani* and CLs or MLs caused by *L braziliensis*, *L guyanensis*, and *L panamensis* in 2014. The use of miltefosine for the treatment of VLs initially demonstrated high clinical cure rates in India; however, subsequent trials within this region and in other countries have found a cure rate closer to 75% at 6 to 12 months posttreatment. Miltefosine demonstrates a similar degree of variability in the treatment of New World CL, with studies in Colombia demonstrating a >90% cure rate but only 53% in Guatemala.[35] The variation in clinical efficacy is suspected to be due in part to species and strain variation between these regions. Among anti-leishmanial drugs documented in the World Health Organization (WHO) List of Essential Medicines, miltefosine is the only oral treatment.

Liposomal amphotericin B, a polyene antibiotic that disrupts the parasite cell membrane through inhibition of ergosterol synthesis, is FDA-approved for treatment of visceral leishmaniasis in the United States. In studies submitted to the FDA, liposomal amphotericin B demonstrated a 100% cure rate in 2 European clinical trials when using regimens with a total dose >21 mg/kg.[36,37] Additional studies in Brazil, Kenya, and India demonstrated similar levels of clinical effectiveness (83%–100%) at various dosages (6–20 mg/kg).[38,39] Although not approved for the treatment of nonvisceral disease, liposomal amphotericin B has also demonstrated clinical effectiveness in both cutaneous and mucocutaneous disease.[40–42]

Dating back to World War II, pentavalent antimony (SbV) has been used for treatment of VL, ML, and CL. The SbV may be administered as a series of intralesional injections, intramuscular injections, or diluted in saline and administered intravenously. Although the exact mechanism of action remains poorly understood, inhibition of parasitic trypanothione reductase by trivalent antimony (ie, the reduced form of SbV), direct inhibition of glycolysis, and activation of the host immune response have been investigated as potential mechanisms.[43] The SbV treatment may be considered for first-line treatment of VLs, excluding some regions in India, where resistance rates >40% have been identified.[44] A formulation of SbV, sodium stibogluconate, was previously available in the United States via an Investigational New Drug protocol from the Centers for Disease Control and Prevention (CDC) Drug Services; however, the manufacturer ceased production of this drug in 2020.[45]

Diagnosis and Identification

Quick and accurate diagnosis of leishmaniasis is important to prevent severe illness and identify those at risk for visceral and mucocutaneous disease. Diagnostic algorithms will vary based on clinical presentation and epidemiological information (**TABLE 2**). Diagnosis of VL is

Downloaded from https://academic.oup.com/labmed/article/54/4/363/6873137 by guest on 24 February 2025

FIGURE 2. A, Typical "pizza lesion" on the skin of a patient presenting with cutaneous leishmaniasis. B, Impression smear of a skin biopsy specimen stained with Giemsa, showing many liberated amastigotes. Note the presence of a large oval nucleus and a small rod-shaped kinetoplast in most of the amastigotes. C, Spleen biopsy of a patient presenting with kala-azar, stained with H&E, showing many amastigotes; the nucleus and kinetoplast are not visible in all of the amastigotes but enough to make a reliable diagnosis. FIGURE 2A courtesy of the Public Health Image Library (Centers for Disease Control and Prevention); FIGURE 2C courtesy of Dr Sarah Sapp (Centers for Disease Control and Prevention).

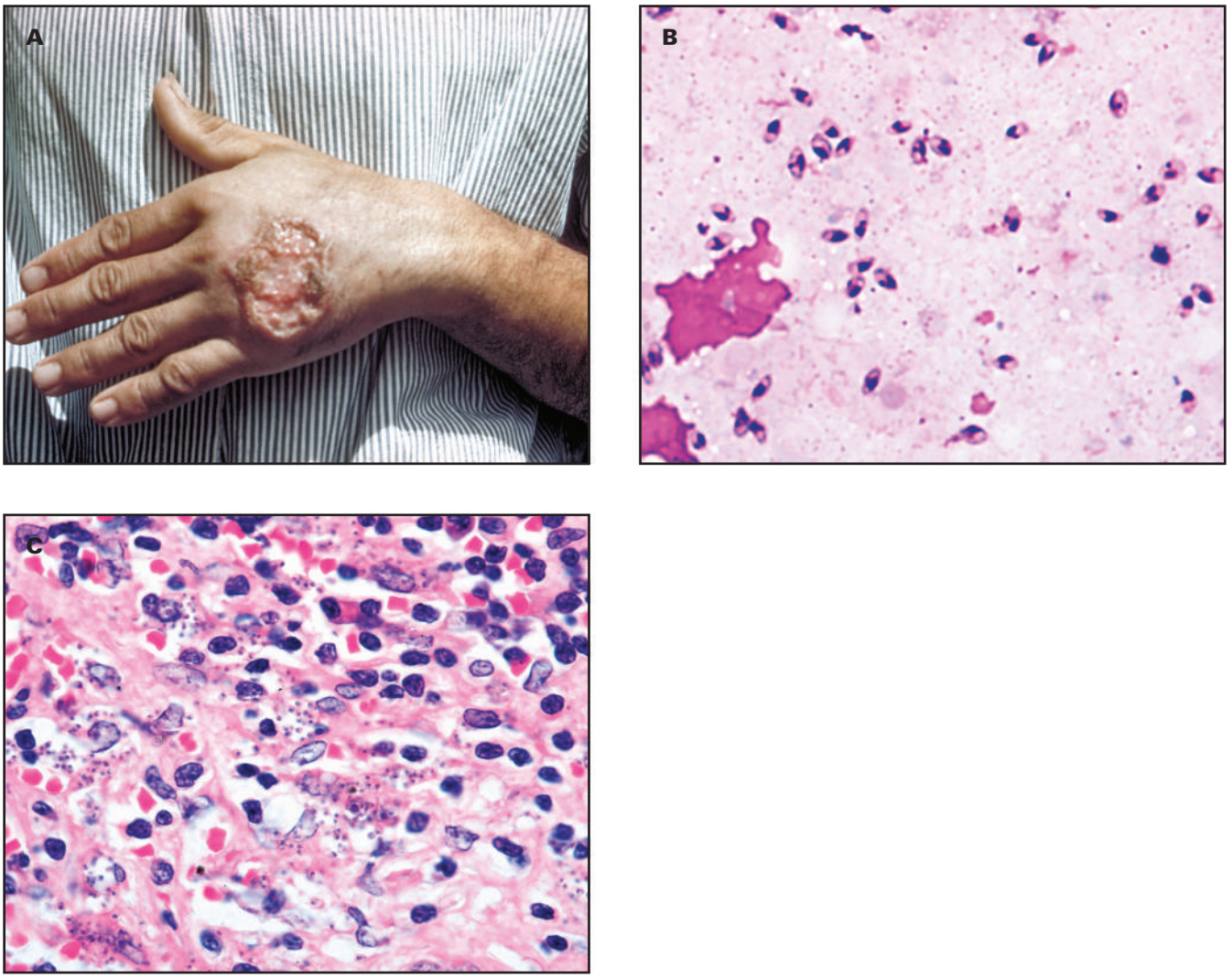

typically by antibody detection. Diagnosis of CL is usually achieved by microscopy. Further typing or species-level identification by isoenzyme analysis or molecular methods is necessary in cases of CL where species that cause ML cocirculate, as it could affect the clinical management of the patient.

Microscopy

Microscopy allows for rapid detection of *Leishmania* amastigotes, but it does not allow for species-level identification. Amastigotes can be detected in a variety of clinical specimens, including skin, bone marrow, spleen, liver, lymph nodes, and buffy coat of peripheral blood.[46]

In cases of CL, detection of amastigotes is usually achieved in impression smears of skin biopsies and scrapings stained with Giemsa (**FIGURE 2B**). Punch biopsy specimens should be collected under sterile conditions on skin precleaned with 70% ethanol. The biopsies should be collected at the raised border of the lesion where amastigotes are actively dividing and not in the center of the lesion.[47] Amastigotes are round to ovoid and measure 1 to 5 μm long. They possess a large round nucleus and a small rod-shaped kinetoplast.[48] Under normal conditions, promastigotes are not visible in clinical specimens. However, if there is a delay in processing and the specimen is allowed to sit at room temperature, amastigotes may begin transforming into promastigotes. Promastigotes are larger, measuring 10 to 12 μm long, are ovoid to spindle-shaped, and possess a large central nucleus, a small anterior kinetoplast, and a single anterior flagellum.[48] Amastigotes are more challenging to detect in specimens processed for histopathology, as the plane of sectioning can affect the detection of the nucleus and kinetoplast. Both structures should be visualized before rendering a definitive diagnosis (**FIGURE 2C**).[48]

Downloaded from https://academic.oup.com/labmed/article/54/4/363/6873137 by guest on 24 February 2025

TABLE 2. Comparison of Diagnostic Methods of Leishmaniasis, Their Clinical Utility, Advantages, and Disadvantages

Diagnostic Method	Clinical Utility	Advantages	Disadvantages
Serology	Visceral[a]	Rapid; low cost; ease of use	Variable sensitivity based on antigen and local epidemiology; few FDA-cleared assays in US
Smear (touch prep)	Cutaneous,[a] mucocutaneous,[a] visceral	Rapid; low cost; minimal equipment needs	Does not allow identification to species level; requires fresh tissue; visceral specimens difficult to obtain; requires maintaining competency on parasite microscopy
Histopathology	Cutaneous, mucocutaneous, visceral	Can be performed on fixed specimens; useful when leishmaniasis was not included in the original diagnosis	Does not allow for identification to species level; requires specialized training in histopathology; morphologic features of amastigotes may overlap with other organisms
Culture	Visceral, cutaneous, mucocutaneous	Allows for isolation of organisms; can be used for further testing (molecular, isoenzyme analysis)	Insensitive; time-consuming; labor-intensive; limited availability; requires fresh tissue
Isoenzyme analysis	Visceral, cutaneous, mucocutaneous	Allows for species-level identification; historically used method of *Leishmania typing*	Time-consuming; often requires isolates from culture; limited availability; multiple classification methods
Molecular testing	Visceral, cutaneous, mucocutaneous	Rapid; allows for species-level ID; can be performed on fresh specimens and FFPE blocks	Expensive; limited availability; variable sensitivity based on target; requires specialized training; may be difficult to maintain proficiency

[a]*Primary method for diagnosis.*

Microscopy is typically not performed for the diagnosis of VLs, although amastigotes may be seen in biopsies and impression smears of bone marrow, liver, spleen, and lymph nodes. Direct examination of spleen specimens has the highest sensitivity, followed by bone marrow, lymph nodes, and then liver. However, due to the risk of postprocedure hemorrhage, bone marrow biopsy is generally preferred over splenic biopsy. Direct examination of buffy coat of peripheral blood appears to be the least sensitive specimen, but all specimens can achieve nearly 100% sensitivity when cultures are prepared.[46]

Regardless of the specimen type, it is not possible to identify *Leishmania* to the species level based on morphology of the amastigotes. Additionally, amastigotes of *Leishmania* are morphologically indistinguishable from those of *Trypanosoma cruzi*; however, epidemiologic information and clinical presentation are usually sufficient to distinguish between these two organisms. Amastigotes of *Leishmania* need to be differentiated from other small intracellular pathogens, including *Histoplasma capsulatum* and microsporidia. Yeast cells of *H capsulatum* typically demonstrate a surrounding "halo" that does not take up Giemsa stain and lacks the characteristic nucleus and kinetoplast of a *Leishmania* amastigote. Grocott's methenamine silver stain can be helpful for separating the 2, as yeast cells of *H capsulatum* are Grocott's methenamine silver-positive, whereas amastigotes of *Leishmania* are not.[48] Spores of microsporidia are often vacuolated, lack a visible nucleus and kinetoplast, and will often stain with an apical dot using periodic acid-Schiff stain, which amastigotes of *Leishmania* will not.[48]

Serologic Diagnosis

Antibody detection is the primary method for the diagnosis of VL, but it has little to no value for cutaneous disease. Conventional methods for antibody detection include gel diffusion, complement fixation test, indirect hemagglutination assays, immunofluorescent assays (IFAs), enzyme immunoassay (EIA), and countercurrent immunoelectrophoresis.[49]

The IFA is not commonly used, and the technology required (a microscope with fluorescent capabilities) makes its application prohibitive in field settings.[50] Although IFA has a relatively high specificity (79%–100%), it has relatively low sensitivity (11%–82%).[51]

The EIAs demonstrate good sensitivity, but specificity varies based on the antigen used. Assays developed using crude soluble antigen have a sensitivity of 80% to 100% but there a risk of cross-reactivity with *Trypanosoma* spp, *Mycobacterium tuberculosis*, and *Toxoplasma gondii*.[49] The use of recombinant K39 antigen, a glycoprotein derived from the highly conservative kinesin region of *L infantum* (as *L chagasi*) found on amastigote and promastigote stages, shows a sensitivity of 100% and specificity of 96%.[49,50] This EIA also shows promising clinical use and prognosis in patients with HIV.[50] Studies evaluating a rK28 antigen EIA for Mediterranean VL patients demonstrated comparable sensitivity and specificity to the rK39 antigen.[51]

Direct agglutination tests (DATs) show varying sensitivity of 91% to 100% and specificity of 72% to 100%.[49] A DAT can be performed on plasma, serum, and urine.[51] Unfortunately, routine testing by DAT has several challenges, including the fragility of an aqueous antigen, batch-to-batch variation of antigen, antigen cost, long incubation time, relative complexity of the assay, and limited production facilities of antigen production.[49,50]

An immunochromatographic strip test (ICT) using the rK39 antigen is available for diagnosing VL. Initial clinical evaluation of this assay shows a sensitivity of 100% and specificity of 98%.[49,50] The assay produces a result in about 15 minutes and is shown to be a reliable indicator of VL.[50] A multicenter study including countries in Africa and the Indian subcontinent found consistent results between geographic areas, with a sensitivity of 98.4% to 100% and specificity of 81.2% to 96.4%. The Kalazar Detect Rapid Test (InBios International), which uses the rK39 antigen, is FDA-cleared for use in the United States and Conformité Européenne marked for use in the European Union. A study in the United States comparing the InBios assay with the IFA developed by the CDC showed agreement, sensitivity, and specificity of 98%, 90%, and 100% respectively.[52] There is a potential for increased sensitivity and specificity of the ICT assay using different antigens. For example, ICT assays using the rK28 antigen showed improved sensitivities in Sudan (95.9%) and Bangladesh (98.1%) in diagnosing VL.

Molecular Diagnosis

Many targets capable of detecting *Leishmania* have been described along with methods to resolve an isolate to the subgenus, complex, or species level. Molecular targets include the ribosomal sequences (*18S rRNA*

Downloaded from https://academic.oup.com/labmed/article/54/4/363/6873137 by guest on 24 February 2025

gene, ITS1 loci, ITS2 loci), heat shock protein (hsp)70, and kinetoplast DNA (kDNA). The *18S rRNA* gene is a well-recognized target for identification of bacterial and fungal species via sequencing.[53,54] In *Leishmania*, the 18S region is limited to discrimination of *Leishmania* species from other kinetoplastids, whereas the ITS1/2 regions offer higher resolution and the ability to provide species level identification in some situations.[55,56] Despite the ITS2 region showing excellent ability to separate *Leishmania* species, it may suffer from poorer sensitivity in comparison to different targets or quantitative polymerase chain reaction (qPCR) methods.[57] The *hsp70* gene is another target demonstrating excellent resolution in separating *Leishmania* species complexes.[56] A recent study examined *hsp70* sequencing for a set of 135 clinical isolates for which multilocus enzyme electrophoresis (MLEE) or orthogonal genetic identification was performed. A total of 130 were grouped with the correct species, 3 were grouped with the incorrect species but correct species complex, and 3 isolates did not group with a species.[58] The *hsp70* locus also contains potentially prognostic information on treatment response. Researchers have identified *hsp70* variants associated with resistance to antimony and miltefosine.[59,60] Finally, kDNA is another target under investigation. The kDNA genome consists of thousands of copies of ~1 kilobase (kb) circular DNA (termed "minicircles") and dozens of copies of ~30 kb circular DNA (termed "maxicircles"). For species determination using kDNA, the cytochrome *b* gene has been investigated, but demonstrated poor separation between *L donovani/L infantum* and *L braziliensis/L peruviana* species.[61] Advantages of kDNA include an extremely high copy-number-to-parasite ratio, thus providing a sensitive detection method in the setting of low parasite burden. Unfortunately, this increased sensitivity may be limited by the prevalence of sequence heterogeneity among minicircles.[62] In addition to pathogen detection and species identification, molecular testing for *Leishmania* may also be useful for evaluating response to treatment and relapse risk.[63]

The quality of the sample provided for molecular analysis should be considered when assessing test performance. In the case of VL, splenic aspirates have demonstrated the highest sensitivity (93%–99%), with bone marrow aspirates and peripheral blood demonstrating lower sensitivity (53% to 86% and 53% to 65%, respectively).[64] However, splenic aspirate is a highly invasive procedure often requiring imaging guidance and a risk of postprocedural hemorrhage. Due to these risks, bone marrow aspirate is the most often recommended site for diagnostic biopsies of VL.[65] For cutaneous disease, molecular testing improves on the sensitivity of histopathologic examination.[66] Currently there are no commercially available FDA-approved molecular detection kits for *Leishmania*, although testing may be available through the CDC and reference laboratories. Several companies have manufactured primer and probe kits for use in qPCR, however, these assays require laboratory validation prior to clinical use.

Isoenzyme Analysis and Molecular Typing Systems

Isoenzyme analysis or MLEE is the WHO gold standard for identification of *Leishmania* species; however, this assay is only offered at a limited number of public health and reference laboratories.[65] One of the primary limitations of MLEE is that it requires a cultured isolate of *Leishmania* parasites. An MLEE cannot be performed directly from clinical specimens, and culture yield from biopsy-proven CL ranges from 90% to 50%, depending on species.[67] Various classification systems for MLEE results have been developed, with the Montpellier system (MON) developed in France being the most widely applied. This system analyzes 15 enzyme loci to assign a "zymodeme" to individual isolates.[68] Despite being a labor-intensive process, the longevity of this assay means it has accumulated the greatest amount of data for typing of *Leishmania* species and may outperform molecular assays for strain typing.[69]

Conclusion

Leishmaniasis is a serious and potentially life-threatening disease caused by protozoan parasites of the genera *Leishmania* and *Endotrypanum*. Naturally endemic to tropical and subtropical parts of the world, global travel has made leishmaniasis a worldwide medical and public health burden. There are 3 main clinical presentations of the disease: cutaneous, mucocutaneous, and visceral. Rapid diagnosis and species-level identification is crucial for successful management and prevention of morbidity. Serologic methods such as rapid antigen tests allow for noninvasive diagnosis of VL and initiation of therapy. Despite advances in molecular detection, diagnosis of CL still requires careful microscopic examination and integration of epidemiologic and clinical data. In situations of cutaneous disease, exclusion of species associated with ML is important to guide therapy and clinical follow-up. Historically, species-level identification has been performed by isoenzyme analysis, a time-consuming method relying on culturing the *Leishmania* parasite. Today, molecular methods are shortening the time to result by testing directly from clinical samples and using targets with increased diagnostic specificity.

Acknowledgments

The authors thank Dr Marcos de Almeida (Centers for Disease Control and Prevention, Atlanta, GA, USA) for reviewing the manuscript prior to submission. Dr Sarah Sapp (Centers for Disease Control and Prevention, Atlanta, GA, USA) provided **FIGURE 2C**.

Conflict of Interest Disclosure

The authors have nothing to disclose.

REFERENCES

1. Okwor I, Uzonna J. Social and economic burden of human leishmaniasis. *Am J Trop Med.* 2016;94(3):489–493. doi:10.4269/ajtmh.15-0408.
2. Alvar J, Vélez ID, Bern C, Herrero M, et al. Leishmaniasis worldwide and global estimates of its incidence. *PLoS One.* 2012;7(5):e35671. doi:10.1371/journal.pone.0035671.
3. Liautaud B, Vignier N, Miossec C, et al. First case of visceral leishmaniasis caused by *Leishmania martiniquensis*. *Am J Trop Med.* 2015;92(2):317–319. doi:10.4269/ajtmh.14-0205.
4. Mathison BA, Sapp SGH. An annotated checklist of the eukaryotic parasites of humans, exclusive of fungi and algae. *Zookeys.* 2021;1069:1–313.
5. Espinosa OA, Serrano MG, Camargo EP, Teixeira MMG, Shaw JJ. An appraisal of the taxonomy and nomenclature of trypanosomatids presently classified as *Leishmania* and *Endotrypanum*. *Parasitology.* 2018;145(4):430–442. doi:10.1017/S0031182016002092.
6. Mann S, Frasca K, Scherrer S, et al. A review of leishmaniasis: current knowledge and future directions. *Curr Trop Med Rep.* 2021;8(2):121–132. doi:10.1007/s40475-021-00232-7.
7. Antinori S, Cascio A, Parravicini C, et al. Leishmaniasis among organ transplant recipients. *Lancet Infect Dis.* 2008;8(3):191–199.
8. Bennett, JE, Dolin R, Blaser MJ. *Mandell, Douglas, and Bennett's Infectious Disease Essentials*. 9th ed. Philadelphia, PA: Elsevier; 2020:4176.

Downloaded from https://academic.oup.com/labmed/article/54/4/363/6873137 by guest on 24 February 2025

9. Tian X, Wei F, Wang L, et al. Herceptin enhances the antitumor effect of natural killer cells on breast cancer cells expressing human epidermal growth factor receptor-2. *Frontiers in Immunology.* 2017;8:1426. doi:10.3389/fimmu.2017.01426.
10. Galvao-Castro B, Sá Ferreira JA, Marzochi KF, Marzochi MC, Coutinho SG, Lambert PH. Polyclonal B cell activation, circulating immune complexes and autoimmunity in human American visceral leishmaniasis. *Clin Exp Immunol.* 1984;56(1):58–66.
11. van Griensven J, Diro E. Visceral leishmaniasis. *Infect Dis Clin North Am.* 2012;26(2):309–322. doi:10.1016/j.idc.2012.03.005.
12. Alvar J, Aparicio P, Aseffa A, et al. The relationship between leishmaniasis and AIDS: the second 10 years. *Clin Microbiol Rev.* 2008;21(2):334–359, table of contents. doi:10.1128/CMR.00061-07.
13. Badaro R, Jones TC, Lorenco R, et al. A prospective study of visceral leishmaniasis in an endemic area of Brazil. *J Infect Dis.* 1986;154(4):639–649. doi:10.1093/infdis/154.4.639.
14. Pearson RD, Cox G, Jeronimo SM, et al. Visceral leishmaniasis: a model for infectioninduced cachexia. *Am J Trop Med Hyg.* 1992;47(1 Pt 2):8–15.
15. Lyons S, Veeken H, Long J. Visceral leishmaniasis and HIV in Tigray, Ethiopia. *Trop Med Int Health.* 2003;8(8):733–739.
16. Aronson N, Herwaldt BL, Libman M, et al. Diagnosis and treatment of leishmaniasis: clinical practice guidelines by the Infectious Diseases Society of America (IDSA) and the American Society of Tropical Medicine and Hygiene (ASTMH). *Clin Infect Dis.* 2016;63(12):e202–e264. doi:10.1093/cid/ciw670.
17. Rahman KM, Islam, S, Rahman MW, et al. Increasing incidence of post-kala-azar dermal leishmaniasis in a population-based study in Bangladesh. *Clin Infect. Dis.* 2010;50(1):73–76.
18. Zijlstra EE, Khalil EAG, Kager PA, El-Hassan AM. Post-kala-azar dermal leishmaniasis in the Sudan: clinical presentation and differential diagnosis. *Brit J Dermatol*. 2000;143(1):136–143. doi:10.1046/j.1365-2133.2000.03603.x.
19. Siriwardana HV, Noyes HA, Beeching NJ, Chance ML, Karunaweera ND, Bates PA. *Leishmania donovani* and cutaneous leishmaniasis, Sri Lanka. *Emerg Infect Dis.* 2007;13(3):476–478. doi:10.3201/eid1303.060242.
20. Burza S, Croft SL, Boelaert M. Leishmaniasis. *Lancet.* 2018;392(10151):951–970. doi:10.1016/S0140-6736(18)31204-2.
21. Weigle K, Saravia NG. Natural history, clinical evolution, and the host-parasite interaction in New World cutaneous leishmaniasis. *Clin Exp.* 1996;14(5):433–450.
22. Davies CR, Llanos-Cuentas EA, Pyke SD, Dye C. Cutaneous leishmaniasis in the Peruvian Andes: an epidemiological study of infection and immunity. *Epidemiol Infect.* 1995;114(2):297–318. doi:10.1017/s0950268800057964.
23. Jones TC, Johnson WD, Barretto AC, et al. Epidemiology of American cutaneous leishmaniasis due to *Leishmania braziliensis*. *J Infect Dis.* 1987;156(1):73–83. doi:10.1093/infdis/156.1.73.
24. Weigle KA, Santrich C, Martinez F, Valderrama L, Saravia NG. Epidemiology of cutaneous leishmaniasis in Colombia: a longitudinal study of the natural history, prevalence, and incidence of infection and clinical manifestations. *J Infect Dis.* 1993;168(3):699–708. doi:10.1093/infdis/168.3.699.
25. Herwaldt BL, Arana BA, Navin TR. The natural history of cutaneous leishmaniasis in Guatemala. *J Infect Dis.* 1992;165(3):518–527. doi:10.1093/infdis/165.3.518.
26. Cincura C, de Lima CMF, Machado PRL, et al. Mucosal leishmaniasis: a retrospective study of 327 cases from an endemic area of *Leishmania (Viannia) braziliensis. Am J Trop Med Hyg.* 2017;97(3):761–766.
27. Mahdi M, Elamin E, Melville S, et al. Sudanese mucosal leishmaniasis: isolation of a parasite within the *Leishmania donovani* complex that differs genotypically from *L. donovani* causing classical visceral leishmaniasis. *Infect Genet Evol.* 2005;5(1):29–33. doi:10.1016/j.meegid.2004.05.008.
28. Shirian S, Oryan A, Hatam GR, Daneshbod Y. Three *Leishmania*/L. species—*L. infantum, L. major, L. tropica*—as causative agents of mucosal leishmaniasis in Iran. *Pathog Glob Health.* 2013;107(5):267–272. doi:10.1179/2047773213Y.0000000098.
29. Osorio LE, Castillo CM, Ochoa MT. Mucosal leishmaniasis due to *Leishmania (Viannia) panamensis* in Colombia: clinical characteristics. *Am J Trop Med Hyg.* 1998;59(1):49–52.
30. Silva L, Damrose E, Fernandes AM. Laryngeal leishmaniasis, a rare manifestation of an emerging disease. *Euro Ann Otorhinolaryngol Head Neck Dis.* 2017;134(3):211–212. doi:10.1016/j.anorl.2015.11.013.
31. Ives A, Ronet C, Prevel F, et al. *Leishmania* RNA virus controls the severity of mucocutaneous leishmaniasis. *Science.* 2011;331(6018):775–778. doi:10.1126/science.1199326.
32. Valencia BM, Lau R, Kariyawasam R, et al. *Leishmania* RNA virus-1 is similarly detected among metastatic and non-metastatic phenotypes in a prospective cohort of American Tegumentary Leishmaniasis. *PLoS Negl Trop Dis*. 2022;16(1):e0010162. doi:10.1371/journal.pntd.0010162.
33. Dereure J, Thanh HD, Lavabre-Bertrand T, et al. Visceral leishmaniasis: persistence of parasites in lymph nodes after clinical cure. *J Infect.* 2003;47(1):77–81. doi:10.1016/s0163-4453(03)00002-1.
34. Mendonca MG, de Brito MEF, Rodriques EHG, et al. Persistence of *Leishmania* parasites in scars after clinical cure of American cutaneous leishmaniasis: is there a sterile cure? *J Infect Dis.* 2004;189(6):1018–1023.
35. Soto J, Toledo J, Gutierrez P, et al. Treatment of American cutaneous leishmaniasis with miltefosine, an oral agent. *Clin Infect Dis.* 2001;33(7):e57E57–e61. doi:10.1086/322689.
36. Davidson RN, di Martino L, Gradoni L, et al. Short-course treatment of visceral leishmaniasis with liposomal amphotericin B (AmBisome). *Clin Infect Dis.* 1996;22(6):938–943. doi:10.1093/clinids/22.6.938.
37. Davidson RN, Di Martino L, Gradoni L, et al. Liposomal amphotericin B (AmBisome) in Mediterranean visceral leishmaniasis: a multi-centre trial. *Q J Med.* 1994;87(2):75–81.
38. Berman JD, Badaro R, Thakur CP, et al. Efficacy and safety of liposomal amphotericin B (AmBisome) for visceral leishmaniasis in endemic developing countries. *Bull World Health Organ.* 1998;76(1):25–32.
39. Thakur CP, Pandey AK, Sinha GP, Roy S, Behbehani K, Olliaro P. Comparison of three treatment regimens with liposomal amphotericin B (AmBisome) for visceral leishmaniasis in India: a randomized dose-finding study. *Trans R Soc Trop Med Hyg.* 1996;90(3):319–322. doi:10.1016/s0035-9203(96)90271-0.
40. Motta JO, Sampaio RN. A pilot study comparing low-dose liposomal amphotericin B with N-methyl glucamine for the treatment of American cutaneous leishmaniasis. *J Eur Acad Dermatol Venereol.* 2012;26(3):331–335.
41. Solomon M, Pavlotsky F, Leshem E, et al. Liposomal amphotericin B treatment of cutaneous leishmaniasis due to *Leishmania tropica*. *J Eur Acad Dermatol Venereol.* 2011;25(8):973–977.
42. Solomon M, Pavlotzky F, Barzilai A, Schwartz E. Liposomal amphotericin B in comparison to sodium stibogluconate for *Leishmania braziliensis* cutaneous leishmaniasis in travelers. *J Am Acad Dermatol*. 2013;68(2):284–289.
43. Haldar AK, Sen P, Roy S. Use of antimony in the treatment of leishmaniasis: current status and future directions. *Mol Cell Biol.* 2011;2011:571242. doi:10.4061/2011/571242.
44. Das VN, Ranjan A, Bimal S, et al. Magnitude of unresponsiveness to sodium stibogluconate in the treatment of visceral leishmaniasis in Bihar. *Natl Med J India.* 2005;18(3):131–133.
45. US Centers for Disease Control and Prevention. CDC Drug Service—Our Formulary. https://www.cdc.gov/laboratory/drugservice/formulary.html#prod-box. December 29, 2021. Accessed February 9, 2022.
46. Thakur S, Joshi J, and Kaur S. Leishmaniasis diagnosis: an update on the use of parasitological, immunological and molecular

Downloaded from https://academic.oup.com/labmed/article/54/4/363/6873137 by guest on 24 February 2025

methods. *J Parasit Dis.* 2020;44:253–272. doi:10.1007/s12639-020-01212-w.

47. US Centers for Disease Control and Prevention. Leishmaniasis—Resources for Health Professionals. 2020. https://www.cdc.gov/parasites/leishmaniasis/health_professionals/index.html. Accessed December 9, 2021.
48. Mathison BA, Pritt BS. Parasitology. In: Pritt BS, ed. *Atlas of Fundamental Infectious Diseases Histopathology: A Guide for Daily Practice.* Northfield, IL: College of American Pathologists; 2018:193–288.
49. Sundar S, Rai M. Laboratory diagnosis of visceral leishmaniasis. *Clin Vaccine Immunol.* 2002;9(5):951–958. doi:10.1128/cdli.9.5.951-958.2002.
50. Srivastava P, Dayama A, Mehrotra S, Sundar S. Diagnosis of visceral leishmaniasis. *Trans R Soc Trop Med Hyg.* 2011;105(1):1–6. doi:10.1016/j.trstmh.2010.09.006.
51. Sarkari B, Rezaei Z, Mohebali M. Immunodiagnosis of visceral leishmaniasis: current status and challenges: a review article. *Iran J Parasitol.* 2018;13(3):331–341.
52. Welch RJ, Anderson BL, Litwin CM. Rapid immunochromatographic strip test for detection of anti-K39 immunoglobulin G antibodies for diagnosis of visceral leishmaniasis. *Clin Vaccine Immunol.* 2008;15(9):1483–1484. doi:10.1128/cvi.00174-08.
53. Fontana C, Favaro M, Pelliccioni M, Pistoia ES, Favalli C. Use of the MicroSeq 500 16S rRNA gene-based sequencing for identification of bacterial isolates that commercial automated systems failed to identify correctly. *J Clin Microbiol.* 2005;43(2):615–619. doi:10.1128/JCM.43.2.615-619.2005.
54. Pryce TM, Palladino S, Kay ID, Coombs GW, et al. Rapid identification of fungi by sequencing the ITS1 and ITS2 regions using an automated capillary electrophoresis system. *Med Mycol J.* 2003;41(5):369–381.
55. Uliana SR, Affonso MH, Camargo EP, Floeter-Winter LM. *Leishmania*: genus identification based on a specific sequence of the 18S ribosomal RNA sequence. *Exp Parasitol.* 1991;72(2):157–163.
56. Van der Auwera G, Ravel C, Verweij JJ, Bart A, Schönian G, Felger I. Evaluation of four single-locus markers for *Leishmania* species discrimination by sequencing. *J Clin Microbiol.* 2014;52(4):1098–1104. doi:10.1128/JCM.02936-13.
57. de Almeida ME, Steurer FJ, Koru O, Herwaldt BL, Pieniazek NJ, da Silva AJ. Identification of *Leishmania* spp. by molecular amplification and DNA sequencing analysis of a fragment of rRNA internal transcribed spacer 2. *J Clin Microbiol.* 2011;49(9):3143–3149. doi:10.1128/JCM.01177-11.
58. Van der Auwera G, Maes I, De Doncker S, et al. Heat-shock protein 70 gene sequencing for *Leishmania* species typing in European tropical infectious disease clinics. *Eurosurveillance.* 2013;18(30):20543.
59. Brochu C, Haimeur A, Ouellette M. The heat shock protein HSP70 and heat shock cognate protein HSC70 contribute to antimony tolerance in the protozoan parasite *Leishmania*. *Cell Stress Chaperones.* 2004;9(3):294–303. doi:10.1379/csc-15r1.1.
60. Vacchina P, Norris-Mullins B, Carlson ES, Morales MA. A mitochondrial HSP70 (HSPA9B) is linked to miltefosine resistance and stress response in *Leishmania donovani*. *Parasit Vectors.* 2016;9(1):621. doi:10.1186/s13071-016-1904-8.
61. Van der Auwera G, Dujardin JC. Species typing in dermal leishmaniasis. *Clin Microbiol Rev.* 2015;28(2):265–294. doi:10.1128/CMR.00104-14.
62. Ceccarelli M, Galluzzi L, Migliazzo A, Magnani M. Detection and characterization of *Leishmania (Leishmania)* and *Leishmania (Viannia)* by SYBR green-based real-time PCR and high resolution melt analysis targeting kinetoplast minicircle DNA. *PLoS One.* 2014;9(2):e88845. doi:10.1371/journal.pone.0088845.
63. Antinori S, Calattini S, Longhi E, et al. Clinical use of polymerase chain reaction performed on peripheral blood and bone marrow samples for the diagnosis and monitoring of visceral leishmaniasis in HIV-infected and HIV-uninfected patients: a single-center, 8-year experience in Italy and review of the literature. *Clin Infect Dis.* 2007;44(12):1602–1610. doi:10.1086/518167.
64. van Griensven J, Diro E. Visceral leishmaniasis: recent advances in diagnostics and treatment regimens. *Infect Dis Clin North Am.* 2019;33(1):79–99. doi:10.1016/j.idc.2018.10.005.
65. WHO Expert Committee on the Control of the Leishmaniases. Control of the leishmaniases: report of a meeting of the WHO Expert Committee on the Control of Leishmaniases; Geneva, 22–26 March 2010. WHO Technical Report Series. Geneva, Switzerland: World Health Organization. 2010:xiii, 186.
66. Shirian S, Oryan A, Hatam G, Panahi S, Daneshbod Y. Comparison of conventional, molecular, and immunohistochemical methods in diagnosis of typical and atypical cutaneous leishmaniasis. *Arch Pathol Lab Med.* 2014;138(2):235–240. doi:10.5858/arpa.2013-0098-OA.
67. Romero GA, Vinitius de Farias Guerra M, Gomes Paes M, de Olivieira Macedo V. Comparison of cutaneous leishmaniasis due to *Leishmania (Viannia) braziliensis* and *L. (V.) guyanensis* in Brazil: clinical findings and diagnostic approach. *Clin Infect Dis.* 2001;32(9):1304–1312.
68. Rioux JA, Lanotte G, Serres E, Pratlong F, Bastien P, Perieres J. Taxonomy of *Leishmania*. Use of isoenzymes. Suggestions for a new classification. *Ann Parasitol Hum Comp*. 1990;65(3):111–125. doi:10.1051/parasite/1990653111.
69. Harris E, Kropp G, Belli A, Rodriguez B, Agabian N. Single-step multiplex PCR assay for characterization of New World *Leishmania* complexes. *J Clin Microbiol.* 1998;36(7):1989–1995. doi:10.1128/JCM.36.7.1989-1995.1998.

Downloaded from https://academic.oup.com/labmed/article/54/4/363/6873137 by guest on 24 February 2025

SCIENCE

Association of CEA, NSE, CYFRA 21-1, SCC-Ag, and ProGRP with Clinicopathological Characteristics and Chemotherapeutic Outcomes of Lung Cancer

Huijuan Bi, MSc,[1] Lina Yin, BA,[1] Wenhao Fang, BA,[1] Shenglan Song, BA,[1] Shan Wu, MSc,[2] and Jilu Shen, MD[1,]*

[1]Department of Clinical Laboratory, Anhui Public Health Clinical Center, The First Affiliated Hospital of Anhui Medical University North District, Hefei, China, [2]Department of Oncology, Anhui Public Health Clinical Center, The First Affiliated Hospital of Anhui Medical University North District, Hefei, China. *To whom correspondence should be addressed: shenjilu@126.com.

Keywords: lung cancer, neuron-specific enolase, cytokeratin 19 fragment, pro-gastrin-releasing peptide, chemotherapy, squamous cell carcinoma antigen

Abbreviations: CEA, carcinoembryonic antigen; NSE, neuron-specific enolase; CYFRA21-1, cytokeratin 19 fragment; SCC-Ag, squamous cell carcinoma antigen; ProGRP, pro-gastrin-releasing peptide; TNM, tumor-node-metastasis; SCLC, small cell lung cancer; LAC, lung adenocarcinoma; LSCC, lung squamous cell carcinoma; LC, lung cancer; CR, complete response; PR, partial response; SD, stable disease; PD, progressive disease; ROC, receiver operating characteristic; AUC, areas under the curve

Laboratory Medicine 2023;54:372-379; https://doi.org/10.1093/labmed/lmac122

ABSTRACT

Objective: The aim of this study was to investigate the association of serum carcinoembryonic antigen (CEA), nerve-specific enolase (NSE), cytokeratin 19 fragment (CYFRA21-1), squamous cell carcinoma antigen (SCC-Ag), and pro-gastrin-releasing peptide (ProGRP) with the clinicopathological characteristics and chemotherapeutic outcomes of patients with lung cancer.

Methods: A total of 189 patients with lung cancer (lung cancer group) diagnosed at the Fourth Affiliated Hospital of Anhui Medical University from January 2020 to December 2021 were included. During the same period, 199 patients with benign lung disorders were included as the benign lung disease group and 75 healthy people were selected as the control group. The serum concentrations of CEA, NSE, CYFRA21-1, SCC-Ag, and ProGRP in all the 3 groups were analyzed and compared in patients with different lung cancer tumor-node-metastasis (TNM) stages and pathological classifications. A total of 11 patients with small cell lung cancer (SCLC) and 18 patients with lung adenocarcinoma (LAC) were further evaluated for the dynamic changes of CEA, NSE, CYFRA21-1, SCC-Ag, and ProGRP before chemotherapy and during the 6 courses of chemotherapy, and the outcome of chemotherapy was evaluated every 2 courses.

Results: The serum concentrations of CEA, NSE, CYFRA21-1, SCC-Ag, and ProGRP in the lung cancer group were significantly higher than those in the control group ($P < .05$). We found statistically significant differences in serum CEA, NSE, CYFRA 21-1, SCC-Ag, and ProGRP among patients with different pathological types (LAC, squamous cell carcinoma, or SCLC) and different stages (I–IV). The ProGRP and NSE had the highest expression in SCLC, CEA showed the highest expression in LAC, whereas CYFRA21-1 and SCC-Ag showed the highest expression in lung squamous cell carcinoma (LSCC). The concentrations of all the markers were elevated in the advanced pathological stages. The receiver operating characteristic curve analysis showed that the diagnostic value of the combined detection of CEA, NSE, CYFRA 21-1, SCC-Ag, and ProGRP for lung cancer was significantly higher than using a single biomarker ($P < .05$). Our dynamic monitoring results show that ProGRP progressively decreased in remission cases of SCLC and CEA progressively decreased in LAC remission cases.

Conclusion: CEA, NSE, CYFRA 21-1, SCC-Ag, and ProGRP have good clinical value in the early diagnosis, differential diagnosis, and progression monitoring of lung cancer. The ProGRP and CEA concentrations are beneficial for evaluating the outcome of chemotherapy in SCLC and LAC. The combined detection of multiple biomarkers shows improved clinical value in the early diagnosis of lung cancer.

Lung cancer (LC) is the most common malignancy in men and the leading cause of cancer-related mortality worldwide, the third most common cancer after breast cancer and colorectal cancer.[1] In recent years, the incidence and mortality of LC have been increasing rapidly in China, where the mortality rate of LC ranks first among all cancers, and the 5-year survival rate is only about 15%.[2] The high incidence and mortality rates of LC are caused by external factors such as pollution and unhealthy living habits, but more important are the characteristics of LC itself: the symptoms of LC in the early stages are relatively insidious and most LCs are in the intermediate or late stages by the time they are diagnosed, missing the optimal treatment time. Therefore, the early diagnosis and

© The Author(s) 2022. Published by Oxford University Press on behalf of American Society for Clinical Pathology. All rights reserved. For permissions, please e-mail: journals.permissions@oup.com

Downloaded from https://academic.oup.com/labmed/article/54/4/372/6772479 by guest on 24 February 2025

accurate localization of LC are crucial strategies to improve the survival rate of patients with LC.

At present, the diagnosis of LC mainly relies on radiological and pathological examinations, which confirm only late-stage tumors, resulting in poor clinical treatment effect.[3] Serum tumor markers are a class of molecules that exist in tumor tissues and host body fluids, which can reflect the existence and characteristics of tumors. With the advantages of noninvasiveness, simplicity, and affordability, serum tumor markers have become an important auxiliary evaluation method for clinical LC monitoring and provide reference for the diagnosis and treatment of LC patients.[4] The accurate diagnosis of LC is crucial for patients to choose the most appropriate individualized treatment. Therefore, there is an urgent need to identify sensitive and specific biomarkers for early diagnosis of LC.

k 21z Carcinoembryonic antigen (CEA) is a broad-spectrum tumor marker that is commonly used in the diagnosis of gastrointestinal tumors, LC, and breast cancer.[5,6] Neuron-specific enolase (NSE) is an enolase involved in the glycolysis pathway that exists in nerve tissue and neuroendocrine tissue. It has been reported that the expression of NSE is elevated in tumors originating in neuroendocrine tissue.[7] A fragment of cytokeratin 19 known as CYFRA21-1 is currently considered to be a biomarker for non–small cell lung cancer (SCLC).[8] Squamous cell carcinoma antigen (SCC-Ag) is a squamous cell antigen first discovered in cervical cancer. Due to being widely expressed in malignant epithelial cells, SCC-Ag is the most preferred tumor marker for cervical squamous cell carcinoma. Previous studies[9–11] have found that SCC-Ag is more specific than CEA in lung squamous cell carcinoma (LSCC) and was not interfered with by factors such as smoking. Pro-gastrin-releasing peptide (ProGRP) is the precursor of gastrin-releasing peptide. Several studies have shown that the expression of ProGRP fragments is increased in the sera of patients with SCLC, which can be used as a novel diagnostic marker for SCLC.[12–15] These tumor markers are considered by the Chinese National Society of Clinical Biochemistry Laboratory Medicine Practice Guidelines to be commonly used serum tumor markers for LC.[16] These tumor markers are also used routinely for LC screening in our hospital. To evaluate the comprehensive values of these biomarkers in the diagnosis, differential diagnosis, and efficacy evaluation of LC, this study selected 189 lung cancer patients diagnosed in our hospital from January 2020 to December 2021 and analyzed the serum levels of CEA, NSE, CYFRA 21-1, SCC-Ag, and ProGRP in patients with LC. The association between these biomarkers and the pathological characteristics and chemotherapeutic outcomes of LC was investigated.

Materials and Methods

Subjects

A total of 189 cases of LC patients (LC group) diagnosed in the Fourth Affiliated Hospital of Anhui Medical University from January 2020 to December 2021 were included. In the LC group, there were 140 males and 49 females with an average age of 66.95 ± 10.35 years. The cancers were classified as 29 SCLCs, 53 squamous cell carcinomas, 91 adenocarcinomas, and 16 other types. International TNM staging of LC indicated 15 cases of stage I, 14 cases of stage II, 56 cases of stage III, and 104 cases of stage IV. A total of 199 patients with benign lung disorders (chronic obstructive pulmonary disease, pneumonia, bronchiectasis, pulmonary tuberculosis, etc) admitted to our hospital during the same period were selected as the benign lung disease group, including 125 males and 74 females, with an average age of 62.6 ± 15.5 years. Another 75 healthy individuals admitted in our hospital during the same period were selected as the healthy control group. The healthy controls had normal heart, liver, lung, and kidney function, no infectious lesions, no radiological or histological confirmed LC or benign lung diseases and had taken no medication within 2 weeks. In the control group, there were 34 males and 41 females, with an average age of 58.2 ± 12.5. As shown in **TABLE 1**, there was no significant difference in age and gender of the 3 groups ($P > .05$).

Inclusion and Exclusion Criteria

All LC patients included in the study were diagnosed by blood test, radiological, or histological test (sputum cytology, percutaneous lung puncture or fiberoptic bronchoscopy, pathological diagnosis), and had no family history of LC or other major diseases. All individuals included signed their own informed consent. Exclusion criteria for the study included individuals with cognitive disorders and any individuals who prematurely dropped out of the study.

Biomarker Detection Method

Sample Collection

Twenty-four hours after admission or 6 to 8 hours after treatment, 5 mL of cubital venous blood was collected from each patient. The blood samples were kept at room temperature for 30 min and centrifuged at 3500 rpm for 10 min before serum samples were separated and stored at −20°C. The serum levels of CEA, NSE, CYFRA21-1, SCC-Ag, and ProGRP in each group were detected by electrochemiluminescence immunoassay.

Instruments and Reagents

The concentrations of CEA, NSE, CYFRA21-1, SCC-Ag, and ProGRP in all serum samples were detected by Roche electrochemiluminescence automatic immunoassay analyzer (Roche Cobas e601) according to the manufacturers instructions. The reagents used in this study were all from Roche.

Criteria for Positive Results

According to the corresponding manufacturer's recommendations, the following thresholds were used as the limit of the normal range: CEA ≥ 6.5 ng/mL, NSE ≥ 16.3 ng/mL, CYFRA21-1 ≥ 3.3 ng/mL, SCC-Ag ≥ 1.8 ng/mL, and ProGRP ≥ 66.0 pg/mL; these were used as the positive cutoff values for the diagnosis of LC. The reference range is from the Roche instructions and has been clinically verified.

Evaluation of Clinical Outcomes

The short-term efficacy evaluation criteria were divided into complete response (CR), partial response (PR), stable disease (SD), and progressive

TABLE 1. Age and Gender of the Patients in the 3 Groups

Characteristic	Cancer (n = 189)	Benign Lung Disease (n = 199)	Healthy Control (n = 75)
Age, y	66.95 ± 10.35	62.6 ± 15.5	58.2 ± 12.5
Gender			
Male	140	125	34
Female	49	74	41

Downloaded from https://academic.oup.com/labmed/article/54/4/372/6772479 by guest on 24 February 2025

TABLE 2. CEA, NSE, CYFRA21-1, SCC-Ag, and ProGRP Concentrations among the 3 Groups[a]

Group	CEA (0–6.5 ng/mL)	NSE (0–16.3 ng/mL)	CYFRA21-1 (≤3.3 ng/mL)	SCC-Ag (≤1.8 ng/mL)	ProGRP (0–66 pg/mL)
Control (n = 75)	1.69 (0.20–8.28)	9.91 (2.91–35.50)	1.62 (0.53–3.73)	0.69 (0.14–8.18)	34.95 (14.12–93.64)
Benign lung disease (n = 199)	3.57 (0.50–145.40)	14.76 (0.50–83.63)	3.85 (0.74–115.90)	1.24 (0.22–11.96)	46.75 (17.73–236.69)
LC (n = 189)	30.29[b,c] (0.66–1000)	31.12[b,c] (6.75–1126)	9.84[b,c] (1.16–176.90)	1.94[b] (0.01–35.31)	274.68[b,c] (16.39–5000)

CEA, carcinoembryonic antigen; CYFRA21-1, cytokeratin 19 fragment 21-1; LC, lung cancer; NSE, neuron-specific enolase; ProGRP, pro-gastrin-releasing peptide; SCC-Ag, squamous cell carcinoma antigen.
[a]*Data are shown as median (minimum – maximum).*
[b]*P < .05 compared with the control group.*
[c]*P < .05 compared with the benign lung disease group.*

disease (PD) according to the World Health Organization efficacy evaluation criteria for solid tumors.[17] The visible lesions disappeared completely for more than 1 month for CR. For PR, the product of the largest tumor diameter and the largest vertical diameter were decreased by more than 50%. In an SD, the product of the largest tumor diameter and the largest vertical diameter decreased by <50% or increased by <25% and in PD, the product of the largest tumor diameter and the largest vertical diameter in one or more lesions increased >25%.

Statistics

Statistical analysis was performed using SPSS 19.0 software. The quantitative data were presented as median since some data showed skewed distribution. The Mann-Whitney *U* or Kruskal-Wallis *H* test were used for comparison between groups. The enumeration data were analyzed using the paired χ^2 test. The receiver operating characteristic (ROC) curve was used to analyze and evaluate the clinical diagnostic performance of CEA, NSE, CYFRA21-1, SCC-Ag, and ProGRP for LC. $P < .05$ was considered to be statistically significant.

Results

Comparison of CEA, NSE, CYFRA21-1, SCC-Ag, and ProGRP Concentrations

As shown in **TABLE 2** and **FIGURE 1**, the serum concentrations of CEA, NSE, CYFRA21-1, SCC-Ag, and ProGRP in the LC group were significantly higher than those of the healthy control group ($P < .01$). Compared with the benign disease group, the serum concentrations of CEA, NSE, CYFRA21-1, and ProGRP in the LC group were also increased significantly ($P < .01$) except for SCC-Ag level ($P > .05$). Comparing the serum concentrations of CEA, NSE, CYFRA21-1, SCC-Ag, and ProGRP between patients with early stage (stage I–II) LC and normal controls, it was found that the serum concentrations of CEA, NSE, CYFRA21-1, SCC-Ag, and ProGRP were significantly increased in patients with early stage LC ($P < .01$) (**TABLE 3**).

Association between Serum CEA, NSE, CYFRA21-1, SCC-Ag, and ProGRP Concentrations with Pathological Types and Stages of LC

The serum concentrations of CEA, NSE, CYFRA 21-1, SCC-Ag, and ProGRP in LAC, LSCC, and SCLC were significantly different ($P < .01$). As shown in **TABLE 4**, serum NSE and ProGRP showed the highest expression in SCLC, CEA showed the highest expression in LAC, and CYFRA21-1 and SCC-Ag had the highest expression in LSCC. Moreover, the serum concentrations of CEA, NSE, CYFRA 21-1, SCC-Ag, and ProGRP in patients with different pathological stages of LC showed significant difference ($P < .01$). Furthermore, as shown in **TABLE 5**, the serum concentrations of CEA, NSE, CYFRA 21-1, SCC-Ag, and ProGRP in patients with stage I-II LC were significantly lower than those in patients with stage III-IV LC ($P < .01$).

Value of Single and Combined CEA, NSE, CYFRA21-1, SCC-Ag, and ProGRP Detection in Differential Diagnosis of LC

The ROC curve analysis showed that the areas under the curve (AUC) of single detection using CEA, NSE, CYFRA 21-1, SCC-Ag, and ProGRP for the diagnosis of LC were 0.861, 0.836, 0.939, 0.697, and 0.721, respectively. The AUC of combined detection for the diagnosis of LC using all 5 markers was 0.960, showing the diagnostic value of the combined detection was significantly higher than that of single detection ($P < .01$) (**FIGURE 2** and **TABLE 6**).

Value of CEA, NSE, CYFRA21-1, SCC-Ag, and ProGRP in Evaluating the Outcome of Chemotherapy

By dynamic detection of serum CEA, NSE, CYFRA 21-1, SCC-Ag, and ProGRP in 29 patients with LC (11 SCLC and 18 LAC) before and after each of the 6 courses of treatment, we found that the serum ProGRP of 8 PR patients with SCLC (including 1 case of CR and 7 cases of PR) gradually decreased with the progress of treatment (**FIGURE 3**, solid line), whereas the ProGRP level was not significantly changed in 3 PD patients and showed a progressive increase trend in the late stages of the disease (**FIGURE 3**, dotted line). Among the 18 patients with LAC, 10 patients with PR showed a progressive decrease in CEA levels (**FIGURE 4**, solid line), 4 patients with SD showed a stable level of CEA with minor fluctuations, and 4 patients with PD showed an increasing trend of CEA level (**FIGURE 4**, dotted line).

Discussion

LC ranks first in morbidity and mortality of types of malignant tumors every year in China.[18,19] Because of the lack of obvious symptoms and specific clinical manifestations in the early stages, LC is usually diagnosed in advanced stages, missing the time for optimal treatment, resulting in a very low survival rate.[20] Therefore, the ability to accurately diagnose early stage LC and monitor its response to treatment is one of the main strategies to improve the survival rate of LC patients. Serum tumor markers are a class of molecules found in tumor tissues and host body fluids that can be used to indicate the presence and development of tumors and monitor the response to treatments. Serum tumor markers are more sensitive than computed tomographic imaging and other evaluation methods in the early stages of cancer.[21] Therefore, serum tumor markers may become effective indicators for early diagnosis of tumors

Downloaded from https://academic.oup.com/labmed/article/54/4/372/6772479 by guest on 24 February 2025

FIGURE 1. Expression of carcinoembryonic antigen (CEA) (A), neuron-specific enolase (NSE) (B), cytokeratin 19 fragment (CYFRA 21-1) (C), squamous cell carcinoma antigen (SCC-Ag) (D), and pro-gastrin-releasing peptide (ProGRP) (E) in lung cancer patients. $P < .01$ for all comparisons.

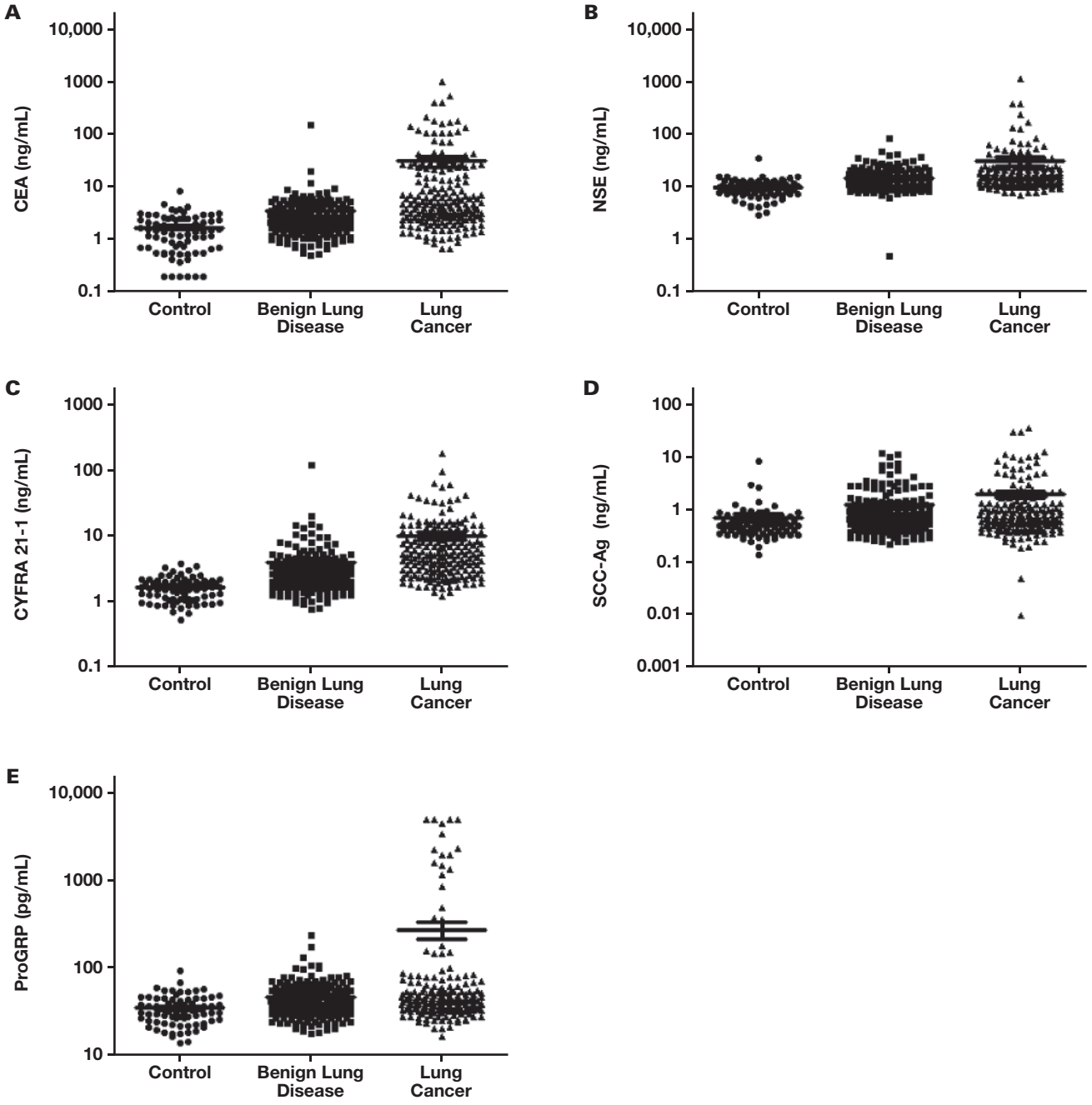

TABLE 3. CEA, NSE, CYFRA21-1, SCC-Ag, and ProGRP Concentrations between Patients with Early Stage Lung Cancer and the Control Group

	CEA (0–6.5 ng/mL)	NSE (0–16.3 ng/mL)	CYFRA21-1 (≤3.3 ng/mL)	SCC-Ag (≤1.8 ng/mL)	ProGRP (0–66 pg/mL)
Control (n = 75)	1.69 (0.20–8.28)	9.91 (2.91–35.50)	1.62 (0.53–3.73)	0.69 (0.14–8.18)	34.95 (14.12–93.64)
Stage I–II (n = 29)	3.45 (1.03–9.64)	12.64 (7.69–35.80)	3.63 (1.55–12.00)	0.81 (0.05–2.38)	44.57 (21.49–144.78)
Z	–4.654	–2.925	–5.691	–2.672	–2.715
P	.000	.003	.000	.008	.007

CEA, carcinoembryonic antigen; CYFRA21-1, cytokeratin 19 fragment 21-1; NSE, neuron-specific enolase; ProGRP, pro-gastrin-releasing peptide; SCC-Ag, squamous cell carcinoma antigen.

Downloaded from https://academic.oup.com/labmed/article/54/4/372/6772479 by guest on 24 February 2025

TABLE 4. Serum Concentrations of CEA, NSE, CYFRA21-1, SCC-Ag, and ProGRP in Patients with Different Pathological Types of LC[a]

Group	CEA	NSE	CYFRA21-1	SCC-Ag	ProGRP
LAC (n = 91)	5.81 (0.67–514.40)	14.00 (7.69–1126.00)	4.19 (1.36–54.83)	0.60 (0.01–28.55)	39.78 (16.39–154.23)
LSCC (n = 54)	3.47 (0.66–24.41)	13.92 (6.75–237.30)	6.83 (1.67–176.90)	1.48 (0.45–35.31)	38.74 (23.61–81.28)
SCLC (n = 29)	4.55 (0.88–1000)	33.02 (9.61–370.0)	3.70 (1.16–41.82)	0.56 (0.27–2.12)	848.42 (27.73–5000)
χ^2	10.968	32.275	18.323	44.461	49.564
P	.012	.000	.000	.000	.000

CEA, carcinoembryonic antigen; CYFRA21-1, cytokeratin 19 fragment 21-1; LAC, lung adenocarcinoma; LC, lung cancer; LSCC, lung squamous cell carcinoma; NSE, neuron-specific enolase; ProGRP, pro-gastrin-releasing peptide; SCC-Ag, squamous cell carcinoma antigen; SCLC, small cell lung cancer.
[a]Data are shown as median (minimum – maximum). Among the 189 LC cases, 15 cases were not classified as LAC, LSCC, or SCLC; these cases were excluded from this analysis.

TABLE 5. Serum Concentrations of CEA, NSE, CYFRA21-1, SCC-Ag, and ProGRP in Patients with Different Pathological Stages of LC[a]

Group	CEA	NSE	CYFRA21-1	SCC-Ag	ProGRP
Stage I (n = 15)	2.62 (1.03–6.65)	11.26 (7.69–17.31)	2.28 (1.55–4.87)	0.60 (0.05–2.18)	39.78 (27.76–47.57)
Stage II (n = 14)	3.93 (1.44–9.64)	11.85 (8.08–35.80)	4.40 (1.62–12.00)	0.82 (0.30–2.38)	43.52 (21.49–144.78)
Stage III (n = 56)	4.64 (0.66–173.90)	13.24 (7.86–80.89)	5.70 (1.16–94.22)	0.98 (0.24–28.68)	39.09 (20.30–5000)
Stage IV (n = 104)	6.26 (0.67–1000)	16.65 (6.75–1126.00)	5.33 (1.36–176.90)	0.70 (0.01–35.31)	46.18 (16.39–5000)
χ^2	16.319	27.008	21.350	8.852	9.558
P	.001	.000	.000	.031	.023

CEA, carcinoembryonic antigen; CYFRA21-1, cytokeratin 19 fragment 21-1; LC, lung cancer; NSE, neuron-specific enolase; ProGRP, pro-gastrin-releasing peptide; SCC-Ag, squamous cell carcinoma antigen.
[a]Data are shown as median (minimum – maximum).

and monitoring the effect of chemotherapeutic outcomes.[22] At present, the commonly used tumor markers for screening and monitoring LC include CEA, NSE, CYFRA21-1, SCC-Ag, and ProGRP. Although some studies have analyzed the association of the high expression of these tumor markers with LC,[23,24] it is still unclear whether these tumor markers are associated with different types of LC or different responses to chemotherapy. This study selected 189 patients with LC diagnosed from January 2020 to December 2021. By analyzing the concentrations of serum CEA, NSE, CYFRA 21-1, SCC-Ag, and ProGRP, we explored the association of these markers with the pathological characteristics of LC and the efficacy of chemotherapy.

FIGURE 2. Receiver operating characteristic curves of diagnosis using single or combined carcinoembryonic antigen (CEA), neuron-specific enolase (NSE), cytokeratin 19 fragment (CYFRA21-1), squamous cell carcinoma antigen (SCC-Ag), and pro-gastrin-releasing peptide (ProGRP).

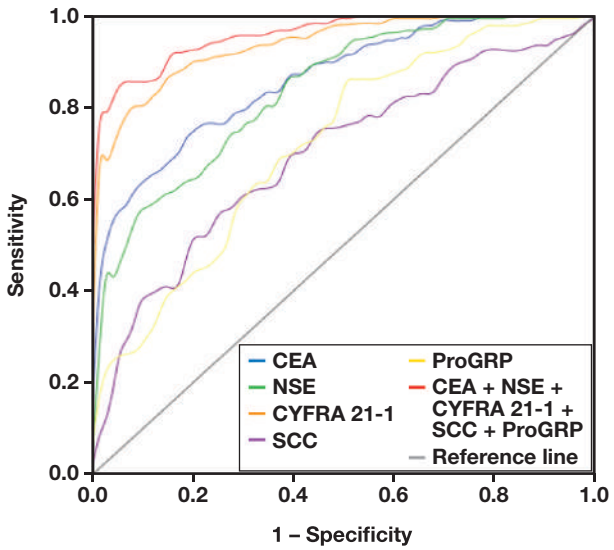

Our results showed that the serum concentrations of CEA, NSE, CYFRA21-1, SCC-Ag, and ProGRP were the highest in the LC group followed by the benign lung disease group and were the lowest in the healthy control group ($P < .01$), suggesting that CEA, NSE, CYFRA21-1, SCC-Ag, and ProGRP can assist in the diagnosis and differential diagnosis of LC. In this study, there was no significant difference in SCC-Ag between the benign lung disease group and the LC group, which may be due to the ratio of various types of benign lung diseases in this study. Studies[25] have reported that SCC-Ag was significantly increased in the pneumonia group, which was slightly lower than that in the LSCC group. Since there were more cases of pneumonia in the benign lung disease group included in this study, this may have increased the average level of SCC-Ag in this group and reduced the difference to the LC group. Comparing the concentrations of CEA, NSE, CYFRA21-1, SCC-Ag, and ProGRP between patients with early-stage LC and the control group, the results showed that the concentrations of CEA, NSE, CYFRA21-1, SCC-Ag, and ProGRP were increased significantly in patients with early-stage LC. This suggests that serum CEA, NSE, CYFRA21-1, SCC-Ag, and ProGRP can assist in the early diagnosis of LC. Further analysis of the

Downloaded from https://academic.oup.com/labmed/article/54/4/372/6772479 by guest on 24 February 2025

TABLE 6. AUC of CEA, NSE, CYFRA21-1, SCC-Ag, ProGRP Alone and in Combination for the Diagnosis of LC

Detection	AUC	SEM	*P* Value	95% Confidence Interval	
				Lower Limit	Upper Limit
CEA	0.861	0.023	<.001	0.816	0.906
NSE	0.836	0.026	<.001	0.785	0.888
CYFRA21-1	0.939	0.014	<.001	0.912	0.965
SCC-Ag	0.697	0.034	<.001	0.630	0.764
ProGRP	0.721	0.035	<.001	0.653	0.789
Combined	0.960	0.010	<.001	0.940	0.980

AUC, area under the curve; CEA, carcinoembryonic antigen; CYFRA21-1, cytokeratin 19 fragment 21-1; LC, lung cancer; NSE, neuron-specific enolase; ProGRP, pro-gastrin-releasing peptide; SCC-Ag, squamous cell carcinoma antigen; SEM, standard error of the mean.

FIGURE 3. Serum pro-gastrin-releasing peptide (ProGRP) concentrations before or after chemotherapy in 11 small cell lung carcinoma patients. The dotted line represents 3 progressive disease patients, the solid line represents 8 patients with remission. The y-axis shows the logarithmic value of ProGRP concentration; the x-axis represents the chemotherapy courses.

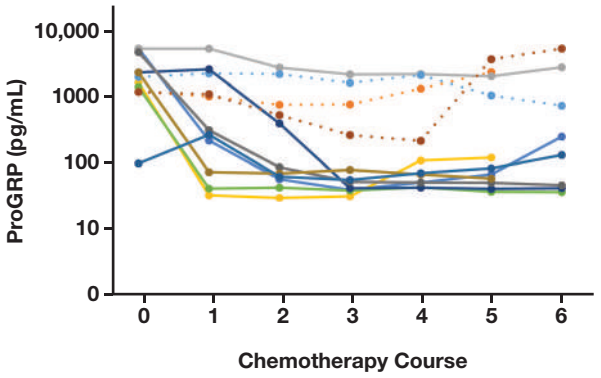

FIGURE 4. Serum carcinoembryonic antigen (CEA) concentrations before or after chemotherapy in 18 lung adenocarcinoma patients. The dotted line shows 8 stable disease or progressive disease patients, the solid line represents 10 partial response patients. The y-axis shows the concentration of CEA; the x-axis represents the chemotherapy courses.

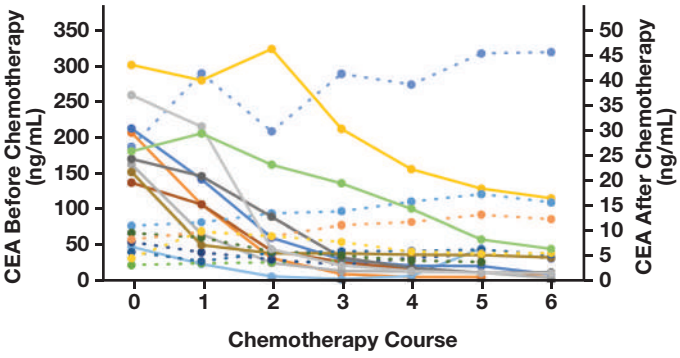

relationship between clinical data and the serum markers showed that CEA was the highest in lung adenocarcinoma (LAC), CYFRA21-1 and SCC-Ag were the highest in LSCC, and serum NSE and ProGRP showed the highest expression in SCLC ($P < .01$). This suggests that CEA, NSE, CYFRA 21-1, SCC-Ag, and ProGRP can effectively assist in the pathological classification of LC. The markers NSE and ProGRP have good clinical value in distinguishing SCLC and NSCLC, CEA has good clinical value in the differential diagnosis of LAC and CYFRA21-1, and SCC-Ag has good clinical value in diagnosis of LSCC. The concentrations of CEA, NSE, CYFRA 21-1, SCC-Ag, and ProGRP in patients with LC at different stages have significant differences. The serum concentrations of CEA, NSE, CYFRA 21-1, SCC-Ag, and ProGRP in patients with stage I-II LC were significantly lower than those in patients with stage III-IV LC ($P < .01$). The later the stage, the higher the concentration, indicating that the concentrations of CEA, NSE, CYFRA 21-1, SCC-Ag, and ProGRP increase significantly with the progression of LC, which makes them potential markers for monitoring disease process, assisting in pathological and stage classification, and guiding early clinical chemotherapy strategies.

A large number of studies have shown that the sensitivity and specificity of single molecules as tumor markers requires further improvement,[26] which is consistent with our finding that some tumor markers were also elevated in benign lung diseases. To improve the sensitivity and specificity of detection and reduce misdiagnosis rate, we compared the value of individual and combined diagnosis of LC by ROC curve. Our results showed that the AUC of CEA, NSE, CYFRA 21-1, SCC-Ag, and ProGRP alone for diagnosing LC were 0.861, 0.836, 0.939, 0.697, and 0.721, respectively. The AUC of the combined detection of the 5 markers for LC was 0.960, indicating that the combined detection of CEA, NSE, CYFRA 21-1, SCC-Ag, and ProGRP has a significantly higher diagnostic value for LC than single-marker detection. This result is consistent with the results of Chen et al,[27] suggesting that the combined detection of CEA, NSE, CYFRA 21-1, SCC-Ag, and ProGRP can effectively improve the sensitivity and specificity of diagnosis, reduce misdiagnosis rate, and beneficial for the early diagnosis, treatment, and prognosis of LC.

To evaluate the ability of these serum tumor markers in monitoring the response to chemotherapy, we performed dynamic detection of serum CEA, NSE, CYFRA 21-1, SCC-Ag, and ProGRP in 29 patients with LC (11 SCLC and 18 LAC) before and after each of the 6 courses of treatment. We found that the serum ProGRP of 8 PR patients with SCLC (including 1 case of CR and 7 cases of PR) gradually decreased with the progress of treatment (**FIGURE 3**, solid line), whereas the ProGRP concentration was not significantly changed in 3 PD patients and showed a progressive increase trend in the late stages of the disease (**FIGURE 3**, dotted line). Among the 18 patients with LAC, 10 PR patients showed a progressive decrease in CEA concentration (**FIGURE 4**, solid line), 4 SD patients showed a stable concentration of CEA with minor fluctuations, and 4 PD patients showed an increasing trend of CEA concentration (**FIGURE 4**, dotted line). These

Downloaded from https://academic.oup.com/labmed/article/54/4/372/6772479 by guest on 24 February 2025

results are consistent with previous research by Barchiesi et al,[28] who prospectively collected and measured serum ProGRP, NSE, CYFRA21-1, SCC-Ag, and CEA in patients with LC and found that ProGRP is an accurate biomarker for diagnosing SCLC and distinguishing SCLC from non-SCLC. Furthermore, the ProGRP concentration was reduced in LC patients who responded to chemotherapy. These results all suggest that serum ProGRP and CEA are useful in monitoring chemotherapy outcomes in patients with SCLC and LAC. By detecting tumor markers, the efficacy of different regimens can be determined, which is crucial for the selection of optimal treatment. Considering the limited size and region of the patients included in this study, future research with larger sample size and wider geographical distribution of subjects is needed to further validate the value of the biomarkers investigated in this study.

In conclusion, serum concentrations of CEA, NSE, CYFRA 21-1, SCC-Ag, and ProGRP can be used to assist the early diagnosis, differential diagnosis, pathological classification, and staging of LC, monitor the disease process, evaluate the sensitivity of patients to chemotherapy regimens, and eventually provide suggestions for the selection of optimal treatment regimens. The combinational detection of multiple markers can effectively improve the sensitivity and specificity of LC diagnosis, reduce misdiagnosis rate, benefit the early detection of LC, and has good clinical value for the early diagnosis of LC.

Funding

This study was funded by University Cooperation and Public Health Collaborative Innovation Project of Anhui Provincial Department of Education (GXXT-2020-016) and Research Funding of Anhui Institute of Translational Medicine (2021zhyx-C55).

Conflict of Interest Disclosure

The authors have nothing to disclose.

REFERENCES

1. Bade BC, Dela Cruz CS. Lung cancer 2020: epidemiology, etiology, and prevention. *Clin Chest Med.* 2020;41(1):1–24. doi:10.1016/j.ccm.2019.10.001.
2. Wu F, Wang L, Zhou C. Lung cancer in China: current and prospect. *Curr Opin Oncol.* 2021;33(1):40–46. doi:10.1097/CCO.0000000000000703.
3. Nooreldeen R, Bach H. Current and future development in lung cancer diagnosis. *Int J Mol Sci .* 2021;22(16):8661. doi:10.3390/ijms22168661.
4. Villalobos P, Wistuba II. Lung cancer biomarkers. *Hematol Oncol Clin North Am.* 2017;31(1):13–29. doi:10.1016/j.hoc.2016.08.006.
5. Hao C, Zhang G, Zhang L. Serum CEA levels in 49 different types of cancer and noncancer diseases. *Prog Mol Biol Transl Sci.* 2019;162:213–227. doi:10.1016/bs.pmbts.2018.12.011.
6. Grunnet M, Sorensen JB. Carcinoembryonic antigen (CEA) as tumor marker in lung cancer. *Lung Cancer.* 2012;76(2):138–143. doi:10.1016/j.lungcan.2011.11.012.
7. Lu L, Zha Z, Zhang P, Li D, Liu G. NSE, positively regulated by LINC00657-miR-93-5p axis, promotes small cell lung cancer (SCLC) invasion and epithelial-mesenchymal transition (EMT) process. *Int J Med Sci.* 2021;18(16):3768–3779. doi:10.7150/ijms.58415.
8. Mazzone PJ, Wang XF, Han X, Choi H, Seeley M, Scherer R, Doseeva V. Evaluation of a serum lung cancer biomarker panel. *Biomark Insights.* 2018;13:1–5. doi:10.1177/1177271917751608.
9. Zhou W, Yang Y, Wang Z, Liu Y, Lari Najafi M. Impact of HSP90α, CEA, NSE, SCC, and CYFRA21-1 on lung cancer patients. *J Healthc Eng* 2021;2021:6929971. doi:10.1155/2021/6929971.
10. Zheng Q, Zhang L, Tu M, et al. Development of a panel of autoantibody against NSG1 with CEA, CYFRA21-1, and SCC-Ag for the diagnosis of esophageal squamous cell carcinoma. *Clin Chim Acta.* 2021;520:126–132. doi:10.1016/j.cca.2021.06.013.
11. Li Q, Sang S. Diagnostic value and clinical significance of combined detection of serum markers CYFRA21-1, SCC Ag, NSE, CEA and ProGRP in non-small cell lung carcinoma. *Clin Lab.* 2020;66(11). doi:10.7754/Clin.Lab.2020.191243.
12. Nakamura H, Nishimura T. History, molecular features, and clinical importance of conventional serum biomarkers in lung cancer. *Surg Today.* 2017;47(9):1037–1059. doi:10.1007/s00595-017-1477-y.
13. Wojcik E, Kulpa JK. Pro-gastrin-releasing peptide (ProGRP) as a biomarker in small-cell lung cancer diagnosis, monitoring and evaluation of treatment response. *Lung Cancer (Auckl).* 2017;8:231–240. doi:10.2147/LCTT.S149516.
14. Dong A, Zhang J, Chen X, Ren X, Zhang X. Diagnostic value of ProGRP for small cell lung cancer in different stages. *J Thorac Dis* 2019;11(4):1182–1189. doi:10.21037/jtd.2019.04.29.
15. Korkmaz ET, Koksal D, Aksu F, et al. Triple test with tumor markers CYFRA 21.1, HE4, and ProGRP might contribute to diagnosis and subtyping of lung cancer. *Clin Biochem.* 2018;58:15–19. doi:10.1016/j.clinbiochem.2018.05.001.
16. Chinese Medical Association; Oncology Society of Chinese Medical Association; Chinese Medical Association Publishing House. Chinese Medical Association guidelines for clinical diagnosis and treatment of lung cancer (2019 edition)]. *Zhonghua Zhong Liu Za Zhi.* 2020;42(4):257–287. doi:10.3760/cma.j.cn112152-20200120-00049.
17. Duffaud F, Therasse P. Nouvelles recommandations pour l'évaluation de la réponse tumorale dans les tumeurs solides [New guidelines to evaluate the response to treatment in solid tumors]. *Bull Cancer.* 2000;87(12):881–886.
18. Cao M, Chen W. Epidemiology of lung cancer in China. *Thorac Cancer.* 2019;10(1):3–7. doi:10.1111/1759-7714.12916.
19. Yang D, Liu Y, Bai C, Wang X, Powell CA. Epidemiology of lung cancer and lung cancer screening programs in China and the United States. *Cancer Lett*. 2020;468:82–87. doi:10.1016/j.canlet.2019.10.009.
20. Gao S, Li N, Wang S, et al. Lung Cancer in People's Republic of China. *J Thorac Oncol.* 2020;15(10):1567–1576. doi:10.1016/j.jtho.2020.04.028.
21. Vos D, Rao S, Pierce JD, et al. The past, present, and future (liquid biopsy) of serum tumor markers in lung cancer: a primer for the radiologist. *J Comput Assist Tomogr.* 2021;45(6):950–958. doi:10.1097/RCT.0000000000001204.
22. Dal Bello MG, Filiberti RA, Alama A, et al. The role of CEA, CYFRA21-1 and NSE in monitoring tumor response to nivolumab in advanced non-small cell lung cancer (NSCLC) patients. *J Transl Med.* 2019;17(1):74. doi:10.1186/s12967-019-1828-0.
23. Li Y, Tian X, Gao L, et al. Clinical significance of circulating tumor cells and tumor markers in the diagnosis of lung cancer. *Cancer Med.* 2019;8(8):3782–3792. doi:10.1002/cam4.2286.
24. Muley T, Rolny V, He Y, et al. The combination of the blood based tumor biomarkers cytokeratin 19 fragments (CYFRA 21-1) and carcinoembryonic antigen (CEA) as a potential predictor of benefit from adjuvant chemotherapy in early stage squamous cell carcinoma of the lung (SCC). *Lung Cancer.* 2018;120:46–53. doi:10.1016/j.lungcan.2018.03.015.
25. Tutar N, Yetkin NA, Yazıcı C, Önal O, Kontaş O, Keleştemur F. Clinical significance of progastrin-releasing peptide, neuron-specific enolase, chromogranin a, and squamous cell cancer antigen in pulmonary neuroendocrine tumors. *Turk J Med Sci.* 2019;49(3):774–781. doi:10.3906/sag-1810-147.

Downloaded from https://academic.oup.com/labmed/article/54/4/372/6772479 by guest on 24 February 2025

26. Wu H, Wang Q, Liu Q, Zhang Q, Huang Q, Yu Z. The serum tumor markers in combination for clinical diagnosis of lung cancer. *Clin Lab.* 2020;66(3).2189-2195. doi:10.7754/Clin.Lab.2019.190533.

27. Chen Z, Liu X, Shang X, Qi K, Zhang S. The diagnostic value of the combination of carcinoembryonic antigen, squamous cell carcinoma-related antigen, CYFRA 21-1, neuron-specific enolase, tissue polypeptide antigen, and progastrin-releasing peptide in small cell lung cancer discrimination. *Int J Biol Markers.* 2021;36(4):36–44. doi:10.1177/17246008211049446.

28. Barchiesi V, Simeon V, Sandomenico C, et al. Circulating progastrin-releasing peptide in the diagnosis of Small Cell Lung Cancer (SCLC) and in therapeutic monitoring. *J Circ Biomark.* 2021;10:9–13. doi:10.33393/jcb.2021.2212.

Downloaded from https://academic.oup.com/labmed/article/54/4/372/6772479 by guest on 24 February 2025

The Interpretation of Mirror Pattern Bands During Oligoclonal Immunoglobulin Isoelectric Focusing Electrophoresis: A Retrospective Study

JinLing Wang, MD, PhD,[1] Lei Li, MD,[1] YanBing Zhang, MD,[1] PeiChang Wang, PhD[1,]*

[1]Department of Clinical Laboratory, Xuanwu Hospital, Capital Medical University, Beijing, China. *To whom correspondence should be addressed: peichangwang1905@163.com.

Keywords: oligoclonal bands, mirror pattern bands, isoelectric focusing electrophoresis, immunofixation electrophoresis

Abbreviations: OCB, oligoclonal band; CSF, cerebrospinal fluid; IFE, immunofixation electrophoresis; QALB, CSF/serum albumin quotient; IgG, immunoglobulin G; MS, multiple sclerosis; CNS, central nervous system; IEF, isoelectric focusing electrophoresis; BBB, blood-brain barrier; ALB, albumin; MM, multiple myeloma; MGUS, monoclonal gammopathy of undetermined significance; MGNS, monoclonal gammopathy of neurological significance; GBS, Guillain-Barré syndrome; CIDP, chronic inflammatory demyelinating polyradiculoneuropathy; M protein, monoclonal protein

Laboratory Medicine 2023;54:380-387; https://doi.org/10.1093/labmed/lmac126

ABSTRACT

Objective: Mirror patterns are incidental types that accompany the analysis of the oligoclonal band (OCB) in cerebrospinal fluid (CSF). However, their interpretation remains controversial. In this study, we analyzed all graphic results of mirror patterns from 86 patients to provide an optimal interpretation scheme for mirror patterns.

Methods: Matched CSF and serum specimens were obtained from patients with various neurological disorders that required OCB analysis. A total of 86 patients were screened and serum immunofixation electrophoresis (IFE) was performed in all 86. The interobserver agreement for interpreting mirror patterns by visual inspection was tested. The method agreement between the visual inspection and IFE was also evaluated. The CSF/serum albumin quotient (QALB) was calculated to determine the blood-brain barrier integrity of all patients.

Results: Of the 86 patients with mirror patterns, 19.8% (17/86) had typical mirror bands and most (80.2%) had atypical mirror bands. There was a good agreement between the 2 observers in interpreting typical mirror patterns. However, kappa statistics analysis showed poor agreement regarding the interpretation of atypical mirror bands by visual observation alone (kappa value, –0.026 to 0.314 between 2 observers). The disagreement was pronounced between the visual inspection and validation of IFE (kappa value, –0.0238 to 0.176 between the first observer and IFE; –0.322 to 0.118 between the second observer and IFE). The normal QALB rates in the type V groups were significantly higher than those in the type IV group and the positive QALB rates in the type IV were significantly higher than those in the type V.

Conclusion: Visual inspection to interpret mirror pattern bands is unreliable. Considering the completely different clinical significance between type IV and type V and high risk of potential misinterpretations, it is necessary to perform IFE on all the atypical mirror types to discriminate atypical type IV from atypical type V.

Intrathecal oligoclonal immunoglobulin G (IgG) band synthesis has the highest specificity for clinically definite multiple sclerosis (MS) but may also occur in the context of central nervous system (CNS) infection and other inflammatory conditions.[1,2] Therefore, the detection of intrathecal IgG synthesis is a routine part of the cerebrospinal fluid (CSF) workup. Isoelectric focusing (IEF) on agarose gels followed by immunoblotting is widely recognized as the gold standard for detecting the presence of IgG OCBs.[2–4] There are 5 classic patterns in IEF gels. Type I patterns have no bands in the CSF and serum sample, type II have oligoclonal IgG bands in CSF not in the serum sample, and type III have oligoclonal bands in CSF and additional identical oligoclonal bands in the CSF and the serum sample.[5] Type IV and type V are mirror patterns (identical serum and CSF OCBs), which are indicative of serum proteins (including polyclonal and monoclonal immunoglobulins) entering the CSF by passive diffusion or through disruption of the blood-brain barrier (BBB). Albumin (ALB) produced only outside the CNS cannot easily cross an intact BBB. However, ALB can cross the BBB and enter the CSF when BBB is damaged by various CNS diseases. The CSF/serum ALB quotient (QALB) is the indicator most frequently used to evaluate BBB intactness.

The clinical significance of mirror pattern bands has been relatively clarified. Type IV, identical oligoclonal bands in CSF and serum samples, is indicative of a systemic, not intrathecal, immune reaction, with a leaky or normal or abnormal BBB and OCB passively transferred in CSF; and type V, monoclonal bands in CSF and serum samples, indicate the presence of a monoclonal IgG component. Typical type IV features

© The Author(s) 2022. Published by Oxford University Press on behalf of American Society for Clinical Pathology. All rights reserved. For permissions, please e-mail: journals.permissions@oup.com

Downloaded from https://academic.oup.com/labmed/article/54/4/380/6794938 by guest on 24 February 2025

irregularly spaced bands, whereas the typical type V has characteristic spaces in symmetric steps among bands and tend to be evenly distributed because the monoclonal proteins form clusters and are more prominent, with higher concentrations and stronger immunoreaction.[6–9] The interpretation of OCB is expert-dependent and involves visual analysis. Interobserver agreement in the interpretation of typical pattern types is very good.[10] However, in clinical practice, the typical mirror patterns are in the minority, and the bands in the vast majority of mirror patterns actually vary from person to person, showing either lower intensity of bands, a smaller number of bands, or both. Those are referred to as "atypical mirror pattern bands." Although it may be relatively easy to interpret the typical mirror pattern as typical type IV or typical type V, it is challenging to correctly interpret atypical mirror pattern bands depending only on visual observation, even for specialized laboratory personnel, causing misinterpretations of results with significant diagnostic implications.[11,12] Immunofixation electrophoresis (IFE) is a technique that possesses the high specificity (antigen-antibody reaction) and high sensitivity of monoclonal immunoglobulin to detect monoclonal components in serum, which is the definitive test for confirming the presence of M protein.[13] The main objective of our study was to evaluate the agreement between 2 experienced professionals and 2 methods, by visual inspection and IFE, in interpreting mirror patterns. Another aim was to determine whether emergence of mirror patterns necessarily indicates damage of the BBB by analyzing QALB levels. We present and analyze the characteristics of equivocal atypical mirror patterns in the form of representative OCB graphic results, which would explain why the interpretation of atypical mirror patterns by visual inspection alone is unsatisfactory.

Materials and Methods

Sample Acquisition and Grouping

We retrospectively studied the OCB data of consecutive patients who required lumbar puncture and underwent routine OCB assays with paired CSF and serum samples using isoelectric focusing followed by immunoblotting over a period of 4 years (May 2017 to January 2022) at Xuanwu Hospital. Inclusion criteria for further studies were those whose OCB results showed mirror pattern bands, that is, identical bands, in both CSF and serum. A total of 86 paired CSF/serum samples were screened. Following the recommendations of Freedman et al,[8] the OCB results were visually inspected and identified as either type IV or type V. Two laboratory experts experienced in OCB analysis were involved in the visual inspection in a blinded fashion.

TABLE 1. Interobserver Agreement on IEF Mirror Pattern Types by Visual Inspection Alone

IEF—Visual Inspection					
Observer 1			Observer 2		
Classification	Typical type IV	Typical type V	Atypical type IV	Atypical type V	Total
Typical type IV	11	0	0	0	11 (12.8%)
Typical type V	0	6	0	0	6 (6.9%)
Atypical type IV	0	0	22	4	26 (30.2%)
Atypical type V	0	0	29	14	43 (50%)
Total	11 (12.8%)	6 (6.9%)	51 (59.3%)	18 (20.9%)	86

IEF, isoelectric focusing electrophoresis.

FIGURE 1. Typical type IV and V. Typical immunoglobulin G (IgG) mirror patterns detected in paired cerebrospinal fluid (CSF)/serum sample and corresponding serum results from immunofixation electrophoresis (ELP). Arrows indicate the prominent bands regions. Anode is at the top (the followings are the same). A, Typical type IV and immunofixation of corresponding serum sample. B, Typical type V and immunofixation of corresponding serum sample.

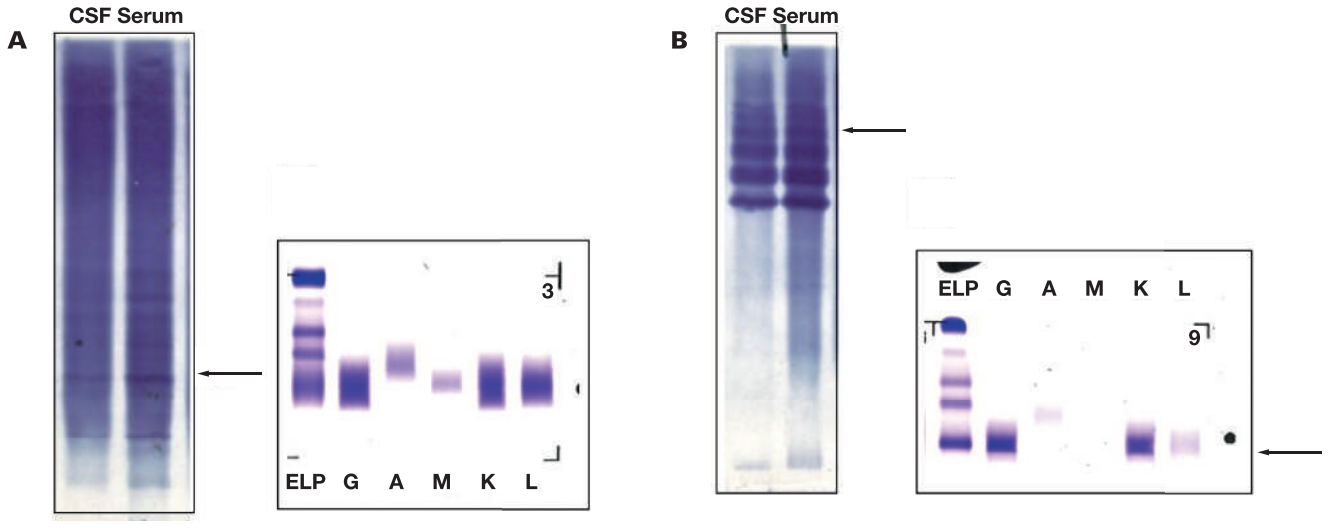

Downloaded from https://academic.oup.com/labmed/article/54/4/380/6794938 by guest on 24 February 2025

Subsequently, all 86 serum samples were subjected to IFE to determine the presence or absence of M protein so that the controversial mirror patterns could be validated as either type IV or type V. The 86 patients were classified into 2 groups according to their OCB results. The first group included typical type IV and typical type V, which could be directly and accurately interpreted based on visual observation alone without the help of IFE verification. The second group comprised the samples with bands that seemed like type V but were actually type IV or vice versa—they were defined as atypical type IV and atypical type V.

Oligoclonal Band Determination and Immunofixation Electrophoresis

IgG and ALB in CSF and serum were quantified using kinetic nephelometry (Beckman Coulter IMMAGE800). Paired serum/CSF samples were used to analyze the IgG-specific OCB performed with IgG IEF on agarose gel, followed by immunofixation (HYDRASYS FOCUSING, Sebia).[14,15] Before IEF, the serum samples were diluted in deionized water to reach the same IgG concentration as that of the parallel CSF samples. Serum samples were run in parallel with CSF samples. The patterns were interpreted qualitatively by comparing the presence or absence of OCB in CSF and serum. The presence of 2 or more bands in the electrophoresis lanes was considered to be a positive reaction.[8] The band patterns of IEF that matched both types IV and type V were our research objects.

The IFE was performed using a commercial hydrogel kit with the Sebia HYDRASYS 2 automated electrophoresis system (Sebia). The IFE method used polyclonal antihuman serum samples to identify IgG, IgA, IgM, and total light chains κ and λ.

Reference Standard Criteria for QALB

The QALB was calculated to determine BBB integrity as follows[16]: [CSF albumin (mg/mL)/serum albumin (mg/mL)] × 1000. The calibration standards were prepared as follows: normal: QALB ≤7; mild impairment: 7< QALB ≤10; moderate impairment: 10< QALB ≤30; severe impairment: QALB >30.

Statistical Analysis

IBM SPSS 26.0 software (SPSS) was used for the statistical analysis. The frequency distributions were analyzed using the χ^2 test. Comparisons of nonparametric data, such as the evaluation of interobserver agreement, were analyzed by kappa statistics. A K-value <0 indicated poor agreement, 0.01 to 0.2 slight, 0.21 to 0.4 fair, 0.41 to 0.6 moderate, 0.61 to 0.8 substantial, and 0.81 to 1.0 approximately perfect agreement. A *P* value <.05 was considered significant statistically.

Results

There was very good agreement with respect to the judgment and interpretation for typical mirror patterns (17/86) between the 2 observers depending on results from IEF alone (**TABLE 1**) (according to the consensus classification,[5] typical IV and typical V are shown in **FIGURE 1**); however, when identifying atypical mirror patterns (69/86), which showed weak, indistinct, and fewer bands, interobserver agreement by visual inspection was slight (K-value 0.144, **TABLES 1** and **2**). The results of IFE for these 69 serum samples, with atypical mirror patterns included 44 atypical type IV and 25 atypical type V. Disagreements between observer 1 and IFE and observer 2 and IFE were substantial (K-value = −0.031 and −0.102, respectively; **TABLES 2** and **3**). Therefore, the correct interpretation of mirror patterns by visual inspection alone was unreliable.

There were 17 (19.8%) typical mirror patterns, including 11 typical type IV and 6 typical type V, which were easily identified by visual inspection. Only 1 graph of typical type IV and 1 of typical type V were chosen as representative and are shown in **FIGURE 1** (other results are not shown). The typical type IV pattern is irregularly spaced bands in both CSF and serum. The typical type V pattern has spaces in symmetric steps among bands and tends to be evenly distributed because the monoclonal proteins form clusters and are more prominent with higher concentrations and stronger immunoreaction. The others (80.2%) were atypical mirror patterns including 44 atypical type IV and 25 atypical type V. Six atypical type IV results from IEF and corresponding serum IFE were used to represent 44 atypical type IV, as shown in **FIGURE 2**. All the patterns from IEF in **FIGURE 2** were highly prone to confuse observers because they look like type V if reviewed without the confirmation of IFE. The 6 representative atypical type V cases from IEF and the corresponding IFE results are shown in **FIGURE 3**. These seemed to be type IV, which made them subject to disagreement among experienced observers when evaluated by visual observation alone.

Normal QALB values were used as the reference standards, and positive cases were defined as those exceeding the upper limit. The QALB stratification analysis in the 4 groups (typical type IV, typical type V, atypical type IV, atypical type V) showed that the ranges of QALB ≤7 (normal) were dominant in both typical type V (83.3%) and atypical type V groups (72%), and the ranges of 10< QALB ≤7 were dominant in both typical type IV (54.5%) and atypical type IV groups (47.7%). The results showed the normal QALB rates in type V groups were significantly higher than those in the type IV group and the positive QALB rates in the type IV were significantly higher than those in the type V (**TABLE 4**, $P < .01$). Our results

TABLE 2. Interobserver Agreement Analysis on Differentiating Atypical Mirror Patterns and Agreement Analysis Between Visual Inspection and IFE/Combined IFE

	K-value (95% CI)	*P* value
IEF alone, interobserver	0.144 (−0.026–0.314)	.115
Observer 1 vs IEF+IFE	−0.031 (−0.0238–0.176)	.746
Observer 2 vs IEF+IFE	−0.102 (−0.322–0.118)	.385

CI, confidence interval; IEF, isoelectric focusing electrophoresis; IFE, immunofixation electrophoresis.

TABLE 3. Agreement on IEF Atypical Mirror Pattern Types by Visual Inspection and Combined IFE

IEF alone	IEF+IFE			IEF alone	IEF+IFE		
Observer 1	Atypical type IV	Atypical type V	Total	Observer 2	Atypical type IV	Atypical type V	Total
Atypical type IV	16	10	26	Atypical type IV	31	20	51
Atypical type V	28	15	43	Atypical type V	13	5	18
Total	44	25	69	Total	44	25	69

Downloaded from https://academic.oup.com/labmed/article/54/4/380/6794938 by guest on 24 February 2025

FIGURE 2. Atypical type IV. The bands of those samples appear to be type V (space in symmetric steps among bands and relatively prominent bands). A, B, C, D, E, and F are 6 representative oligoclonal band results and corresponding serum results from immunofixation electrophoresis (ELP) that show no specific bands. CSF, cerebrospinal fluid.

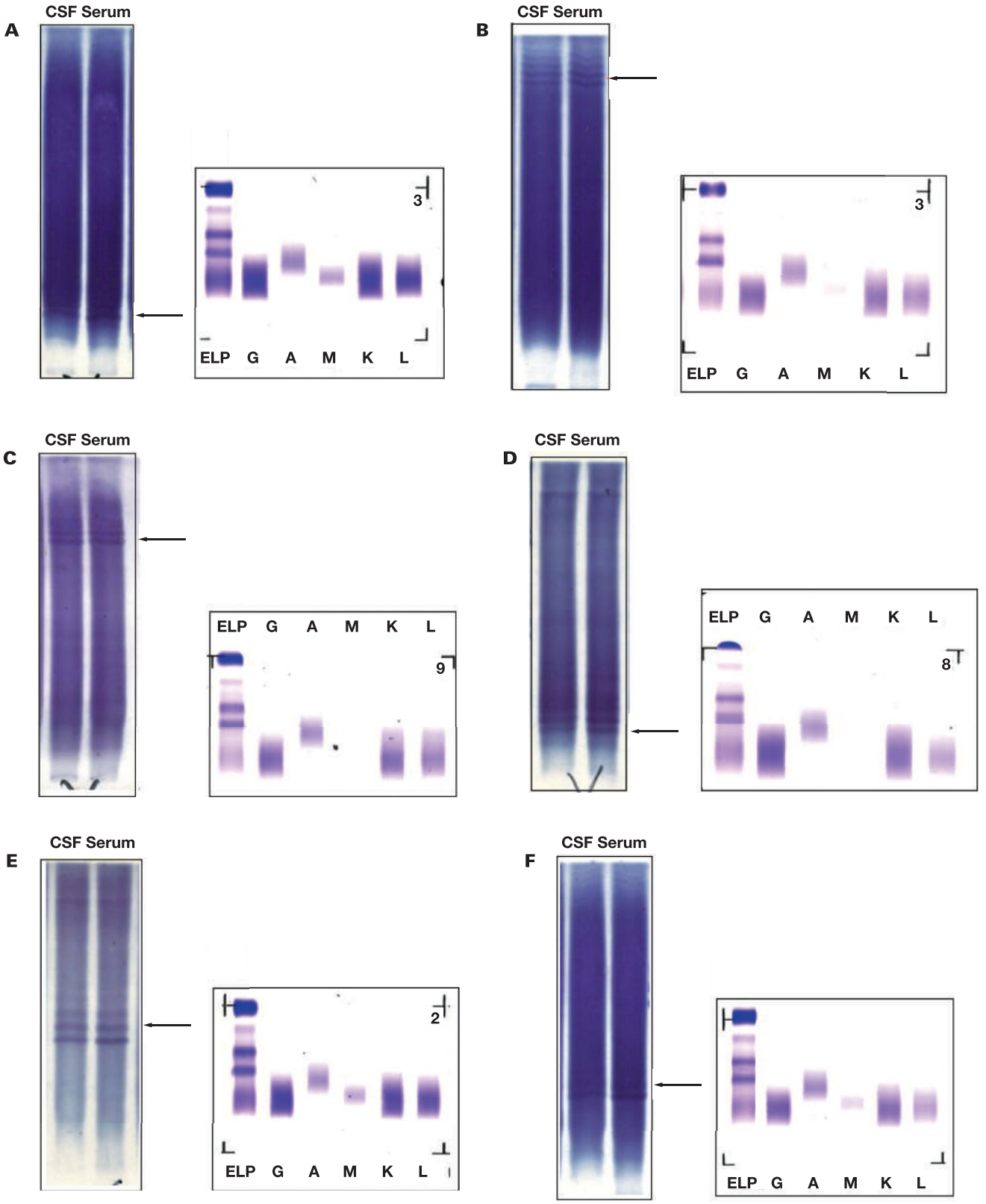

Downloaded from https://academic.oup.com/labmed/article/54/4/380/6794938 by guest on 24 February 2025

FIGURE 3. Atypical type V. The bands of those samples appear to be type IV (irregularly spaced bands). A, B, C, D, E, and F are 6 representative oligoclonal band results and corresponding serum results from immunofixation electrophoresis (ELP) that show obvious positive monoclonal (M) protein (B, C, D, E) or weak positive M protein (A, F) (with immunoglobulin G (IgG)-κ or IgG-λ). CSF, cerebrospinal fluid.

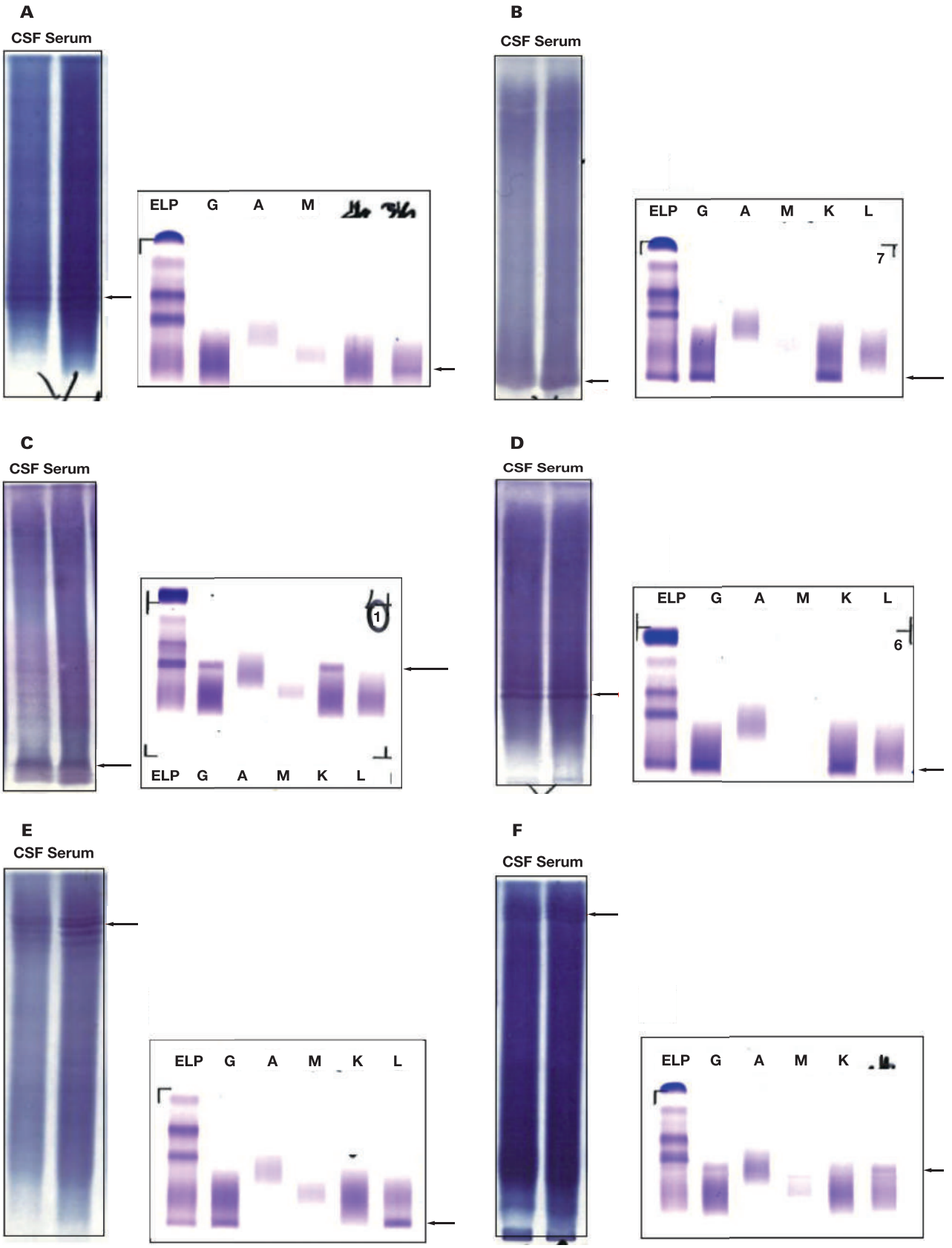

Downloaded from https://academic.oup.com/labmed/article/54/4/380/6794938 by guest on 24 February 2025

2023;54:380-387 | https://doi.org/10.1093/labmed/lmac126

TABLE 4. Comparison of the QALB Positive Rates in the Four Groups[a]

Variable QALB	Type IV		Type V		*P* value
	Typical type IV (n = 11)	Atypical type IV (n = 44)	Typical type V (n = 6)	Atypical type V (n = 25)	
QALB ≤7 (normal)	2 (18.2)[b]	11 (25)[b]	5 (83.3)	18 (72)	<.01
7< QALB ≤10	6 (54.5)[b]	21 (47.7)[b]	1 (16.7)	6 (24)	<.01
10< QALB ≤30	2 (18.2)	10 (22.7)	0 (0)	1 (4)	—
QALB >30	1 (9.1)	2 (4.5)	0 (0)	0 (0)	—
Total abnormal	9 (81.8)[b]	33 (75)[b]	1 (16.7)	7 (28)	<.01

QALB, cerebrospinal fluid/serum albumin quotient.
[a]Data are given as No. (%).
[b]Compared to type V group (P < .01).

indicate that the emergence of mirror pattern bands did not necessarily indicate an abnormal BBB; passive transfer in the CSF from serum was also a possible reason. Moreover, the permeability of BBB in type IV groups was significantly higher than that in type V ($P < .01$).

Discussion

The detection of OCB is routinely applied in the diagnostic workup of inflammatory CNS disorders, especially in the early stage of MS.[8,17] The vast majority of previous studies have focused on the MS and CSF-restricted OCBs, that is, type II.[11,15,18–21] Mirror pattern bands are incidental findings during CSF OCB analysis.[22] They are not uncommon; however, the correct interpretation of mirror patterns has not been given adequate attention. The discrimination between the 2 mirror patterns, type IV and type V, by visual inspection is controversial, and misinterpretation often occurs. In this retrospective study, we first demonstrated that rater-dependent interpretation of mirror patterns was untrustworthy and also illustrated why the high rate of misinterpretation occurs, by means of 86 patients with a variety of neurological disorders whose OCB results showed mirror patterns. We then divided the 86 samples into 2 groups: typical mirror patterns (17/86, 19.8%) and atypical mirror patterns (69/86, 80.2%). According to the consensus results of IEF, agreement concerning typical mirror patterns between 2 experienced observers was satisfactory by visual observation alone (11 typical type IV patterns and 6 typical type V patterns were correctly identified by both observers). However, interobserver disagreement was prominent in identification of atypical mirror patterns. Indeed, the differentiation between atypical type IV and atypical type V by visual inspection was disputable in some cases. There are 2 reasons that could account for this. First, IEF is the most sensitive method for discriminating monoclonal and oligoclonal bands because IEF can capture any abnormal overexpression of IgG both in CSF and serum in the form of bands.[23,24] The IEF can resolve what would be a single band in other electrophoretic techniques, for example, by IFE into multiple bands differing by 1 U of charge.[8,25] This peculiarity is probably due to posttranslational modifications such as glycosylation. This is 1 reason why it is hard to distinguish between monoclonal and oligoclonal bands by visual observation. Besides, although IFE is widely regarded as the gold standard technique to detect monoclonal components in serum, the relatively weaker capability of IFE than IEF[26] to separate immunoglobulins makes IFE the poorer choice to detect OCBs. This also might account for why an IFE gel often looks like a polyclonal without bands even if OCBs appear in the gel. Therefore, IFE was used in this study solely to rule out or confirm the presence of monoclonal proteins rather than verifying the presence of OCBs in serum. Second, every individual has been exposed to different antigens during their life and unique IEF patterns may indicate this when some IgG clones are overrepresented. Both of these factors contribute to large individual differences in mirror patterns, which exacerbate the difficulty of interpretation.

On one hand, in some individuals, systemic inflammation and immune response are very active, which results in strong intensity of mirror bands that appear to share similar characteristics with monoclonal bands. In this study, for example, the bands in **FIGURE 2E** were sharp and clearly visible and without the confirmation of IFE, the evaluation as type V would be arbitrary. Misdiagnosis or delayed diagnosis would be inevitable. On the other hand, in some cases, some weak and less sharp bands than typical type V were mistaken for type IV by visual observation. In our study, the impressive case shown in **FIGURE 3B** was a good case in point. The bands were relatively weak and near the cathode, which was not easy to detect at the first glance, and the pattern was evaluated as type V. Both observers in our study failed to precisely recognize this kind of pattern. Interestingly, this case was diagnosed as multiple myeloma (MM) during hospitalization due to the results of the OCB test in the early stage. Moreover, it was also worth noting that in some cases, bands such as shown in **FIGURE 3A** and **3F**, whose IEF results resembled those of type IV, had relatively weak and subtle pathological bands on both IEF and IFE. This was why those cases were easily misinterpreted as type IV. Another example was 2 cases shown in **FIGURE 2F** and **FIGURE 3D**, respectively. The bands in the IEF were very similar in both location and intensity; however, they were actually type IV and type V after the verification of IFE. Interpretation of atypical mirror pattern types, that is, those with few and weak bands, is critical, and misinterpretation might yield false-negative or false-positive results even by experienced laboratory personnel.

The secretion of a monoclonal immunoglobulin, referred to as a monoclonal protein (M protein), is the hallmark of monoclonal gammopathies, comprising a spectrum of clonal plasma cell disorders.[27] Monoclonal gammopathy of undetermined significance (MGUS), MM, and Waldenström macroglobulinemia belong to these disorders. The MGUS is present in more than 3% to 4% of the population older than 50 years[28] and is regarded as a premalignant precursor of MM. It is often categorized as a low tumor burden disease as well,[29] and almost all cases of MM are preceded by MGUS.[27,30] Monoclonal gammopathies or underlying lymphoplasmacytic disorders can affect the peripheral nervous system by various mechanisms.[31] Almost 10% of patients with neuropathy of unknown cause have paraprotein,[32] which is defined as monoclonal gammopathy of neurological significance (MGNS). MGUS is most often asymptomatic; however, MGNS should be considered when

Downloaded from https://academic.oup.com/labmed/article/54/4/380/6794938 by guest on 24 February 2025

M protein and peripheral nervous disorders are both present.[33] In our study, all 86 patients came to our hospital with a variety of neurological disorders, such as peripheral neuropathy (weakness and numbness in the arms and hands, sensory and motor dysfunctions), headache, confusion, and slurred speech and so forth. Among 25 patients with atypical type V, 2 cases were diagnosed as MM, 4 cases were POMES (polyneuropathy, organomegaly, endocrinopathy, M-protein, skin changes) syndrome, 7 cases were MGUS, and 12 cases were given MGNS as the final diagnosis. Among 44 patients with atypical type IV, according to the final diagnosis, 6 cases were diagnosed as Guillain-Barrè syndrome (GBS), 12 cases were chronic inflammatory demyelinating polyradiculoneuropathy (CIDP), 6 cases were peripheral neuropathy, 6 cases were autoimmune diseases including systemic lupus erythematosus and Behçet's disease, 11 cases were demyelinating diseases, and 3 cases were autoimmune encephalitis. Moreover, the results of QALB stratification analysis on the 86 patients were basically consistent with clinical diagnosis and disease feature; for example, patients with CIDP and GBS with systemic inflammation have different degrees of BBB damage and type IV is dominant in those patients. The presence of OCBs is due mostly to the increased BBB permeability. The MM patients mostly have normal BBB, and type V from passive diffusion of serum dominates in those patients.

The detection of M protein was an incidental finding of the OCB test, which was originally meant to investigate the presence or absence of intrathecal immune responses, especially MS. The onset of MS usually shares similar symptoms with peripheral nervous system abnormalities. Therefore, monoclonal gammopathy must be differentiated from systemic inflammation if mirrored IgG bands are present in both CSF and serum. As a routine hospital admission test, OCB by IFE could provide clues for a diagnosis of monoclonal gammopathy in a timely manner. Correct interpretation of OCB patterns, especially the mirror pattern types, is a prerequisite.

Our findings indicate both poor interobserver agreement and rather poor agreement between direct visual inspection and verification of IFE for the evaluation of atypical mirror patterns. To reduce the expert-dependent variability and unreliability and to diminish errors in visual analysis of atypical mirror pattern types, it is necessary to perform IFE on every patient serum whose paired CSF/serum OCB result shows mirror pattern types. Our findings are not aimed at solving the diagnostic dilemma between MS, MGUS, MM, and other peripheral neuropathies, but to eliminate misinterpretations of atypical pattern bands and provide timely and appropriate diagnostic thinking.

There are some limitations of the study. Owing to page limitations, it is unlikely that all 69 atypical mirror patterns will be presented in the form of graphical data. It is also inevitable that there is a loss of image detail to some extent when OCB images are scanned. However, the prominent disagreement in interpreting mirror patterns bands by visual observation is enough to draw attention, especially considering the different clinical significance of mirror pattern types. In addition, there is a need for long-term follow-up studies of the atypical type V pattern regarding whether the appearance of weak and indistinct M proteins (eg, cases in **FIGURE 3A** and **3F**) is transient or permanent and what the prognostic features are.

Conclusions

There is poor interobserver agreement and rather poor agreement between direct visual inspection and combined IFE for interpreting atypical mirror patterns. To reduce the expert-dependent variability and unreliability and to diminish errors of visual analysis on atypical mirror pattern types, it is crucial to perform IFE on every patient serum whose paired CSF/serum OCB result showed mirror pattern types.

Acknowledgments

This study was approved by the Ethics Committee of Xuanwu Hospital of the Capital Medical University (Beijing, China), and written informed consent was obtained from all participants. The datasets generated and/or analyzed during the present study are available from the corresponding author on reasonable request.

Conflict of Interest Disclosure

The authors have nothing to disclose.

REFERENCES

1. Davies G, Keir G, Thompson EJ, Giovannoni G. The clinical significance of an intrathecal monoclonal immunoglobulin band: a follow-up study. *Neurology.* 2003;60(7):1163–1166.
2. Link H, Huang YM. Oligoclonal bands in multiple sclerosis cerebrospinal fluid: an update on methodology and clinical usefulness. *J Neuroimmunol.* 2006;180(1–2):17–28.
3. Villar LM, Masterman T, Casanova B, et al. CSF oligoclonal band patterns reveal disease heterogeneity in multiple sclerosis. *J Neuroimmunol.* 2009;211(1–2):101–104.
4. Abraira V, Alvarez-Cermeno JC, Arroyo R, et al. Utility of oligoclonal IgG band detection for MS diagnosis in daily clinical practice. *J Immunol Methods.* 2011;371(1–2):170–173.
5. Andersson M, Alvarez-Cermeno J, Bernardi G, et al. Cerebrospinal fluid in the diagnosis of multiple sclerosis: a consensus report. *J Neurol Neurosurg Psychiatry.* 1994;57(8):897–902.
6. Chen Y. Multiple cerebrospinal fluid bands with accompanying serum bands. *Clin Chem.* 2014;60(12):1582–1583.
7. Petzold A. Intrathecal oligoclonal IgG synthesis in multiple sclerosis. *J Neuroimmunol.* 2013;262(1–2):1–10.
8. Freedman MS, Thompson EJ, Deisenhammer F, et al. Recommended standard of cerebrospinal fluid analysis in the diagnosis of multiple sclerosis: a consensus statement. *Arch Neurol.* 2005;62(6):865–870.
9. Chen Y, Watts G. Systemic inflammation or monoclonal gammopathy? *Arch Pathol Lab Med.* 2011;135(12):1527–1529.
10. Nováčková LZ. Detection of oligoclonal IgG bands in cerebrospinal fluid and serum: comparison between commercial immunofixation method and home-made affinity immunoblotting method and evaluation of interobserver agreement. *Klin Biochem Metab.* 2011;19(40):229–233.
11. Carta S, Ferraro D, Ferrari S, Briani C, Mariotto S. Oligoclonal bands: clinical utility and interpretation cues. *Crit Rev Clin Lab Sci.* 2022:1–14.
12. Awad A, Hemmer B, Hartung HP, Kieseier B, Bennett JL, Stuve O. Analyses of cerebrospinal fluid in the diagnosis and monitoring of multiple sclerosis. *J Neuroimmunol.* 2010;219(1–2):1–7.
13. Zhu S, Li W, Lin M, Li T. Serum protein electrophoresis and immunofixation electrophoresis detection in multiple myeloma. *J Coll Physicians Surg Pak.* 2021;30(7):864–867.
14. Sadaba MC, Gonzalez Porque P, Masjuan J, Alvarez-Cermeno JC, Bootello A, Villar LM. An ultrasensitive method for the detection of oligoclonal IgG bands. *J Immunol Methods.* 2004;284(1–2):141–145.
15. Hegen H, Zinganell A, Auer M, Deisenhammer F. The clinical significance of single or double bands in cerebrospinal fluid isoelectric

Downloaded from https://academic.oup.com/labmed/article/54/4/380/6794938 by guest on 24 February 2025

focusing: a retrospective study and systematic review. *PLoS One.* 2019;14(4):e0215410.

16. Uher T, Horakova D, Tyblova M, et al. Increased albumin quotient (QAlb) in patients after first clinical event suggestive of multiple sclerosis is associated with development of brain atrophy and greater disability 48 months later. *Mult Scler.* 2016;22(6):770–781.
17. Polman CH, Reingold SC, Banwell B, et al. Diagnostic criteria for multiple sclerosis: 2010 revisions to the McDonald criteria. *Ann Neurol.* 2011;69(2):292–302.
18. Simonsen CS, Flemmen H, Lauritzen T, Berg-Hansen P, Moen SM, Celius EG. The diagnostic value of IgG index versus oligoclonal bands in cerebrospinal fluid of patients with multiple sclerosis. *Mult Scler J Exp Transl Clin.* 2020;6(1):2055217319901291.
19. Avasarala JR, Cross AH, Trotter JL. Oligoclonal band number as a marker for prognosis in multiple sclerosis. *Arch Neurol.* 2001;58(12):2044–2045.
20. Link H, Huang Y-M. Oligoclonal bands in multiple sclerosis cerebrospinal fluid: an update on methodology and clinical usefulness. *J Neuroimmunol.* 2006;180(1):17–28.
21. Franciotta D, Avolio C, Lolli F. Between-laboratory variability in oligoclonal IgG band numbering. *Clin Chem.* 2005;51(1):270–272.
22. Chen Y. Laboratory performance on reporting monoclonal gammopathy during cerebrospinal fluid oligoclonal banding analysis from external quality assessment surveys. *J Appl Lab Med.* 2018;3(2):261–266.
23. Cornell FN. Isoelectric focusing, blotting and probing methods for detection and identification of monoclonal proteins. *Clin Biochem Rev.* 2009;30(3):123–130.
24. Wurster U. The clinical significance of an intrathecal monoclonal immunoglobulin band: a follow-up study. *Neurology.* 2004;62(7):1237.
25. Chen Y. Laboratory performance on reporting monoclonal gammopathy during cerebrospinal fluid oligoclonal banding analysis from external quality assessment surveys. *J Appl Lab Med.* 2018;3(2):261–266.
26. Kušnierová P, Zeman D, Revendová K, Dlouhý O. Detection of monoclonal free light chains by immunofixation electrophoresis and isoelectric focusing - comparison with the quantitative method of determination. *Scand J Clin Lab Invest.* 2020;80(7):556–561.
27. Chaudhry HM, Mauermann ML, Rajkumar SV. Monoclonal Gammopathy-associated peripheral neuropathy: diagnosis and management. *Mayo Clin Proc.* 2017;92(5):838–850.
28. Go RS, Swanson KM, Sangaralingham LR, Habermann EB, Shah ND. Clinical prevalence (diagnosed cases) of monoclonal gammopathy of undetermined significance in the US: estimating the burden on health care. *Leukemia*. 2016;30(6):1443–1446.
29. Willrich MAV, Murray DL, Kyle RA. Laboratory testing for monoclonal gammopathies: focus on monoclonal gammopathy of undetermined significance and smoldering multiple myeloma. *Clin Biochem.* 2018;51:38–47.
30. Dhodapkar MV. MGUS to myeloma: a mysterious gammopathy of underexplored significance. *Blood.* 2016;128(23):2599–2606.
31. Naddaf E, Mauermann ML. Peripheral neuropathies associated with monoclonal gammopathies. *Continuum (Minneap Minn).* 2020;26(5):1369–1383.
32. Visentin A, Pravato S, Castellani F, et al. From biology to treatment of monoclonal gammopathies of neurological significance. *Cancers (Basel).* 2022;14(6).
33. Abildgaard N. [Monoclonal gammopathies]. *Ugeskr Laeger.* 2021;183(42).

Downloaded from https://academic.oup.com/labmed/article/54/4/380/6794938 by guest on 24 February 2025

Long-Term Dynamic of Anti-TrimericS and Anti-RBD Antibodies in Naive and COVID-19 Recovered mRNA-1273 Vaccine Recipients

Annick Ocmant, PharmD,[1] Sandrine Roisin, MD,[1] Delphine Mathieu, MD,[2] Jonathan Brauner, MD,[1] Frédéric De Leener, MD[3]

[1]Department of Laboratory Medicine, Centre Hospitalier Universitaire (CHU) de Tivoli, La Louvière, Belgium, [2]Department of Infectious Diseases, Centre Hospitalier Universitaire (CHU) de Tivoli, La Louvière Belgium, [3]Department of Internal Medicine, Centre Hospitalier Universitaire (CHU) de Tivoli, La Louvière Belgium. *To whom correspondence should be addressed: aocmant@chu-tivoli.be.

Keywords: SARS-CoV-2, serology, RBD, spike protein, vaccine, kinetic

Abbreviations: IgG, immunoglobulin G; RBD, receptor-binding domain; S, spike; PCR, polymerase chain reaction; BAU, binding antibodies units; AU, arbitrary units; IQR, interquartile range; CE, European Conformity

Laboratory Medicine 2023;54:388-391; https://doi.org/10.1093/labmed/lmac127

ABSTRACT

Objective: Patients and physicians are increasingly requesting their clinical laboratory to provide SARS-CoV-2 serology interpretation. Our study aimed to assess the evolution of SARS-CoV-2 antibodies in Moderna-vaccinated health care workers.

Methods: We analyzed the evolution of mRNA-1273 (Moderna)–elicited antibodies by 2 high-throughput assays, TrimericS IgG (Diasorin) and SARS-CoV-2 IgG-II (Abbott).

Results: After the first injection, the COVID-19–recovered vaccinees showed a serological response as strong as that observed 1 month after the second injection in participants without COVID-19 history. Although remaining above the positivity thresholds, the TrimericS immunoglobulin G (IgG) and anti-RBD (receptor-binding domain) IgG levels fell considerably between 1 and 7 months postvaccination, dropping to 10.6% and 13% for the COVID-19 recovered subgroup and to 11.7% and 9.3% for the COVID-19 naive subgroup.

Conclusion: Regardless of the test used, a decrease in circulating anti-SARS-CoV-2 IgG levels should be expected a few months after vaccination. As this decline does not preclude the efficacy of immune response, caution is necessary when interpretating postvaccination serological data.

Vaccination strategy turned out to be of paramount importance in the fight against the severe acute respiratory syndrome caused by the SARS-CoV-2 virus. Several vaccines were widely permitted and used to reduce mortality and morbidity as well as to halt the spread of the virus; the mRNA-1273 vaccine, encoding the prefusion stabilized full-length spike (S) protein of SARS-CoV-2, has been used in worldwide mass vaccination programs.

Various studies about postvaccination immune status have been published. Their designs differ depending on the target antibody, time since vaccination, type of vaccine administered, and the studied population. More specifically, the immunoassays varied according to the detected antibodies that were directed to either the SARS-CoV-2 nucleocapsid, the S protein[1] or the receptor-binding domain (RBD).[2] Although the serology after BNT612b25 (Pfizer-BioNTech) vaccination has been largely studied, serological data after mRNA-1273 (Moderna) vaccination are scarcer. In a trial of about 30 participants, the persistence of anti-RBD for up to 6 months after the second mRNA-1273 dose was clearly shown.[3,4] In a larger cohort, antibodies to S1/S2[1] or RBD[5] had already declined after 3 and 4 months and decayed more severely by 6 months after vaccination, especially among those who had not suffered from COVID-19 before the vaccination.[6]

We present here a longitudinal study to assess the development of SARS-CoV-2 antibodies in Moderna-vaccinated health care workers. Two commercially available high-throughput serological tests were assumed as the most suitable to our purpose. The quantitative LIAISON SARS-CoV-2-TrimericS IgG assay (Diasorin) was selected because it uses a recombinant trimer of S1/S2 close to the native transmembrane S glycoprotein as the capture antigen. The S1 subunit includes the RBD that interacts with angiotensin-converting enzyme-2 host cell receptor. The assay SARS-CoV-2 IgG II quant (Abbott) was also selected here, since it points to the RBD antigen, one of the most immunogenic regions of the coronavirus and the main target for neutralizing antibodies.[7] For both immunoassays, a dilution protocol was used to provide a more accurate appraisal of antibodies rates.[8] In contrast to the study of Kanji et al,[9] which used the same tests, we collected a baseline blood sample to categorize the vaccinees as COVID-19 naive or infection-recovered before the first dose of vaccine.

Material and Methods

This study was conducted from December 2020 to September 2021 and included 620 serum samples from 155 health care workers (120 females,

© The Author(s) 2022. Published by Oxford University Press on behalf of American Society for Clinical Pathology. All rights reserved. For permissions, please e-mail: journals.permissions@oup.com

Downloaded from https://academic.oup.com/labmed/article/54/4/388/6885749 by guest on 24 February 2025

35 males) of a university hospital in Belgium. The median age was 44 years (range 25–67 years). As recommended for the Moderna vaccine, the 2-dose series was administrated 28 days apart. For each participant, a blood sample was obtained at 3 different points in time: 1 month (28 days) after the first mRNA-1273 injection (T1), then 1 month (range, 25–38 days) (T2) and 7 months (range, 197–225 days) (T3) after the second injection. An initial specimen (T0) collected during the month preceding the first injection was also obtained. All samples were frozen until analyzed. The study was approved by an ethics committee (approval number1386) in accord with the ethical standards established by the institution in which the experiments were performed. All participants also filled out a questionnaire about their clinical manifestations in the case of a COVID-19 infection prior to vaccination.

Participants were classified into 2 groups, the COVID-19–recovered and the COVID-19–naive subgroups, based on their prevaccination status with regard to COVID-19 infection. A COVID-19 infection was defined by either a positive reverse transcription polymerase chain reaction (PCR) on a nasopharyngeal swab or, in case no PCR was available, by a positive serology to Tri-S-CoV-2 IgG or CoV-2 IgG II prior to vaccination. We also considered 2 seronegative people who had undeniably suffered from a symptomatic form of COVID-19 infection a few days around the first (T0) blood sampling.

Blood specimens were analyzed according to the manufacturer's instructions[10,11] using the Diasorin SARS-CoV-2 TrimericS IgG assay (Tri-S-CoV-2 IgG) on a LIAISON XL automate and the Abbott SARS-Cov-2 IgG II quant on an Alinity i platform (CoV-2 IgG-II). The SARS-CoV-2 TrimericS IgG results are reported in binding antibodies units (BAU) per milliliter since they are aligned on the first World Health Organization International Standard for anti-SARS-CoV-2 immunoglobulin binding activity (NIBSC 20-136). The Diasorin conversion factor is BAU/mL = 2.6 × AU/mL (arbitrary units/mL). The positivity thresholds were 33.8 BAU/mL for Diasorin and 50 AU/mL for Abbott. The suppliers' instructions for use mentioned a high positive concordance between those cutoffs and a positive neutralization test, namely a microneutralization titer ≥1/10 for Diasorin and a plaque reduction neutralization titer ≥1/20 for Abbott. In addition, postvaccinal antibody levels were also assessed against other limits related to high neutralizing antibodies titers. According to the Diasorin CE-marked notice, a high microneutralization assay titer threshold (≥1:80) corresponds to antibody levels higher than 520 BAU/mL, whereas the threshold of 1:80 is 960 AU/mL in the Abbott kit.

When results were over the analytical interval, a 20-fold dilution (Liaison XL) or a 2-fold dilution (Alinity i) made it possible to extend the range of measurement from 2080 to 41,600 BAU/mL and from 40,000 to 80,000 AU/mL, respectively.

Statistical analysis was performed using GraphPadPrism 8.4.2 (GraphPad).

Results

A prevaccinal SARS-CoV-2 infection was identified in 34.2% (53/155) of the participants; Tri-S-CoV-2 IgG was the only antibody present in 3 of those 53, CoV-2 IgG II in 5 of the 53, and both were positive in 37 of the 53. An infection was identified for 6 of the 53 seronegative participants from a positive reverse transcription PCR test. Finally, 2 of the 53 suffered from an evident symptomatic COVID-19 disease around the time of the T0 blood draw for which they were seronegative at baseline. Forty-seven were symptomatic; the illness was characterized mostly by generalized symptoms such as fever, fatigue (41/47), or respiratory impairment (33/47). Anosmia or agueusia was present in 25 of the 47, and 13 of 47 had abdominal or other minor symptoms.

Before vaccination (T0), all COVID-19–naïve subjects were seronegative for SARS-CoV-2 IgG. Among the COVID-recovered cohort, the median (interquartile range, IQR) antibody levels were 87 BAU/mL (IQR: 30-145 BAU/mL) for TrimericSCoV-2 IgG and 187 AU/mL (IQR: 69-631 AU/mL) for CoV-2 IgG II. At T1, TrimericSCoV-2 IgG as well as CoV-2 IgG II were positive in all of the 155 participants. The concentrations of Tri-S-CoV-2 IgG were significantly ($P < .0001$) higher in the COVID-19–recovered subgroup with median (IQR) values of 11,600 BAU/mL (IQR: 5315–22,400 BAU/mL) compared to 938.5 BAU/mL (IQR: 534–1445 BAU/mL) among those with no history of infection. The evolution of CoV-2 IgG II followed the same trend with 25,439 AU/mL (IQR: 11,608–52,915 AU/mL) and 3077 AU/mL (IQR: 1519–5070 AU/mL), respectively.

The second injection boosted the production of antibodies, but the magnitude of the response varied, with the strongest increase observed among noninfected vaccinees. Tri-S-CoV-2 IgG reached 3985 BAU/mL (IQR: 2910–6143 BAU/mL) and CoV-2 IgG II increased to 16796 AU/mL (IQR: 12,982–24,755 AU/mL). In contrast, among COVID-19–recovered participants, the Tri-S-CoV-2 IgG levels are similar (P = not significant) to T1 (median 11,500 BAU/mL; IQR: 6,330–20,950) whereas CoV-2 IgG II are slightly higher (median 31702 AU/mL; IQR: 23,525–52,684 AU/mL) as compared to T1 ($P = .0025$). It is worth mentioning that at T1, the vaccinees who recovered from COVID-19 mounted a higher anti-S response ($P < .0001$) and an anti-RBD response as strong as that observed at T2 in COVID-naive individuals ($P = .0138$).

As shown in **FIGURE 1**, the humoral immune response 7 months after the second injection (T3) was reduced in comparison to that observed after 1 month (T2), although remaining above the predefined positivity thresholds. The seropositive rates notably remained at 100% for both assays, but the antibody levels significantly ($P < .0001$) declined in COVID-19 recovered and in the naive subgroup compared to T2. The IQR range for Tri-S-CoV-2 IgG was 719.5 to 1930 BAU/mL with a median value of 1310 BAU/mL for the first group as opposed to 305.8 to 945.8 BAU/mL with a median of 510 BAU/mL for the second group. Similarly, the IQR for CoV-2 IgG II was 2046 to 8667 AU/mL with a median of 3819 AU/mL vs 1002 to 2514 AU/mL with a median of 1518 AU/mL.

The results were also analyzed using limits related to the presence of higher neutralizing antibodies titers. At T3, the number of COVID-19 naive subjects that maintained a Tri-S-CoV-2 IgG level above this limit is lower (47%) than the 85% of the COVID-19 recovered subjects. When the respective limit is applied in the case of CoV-2 IgG-II, the difference between the 2 groups is less marked, as the rate of positivity is respectively 79% and 94%. In addition to the fact that the assays do not measure the same antibody, the different techniques used by manufacturers to describe the relation between binding antibodies and neutralizing antibodies may also account for this observation.

FIGURE 2 illustrates the considerable drop in antibody levels by individual. For each participant, the magnitude of the reduction is expressed in percentages of T3 to T2 antibody levels (T3/T2 ratio). Seven participants were excluded because their T2 antibodies values were over the linearity range. One participant whose antibodies concentrations were much higher on T3 than on T2 was considered an outlier. The median (range) of T3/T2 ratio is 10.6% (3.9%–71.2%) for Tri-S-CoV-2 IgG and

Downloaded from https://academic.oup.com/labmed/article/54/4/388/6885749 by guest on 24 February 2025

FIGURE 1. Evolution of anti-spike antibodies (Diasorin SARS-CoV-2 TrimericS immunoglobulin G [IgG]) (A) and anti-receptor-binding domain antibody (Abbott SARS-CoV-2 IgG-II) (B) levels from the time before the vaccination (T0) to 1 month after the first dose (T1) and 1 month (T2) to 7 months (T3) after the second dose of mRNA-1273 vaccine. Log scaled results from individuals with (n = 53) or without (n = 102) prior SARS-CoV-2 infection are represented. Error bars represent the median values with the interquartile range. Dashed lines represent the respective manufacturer's thresholds for the presence of antibodies (positivity threshold) and the limits consistent with higher SARS-CoV-2 neutralizing antibody titers. AU, arbitrary units; BAU, binding antibodies units.

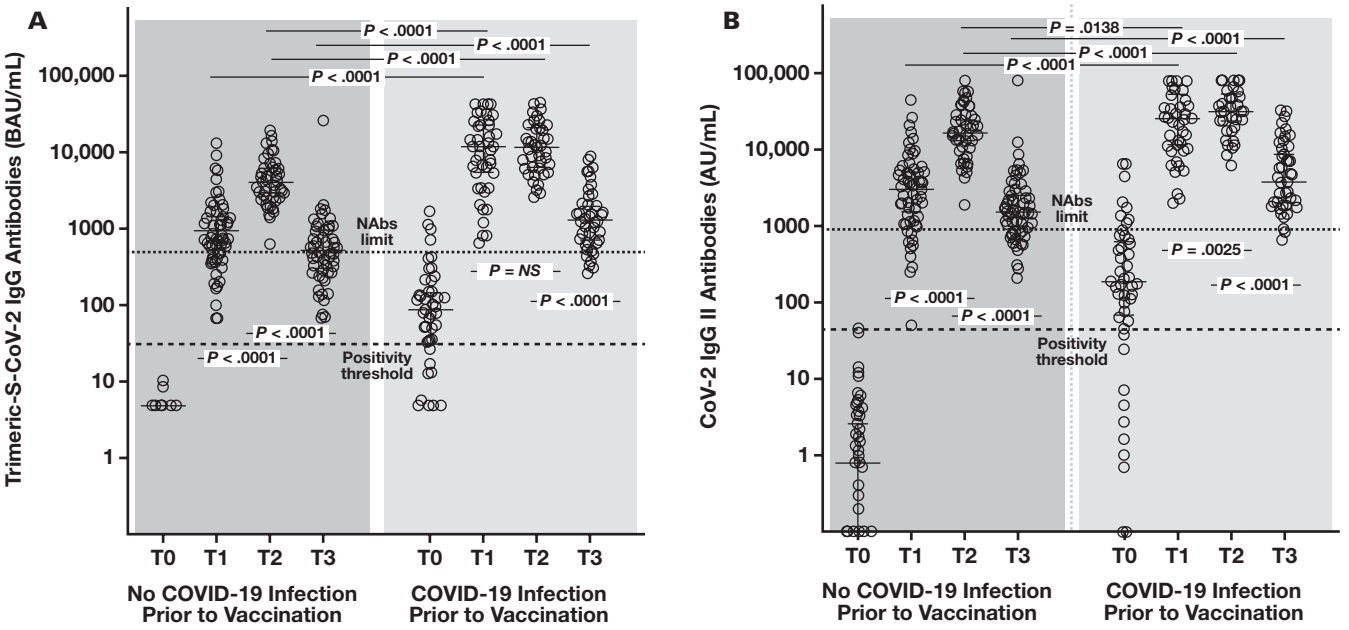

FIGURE 2. Relationship between the decrease of anti-spike antibody titers (Diasorin-Tri-S-CoV-2 immunoglobulin G [IgG]) and that of anti-receptor-binding domain levels (Abbott-Cov-2 IgG-II) from 1 month (T2) to 7 months (T3) after the second dose of mRNA-1273 vaccine. Results are expressed as the ratio (%) of antibody levels at T3 to the respective levels at T2. The graphs include individuals previously infected by SARS-CoV-2 (r = 0.7238) (A) or not (r = 0.8305) (B).

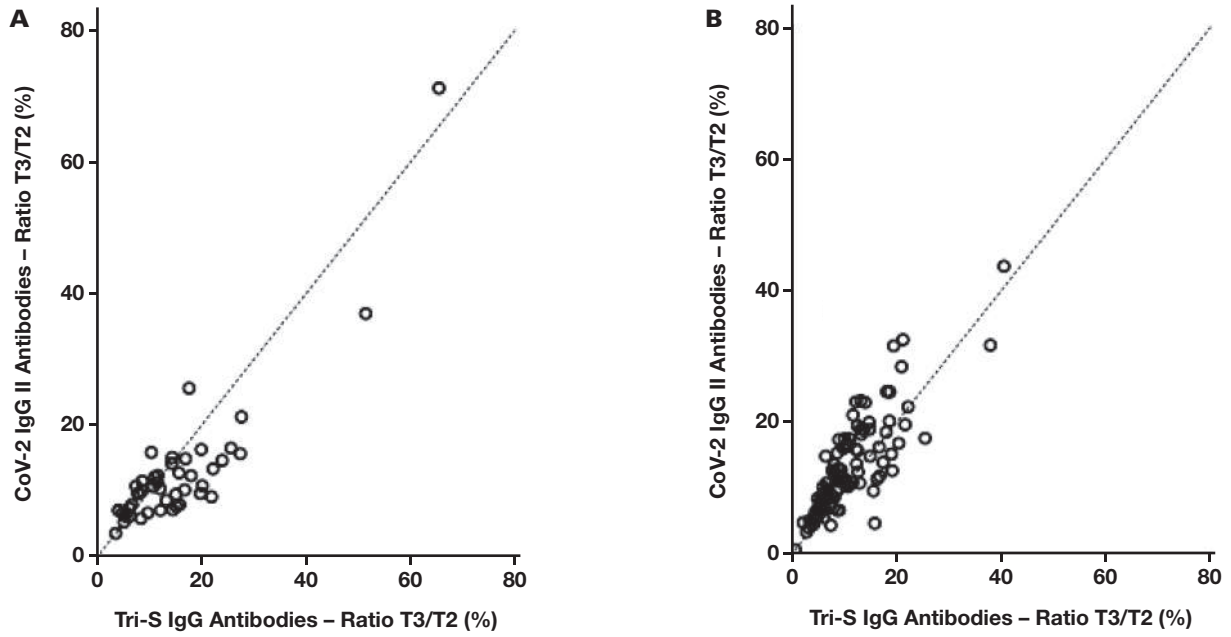

13% (3.9%–65.5%) for CoV-2 IgG II among virus-exposed individuals (n = 46) and 11.7% (0.9%–43.8%) and 9.3% (0.9%–40.6%) among the COVID-19 naive participants (n = 101). The declines of anti-S and anti-RBD are moderately correlated in both subgroups (Spearman r = 0.7238 and 0.8305, respectively).

Discussion

In this study, we analyzed the long-term kinetic and magnitude of vaccine-elicited antibodies at multiple time points after mRNA-1273 vaccination. The antibody response was assessed by 2 widespread serological commercial assays for IgG anti-SARS-CoV-2, one targeting the spike protein, the other

Downloaded from https://academic.oup.com/labmed/article/54/4/388/6885749 by guest on 24 February 2025

the RBD. A strong vaccine-induced humoral response was measured by both assays from the first dose of vaccine. The second injection clearly intensified the antibody response in naive individuals, to a lesser extent in COVID-19 recovered vaccinees. In the latter group, anti-S levels did not change even after the second injection. As discussed, for the BNT162b2 mRNA vaccine,[12] we also observed that the first injection acted as a boost in previously infected subjects so that their humoral response was comparable to that measured after the second dose in subjects without prior evidence of infection.

Regarding the development of the immune response, an initial increase rapidly followed by a progressive decrease and later a stabilization of antibody level is expected. Seven months after the second dose, the magnitude of the humoral immune response to both S protein and RBD declined substantially, by about a factor of 10, in all but 1 participant. The declines of anti-S and anti-RBD, expressed as the ratio of T3 antibodies levels to T2 levels, are correlated. These declines appeared whether the subject had had a SARS-CoV-2 infection preceding the vaccination or not. Given the higher antibody levels after the second injection, vaccine recipients previously infected with SARS-CoV-2 maintained a more sustained response 7 months after the second dose compared to naive vaccinees. Although the anti-RBD assay highlights a greater drop among noninfected subjects as compared to COVID-19 recovered, the T3/T2 ratio of anti-S that reflects the decay rate is comparable in both cohorts. Nevertheless, there is no evidence of any clinical relevance, this difference being probably more related to the peculiar features of each assay. Overall, despite a decline in magnitude over time, the immune response could remain powerful. Whether reduced antibody levels are linked or not to an altered humoral immunity is not obvious. Indeed, through a potent cellular immune response, sufficient protection has been demonstrated despite undetectable circulating IgG.[13]

Protective immunity is associated with neutralizing antibodies capable of preventing the virus from entering the host cells. No neutralizing test was performed in this study. However, based on data found in the instructions for use of the CE-marked reagents, we observed that 7 months after vaccination, most participants maintained anti-S and anti-RBD titers showing the expected presence of high levels of neutralizing antibodies. However, caution is required when extrapolating binding test results to neutralization. Indeed, serological tests do not accurately reflect neutralizing capacity, as many discrepancies have been shown between neutralizing and serological data.[14] The positivity threshold provides information regarding the presence of antibodies, and even high titers do not guarantee a protective immunity.[15] The reinfections observed in the presence of specific IgG raised the question of the relevance of serology testing to presume protection in further exposure to SARS-CoV-2. Moreover, the commercialized serological tests, even when targeting RBD, do not simulate a neutralization test.[16] Also, the peak of antibody titers could be indicative,[17] perhaps more than later titers, in predicting a breakthrough of the infection. In summary, all these limitations must be kept in mind when interpretating serological data from clinical laboratories. In addition, the vaccine-induced antibodies could bind differently to a mutated virus. Considering the recently emerged virus variants and COVID-19 vaccine booster shots, the extension of immune monitoring could provide relevant information on the long-term evolution of the immune response.

Acknowledgments

We thank all sample donors and the staff of the laboratory department of the CHU-Tivoli for their useful technical assistance.

Conflict of Interest Disclosure

The authors have nothing to disclose.

REFERENCES

1. Tré-Hardy M, Cupaiolo R, Wilmet A, et al. Waning antibodies in SARS-CoV-2 naïve vaccinees: results of a three-month interim analysis of ongoing immunogenicity and efficacy surveillance of the mRNA-1273 vaccine in healthcare workers. *J Infect.* 2021;83(3):381–412. doi:10.1016/j.jinf.2021.06.017.
2. Favresse J, Bayart JL, Mullier F, et al. Antibody titres decline 3-month post-vaccination with BNT162b2. *Emerg Microbes Infect.* 2021;10(1):1495–1498. doi:10.1080/22221751.2021.1953403.
3. Doria-Rose N, Suthar MS, Makowski M, et al. mRNA-1273 Study Group. Antibody persistence through 6 months after the second dose of mRNA-1273 vaccine for Covid-19. *N Engl J Med.* 2021;384(23):2259–2261.
4. Widge AT, Rouphael NG, Jackson LA, et al. Durability of responses after SARS-CoV-2 mRNA-1273 vaccination. *N Engl J Med.* 2021;384(1):80–82.
5. Brisotto G, Muraro E, Montico M, et al. IgG antibodies against SARS-CoV-2 decay but persist 4 months after vaccination in a cohort of healthcare workers. *Clin Chim Acta.* 2021;523:476–482.
6. Tré-Hardy M, Cupaiolo R, Wilmet A, et al. Immunogenicity of mRNA-1273 COVID vaccine after 6 months surveillance in health care workers; a third dose is necessary. *J Infect.* 2021;83(5):559–564.
7. Nam M, Seo JD, Moon HW, et al. Evaluation of humoral immune response after SARS-CoV-2 vaccination using two binding antibody assays and a neutralizing antibody assay. *Microbiol Spectr.* 2021;9(3):e0120221.
8. Favresse J, Douxfils J. Importance of sample dilution in the evaluation of the antibody response after SARS-CoV-2 vaccination. *J Infect.* 2022;84(1):94–118.
9. Kanji JN, Bailey A, Fenton J, et al. Detection of SARS-CoV-2 antibodies formed in response to the BNT162b2 and mRNA-1237 mRNA vaccine by commercial antibody tests. *Vaccine.* 2021;39(39):5563–5570.
10. DiaSorin. Package insert of CE marked LIAISON SARS-CoV-2 TrimericS IgG, Version FR-54286, February 2021.
11. Abbott Laboratories. Package insert of CE marked Alinity i SARS-CoV-2 IgG II Quant, Version FR-H13946R01. December 2020.
12. Ebinger JE, Fert-Bober J, Printsev I, et al. Antibody responses to the BNT162b2 mRNA vaccine in individuals previously infected with SARS-CoV-2. *Nat Med.* 2021;27(6):981–984.
13. Schwarzkopf S, Krawczyk A, Knop D, et al. Cellular immunity in COVID-19 convalescents with PCR-confirmed infection but with undetectable SARS-CoV-2-specific IgG. *Emerg Infect Dis.* 2021;27(1):122–129.
14. Gillot C, Favresse J, Maloteau V, et al. Dynamics of neutralizing antibody responses following natural SARS-CoV-2 infection and correlation with commercial serologic tests. a reappraisal and indirect comparison with vaccinated subjects. *Viruses.* 2021;13(2329).
15. Douxfils J, Gillot C, Mullier F, et al. Post-SARS-CoV-2 vaccination specific antibody decrease—thresholds for determining seroprevalence and seroneutralization differ. *J Infect.* 2021;83(4):e4–e5.
16. Bal A, Pozzetto B, Trabaud MA, et al. Evaluation of high-throughput SARS-CoV-2 serological assays in a longitudinal cohort of patients with mild COVID-19: clinical sensitivity, specificity, and association with virus neutralization test. *Clin Chem.* 2021;67(5):742–752.
17. Bergwerk M, Gonen T, Lustig Y, et al. Covid-19 breakthrough infections in vaccinated health care workers. *N Engl J Med.* 2021;385(16):1474–1484.

Downloaded from https://academic.oup.com/labmed/article/54/4/388/6885749 by guest on 24 February 2025

A Retrospective Case-Control Study on the Diagnostic Values of Hemostatic Markers in Hypertensive Disorder of Pregnancy

Qiujin Sun, MS,[1] Yifan Lu, MS,[2] Junhui Zhong, BS,[3] Xianchun Yang, BS,[1] Lu Zhong, BS,[1] Wenwen Zhang, BS,[1] Yanhua Weng, BS,[1] Zhengwen Xu, BS,[2] Yanhong Zhai, MD,[2] Zheng Cao, PhD,[2,]*

[1]Department of Clinical Laboratory, Beijing Chaoyang District Maternal and Child Health Care Hospital, Beijing, China, [2]Department of Laboratory Medicine, Beijing Obstetrics and Gynecology Hospital, Capital Medical University, Beijing Maternal and Child Health Care Hospital, Beijing, China, [3]Peking University School of Public Health, Beijing, China. *To whom correspondence should be addressed: zhengcao2011@ccmu.edu.cn.

Keywords: preeclampsia, hypertension, pregnancy, diagnosis, hemostatic marker, coagulation

Abbreviations: HDP, hypertensive disorder of pregnancy; tPAI-C, tissue-type plasminogen activator and inhibitor-1 complex; HC, healthy pregnancy control; GH, gestational hypertension; PE, preeclampsia; HELLP, hemolysis, elevated liver enzymes, and low platelets; FDP, fibrinogen degradation products; TM, thrombomodulin; TAT, thrombin-antithrombin complex; PIC, plasmin inhibitor-plasmin complex; MPE, mild PE; SPE, severe PE; BP, blood pressure; AST, aspartate aminotransferase; ROC, receiver operating characteristic; GW, gestational weeks; BMI, body mass index; WBC, white blood cell; RBC, red blood cell; PLT platelet; AUC, area under the curve; CI, confidence interval

Laboratory Medicine 2023;54:392-399; https://doi.org/10.1093/labmed/lmac128

ABSTRACT

Objective: The purpose of this study was to evaluate the diagnostic performance of the following hemostatic markers in hypertensive disorder of pregnancy (HDP): tissue-type plasminogen activator and inhibitor-1 complex (tPAI-C), thrombomodulin, thrombin-antithrombin complex, plasmin inhibitor-plasmin complex, D-dimer, and fibrinogen degradation products.

Methods: A total of 311 individuals diagnosed with HDP and 187 healthy controls (HC) of matched gestational age were admitted, including 175 subjects with gestational hypertension, 94 with mild preeclampsia, and 42 with severe preeclampsia.

Results: Compared with those of the HC group, the plasma concentrations of all the hemostatic markers continuously increased with the clinical severity of the hypertensive disorder, regardless of their statistical significance. In the receiver operating characteristic analysis, tPAI-C displayed the best discrimination performance.

Conclusion: The tPAI-C level was consistently and significantly elevated across the different HDP groups when compared with the HC group, suggesting aggravated fibrinolysis disorder increasing with the severity of the HDP.

Hypertensive disorder of pregnancy (HDP) includes a set of disorders with elevated blood pressure (BP) in pregnancy, such as gestational hypertension (GH), preeclampsia (PE), eclampsia, and chronic hypertension. The prevalence of HDP in China is approximately 7.8% to 12.3%, which has grown rapidly over the past decade and poses a major threat to maternal and perinatal health.[1,2]

During normal pregnancy, a hypercoagulable state develops as a physiologic adaptation to prevent major hemorrhage during and after placental separation. This hypercoagulable state may contribute to the increased susceptibility of pregnant women to thrombotic disorders.[2,3] Complex associations between pregnant hypertension disorders and dysregulated coagulation functions have been reported. It is thought that abnormal development of placental vessels in early pregnancy might lead to inadequate perfusion of the placenta, resulting in hypertension and other relevant disorders.[4] Further, placental ischemia-increased trophoblast deportation has been related to the activation of coagulation and fibrinolysis and even thrombogenesis.[5] In patients with severe PE with hemolysis, elevated liver enzymes, and low platelets (HELLP) syndrome whose pathophysiology remains partially unknown, abnormal vascular tone, vasospasm, and coagulation defects have been frequently detected.[6,7] Despite the apparent connection between microvascular endothelial damage and intravascular platelet activation and HDP, the diagnostic value of hemostatic markers in such disorders has not been thoroughly investigated.

Diagnostic criteria for HDP are currently based on clinical symptoms such as BP and proteinuria. However, there are hardly any specific circulating biomarkers for the diagnosis of HDP such as PE,[1,8] which poses a serious challenge for early diagnosis of disease to avoid severe pregnant outcomes in clinical practice. In this study, we aimed to assess the diagnostic performance of conventional and nonconventional hemostatic markers in women with HDP, including fibrinogen degradation products (FDP), D-dimer, tissue-type plasminogen activator and inhibitor-1 complex (tPAI-C), thrombomodulin (TM), thrombin-antithrombin complex (TAT), and plasmin inhibitor-plasmin complex (PIC).

© The Author(s) 2022. Published by Oxford University Press on behalf of American Society for Clinical Pathology. All rights reserved. For permissions, please e-mail: journals.permissions@oup.com

Downloaded from https://academic.oup.com/labmed/article/54/4/392/6820974 by guest on 24 February 2025

Methods

Subjects

This case-control study included 498 singleton pregnant women admitted to Chaoyang District Maternal and Child Health Hospital in Beijing from October 2019 to December 2020. None of these patients had preexisting hypertension before pregnancy. The enrolled subjects were divided into the following groups according to their diagnosis at delivery, including healthy pregnancy control (HC) (n = 187), GH (n = 175), mild PE (MPE) (n = 94), severe PE (SPE) without HELLP (n = 33), SPE with HELLP (n = 9), and HDP (n = 311, the combination of GH, MPE, and SPE cases). The results of the 6 hemostatic markers were retrieved from the patients' historical medical records and retrospectively analyzed.

Diagnostic Criteria for HDP

The following diagnosis criteria were applied in the present study for HDP.[9] A diagnosis of GH was given if a previously normotensive patient's BP was ≥140/90 mm Hg on 2 occasions (at least 4 hours apart) during pregnancy after 20 weeks gestation, without the presence of proteinuria or other clinical features suggestive of preeclampsia. An MPE was defined by BP ≥140/90 mm Hg and proteinuria ≥0.3 g/24 h after 20 weeks of gestation (with or without signs and symptoms of significant end-organ dysfunction). A diagnosis of SPE was made if a patient with PE presented with one of the following conditions: (1) systolic BP ≥160 mm Hg or diastolic BP ≥110 mm Hg; (2) proteinuria ≥5.0 g/24 h (with signs and symptoms of significant end-organ dysfunction); (3) persistent headache or visual disturbance or other brain and nerve symptoms; (4) persistent upper abdominal pain, subcapsular hematoma, or liver rupture symptoms; (5) abnormal liver function including elevated liver enzyme alanine aminotransferase or aspartate aminotransferase (AST) level; (6) renal function abnormality/oliguria (24-hour urine volume <400 mL or hourly urine volume <17 mL) or creatinine >106 μmol/L; (7) hypoalbuminemia with pleural effusion or peritoneal effusion; (8) platelet $<100 \times 10^9$/L; (9) hemolysis, anemia, jaundice, or pulmonary edema; or (10) fetal growth restriction or oligohydramnios. The diagnostic criteria for HELLP were hemolysis, increased lactate dehydrogenase (≥600 IU/L), increased AST (≥70 IU/L), and low platelets ($<100 \times 10^9$/L).[10]

The exclusion criteria were as follows: (1) use of anticoagulant, antitumor, antihypertensive, or antiplatelet drugs in the month prior to study entry; (2) multiple pregnancies; (3) a medical history of trauma and surgery; or (4) a medical history of cardiac, hepatic, renal, hematologic, or immune system disease and tumor.

The HC subjects are defined as normotensive healthy pregnant women without any of the above-mentioned diseases or other pregnancy complications.

Plasma Sample Collection and Hemostatic Marker Testing

All the plasma samples were collected from the recruited subjects meeting enrollment criteria at the time of diagnosis by the clinician team (sampling gestational weeks shown in **TABLE 1**), by 2.7 mL VACUETTE collection tubes supplemented with 3.2% trisodium citrate. The plasma samples from the HC group were all collected in the early third trimester of pregnancy with roughly matching gestational weeks when compared with the HDP group. The indicated hemostatic marker tests were performed within 4 hours after blood collection.

Instruments and Reagents

D-dimer (Siemens) and FDP (Sysmex) evaluations were performed in a Sysmex CA 7000 Coagulation Analyzer, and the reagent lot numbers were IYR3001 and 30954900, respectively. Measurements of TAT, TM, PIC, and tPAI-C (Sysmex) were performed in a Sysmex HISCL 5000 Immunoassay Analyzer, and the reagent lot numbers were 33610500, 25919900, 29521100, and 30954900 respectively.

Statistical Methods

With the statistical software of IBM SPSS Statistic 23.0, quantitative data were summarized by mean and standard deviation (mean [SD]) (for normally distributed data) or median and interquartile ranges (median [IQR]) (for nonnormally distributed data). Nonparametric Kruskal-Wallis tests were used to compare each group of unpaired data and Kruskal-Wallis ANOVA were used to compare more than 2 groups of unpaired data. *P* values less than .05 were considered statistically significant. Diagnostic performance was assessed with receiver operating characteristic (ROC) curve analysis. Sensitivity, specificity, and cut-off values determined by the Youden's index were reported.

Results

There were no significant differences in age and sampling gestational weeks (GW) between the disease groups and the HC group; slightly lower delivery GW and higher prepregnancy body mass index (BMI) were observed in the HDP groups (including the GH, MPE, and SPE groups) ($P < .05$). Gestational diabetes mellitus was a common chronic condition, and its prevalence was not essentially different among different HDP groups. Interestingly, the incidence of fetal growth restriction, placental abruption, and HELLP syndrome rose with the increasing severity of HDP (**TABLE 1**).

As summarized in **TABLE 2**, of the 2 conventional coagulation tests, D-dimer and FDP were significantly elevated in the MPE group but not in the GH or SPE groups (with or without HELLP). Both the TM and TAT concentrations were found to be statistically increased only in the patients with SPE with HELLP. The plasma level of PIC was more sensitive to PE and it was marginally increased in both MPE and SPE groups. Further, the tPAI-C level was increased across all the HDP groups and nearly doubled in the HELLP patients (**TABLE 2**, **FIGURE 1**). Complete blood count indices for each group are listed in **TABLE 2**, including white blood cell (WBC), red blood cell (RBC), and blood platelet (PLT). Marginally higher WBC, RBC, and PLT were seen in mild HDP groups such as GH and MPE. Spearman rank correlation was used to analyze the correlations between PLT and the hemostatic markers. Interestingly, a negative correlation was observed between PLT and D-dimer, and FDP and TAT in the SPE with HELLP group (**TABLE 2**).

According to the results of the statistical calculations shown in **TABLE 2**, the significantly different hemostatic markers were then subjected to ROC analyses to assess their diagnostic values in different hypertensive diseases of pregnancy (**TABLE 3**, **FIGURE 2**). As shown in **TABLE 3**, tPAI-C displayed the strongest discrimination power, with the highest area under the curve (AUC) values in the SPE with or without HELLP groups ($P < .05$). Specifically, in the SPE without HELLP group, the AUC of tPAI-C was 0.729 (a 95% confidence interval [CI] of 0. 0.616–0.843), followed by that of PIC (0.608, 95% CI = 0.513–0.704). In the SPE with HELLP group, the AUC of tPAI-C was 0.954 (95% CI = 0.916–0.991),

Downloaded from https://academic.oup.com/labmed/article/54/4/392/6820974 by guest on 24 February 2025

TABLE 1. Demographic Data and Pregnancy Complications for the Recruited Subjects[a]

	HC (n = 187)	GH (n = 175)	MPE (n = 94)	SPE (n = 42)
Age (y)	30 (28–32)	30 (27–34)	30 (27–32)	30 (27–34)
P value	—	.089	.576	.310
Sampling GW (wk)	32 (32–33)	32 (31–33)	32 (32–33)	32 (31–32)
P value	—	.961	.377	.091
Delivering GW (wk)	40 (39–40)	38 (37–39)	39 (38–40)	37 (36–39)
P value	—	**<.001**	**<.001**	**<.001**
Prepregnancy BMI (kg/m^2)	20.6 (19.0–22.1)	23.2 (21.3–25.8)	23.4 (21.1–26.3)	23.7 (21.1–25.8)
P value	—	**<.001**	**<.001**	**<.001**
Gestational diabetes mellitus	0	32.0% (56)	34.0% (32)	21.4% (9)
Fetal growth restriction	0	1.7% (3)	4.3% (4)	9.5% (4)
HELLP syndrome	0	0	0	21.4% (9)

BMI, body mass index; GH, gestational hypertension; GW, gestational weeks; HC, healthy pregnancy control; HELLP, hemolysis, elevated liver enzymes, and low platelets syndrome; MPE, mild preeclampsia; SPE, severe preeclampsia.
[a]*Data are presented as median (25th–75th percentile) except where otherwise indicated. Nonparametric Kruskal-Wallis tests were used for data comparison. Bold values indicate significance (*P < *.05).*

TABLE 2. Concentrations of Hemostatic Markers and Complete Blood Count Indices in Different Hypertensive Disorders of Pregnancy[a]

	HC (n = 187)	HDP (n = 311)	GH (n = 175)	MPE (n = 94)	SPE without HELLP (n = 33)	SPE with HELLP (n = 9)
D-dimer (mg/L)	1.42 (1.05–2.08)	1.50 (1.04–2.14)	1.29 (0.97–1.89)	1.69 (1.18–2.34)	1.65 (1.10–3.01)	2.03 (1.36–3.39)
P value	—	.705	.119	**.029**	.180	.090
FDP (mg/L)	4.10 (3.30–5.60)	4.30 (3.50–5.70)	4.20 (3.20–5.10)	4.50 (3.70–6.13)	4.80 (3.70–6.50)	6.30 (4.05–8.85)
P value	—	.165	.813	**.012**	.172	.052
TAT (ng/mL)	8.16 (6.95–10.02)	8.60 (6.79–11.35)	8.38 (6.67–11.14)	8.81 (7.01–11.17)	9.46 (6.61–11.65)	12.18 (9.95–16.72)
P value	—	.182	.671	.227	.310	**.001**
TM (TU/mL)	7.62 (6.77–8.76)	7.68 (6.81–8.83)	7.60 (6.63–8.53)	7.69 (6.98–9.03)	7.93 (7.10–9.29)	10.11 (8.71–11.46)
P value	—	.471	.484	.278	.080	**.001**
PIC (μg/mL)	0.10 (0.08–0.12)	0.10 (0.09–0.13)	0.10 (0.09–0.12)	0.10 (0.09–0.13)	0.11 (0.09–0.12)	0.14 (0.09–0.30)
P value	—	**.005**	.111	**.006**	**.046**	**.015**
tPAI-C (ng/mL)	5.32 (4.62–6.31)	6.16 (4.98–7.71)	6.09 (5.00–7.71)	5.79 (4.87–7.01)	7.45 (5.60–10.21)	10.15 (7.48–13.32)
P value	—	**<.001**	**<.001**	**.001**	**<.001**	**<.001**
WBC (10^9/L)	8.98 (7.99–10.26)	9.22 (8.16–10.92)	9.18 (8.32–10.54)	9.67 (8.23–11.03)	8.43 (7.66–11.07)	7.63 (6.87–8.44)
P value	—	**.033**	**.043**	**.029**	.794	**.025**
RBC (10^{12}/L)	3.88 (3.70–4.06)	4.08 (3.85–4.32)	4.06 (3.85–4.33)	4.09 (3.82–4.30)	4.10 (3.95–4.31)	4.00 (3.30–4.56)
P value	—	**<.001**	**<.001**	**<.001**	**.001**	.899
PLT (10^9/L)	200 (169–236)	215 (184–252)	214 (184–257)	222 (191–252)	205 (173–244)	173 (139–223)
P value	—	**.001**	**.004**	**<.001**	.661	.112
Correlation analysis with PLT (*P* value, *r*)						
D-dimer	0.521, –0.047	0.556, 0.034	0.230, 0.091	0.710, 0.039	0.993, –0.002	0.016, –0.767
FDP	0.166, –0.102	0.977, 0.002	0.715, 0.028	0.408, 0.086	0.589, –0.098	0.012, –0.787
TAT	0.085, –0.126	0.119, –0.088	0.648, –0.035	0.568, –0.060	0.470, –0.130	0.013, –0.783
TM	0.740, 0.024	0.540, –0.035	0.805, –0.019	0.343, –0.098	0.280, 0.194	0.700, –0.150
PIC	0.987, 0.001	0.250, 0.065	0.222, 0.093	0.212, 0.130	0.524, 0.115	0.035, –0.703
tPAI-C	0.161, 0.103	0.232, –0.068	0.541, –0.047	0.718, 0.038	0.625, –0.088	0.067, –0.633

FDP, fibrinogen degradation products; GH, gestational hypertension; HC, healthy pregnancy control; HDP, hypertensive disorders of pregnancy; HELLP, hemolysis, elevated liver enzymes, and low platelets syndrome; MPE, mild preeclampsia; PLT, blood platelet; RBC, red blood cell; SPE, severe preeclampsia; TAT, thrombin-antithrombin complex; TM, thrombomodulin; tPAI-C, tissue-type plasminogen activator and inhibitor-1 complex; WBC, white blood cell.
[a]*P value comparison is between the HC group and the other hypertensive disorder groups. Nonparametric Kruskal-Wallis tests were used for data comparison. Bold values indicate significance (*P < *.05).*

Downloaded from https://academic.oup.com/labmed/article/54/4/392/6820974 by guest on 24 February 2025

FIGURE 1. Box plots representing the plasma levels of the 6 hemostatic markers in different hypertensive disorders of pregnancy, including healthy pregnancy control (HC), hypertensive disorder of pregnancy (HDP), gestational hypertension (GH), mild preeclampsia (MPE), severe preeclampsia without hemolysis, elevated liver enzymes, and low platelets syndrome (SPE without HELLP), and SPE with HELLP. Nonparametric Kruskal-Wallis tests were used in data comparison. *$P < .05$. A, D-dimer. B, Fibrinogen degradation products (FDP). C, Thrombin-antithrombin complex (TAT). D, Thrombomodulin (TM). E, Plasmin inhibitor-plasmin complex (PIC). F, Tissue-type plasminogen activator and inhibitor-1 complex (tPAI-C).

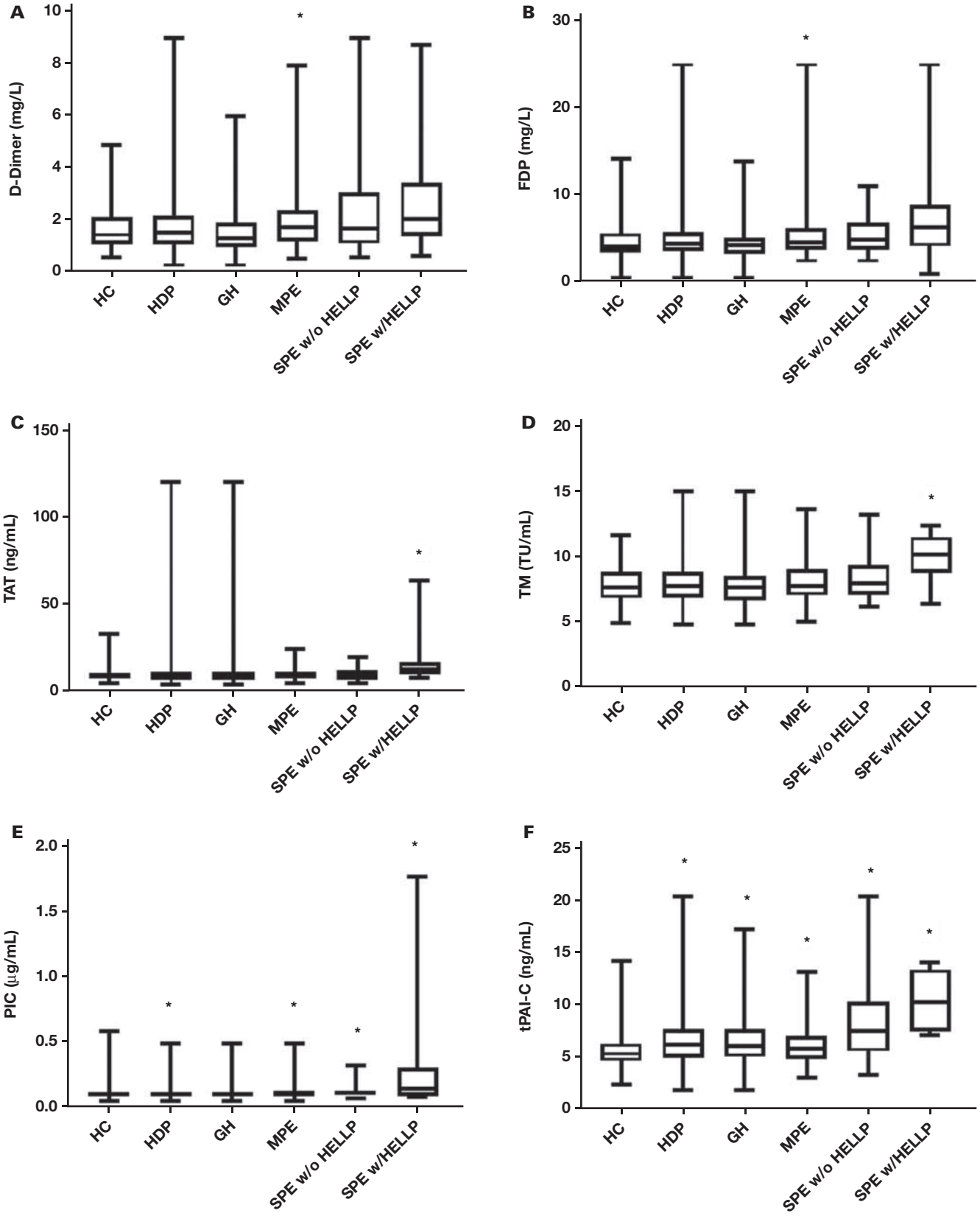

Downloaded from https://academic.oup.com/labmed/article/54/4/392/6820974 by guest on 24 February 2025

TABLE 3. ROC Analysis with the Hemostatic Markers in Different Hypertensive Disorders of Pregnancy

Hypertensive Disorders	Tests	Cutoff	95% Confidence Interval	Sensitivity	Specificity	AUC	*P* Value[a] (Comparison with tPAI-C)
HDP (n = 311)	PIC (μg/mL)	0.08	0.523–0.628	78.14%	35.29%	0.575	**.041**
	tPAI-C (ng/mL)	6.63	0.598–0.694	42.19%	83.42%	0.646	—
GH (n = 175)	tPAI-C (ng/mL)	6.04	0.581–0.696	50.90%	71.70%	0.639	—
MPE (n = 94)	D-dimer (mg/L)	1.46	0.509–0.651	64.90%	52.40%	0.580	.676
	FDP (mg/L)	3.80	0.521–0.662	71.28%	43.32%	0.592	.838
	PIC (μg/mL)	0.11	0.529–0.669	48.90%	67.40%	0.599	.950
	tPAI-C (ng/mL)	5.57	0.531–0.673	60.60%	58.30%	0.602	—
SPE without HELLP (n = 33)	PIC (μg/mL)	0.11	0.513–0.704	54.55%	67.38%	0.608	.102
	tPAI-C (ng/mL)	6.69	0.616–0.843	60.61%	84.49%	0.729	—
SPE with HELLP (n = 9)	TAT (ng/mL)	9.55	0.700–0.933	88.89%	68.45%	0.817	**.036**
	TM (TU/mL)	9.09	0.641–0.988	77.78%	82.35%	0.815	.146
	PIC (μg/mL)	0.11	0.559–0.917	66.67%	74.33%	0.738	**.018**
	tPAI-C (ng/mL)	7.02	0.916–0.991	100.00%	87.17%	0.954	—

AUC, area under receiver operating characteristic curve; FDP, fibrinogen degradation products; GH, gestational hypertension; HDP, hypertensive disorders of pregnancy; HELLP, hemolysis, elevated liver enzymes, and low platelets syndrome; MPE, mild preeclampsia; PIC, plasmin inhibitor-plasmin complex; SPE, severe preeclampsia; TAT, thrombin-antithrombin complex; TM, thrombomodulin; tPAI-C, tissue-type plasminogen activator and inhibitor-1 complex.
[a]Comparison between the AUC of tPAI-C and the AUC of other hemostatic markers in the same disease group. Nonparametric Kruskal-Wallis tests were used for data comparison. Bold values indicate significance (P < .05).

followed by that of TAT (0.817, 95% CI = 0.700–0.933), TM (0.815, 95% CI = 0.641–0.988), and PIC (0.738, 95% CI = 0.559–0.917).

Discussion

Normal pregnancy is invariably accompanied by a prothrombotic state.[11] Compared to nonpregnant women, pregnant women usually have a significant increase in the levels of coagulation factors, reduced fibrinolytic activity, and increased platelet reactivity.[12] This leads to an increased risk of thromboembolic complications. Preeclampsia is a multisystem progressive disorder characterized by hypertension and proteinuria. In addition to inadequate spiral arterial recasts in early pregnancy, overreaction to immune inflammation and damage to the vessel endothelium, coagulation dysfunction, and imbalances in the coagulation and fibrinolytic systems may also contribute to its pathogenesis.[13,14]

The gold standard of PE diagnosis that previously was defined as hypertension plus proteinuria after 20 weeks gestation has now been expanded to hypertension in combination with renal and liver dysfunction and thrombocytopenia.[8] However, the lack of effective circulating markers for PE in clinical practice remains a potential hurdle for its diagnosis and treatment. Based on the pathophysiology of the disease progress, we retrospectively examined the relative changes and diagnostic performance of conventional (D-dimer and FDP) and nonconventional (tPAI-C, TM, TAT, and PIC) hemostatic markers in a group of specific hypertensive disorders during pregnancy, including GH, MPE, and SPE.

A higher TM level was found in the SPE group compared to that of the HC group, which was similar to results described in the Dusse et al[15] study. Increased TM levels in SPE may reflect maternal endothelial activation because of increased ROS production and oxidative stress in this clinical condition.[16] Combined analysis showed that the coagulation system is extensively activated in HDP patients after cytokine storms and that these patients have high circulating levels of thrombomodulatory proteins.[17,18] However, whether endothelial dysfunction is a cause or a consequence of PE is inconclusive. The fact that the TM level was the highest in the SPE group may be explained by potentially more severe endothelial injury and impaired renal function in those patients, as TM is metabolized by the kidneys.[17] However, the TM plasma levels did not differ between SPE and normotensive pregnancy in the study by Alpoim et al.[16] Differences in the TM measurement methodology or the patients' ethnic background might account for the disagreement.

It is worth noting that the tPAI-C concentration was elevated in all the HDP groups. More interestingly, among the 6 markers investigated, tPAI-C demonstrated the best diagnostic performance in discriminating HDP and HC groups, which is consistent with previous studies.[3,19] The decrease in fibrinolysis in normal pregnancy is due to a decrease in tissue-type fibrinogen activator activity accompanied by increased levels of fibrinogen activator inhibitor-1 and fibrinogen activator inhibitor-2,[20] which gradually return to normal levels shortly after delivery. In patients with PE, however, significant endothelial disturbance and procoagulant potential along with aberrant expression of these hemostatic factors were reported in previous studies.[4,21] Therefore, it will be intriguing to assess the predictive value of tPAI-C level in patients with early-onset SPE.

Both tPAI-C and TM play vital roles in coagulation regulation and in fibrinolytic phase; their aberrant levels in plasma are considered important pathological factors in cardiovascular disease.[22,23] In the HDP population, increased plasma levels of these hemostatic markers not only indicate the presence of hypercoagulable status but are also associated with differential scales and phases of endothelium damage. In addition, we found that TAT and PIC were both increased to various degrees in the HDP groups (**TABLE 2**). Similar to our study, Kobayashi et al[24] reported that PIC, TAT, and D-dimer were elevated in early-onset and late-onset SPE groups compared with normal subjects. The pathophysiology of PE is related to endothelial injury, activation of the sympathetic nervous system, and hypercoagulability. Then thrombin formed on the surface of damaged endothelium activates coagulation and stimulates the release of vasoactive substances, which induce vasoconstriction.[25,26] Thrombophilia may be one of the causes of early-onset

Downloaded from https://academic.oup.com/labmed/article/54/4/392/6820974 by guest on 24 February 2025

FIGURE 2. Predictive performance assessment by receiver operating characteristic analysis with the hemostatic markers in different hypertensive disorders of pregnancy. Nonparametric Kruskal-Wallis tests were used to data comparison. A, Hypertensive disorder of pregnancy. B, Gestational hypertension. C, Mild preeclampsia. D, Severe preeclampsia without hemolysis, elevated liver enzymes, and low platelets syndrome (SPE without HELLP). E, SPE with HELLP. FDP, fibrinogen degradation products; PIC, plasmin inhibitor-plasmin complex; TAT, thrombin-antithrombin complex; TM, thrombomodulin; tPAI-C, tissue-type plasminogen activator and inhibitor-1 complex.

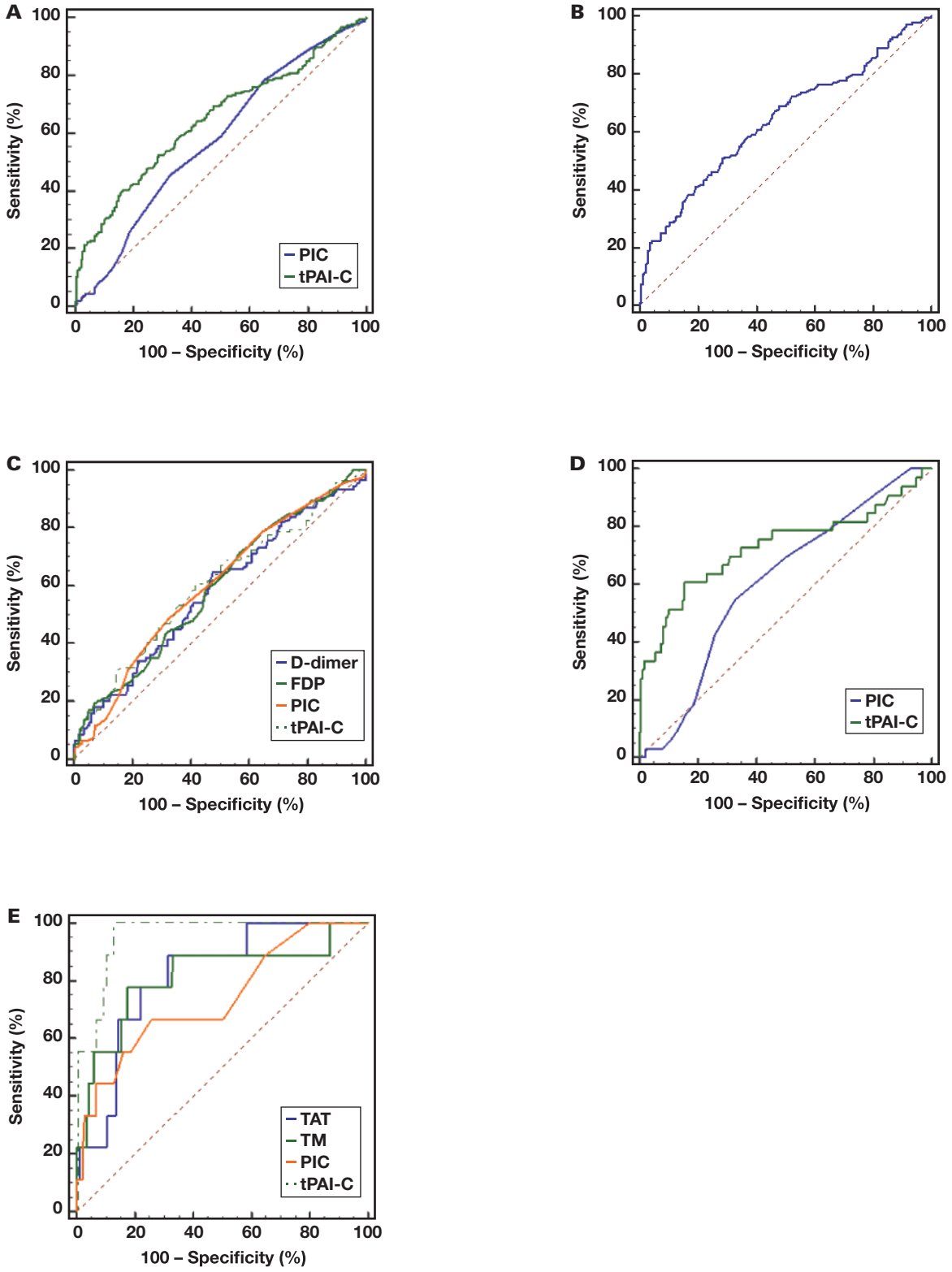

Downloaded from https://academic.oup.com/labmed/article/54/4/392/6820974 by guest on 24 February 2025

PE, as proposed by Dekker et al.[27] Elevated TAT, PIC, and D-dimer reflect intravascular thrombus formation[28] and may suggest that an excessive hypercoagulable state is associated with the termination of pregnancy resulting from the aggravation of PE.[24,28]

Conclusion

Of the 6 hemostatic markers investigated, only the tPAI-C level was consistently and significantly elevated across the different HDP groups when compared with the HC group, suggesting aggravated fibrinolysis disorder increasing with the severity of the HDP.

Supplementary Data

Supplemental figures and tables can be found in the online version of this article at www.labmedicine.com

Acknowledgments

We thank For Li for the kind assistance in LIS data retrieving and Sen Lin for the help in medical records collection.

This study was supported by the Science and Technology Program of Beijing Chaoyang District Maternal and Child Health Care Hospital (No. CYSF2055). The funding body did not take part in the design of the study, the collection, analysis and interpretation of the data, or manuscript writing.

This study was approved by the Ethics Committee of Beijing Chaoyang District Maternal and Child Health Care Hospital (approval number CYFY2019-CYSF2055). Verbal consent from the participants was required as no clinical intervention was involved, which was approved by our institute's ethical committee.

The raw laboratory testing results are provided in **Supplemental Table 1**. According to the patient consent, their relevant demographic and medical records are only available from the corresponding author on reasonable request.

Conflict of Interest Disclosure

The authors have nothing to disclose.

REFERENCES

1. Zhuang C, Gao J, Liu J, et al. Risk factors and potential protective factors of pregnancy-induced hypertension in China: a cross-sectional study. *J Clin Hypertens (Greenwich).* 2019;21(5):618–623. doi:10.1111/jch.13541.
2. Higgins JR, Walshe JJ, Darling MR, Norris L, Bonnar J. Hemostasis in the uteroplacental and peripheral circulations in normotensive and pre-eclamptic pregnancies. *Am J Obstet Gynecol.* 1998;179(2):520–526.
3. Halligan A, Bonnar J, Sheppard B, Darling M, Walshe J. Haemostatic, fibrinolytic and endothelial variables in normal pregnancies and pre-eclampsia. *Br J Obstet Gynaecol.* 1994;101(6):488–492.
4. Luís Belo AS-S, Ann R, Gordon L, Luís P-L, Alexandre Q, Irene R. Elevated tissue plasminogen activator as a potential marker of endothelial dysfunction in pre-eclampsia correlation with proteinuria. *Br J Obstet Gynaecol.* 2002;109(11):1250–1255.
5. Levi M. Pathogenesis and management of peripartum coagulopathic calamities (disseminated intravascular coagulation and amniotic fluid embolism). *Thromb Res.* 2013;131:S32–S34. doi:10.1016/S0049-3848(13)70017-3.
6. Jebbink J, Wolters A, Fernando F, Afink G, van der Post J, Ris-Stalpers C. Molecular genetics of preeclampsia and HELLP syndrome—a review. *Biochim Biophys Acta.* 2012;1822(12):1960–1969.
7. Aloizos S, Seretis C, Liakos N, et al. HELLP syndrome: understanding and management of a pregnancy-specific disease. *J Obstet Gynaecol.* 2013;33(4):331–337.
8. Holger S, Martin H, Theresa A. Combining biomarkers to predict pregnancy complications and redefine preeclampsia: the angiogenic-placental syndrome. *Hypertension.* 2020;75(4):918–926.
9. American College of Obstetricians and Gynecologists' Committee on Practice Bulletins—Obstetrics. ACOG Practice Bulletin No. 203: Chronic Hypertension in Pregnancy. *Obstet Gynecol.* 2019;133(1):e26–e50.
10. Agnès Ditisheim BMS. Diagnosis and management of HELLP syndrome complicated by liver hematoma. *Clin Obstet Gynecol.* 2017;60(1):190–197.
11. Brenner B. Haemostatic changes in pregnancy. *Thromb Res.* 2004;114(5-6):409–414.
12. Thornton P, Douglas J. Coagulation in pregnancy. *Best Pract Res Clin Obstet Gynaecol.* 2010;24(3):339–352.
13. Ives CW, Sinkey R, Rajapreyar I, Tita ATN, Oparil S. Preeclampsia-pathophysiology and clinical presentations: JACC state-of-the-art review. *J Am Coll Cardiol.* 2020;76(14):1690–1702.
14. Phipps E, Prasanna D, Brima W, Jim B. Preeclampsia: updates in pathogenesis, definitions, and guidelines. *Clin J Am Soc Nephrol.* 2016;11(6):1102–1113.
15. Dusse LM, Alpoim PN, Lwaleed BA, de Sousa LP, Carvalho M, Gomes KB. Is there a link between endothelial dysfunction, coagulation activation and nitric oxide synthesis in preeclampsia? *Clin Chim Acta.* 2013;415:226–229.
16. Alpoim PN, Perucci LO, Godoi LC, Goulart COL, Dusse LMS. Oxidative stress markers and thrombomodulin plasma levels in women with early and late severe preeclampsia. *Clin Chim Acta.* 2018;483:234–238.
17. van Aanhold CCL, Bos M, Katrina M, et al. Thrombomodulin is upregulated in the kidneys of women with pre-eclampsia. *Sci Rep.* 2021;11(1):5692.
18. Kobayashi H, Sadakata H, Suzuki K, She MY, Shibata S, Terao T. Thrombomodulin release from umbilical endothelial cells initiated by preeclampsia plasma-induced neutrophil activation. *Obstet Gynecol.* 1998;92(3):425–430.
19. Cadroy Y, Grandjean H, Pichon J, et al. Evaluation of six markers of haemostatic system in normal pregnancy and pregnancy complicated by hypertension or pre-eclampsia. *Br J Obstet Gynaecol.* 1993;100(5):416–420.
20. O'Riordan MN, Higgins JR. Haemostasis in normal and abnormal pregnancy. *Best Pract Res Clin Obstet Gynaecol*. 2003;17(3):385–396.
21. Rousseau A, Favier R, Van Dreden P. Elevated circulating soluble thrombomodulin activity, tissue factor activity and circulating procoagulant phospholipids: new and useful markers for pre-eclampsia? *Eur J Obstet Gynecol Reprod Biol.* 2009;146(1):46–49.
22. Kohler HP, Grant PJ. Plasminogen-activator inhibitor type 1 and coronary artery disease. *N Engl J Med.* 2000;342(24):1792–1801.
23. Okamoto T, Tanigami H, Suzuki K, Shimaoka M. Thrombomodulin: a bifunctional modulator of inflammation and coagulation in sepsis. *Crit Care Res Pract.* 2012;2012:614545.
24. Kobayashi T, Tokunaga N, Sugimura M, Kanayama N, Terao T. Predictive values of coagulation/fibrinolysis parameters for the

Downloaded from https://academic.oup.com/labmed/article/54/4/392/6820974 by guest on 24 February 2025

termination of pregnancy complicated by severe preeclampsia. *Semin Thromb Hemost*. 2001;27(2):137–41.

25. Rbiet MJ, Plantier JL, Dejana E. Thrombin-induced endothelial cell dysfunction. *Br Med Bull*. 1994;50:936–945.
26. Khatun S, Kanayama N, Belayet H, et al. The impact of vasoactive peptides on nitric oxide production in cultured sympathetic neurons. *Neuroscience*. 1999;93:605–609.
27. Dekker GA, de Vries JIP, Doelitzsch PM, et al. Underlying disorders associated with severe early-onset preeclampsia. *Am J Obstet Gynecol.* 1995;173:1042–1048.
28. Hayashi M, Hamada Y, Ohkura T. Thrombin–antithrombin complex and a2-plasmin inhibitor–plasmin complex levels after cesarean section in normal pregnancies and pre-eclampsia. *Int J Gynaecol Obstet*. 2003;82(2):213–6.

Downloaded from https://academic.oup.com/labmed/article/54/4/392/6820974 by guest on 24 February 2025

Comparison of Commercial Low Molecular Weight Heparin and Homemade Anti-Xa Calibrators to a Commercial Specific Anti-Xa Calibrator for Plasma Rivaroxaban Quantification by Anti-Xa Oral Anticoagulant Plasma Concentration Chromogenic Assay

Bita Divsalar, PhD,[1,2] *Tahereh Kalantari, PhD,*[*,1,2] *Soheila Mohebbi, MSc,*[1,2] *Ardeshir Bahmanimehr, PhD,*[3] *Amin Shahsavani, MSc,*[3,4] *Afshin Borhani-Haghighi, MD*[5]

[1]Division of Hematology and Blood Banking, Department of Laboratory Sciences, School of Paramedical Sciences, Shiraz University of Medical Sciences, Shiraz, Iran, [2]Diagnostic Laboratory Sciences and Technology Research Center, School of Paramedical Sciences, Shiraz University of Medical Sciences, Shiraz, Iran, [3]Thalassemia and Hemophilia Genetic, PND Research Center, Dastgheib Hospital, Shiraz University of Medical Sciences, Shiraz, Iran, [4]Hematology Research Center, Shiraz University of Medical Sciences, Shiraz, Iran, [5]Clinical Neurology Research Center, Shiraz University of Medical Sciences, Shiraz, Iran. *To whom correspondence should be addressed: kalantari_t@sums.ac.ir.

Keywords: Anti-Xa, homemade calibrator made by spiked normal pooled plasma, NPP, laboratory, low molecular weight heparin, rivaroxaban

Abbreviations: LMWH, low molecular weight heparin; aPTT, activated partial thrombin time; PT, prothrombin time; HPLC-MS/MS, high-performance liquid chromatography coupled with tandem mass spectrometry; DOAC, direct oral anticoagulant; NPP, normal pooled plasma; PPP, platelet-poor plasma; DMSO, dimethyl sulfoxide; ROC, receiver operating characteristic; ICC, intraclass correlation coefficient; 95 CI, 95% confidence interval; AUC, area under the curve

Laboratory Medicine 2023;54:400-405; https://doi.org/10.1093/labmed/lmac137

ABSTRACT

Objective: The main concern about measuring the concentration of rivaroxaban by anti-Xa assay in some laboratories is the lack of a commercial specific calibrator in emergencies. Therefore, this study aimed at providing a homemade anti-Xa calibrator and commercial low molecular weight heparin (LMWH) anti-Xa calibrator.

Methods: The anti-Xa plasma concentration of rivaroxaban was measured in 70 patients using a commercial specific anti-Xa calibrator, a commercial LMWH anti-Xa calibrator, and a homemade anti-Xa calibrator.

Results: We demonstrated a significant correlation and agreement ($P < .001$) between LMWH-calibrated anti-Xa and the commercial specific calibrator. A significant correlation ($P < .001$) was found between homemade calibrated anti-Xa made by normal pooled plasma and that calibrated with a commercial specific drug. The nonspecific homemade and LMWH calibrators had excellent agreement ($P < .001$) and can be used interchangeably.

Conclusion: Our data showed that for estimating rivaroxaban concentrations, the LMWH calibrator could be used as an alternative calibrator in the anti-Xa assay.

Rivaroxaban is the second new oral anticoagulant approved by the Food and Drug Administration to reduce the risk of stroke and systemic embolism in patients with nonvalvular atrial fibrillation.[1] It targets factor Xa selectively, and by blocking the intrinsic and extrinsic coagulation pathways can inhibit thrombin production.[2] Rivaroxaban has a vital fixed daily dose and does not require routine laboratory monitoring. However, rivaroxaban concentrations are measured in some clinical conditions, such as in patients before surgery to detect a residual anticoagulant effect, patients suspected of overdose, thromboembolic events or bleeding, renal impairment, and in overweight patients.[3,4]

The 2 main objectives of quantifying drug levels in the abovementioned clinical conditions are (1) evaluating the level of anticoagulants in specific clinical situations and (2) excluding clinically relevant circulating drugs.[5] Studies have shown that the expected results of screening tests such as activated partial thrombin time (aPTT) and prothrombin time (PT) are insensitive and nonspecific to distinguish the presence of factor Xa inhibitors or assess their plasmatic concentrations.[6]

The gold standard evaluating rivaroxaban concentration in body fluids is believed to be high-performance liquid chromatography coupled

© The Author(s) 2022. Published by Oxford University Press on behalf of American Society for Clinical Pathology. All rights reserved. For permissions, please e-mail: journals.permissions@oup.com

Downloaded from https://academic.oup.com/labmed/article/54/4/400/6961560 by guest on 24 February 2025

with tandem mass spectrometry (HPLC-MS/MS). However, HPLC is too expensive and complicated to be used in all laboratories and emergencies. Also, performing HPLC-MS/MS procedures requires considerable expertise and can only be done in a small number of clinical laboratories[7,8] In some cases, like life-threatening bleeding, emergency surgery, and acute stroke in a patient requiring thrombolysis treatment, the speed of determining direct oral anticoagulant (DOAC) concentrations may directly affect the patient care.[9] The International Council for Standardization in Hematology recommends chromogenic anti-Xa assays in the absence of HPLC. Studies have shown that the chromogenic anti-Xa assay with a specific control and calibrator can be used to determine the impact of each anti-factor Xa.[10] Therefore, commercial calibrators have been developed to assess the plasma concentrations of rivaroxaban and apixaban based on the anti-Xa chromogenic assay.[8] Studies have shown the ability of rivaroxaban-specific calibrated anti-Xa assays to accurately measure the plasma concentrations of rivaroxaban over a wide range of plasma drug concentrations.[11,12]

Problems that may delay laboratory measurement of drug concentrations in patients in emergencies are the lack of either accessibility of specific methods or information on the anti-Xa oral inhibitor used by the patients.[8] Due to the increasing use of DOACs such as rivaroxaban, the main concern about measuring the concentration of these drugs by the anti-Xa assay in some laboratories is the lack of a commercial specific calibrator in emergencies. However, low molecular weight heparin (LMWH), a possible calibrator for measuring the concentrations of rivaroxaban by anti-Xa assay, is present in most laboratories. As a result, this study aimed to evaluate using a commercial LMWH calibrator to measure rivaroxaban concentrations by anti-Xa chromogenic assay. Our secondary goal was to prepare a homemade calibrator by diluting different concentrations of rivaroxaban powder in normal pooled plasma (NPP) in situations where a commercial specific calibrator of this drug is not available.

Materials and Methods

Subjects

Samples from 70 patients with stroke taking rivaroxaban were collected from October 2020 to March 2021 at the Department of Neurology at Namazi Hospital in the Shiraz University of Medical Science, Shiraz, Iran. Ethical approval and patient consent statements were received for all subjects included in this study. Based on the World Health Organization guidelines, stroke has been characterized by focal or whole neurological deficits that persist owing to vascular origin for more than 24 hours. A standard case report form was used by trained residents in the Department of Neurology to document details. The reports included age, sex, medical history, clinical manifestations, National Institutes of Health Stroke Scale score, neuroimaging examinations, and laboratory test results.

The rivaroxaban concentration was measured by anti-Xa assay using the commercial specific control and calibrator kit for each patient. Venous blood samples for estimation of rivaroxaban concentrations were collected in Vacuette tubes (Greiner BioOne) containing 3.2% trisodium citrate (volume 3.5 mL). All samples were centrifuged in less than 4 hours from the time of collection at room temperature for 15 minutes at 2500*g* to obtain platelet-poor plasma (PPP), aliquoted into labeled tubes, and stored at −70°C until analysis.

The chromogenic anti-Xa assay was done with a LIQUID Anti-Xa Hemosil kit according to the manufacturer's instruction. (IL LAX, Instrumentation Laboratory). Commercial specific control and calibrators were used for rivaroxaban (BIOPHEN Rivaroxaban Calibrator and Control kits). The results were conducted by anti-Xa assay with commercial LMWH calibrator and control kits (BIOPHEN Calibrator and Control kits) and homemade calibrator made by spiked NPP. Methodological differences between assays were represented by a higher plasma dilution for rivaroxaban (1/9) than with LMWH (1/5) to reduce limited range linearity.[8]

Each measurement was done on the ACL TOP coagulation analyzer (ACL TOP 300 CTS, Werfen) and reported in international units per milliliter (LMWH) or nanogram per milliliter (direct anti-Xa inhibitor).

Anti-Xa Assay with Specific Rivaroxaban Calibrator

Plasma concentrations of rivaroxaban were measured using a commercial kit based on the chromogenic anti-Xa assay by the specific control and calibrator kit (BIOPHEN Rivaroxaban Calibrator and Control kits).

Anti-Xa Assay with LMWH Calibrator

The anti-Xa assay was calibrated using a commercial LMWH calibrator (BIOPHEN Calibrator and Control kits) and conducted based on the manufacturer's instructions. Results from the assay are expressed as international units per milliliter of anti-Xa activity.

Anti-Xa Assay with Homemade Calibrator Made by Spiked NPP

Blood samples from 50 healthy volunteers, 25 men and 25 women, were drawn into Vacuette tubes (Greiner BioOne) containing 3.2% trisodium citrate (volume 3.5 mL) and centrifuged at 3000*g* for 15 minutes at 4°C to obtain PPP. Pooled plasma was derived from mixing the PPP of 50 healthy persons, and PT, PTT, and fibrinogen tests were performed on it (PT: 13.2 seconds [sec], control PT: 13.1 sec, INR: 1.1 sec, PTT: 31.6 sec, control PTT: 31 sec, and fibrogen: 298 mg/dL). Plasma samples were aliquoted, transferred into plastic tubes, fast-frozen with liquid nitrogen, and stored at −70°C until analysis. Plasma samples were thawed only once at 37°C. Donors gave informed consent before blood sampling. Volunteers gave written informed consent.

Rivaroxaban powder (Bayer HealthCare Pharmaceuticals) was dissolved in 100% dimethyl sulfoxide (DMSO) (0.01 g rivaroxaban in 5 mL DMSO), which led to a concentration of 2,000,000 ng/mL rivaroxaban in DMSO. Then, 10 µL of this concentration was mixed with 990 µL DMSO to get to a 20,000 ng/mL concentration. After that, 25 µL from this concentration was combined with 975 µL NPP and incubated at 37°C for 20 minutes, which yielded a concentration of 500 ng rivaroxaban in 1 mL NPP. We then made a serial dilution with NPP[13] to obtain the following final concentrations of the calibrator: 500, 250, 100, 50, and 0 ng/mL. The anti-Xa assay was calibrated with this homemade calibrator, and the samples were analyzed within 2 hours. Each measurement was performed in triplicate.

Statistical Analysis

The Pearson correlation test was performed to analyze the correlation between LMWH, homemade, and rivaroxaban specific calibrators. The linear regressions and receiver operating characteristic (ROC) curve analysis were performed using GraphPad Prism v9.0.

Downloaded from https://academic.oup.com/labmed/article/54/4/400/6961560 by guest on 24 February 2025

The intraclass correlation coefficient (ICC) agreement was measured with SPSS v22.

Results

Clinical Characteristics and Indications of Dosage

The anti-Xa plasma concentration of rivaroxaban was measured for 70 persons enrolled in the study prescribed rivaroxaban (rivaroxaban dose 10–20 mg/day) for stroke prevention. The characteristics of the study participants are summarized in **TABLE 1**. The commercial specific calibrated chromogenic anti-Xa assay measured the rivaroxaban concentration as ranged from 10 to 509 ng/mL.

Plasma Measurement of Rivaroxaban Concentration Using Commercial LMWH Calibrated Anti-Xa and Homemade Calibrated Anti-Xa

In this study, we estimated the concentration of rivaroxaban using commercial LMWH calibrated anti-Xa and homemade calibrated anti-Xa made by NPP. In 70 patients, plasma concentrations were measured on the 3 different calibrators by anti-Xa assay. A significant correlation was found between commercial LMWH calibrated anti-Xa and commercial rivaroxaban specific calibrated anti-Xa (r^2 = 0.998, P < .001) (**FIGURE 1A**). There was also a strong linear relationship between homemade calibrated anti-Xa activity and commercial rivaroxaban-specific calibrated anti-Xa (r^2 = 1.00, P < .001) (**FIGURE 1B**). Moreover, a significant correlation was seen between LMWH and homemade calibrated anti-Xa for detecting rivaroxaban concentration (r^2 = .998, P < .001) (**FIGURE 1C**).

Like the Pearson correlation, the ICC estimates the relationship rate between variables (in this case, between multiple assessments of rivaroxaban concentration with different calibrators). However, the ICC also considers the bias distinguishing agreement from the correlation; that means a good agreement (reproducibility) not only requires good correlation but it also requires a lower rate of bias.[14] For this reason, we used the ICC.

TABLE 1. Patients' General Characteristics

Parameter	Mean ± SD
Age, y	66.98 ± 17.08
CHA2DS2-VASc score	3.55 ± 1.79
HAS-BLED score	2.1 ± 1.17
Hemoglobin, g/dL	13.4 ± 1.87
WBC, x 10^9/L	8.21 ± 3.76
RDW, %	14.9 ± 5.5
Platelet, x 10^9/L	214 ± 99.2
MPV, fL	10.2 ± 1.1
Cholesterol, mg/dL	147.7 ± 43.8
ALT, U/L	20.2 ± 15.6
AST, U/L	22.3 ± 7.56
BUN, mg/dL	19.9 ± 7.6
Creatinine, mg/dL	1.15 ± 0.34
Blood glucose, mg/dL	136.3 ± 49.1
GFR, mL/min/1.73 m^2 (MDRD)	54.6 ± 5.1
Fibrinogen, mg/dL	353.88 ± 107.73

ALT, alanine aminotransferase; AST, aspartate aminotransferase; BUN, blood urea nitrogen; GFR, glomular filtration rate; MPV, mean platelet volume; RDW, red cell distribution width.

The ICC agreement between commercial LMWH calibrated anti-Xa and commercial rivaroxaban-specific calibrated anti-Xa was 0.77 (95% confidence interval [95 CI]: −0.035–0.94, P < .001). Also, the ICC agreement between homemade calibrated anti-Xa and commercial rivaroxaban-specific calibrated anti-Xa was 0.6 (95% CI: −0.013–0.88, P < .001). On the other hand, the ICC agreement between homemade and LMWH calibrators was 0.89 (95% CI: 0.80–0.94, P < .001).

The reliability by ICC values for agreement were considered to be poor (<0.40), moderate (0.41–0.61), good (0.61–0.80) and excellent (>0.81).

The ROC curve analysis displayed the sensitivity and specificity of homemade and LMWH calibrators in measuring rivaroxaban concentrations. As shown in **FIGURE 2**, sensitivity and specificity of homemade and LMWH calibrators for measuring the concentration of rivaroxaban was 57% and 91% (area under the curve [AUC]: 0.79, P < .001) as well as 55.71% and 85.71% (AUC: 0.71, P < .001), respectively (**FIGURE 2**). We calculated the highest sensitivity, specificity, positive predictive value, and negative predictive value of the assay with both homemade and LMWH calibrators for each plasma concentration to ensure a reliable method in this study. The sensitivity and specificity of homemade and LMWH calibrators for measuring rivaroxaban concentration was 100% in the concentrations >60.4 and >41.3, respectively, compared with the specific calibrator for rivaroxaban detection (**TABLE 2**).

Discussion

This study evaluated the reliability of 2 commercial LMWH and homemade calibrators with a commercial specific calibrator for measuring rivaroxaban concentration by chromogenic anti-Xa assays.

The main finding of this study was a remarkable correlation and agreement (r^2 = 0.998, P < .001, ICC: 0.77 P < .001) between LMWH and specific calibrators for measuring the concentration of rivaroxaban that clarify the LMWH calibrator as an alternative calibrator to the chromogenic assays in emergencies. There was also a significant correlation (r^2 =1.00, P < .001) and moderate agreement (ICC: 0.6 P < .001) between homemade and commercial specific drug calibrators. The homemade and LMWH calibrators had an excellent agreement (ICC: 0.89 P < .001) and can be used interchangeably.

The ROC analysis displayed that both calibrators (LMWH and homemade) had acceptable specificity for detecting the rivaroxaban concentrations. The sensitivity, specificity, and negative predictive value of homemade and LMWH calibrators for measuring the concentration of rivaroxaban was 100% in concentrations >60.4 and >41.3, respectively, compared to commercial specific calibrators for rivaroxaban detection. We chose cut-off values with the highest sensitivity and negative predictive value to ensure a dependable way to compare these methods in this study.

The expected plasma trough concentration was 44 ng/mL (12–137 ng/mL) for rivaroxaban in 1 stroke prevention study.[10] Our results confirmed that in the event that a commercial specific calibrator for measuring rivaroxaban concentration is not available, an LMWH calibrator could be used as an alternative method for estimating the rivaroxaban concentration with a sensitivity of 100%.

This observation is in line with Maier et al,[15] who suggested that performing a routine heparin anti-Xa assay may play a significant role in assessing anti-Xa concentration when drug-specific tests are

Downloaded from https://academic.oup.com/labmed/article/54/4/400/6961560 by guest on 24 February 2025

FIGURE 1. A, Correlation of anti-Xa rivaroxaban plasma concentration measured with specific and low molecular weight heparin (LMWH) calibrators (r^2 = 0.998, y = 1.13E2 + 0.8x). B, Correlation of anti-Xa rivaroxaban plasma concentration measured with specific and homemade calibrators (r^2 = 1.00, y = 73.85 + 1.22x). C, Correlation of anti-Xa rivaroxaban plasma concentration measured with LMWH and homemade calibrators (r^2 = 0.998, y = 48.39 + 1.53x). The correlation between the calibrators was shown with $P < .001$ in all three graphs (A, B, and C). NPP, normal pooled plasma.

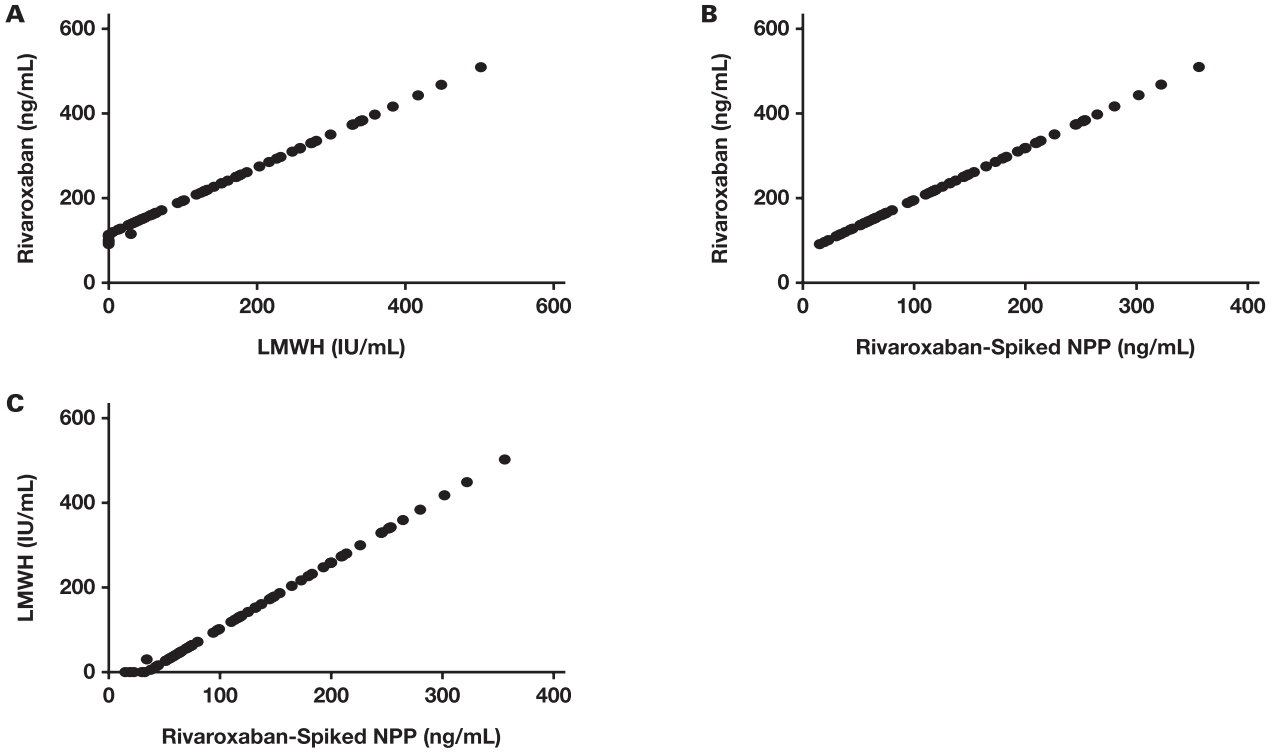

FIGURE 2. Receiver operating characteristic curve analysis of homemade (A) and low molecular weight heparin (B) calibrators for measuring rivaroxaban concentrations.

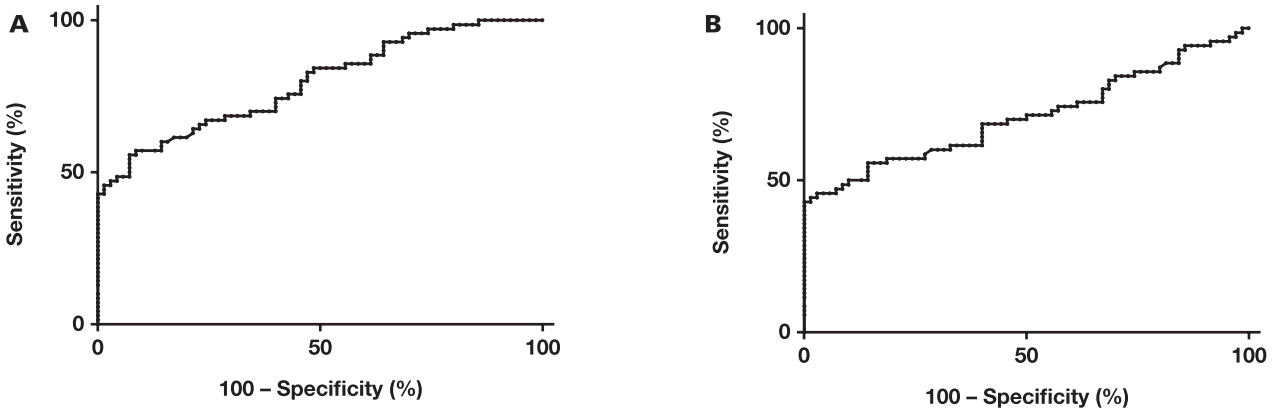

not available and rapid determination of drugs is required and necessary. This study provides data suggesting that the heparin calibrated anti-Xa method is performed using standard coagulation devices in a wide range of US hospitals. Therefore, this may guide appropriate and cost-effective usage and may help in saving anti-Xa antidote.[15] Several studies have shown a strong linear correlation between plasma concentrations of rivaroxaban and the LMWH-calibrated anti-Xa assay.[13,16–18] This correlation is observed at many drug concentrations (20–500 ng/mL). Although the anti-Xa chromogenic assay using a commercial specific calibrator is preferred to quantify the rivaroxaban concentrations, it was shown that the LMWH calibrated anti-Xa assay may be helpful in emergencies to estimate the presence of rivaroxaban. However, the concentration of rivaroxaban should be evaluated with caution.[13,16–18] One study concluded that LMWH-calibrated anti-Xa assays to determine the presence of anti-Xa inhibitors were not recommended. Consequently, it is best for each laboratory to evaluate the sensitivity of the LMWH calibrator method using commercially available direct oral inhibitors.[19]

Downloaded from https://academic.oup.com/labmed/article/54/4/400/6961560 by guest on 24 February 2025

TABLE 2. ROC Curve Analysis for Rivaroxaban Concentrations by Anti-Xa Assay with LMWH and Homemade Calibrators in an Emergency Procedure

	Sensitivity	Specificity	Positive Predictive Value	Negative Predictive Value	AUC	95% CI
Assay with NPP >60.4	100	100	100	100	1	0.95–1
Assay with LMWH >41.3	100	100	100	100	1	0.95–1

AUC, area under the curve; CI, confidence interval; LMWH, low molecular weight heparin; NPP, normal pooled plasma; ROC, receiver operating characteristic.

Oral anti-Xa assays are not readily available in all laboratories due to the cost of the assay, which requires commercial specific calibrators and controls for each drug. Conversely, the LMWH calibrated anti-Xa assay is available in most routine laboratories. The results of a study done by Billoir et al[8] demonstrated that in the absence of specific assays, the LMWH calibrated anti-Xa assay could be used to measure and monitor the inhibitory effects of oral factor Xa before emergency surgery. They also illustrated the possibility of using the LMWH calibrated anti-Xa assay to estimate the plasma concentrations of rivaroxaban and apixaban quantitatively. Their research showed an LMWH anti-Xa activity of <0.50 IU/mL and <30 ng/mL for measuring the plasma concentration of rivaroxaban or apixaban, respectively. They found a cutoff for safe indications of emergency procedures with 100% sensitivity and specificity, indicating the possibility of estimating apixaban or rivaroxaban concentrations using the LMWH calibrator to reduce delay in an emergency.[8] Furthermore, Margetić et al[5] demonstrated the potential of using LMWH calibrated chromogenic anti-Xa assays as an alternative method to determine a significant concentration of rivaroxaban and apixaban in the absence of a chromogenic anti-Xa assay calibrated with a specific drug. However, they explained that a commercial calibrated chromogenic anti-Xa assay should be performed to determine the amount of these drugs if positive results indicate the presence of an oral anti-Xa inhibitor in plasma. Accordingly, they do not recommend use of LMWH calibrator in routine clinical practice as the only practical method for quantifying anti-Xa drugs (rivaroxaban and apixaban).[5] Although the LMWH anti-Xa chromogenic assay appears to allow a quantitative assessment of oral anti-Xa inhibitors, the lack of outcome data with corresponding drug concentrations may decrease the effectiveness of this method in some patients.[18]

Since the LMWH calibrator for measuring the concentration of rivaroxaban has not been standardized between laboratories, significant differences may be seen based on the choice of reagents and the instruments used. Therefore, it is suggested that each laboratory should evaluate the sensitivity of its reagents to rivaroxaban before using the LMWH calibrator.[16]

We made a homemade calibrator using spiked NPP with limited available resources. We estimated a wide range of rivaroxaban concentrations (10–509 ng/mL) with the homemade calibrator, which had acceptable specificity (91%). On the other hand, the sensitivity of both alternative LMWH and homemade calibrators was low (55.71% and 57%, respectively), indicating high bias owing to the small sample size. To make a homemade calibrator using spiked NPP, the optical density of the samples was read, and the calibration curve was drawn manually. For drawing an accurate calibration curve, we had to select an appropriate sample size, and the number of control points must be high. Then, each method was repeated several times. The major limitation of this study was related to the sample size and reagent constraint. As a result, we recommend that future studies should use the appropriate number of samples and control points to draw a precise calibration curve to more accurately evaluate drug concentration.

Conclusion

This study confirmed that if specific calibrators are not available, it is very likely that an LMWH calibrated anti-Xa assay could be used to estimate rivaroxaban concentration. We do not advise the routine use of these assays to estimate rivaroxaban concentration. The LMWH calibrated anti-Xa assay and homemade calibrated anti-Xa activity for estimating rivaroxaban concentration should be used with caution, and it is essential to clearly understand their limitations. Nevertheless, we suggest the use of LMWH and homemade calibrators for each diagnostic laboratory according to their reagents and coagulometer variability, and that they establish their own ranges and cutoffs. We hope our experience is helpful in other laboratories that do not have access to commercial specific calibrators for measuring concentration levels of direct oral anticoagulants by chromogenic anti-Xa assay.

Acknowledgments

Shiraz University of Medical Sciences partially supported this work with grant number 97-19393 and the ethics committee reference number IR.SUMS.REC.1398.691. We appreciate all who participated in this study. We also extend our gratitude to the Thalassemia and Hemophilia Genetic staff, PND Research Center, Dastgheib Hospital, Shiraz University of Medical Sciences, Shiraz, Iran.

Conflict of Interest Disclosure

The authors have nothing to disclose.

REFERENCES

1. January CT, Wann LS, Alpert JS, et al. 2014 AHA/ACC/HRS guideline for the management of patients with atrial fibrillation: a report of the American College of Cardiology/American Heart Association Task Force on Practice Guidelines and the Heart Rhythm Society. *J Am Coll Cardiol.* 2014;64(21):e1–76. doi:10.1016/j.jacc.2014.03.022.
2. Fayyaz M, Abbas F, Kashif T. The role of warfarin and rivaroxaban in the treatment of cerebral venous thrombosis. *Cureus.* 2019;11(5):e4589. doi:10.7759/cureus.4589.
3. Jourdi G, Siguret V, Martin AC, et al. Association rate constants rationalise the pharmacodynamics of apixaban and rivaroxaban. *Thromb Haemost.* 2015;114(07):78–86. doi:10.1160/TH14-10-0877.
4. Martin K, Moll S. Direct oral anticoagulant drug level testing in clinical practice: a single institution experience. *Thromb Res.* 2016;143:40–44. doi:10.1016/j.thromres.2016.04.019.
5. Margetić S, Ćelap I, Delić Brkljačić D, et al. Chromogenic anti-FXa assay calibrated with low molecular weight heparin in patients treated

Downloaded from https://academic.oup.com/labmed/article/54/4/400/6961560 by guest on 24 February 2025

with rivaroxaban and apixaban: possibilities and limitations. *Biochem Med (Zagreb).* 2020;30(1):74–82.

6. Jabet A, Stepanian A, Golmard J-L, et al. Are screening tests reliable to rule out direct oral anticoagulant plasma levels at various thresholds (30, 50, or 100 ng/mL) in emergency situations? *Chest.* 2018;153(1):288–290. doi:10.1016/j.chest.2017.09.047.
7. Mani H, Rohde G, Stratmann G, et al. Accurate determination of rivaroxaban levels requires different calibrator sets but not addition of antithrombin. *Thromb Haemost.* 2012;108(07):191–198. doi:10.1160/TH11-12-0832.
8. Billoir P, Barbay V, Joly LM, Fresel M, Chrétien MH, Le Cam Duchez V. Anti-Xa oral anticoagulant plasma concentration assay in real life: rivaroxaban and apixaban quantification in emergency with LMWH calibrator. *Ann Pharmacother.* 2019;53(4):341–347.
9. Samuelson BT, Cuker A, Siegal DM, Crowther M, Garcia DA. Laboratory assessment of the anticoagulant activity of direct oral anticoagulants: a systematic review. *Chest.* 2017;151(1):127–138. doi:10.1016/j.chest.2016.08.1462.
10. Gosselin RC, Adcock DM, Bates SM, et al. International Council for Standardization in Haematology (ICSH) recommendations for laboratory measurement of direct oral anticoagulants. *Thromb Haemost.* 2018;118(03):437–450. doi:10.1055/s-0038-1627480.
11. Samama MM, Contant G, Spiro TE, et al. Evaluation of the anti-factor Xa chromogenic assay for the measurement of rivaroxaban plasma concentrations using calibrators and controls. *Thromb Haemost.* 2012;107(02):379–387. doi:10.1160/TH11-06-0391.
12. Lindhoff-Last E, Ansell J, Spiro T, Samama MM. Laboratory testing of rivaroxaban in routine clinical practice: when, how, and which assays. *Ann Med.* 2013;45(5-6):423–429. doi:10.3109/07853890.2013.801274.
13. Gosselin R, Grant R, Adcock D. Comparison of the effect of the anti-Xa direct oral anticoagulants apixaban, edoxaban, and rivaroxaban on coagulation assays. *Int J Lab Hematol.* 2016;38(5):505–513.
14. Jinyuan L, Wan T, Guanqin C, Yin L, Changyong F. Correlation and agreement: overview and clarification of competing concepts and measures. *Shanghai Arch Psychiatry* 2016;28(2):115.
15. Maier CL, Asbury WH, Duncan A, et al. Using an old test for new tricks: measuring direct oral anti-Xa drug levels by conventional heparin-calibrated anti-Xa assay. *Am J Hematol.* 2019;94(5):E132–E134. doi:10.1002/ajh.25434.
16. Yates SG, Smith S, Tharpe W, Shen Y-M, Sarode R. Can an anti-Xa assay for low-molecular-weight heparin be used to assess the presence of rivaroxaban? *Transfus Apher Sci.* 2016;55(2):212–215. doi:10.1016/j.transci.2016.06.005.
17. Gosselin RC, Francart SJ, Hawes EM, Moll S, Dager WE, Adcock DM. Heparin-calibrated chromogenic anti-Xa activity measurements in patients receiving rivaroxaban: can this test be used to quantify drug level? *Ann Pharmacother.* 2015;49(7):777–783. doi:10.1177/1060028015578451.
18. Beyer J, Trujillo T, Fisher S, Ko A, Lind SE, Kiser TH. Evaluation of a heparin-calibrated antifactor Xa assay for measuring the anticoagulant effect of oral direct Xa inhibitors. *Clin Appl Thromb Hemost.* 2016;22(5):423–428. doi:10.1177/1076029616629759.
19. Sabor L, Raphaël M, Dogné J-M, Mullier F, Douxfils J. Heparin-calibrated chromogenic anti-Xa assays are not suitable to assess the presence of significant direct factor Xa inhibitors levels. *Thromb Res.* 2017;156:36–38. doi:10.1016/j.thromres.2017.05.024.

Downloaded from https://academic.oup.com/labmed/article/54/4/400/6961560 by guest on 24 February 2025

Prevalence of the Direct Antiglobulin Test and Its Clinical Impact on Multiply Transfused Thalassemia Patients: A Prospective Study Conducted at a Tertiary Care Center in Northern India

Dr Brijesh Kumar Yadav,[1] Dr Rajendra K. Chaudhary,[1,] Dr Harsha Shrivastava,[1] and Dr Priti Elhence[1]*

[1]Department of Transfusion Medicine, Sanjay Gandhi Postgraduate Institute Medical Sciences, Lucknow, India. *To whom correspondence should be addressed: rkcsgpgi@gmail.com.

Keywords: β thalassemia, DAT, ether elution, auto antibody, splenectomy, hepatitis C, serum ferritin, IgG

Abbreviations: DAT, direct antiglobulin test; IgG, immunoglobulin G; RBC, red blood cell; Hb, hemoglobin; AIHA, autoimmune hemolytic anemia; HCV, hepatitis C virus; AHG, antihuman globulin; ELISA, enzyme-linked immunosorbent assay; AOR, adjusted odds ratio

Laboratory Medicine 2023;54:406-410; https://doi.org/10.1093/labmed/lmac140

ABSTRACT

Objective: This study was conducted to estimate prevalence of direct antiglobulin test (DAT) positivity and its impact on transfusion support in patients with thalassemia.

Methods: The DAT testing was performed for patients with β-thalassemia who received transfusion from November 2021 to March 2022. Elution was done for DAT-positive samples.

Results: Of 180 patients, 21 (11.6%) were DAT positive. Immunoglobulin G (IgG) was present in 4 (19%) and IgG+C3d was present in 8 (38%). Only complement was present in 9 (42.8%) patients. The IgG-reactive DATs were associated with pan-reactive eluate. Patients who were DAT-positive had significantly higher levels of serum bilirubin, ferritin, and IgG than those who were DAT-negative.

Conclusion: Autoantibody formation in multiply transfused thalassemia patients is common and merits equal attention as alloimmunization. It is particularly important as DAT-positive red blood cells may undergo clinically significant hemolysis, which may increase the transfusion requirements with associated sequalae such as increased serum ferritin and splenomegaly.

Thalassemia is an inherited hemolytic disorder caused by partial or complete defect in α- or β-globin chain synthesis. The curative treatment for thalassemia is stem cell transplant, in the absence of which severe disease is managed by regular and lifelong red blood cell (RBC) transfusion to keep the hemoglobin (Hb) level between 9 and 11.5 g/dL.[1] Gene therapy by autologous hematopoietic stem cells modified with a lentiviral vector expressing the β-globin gene is a promising approach to completely cure β thalassemia.[2]

A major complication of transfusion therapy in thalassemia is the development of anti-RBC antibodies (alloantibodies and/or autoantibodies). Although formation of alloantibodies occurs due to phenotypic differences between donor and patient RBCs, immunologic disturbances arising from chronic overstimulation of the immune system caused by the joint effect of allogeneic transfusions and splenectomy are responsible for the development of autoantibodies.[3] It is hypothesized that the missing role of the spleen in filtering damaged and conformationally changed RBCs after splenectomy may further augment the immune response and lead to the formation of autoantibodies.[4] Thus, it is not uncommon to find positive direct antiglobulin tests (DATs) in thalassemic patients even when phenotypically matched RBCs have been transfused.

The prevalence of RBC autoantibodies has been estimated to be 6.5% in chronically or intermittently transfused patients[3] as compared to 1.4% in the general population.[5] The autoantibodies can remain silent or cause accelerated clearance of RBCs and autoimmune hemolytic anemia (AIHA),[5] resulting in clinical hemolysis. Autoantibodies may also cause difficulty in cross-matching blood and shorten the duration of RBC survival, requiring immunosuppressive therapy or splenectomy. In some patients, there are anti-RBC autoantibodies present that give a positive DAT without notable RBC destruction.[5] The antibody eluted from the RBCs in such cases often reacts with all RBCs except Rh null RBCs. This prospective study was conducted to estimate the prevalence of DAT positivity and its impact on transfusion support in thalassemia patients. We also studied the association of various clinical and laboratory parameters with DAT positivity.

Materials and Methods

This study was conducted prospectively on participants with β thalassemia for a period of 5 months (from November 2021 to March 2022) after

© The Author(s) 2022. Published by Oxford University Press on behalf of American Society for Clinical Pathology. All rights reserved. For permissions, please e-mail: journals.permissions@oup.com

Downloaded from https://academic.oup.com/labmed/article/54/4/406/6887105 by guest on 24 February 2025

obtaining written informed consent and a waiver from the institutional ethical review board. Patients with connective tissue and autoimmune diseases were excluded from the study.

We used EDTA samples received for routine compatibility testing. No extra sample was taken. Plasma was separated and stored at –80°C in aliquots, which were thawed at room temperature later and used for antibody screening, anti-hepatitis C (HCV) antibody testing, and total serum immunoglobulin G (IgG) estimation. The RBCs were used for performing the DAT.

The DAT was performed by conventional tube technique using AABB standard.[6] Briefly, 1 drop of 2% to 5% suspension of RBCs was dispensed into test tubes and washed 3 times with normal saline, the final wash decanted completely. Two drops of polyspecific antihuman globulin (AHG) reagent (Eryclone Anti-Human Globulin, Tulip Diagnostics) were then added, mixed well, tube-centrifuged at 1000*g* for 30 s, and cells were examined for agglutination. All reactions were graded and recorded.[4] Further distinction of autoantibody was done using monospecific gel cards (IgG/C3cC3d) (DC-Screening I, DiaMed)

Ether elution was performed on all DAT positive samples following the standard method[7] and eluate was tested for the presence of antibody using reagent RBC panel in AHG phase. Antibody screening and identification was performed by the column agglutination technique using commercially available 3-cell (ID-Diacell I-II-III DiaMed) and 11-cell panels (ID-Diapanel, DiaMed), respectively.

Serum IgG concentrations were quantified using the enzyme-linked immunosorbent assay (ELISA) method (Invitrogen, ThermoFisher Scientific). Maximum detection limit of this assay is 0.105 µg/mL (52,500 IU/µL).

Screening for anti-HCV antibody was performed by an enzyme-linked fluorescent assay using a VIDAS Hepatitis panel (bioMérieux Clinical Diagnostics).

Clinical details such as age, sex, age at first transfusion, splenectomy, and transfusion records including number of units transfused and the interval between transfusions, were obtained from the hospital information system. Other biochemical parameters such as hemoglobin, serum total bilirubin, serum conjugated bilirubin, and serum ferritin were obtained from patient files.

Statistical Analysis

All statistical tests were performed using IBM SPSS software for Windows version 20 (IBM). Categorical variables were presented as number and proportions, and continuous variables were presented as median and quartile (χ^2 test). Association was shown by regression (binary logistic). A *P* value of <.05 was considered significant.

Results

A total of 180 participants with β thalassemia who were on regular transfusion therapy over a period of November 2021 to March 2022 at our center were included. Of the 180 patients, 161 (90%) were diagnosed with β thalassemia major and 19 (10%) were diagnosed with β thalassemia intermedia. The majority of these patients were treated exclusively at our institution for thalassemia for the entirety of the study period. Of the 180 patients, 21 (11.6%) were positive for DAT using polyspecific AHG reagent. Patient clinical and demographic details are given in **TABLE 1**. A majority of the patients were male (125/180, 69.4%) with a median age of 13 years. A total of 29 patients (29/180, 16.1%) had undergone splenectomy.

TABLE 2 shows laboratory features in DAT-positive and DAT-negative patients. Alloantibody was present in only 1 DAT-positive patient compared to 9 (5.7%) DAT-negative patients; the difference was not significant (*P* = .866). Only IgG was present in 4 (19%), IgG+C3d was present in 8 (38%), and in the remaining 9 (42.8%) patients, RBCs were coated with complement only. Eluate was pan-reactive in all IgG-coated RBCs and negative in complement-coated RBCs. All DAT-positive patients had significantly higher levels of total bilirubin, serum ferritin, and total serum IgG level compared to DAT-negative patients (*P* < .05). The rate of HCV positivity was also found to be higher in the DAT-positive group than in the DAT-negative group (28.6% vs 1.2%) (*P* < .05).

TABLE 3 shows transfusion requirements in the patients. It was found that total number of units (median) transfused per year and annual consumption of RBCs in milliliters per kilogram per year were higher in DAT-positive patients, 31 vs 24 units and 228.5 vs 152 mL, respectively (*P* < .05).

Although the interval between 2 transfusions was significantly less in DAT-positive patients, alloantibodies were detected in 9 (5%) DAT-negative patients and 1 (4.7%) DAT-positive patient. The specificity of the alloantibodies mostly belonged to RH, Kell, and Kidd specificities (**TABLE 4**).

A positive DAT was associated with splenectomy (*P* = .018), elevated IgG level (*P* = .021), positive HCV Ab (*P* = .018), increased serum ferritin (*P* = .036), decreased transfusion interval (*P* = .018), and increased consumption of RBCs per year (*P* = .013) on multivariate analysis (**TABLE 5**).

Discussion

Although alloimunization is a known complication in multiply transfused thalassemia patients, autoantibody formation is less commonly reported in the literature. Autoantibodies in these patients cause

TABLE 1. Clinical Details of Thalassemia Patients with and without DAT Positivity[a]

Variable	All Patients (n = 180)	DAT-Positive Patients (n = 21)	DAT-Negative Patients (n = 159)	*P* Value
Age, median (quartile), y	13 (9–21)	15 (12.5–22.5)	12 (9–21)	.082
Male	125 (69.4)	16 (76.2)	109 (68.6)	.457
Female	55 (30.6)	5 (23.8)	50 (31.4)	
Thalassemia major	161 (89.4)	20 (95.2)	141 (88.7)	
Thalassemia Intermedia	19 (10.6)	1 (4.8)	18 (11.3)	
Age at first transfusion, median (quartile), y	0.58 (0.41–1.5)	0.75 (0.57–1.13)	0.58 (0.41–1.1.50)	.459
Splenectomy	29 (16.1)	10 (47.6)	19 (11.9)	<.001

DAT, direct antiglobulin test.
[a]*Data are given as No. (%) except where indicated.*

Downloaded from https://academic.oup.com/labmed/article/54/4/406/6887105 by guest on 24 February 2025

TABLE 2. Laboratory Features of Thalassemia Patients with and without DAT Positivity

Laboratory Feature	DAT-Positive (n = 21)	DAT-Negative (n = 159)	*P* Value
Alloimmunization, No. (%)	1 (4.8)	9 (5.7)	.866
Auto antibody, No. (%)			
IgG+C3d	8 (38)	NA	
IgG only	4 (19)		
C3d only	9 (42.8)		
Total bilirubin, median (quartile), mg/dL	1.7 (1.1–2.2)	1.1 (0.7–1.87)	.011
Conjugated bilirubin, median (quartile), mg/dL	0.75 (0.57–1.13)	0.6 (0.44–0.86)	.109
Serum ferritin, median (quartile), ng/mL	3300 (2627–4466)	2090 (1746–2598)	<.001
Total serum IgG[a] level >52,500 IU/dL, No. (%)	16 (76.2)	28 (48.3)	.027
Anti-HCV antibody positive, No. (%)	6 (28.6)	2 (1.2)	<.001

DAT, direct antiglobulin test; HCV, hepatitis C virus; IgG, immunoglobulin G; NA, not applicable.
[a]Measured in all DAT-positive and 58 DAT-negative patients

TABLE 3. Transfusion Support in Thalassemia Patients

Variable	DAT-Positive (n = 21)	DAT-Negative (n = 159)	*P* Value
No. of units transfused/y, median (quartile)	31 (25–38)	24 (21–26)	<.001
Average interval between 2 consecutive transfusions, median (quartile), d	22 (15–28)	27 (24–30)	.002
Annual consumption of RBCs, median (quartile), mL/kg/y	228.5 (138.9–297.1)	152 (115–208)	.013

DAT, direct antiglobulin test.

TABLE 4. Specificity of Alloantibodies in DAT-Positive and DAT-Negative Patients

Antibody	DAT-Positive (n = 21)	DAT-Negative (n = 159)	Total
Anti-E	0	1	1
Anti D + Anti C	0	1	1
Anti C + Anti K	0	1	1
Anti E + Anti K	0	2	2
Anti-K	1	3	4
Anti Jk[a]	0	1	1

DAT, direct antiglobulin test.

hemolysis of the patient's own RBCs as well as transfused RBCs. The DAT is the most sensitive diagnostic tool for detection of in vivo sensitization of RBCs.

A DAT positivity in thalassemia patients can either be due to autoantibodies or residual donor RBCs coated with alloantibodies. However, in our study, DAT positivity was due only to autoantibodies and not alloantibodies.

In the current study, the rate of DAT positivity among patients with β-thalassemia was 11.6% (21/180). The prevalence of autoantibody formation in patients with thalassemia in other countries has been reported as 28.8% in Egypt,[8] 23% in Hong Kong,[9] 22.8% in Albania,[10] and 6.5% in the United States.[11]

In a study from India, Dhawan et al[1] reported a very high rate of autoantibody formation (28.2 %) among 319 multiple transfused patients with β thalassemia major. Similarly, another study from India reported a 15.9% rate of autoantibody formation in this group of patients.[12]

In our study, DAT positivity due to IgG+ complement was found to be an independent predictor of clinically significant hemolysis in patients with β thalassemia with underlying RBC autoimmunity.[5] Amen et al[13] noted that 52% of the autoantibodies detected in their subjects were of IgG in nature; however, none of them caused significant hemolysis. Singer et al[4] found autoantibodies in 25% of those with thalassemia, having IgG specificity in 68.8% and C3d specificity in 32.2% of patients, respectively. Clinically significant AIHA developed in 3 patients: IgG-induced in 1 and IgG with complement in the other 2.[4] In a study from India, IgG only was detected on 56.3% of DAT-positive RBCs.[12] It has been reported that patients with thalassemia major show a significant lymphocytosis, with mainly B-cell changes consistent with ongoing B-cell stimulation associated with chronic exposure to RBC antigens.[14] This B-cell stimulation results in an increase in serum immunoglobulin, immune complexes, and RBCs expressing surface immunoglobulin.

Age at the start of transfusion plays a role in the alloantibody and autoantibody formation. Previous studies have reported a lower frequency of autoantibody formation associated with the early onset of transfusion.[15,16] Consistent with the previous studies, we also observed that early onset of transfusion (0.58 year) was associated with low frequency of autoantibody formation (159/180, 88.3%) compared to late onset (0.75 year) (21/180, 11.6%), however, the difference was not statistically significant (P = .459) (**TABLE 1**). Some authors reported no association between autoantibodies and age of start of transfusion (P = .5, P = .8, respectively).[8,17]

In our study, 47.6% of DAT-positive patients had undergone splenectomy compared to 11.9% of the DAT-negative participants (P < .001). Singer et al[4] observed that 56% of the patients with autoantibodies had undergone splenectomy in their group of patients.

Downloaded from https://academic.oup.com/labmed/article/54/4/406/6887105 by guest on 24 February 2025

TABLE 5. Multivariate Analysis of DAT-Positive Patients

Variable	Regression Coefficient (β)	Adjusted Odds Ratio (95% Confidence Interval)	*P* Value
Serum IgG	–6.237	0.002 (0.000–0.387)	.021
Serum bilirubin conjugated	–3.115	0.044 (0.002–1.180)	.061
Serum ferritin	–0.002	0.998 (0.997–1.000)	.036
Interval between 2 consecutive transfusions	0.584	1.794 (1.106–2.9098)	.018
Annual consumption of packed RBCs	–0.054	0.948 (0.909–0.989)	.013
HCV reactivity	–7.62	0.000 (0.000–0.264)	.018
Splenectomy	–10.3	0.000 (0.000–0.169)	.018

DAT, direct antiglobulin test; HCV, hepatitis C virus; IgG, immunoglobulin G.

Arinsburg et al[3] reported an even higher number of patients with splenectomy (88.1%).

Persons with thalassemia who have undergone splenectomy have higher levels of serum IgG, which is not unexpected, as the spleen is not clearing the RBCs coated with autoantibodies.[18] In our study, 76.2% of DAT-positive patients had serum IgG levels greater than 52,500 IU/dL in contrast to 48.3% of DAT-negative patients (P = .027, **TABLE 2**). Arinsburg et al[3] noted elevated IgG levels in 88.1% of DAT-positive patients. Multiple studies in general patient populations have shown that increased serum IgG levels are associated with a positive DAT. [19,20] Immunological abnormalities in those with thalassemia, including an expansion of circulating B cells and a modest polyclonal gammopathy, are thought to play a role in the abnormal IgG levels.

The HCV positivity among DAT-positive patients was 28.6% in our study, which was significantly higher than that in DAT-negative patients (P < .001, **TABLE 2**). Arinsburg et al[3] reported 60% HCV positivity among DAT-positive subjects. The HCV has been implicated both in the autoantibody formation and autoimmune diseases. The HCV might be involved in the breakdown of self-tolerance triggering autoreactivity.[21] Bhattachrya et al[22] reported very high prevalence of anti-HCV antibodies in multiply transfused thalassemia patients in India. Of 300 patients,75(25%) were found to be HCV positive by ELISA. Among them, 49 (65%) were HCV RNA positive with significant viral load in their blood.

Serum ferritin levels were significantly higher in DAT-positive patients in our study (3300 ng/mL vs 2090 ng/mL, P < .001). This could be due to the combined effect of more transfusions and the higher rate of splenectomy in DAT-positive patients[22] or simply an increased number of transfusions in DAT-positive patients.[23]

The transfusion response in terms of number of units transfused per year, the interval between 2 transfusions, and annual consumption of RBCs was significantly higher among the DAT-positive than the DAT-negative patients (**TABLE 3**). This indicates that DAT-positive RBCs may be undergoing hemolysis more profoundly than DAT-negative RBCs, which is also corroborated by increased levels of serum conjugated bilirubin in DAT-positive patients. However, a previous study reported similar transfusion response among DAT-positive and DAT-negative patients.[3]

On multivariate analysis, a positive DAT in thalassemia was associated with elevated serum IgG levels (adjusted odds ratio [AOR] 0.002, P = .021), elevated serum ferritin (AOR 0.998, P = .036), decreased interval between transfusions (AOR 1.794, P = .018), increased annual consumption of RBCs (AOR 0.948, P = .013), HCV positivity (AOR 0.00, P = .018), and splenectomy (AOR 0.000, P = .018).

We did not find any association between alloimmunization and DAT positivity, which is consistent with Arinsburg et al.[3] In contrast, Jain et al[12] reported significantly higher alloimmunization in patients with positive DAT.

Raised serum conjugated bilirubin level coupled with increased transfusion requirements and decreased transfusion interval in DAT-positive thalassemia patients indicates the development of AIHA. However, due to lack of all the clinical and baseline laboratory information, the DAT-positive subjects in our study cannot be confirmed to have AIHA. This is one of the limitations of this study. Khaled et al[5] reported 25 cases of AIHA among 87 DAT-positive patients. However, it is important for the clinician to closely monitor DAT-positive thalassemia patients for any signs of worsening clinical and laboratory features of hemolysis to rule out the possibility of development of AIHA so that therapeutic interventions can be planned.

Thus, the phenomenon of autoantibody formation in multiply transfused thalassemia patients is not uncommon and merits the same attention as alloimmunization. It is particularly important, as DAT-positive RBCs may undergo clinically significant hemolysis, which may increase the transfusion requirements with associated sequalae such as increased serum ferritin and splenomegaly.

REFERENCES

1. Dhawan HK, Kumawat V, Marwaha N, et al. Alloimmunization and autoimmunization in transfusion dependent thalassemia major patients: study on 319 patients. *Asian J Transfus Sci.* 2014;8(2):84–88. doi:10.4103/0973-6247.137438.
2. Rattananon P, Anurathapan U, Bhukhai K, Hongeng S. The future of gene therapy for transfusion-dependent beta-thalassemia: the power of the lentiviral vector for genetically modified hematopoietic stem cells. *Front Pharmacol.* 2021;12:730873. doi:10.3389/fphar.2021.730873.
3. Arinsburg SA, Skerrett DL, Kleinert D, Giardina PJ, Cushing MM. The significance of a positive DAT in thalassemia patients. *Immunohematology.* 2010;26(3):87–91.
4. Singer ST, Wu V, Mignacca R, Kuypers FA, Morel P, Vichinsky EP. Alloimmunization and erythrocyte autoimmunization in transfusion-dependent thalassemia patients of predominantly Asian descent. *Blood.* 2000;96(10):3369–3373.
5. Khaled MB, Ouederni M, Sahli N, et al. Predictors of autoimmune haemolytic anemia in beta-thalassemia patients with underlying red blood cells autoantibodies. *Blood Cells Mol Dis.* 2019;79:102342.

Downloaded from https://academic.oup.com/labmed/article/54/4/406/6887105 by guest on 24 February 2025

6. Cohn CS, Delaney M, Johnson ST and Katz LM. *Technical Manual*. 20th ed. Bethesda, MD: AABB; 2020.
7. Rubin H. Antibody elution from red blood cells. *J Clin Pathol.* 1963;16(1):70–73.
8. Ahmed AM, Hasan NS, Ragab SH, Kuypers FA, Morel P, Vichinsky EP. Red cell alloimmunization and autoantibodies in Egyptian transfusion-dependent thalassaemia patients. *Arch Med Sci.* 2010;6(4):592–598.
9. Cheng CK, Lee CK, Lin CK. Clinically significant red blood cell antibodies in chronically transfused patients: a survey of Chinese thalassemia major patients and literature review: RBC antibodies in thalassemia major. *Transfusion.* 2012;52(10):2220–2224. doi:10.1111/j.1537-2995.2012.03570.x.
10. Seferi I, Xhetani M, Face M, Burazeri G, Nastas E, Vyshka G. Frequency and specificity of red cell antibodies in thalassemia patients in Albania. *Int J Lab Hematol.* 2015;37(4):569–574. doi:10.1111/ijlh.12362.
11. Vichinsky E, Neumayr L, Trimble S, et al. CDC thalassemia investigators. transfusion complications in thalassemia patients: a report from the Centers for Disease Control and Prevention (CDC). *Transfusion.* 2014;54(4):971–972.
12. Jain A, Agnihotri A, Marwaha N, Sharma RR. Direct antiglobulin test positivity in multi-transfused thalassemics. *Asian J Transfus Sci.* 2016;10(2):161–163. doi:10.4103/0973-6247.164268.
13. Amen R, Shemmari SA, Humood SA, Chawdhury RI, Eyaadi OA, Bashir AA. RBC alloimmunization and autoimmunization among transfusion-dependent thalassemia patients. *Transfusion*. 2003;43(11):1604–1610.
14. Hodge G, Lloyd JV, Hodge S, Story C, Han P. Functional lymphocyte immunophenotypes observed in thalassaemia and haemophilia patients receiving current blood product preparations. *Br J Haematol.* 1999;105(3):817–825. doi:10.1046/j.1365-2141.1999.01385.x.
15. Michail-Merianou V, Pamphili-Panousopoulou L, Piperi-Lowes L, Pelegrinis E, Karaklis A. Alloimmunization to red cell antigens in thalassemia: comparative study of usual versus better-match transfusion programmes. *Vox Sang.* 1987;52(1-2):95–98.
16. Spanos T, Karageorga M, Ladis V, Peristeri J, Hatziliami A, Kattamis C. Red cell alloantibodies in patients with thalassemia. *Vox Sang.* 1990;58(1):50–55. doi:10.1111/j.1423-0410.1990.tb02055.x.
17. Noor HM, Ariffin N, Illuni HI, Rosline H. Red cell autoantibodies among thalassaemia patients in Hospital Universiti Sains Malaysia. *Singapore Med J.* 2007;48(10):922–925.
18. Tovo PA, Miniero R, Barbera C, Sacchetti L, Saitta M. Serum immunoglobulins in homozygous β-thalassemia. *Acta Haematol.* 1981;65(1):21–25. doi:10.1159/000207144.
19. Huh YO, Liu FJ, Rogge K, Chakrabarty L, Lichtiger B. Positive direct antiglobulin test and high serum immunoglobulin G values. *Am J Clin Pathol.* 1988;90(2):197–200. doi:10.1093/ajcp/90.2.197.
20. Szymanski IO, Odgren PR, Fortier NL, Snyder LM. Red blood cell associated IgG in normal and pathologic states. *Blood.* 1980;55(1):48–54.
21. McMurray RW, Elbourne K. Hepatitis C virus infection and autoimmunity. *Semin Arthritis Rheum.* 1997;26(4):689–701. doi:10.1016/s0049-0172(97)80005-4.
22. Bhattacharya KK, Biswas A, Gupta D, Sadhukhan PC. Experience of hepatitis C virus seroprevalence and its genomic diversity among transfusion dependent thalassemia patients in a transfusion centre. *Asian J Transfus Sci.* 2018;12(2):112–116.
23. Shah R, Trehan A, Das R, Marwaha RK. Serum ferritin in thalassemia intermedia. *Indian J Hematol Blood Transfus.* 2014;30(4):281–285. doi:10.1007/s12288-013-0267-y.

Downloaded from https://academic.oup.com/labmed/article/54/4/406/6887105 by guest on 24 February 2025

Identification of Tumor Suppressor Gene LHPP-Based 5-microRNA Signature That Predicts the Early- and Midstage Esophageal Squamous Cell Carcinoma: A Two-Stage Case-Control Study in the Chinese Han Population

Xiang Zhao,[1,a] Xiaocun Zhu,[2,a] Luoshai Wang,[3,a] Yurao Chen,[1] Ronghuai Chen,[1] Zemao Zheng,[1] Hengjin Yang,[1] Wan Xia,[1] Juan Yao, PhD,[1,4,] Kun Zhao, PhD[5]*

[1]Department of Radiation Oncology, Huaian Hospital of Huaian City, Huaian, China, [2]Department of General Surgery and Breast Surgery, Huaian Hospital of Huaian City, Huaian, China, [3]Department of Cardiothoracic Surgery, Huaian Hospital of Huaian City, Huaian, China, [4]Department of Oncology, Taizhou People's Hospital Affiliated to Nantong University, Taizhou, China, and [5]Department of Oncology, Huaian Hospital of Huaian City, Huaian, China. *To whom correspondence should be addressed: tryjyc@ntu.edu.cn. [a]First authors.

Keywords: next-generation sequencing, esophageal squamous cell carcinoma, microRNA, logistic regression model, biomarker, diagnosis

Abbreviations: ESCC, esophageal squamous-cell carcinoma; LHPP, phospholysine phosphohistidine inorganic pyrophosphate phosphatase; BNCC, BeNa Culture Collection; DEMs, differentially expressed miRNAs; SCC, squamous cell carcinoma; CEA, carcinoembryonic antigen; NS, nonsignificant; NC, negative control

Laboratory Medicine 2023;54:411-423; https://doi.org/10.1093/labmed/lmac125

ABSTRACT

Objective: To establish a novel approach for diagnosing early- and midstage esophageal squamous cell carcinoma (ESCC).

Methods: The tumor suppressor gene phospholysine phosphohistidine inorganic pyrophosphate phosphatase (LHPP)–based miRNA signature was identified using next-generation sequencing and 3 biological online prediction systems. This retrospective study established and validated an ESCC prediction model using a test cohort and a validation cohort.

Results: Immunohistochemical staining and real-time quantitative polymerase chain reaction (RT-qPCR) results showed that LHPP protein levels were significantly lower in tissues with early- and midstage ESCC than in adjacent tissues ($P < .01$). Further, we confirmed that miR-15b-5p, miR-424-5p, miR-497-5p, miR-363-5p, and miR-195-5p inhibited LHPP. These 5 miRNAs were significantly elevated in the plasma of early- and midstage ESCC ($P < .05$). An ESCC prediction model combining these 5 miRNAs was established. Finally, in the external validation cohort, the model exhibited high discriminative value (sensitivity/specificity: 84.4%/93.3%).

Conclusions: The prediction model has potential implications for diagnosis of early- and midstage ESCC.

Esophageal squamous cell carcinoma (ESCC) is a malignant tumor of the digestive system.[1] Esophageal cancer has the sixth-highest fatality rate among various malignant tumors. The early symptoms of esophageal cancer are not obvious; therefore, early screening and diagnosis mainly rely on traumatic methods, including the detection of exfoliated esophageal cells and gastrointestinal endoscopy.[2,3] These screening technologies cause trauma to patients during the testing process, making it difficult to achieve large-scale population screening. Hence, exploring diagnostic biomarkers is of great significance for patients with early- and midstage ESCC. Endogenous miRNAs play crucial roles in many biological processes.[4–6] The findings of 2 recent studies[7,8] have suggested that miRNAs, as oncogenes or tumor suppressor genes, may play important roles in the regulation of the occurrence, development, invasion, metastasis, and angiogenesis of various tumors and are related to the occurrence and development of ESCC.

In 2018, Hindupur et al[9] identified a novel tumor suppressor gene, namely, phospholysine phosphohistidine inorganic pyrophosphate phosphatase (LHPP). LHPP is a histidine phosphatase, which has the opposite effect of histidine kinase and can reverse the phosphate group connected to histidine on the protein.[9] Researchers have reported that inhibiting the expression of LHPP can promote the growth of a variety of gastrointestinal tumors, including colorectal cancer,[10] hepatocellular carcinoma,[11] pancreatic cancer,[12] and gastric cancer.[13]

© The Author(s) 2022. Published by Oxford University Press on behalf of American Society for Clinical Pathology. All rights reserved. For permissions, please e-mail: journals.permissions@oup.com

Downloaded from https://academic.oup.com/labmed/article/54/4/411/6821144 by guest on 24 February 2025

FIGURE 1. Flow diagram of early- and midstage esophageal squamous cell carcinoma (ESCC) diagnostic regression model establishment. NGS, next-generation sequencing.

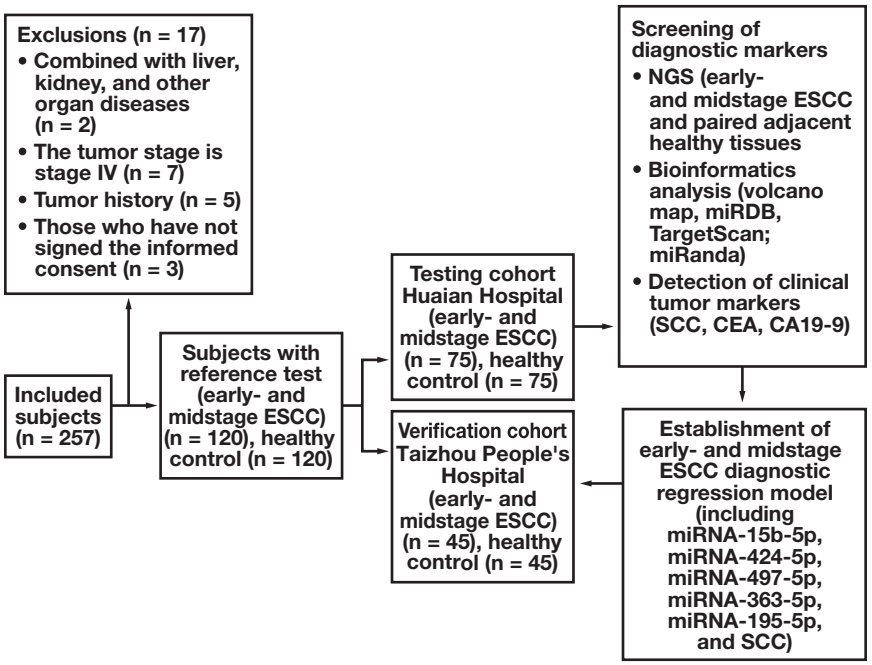

TABLE 1. Primer Sequences

Gene	Primers
LHPP	F: 5′-AGGCTGGGATTTGACATCTC-3′ R: 5′-AGCAGGTATGGTCGCAGG-3′
miR-15b-5p	F: 5′-ATCCAGTGCGTGTCGTG-3′ R: 5′-TGCTTAGCAGCACATCATG-3′
miR-424-5p	F: 5′-GCGGCCAGCAGCAATTCATG-3′ R: 5′-CAGCCACAAAAGAGCACAAT-3′
miR-497-5p	F: 5′-CCTTCAGCAGCACACTGTGG-3′ R: 5′-CAGTGCAGGGTCCGAGGTAT-3′
miR-363-5p	F: 5′-GCAGCAACTAGAAACG-3′ R: 5′-GCACTCATGCCCATTCATCC-3′
miR-195-5p	F: 5′-GGAGTGTAGGCCCAATACCAGA-3′ R: 5′-TGCCACTTAGCAGCACAGAAA-3′
miR-6838-5p	F: 5′-GCACTCCTGGATGCCAATCT-3′ R: 5′-CTCTACAGCTATATTGCCAGCCAC-3′
GAPDH	F: 5′-GCACCGTCAAGGCTGAGAAC-3′ R: 5′-TGGTGAAGACGCCAGTGGA-3′
U6	F: 5′-CTCGCTTCGGCAGCACA-3′ R: 5′-AACGCTTCACGAATTTGCGT-3′

LHPP, phospholysine phosphohistidine inorganic pyrophosphate phosphatase.

So far, there is no study reported in the literature, to our knowledge, regarding the expression level of LHPP in ESCC, so its mechanism of action on tumors is unclear.

In this study, we performed next-generation sequencing (NGS) to analyze and screen out the miRNAs differentially expressed in tissues with ESCC, and combined it with bioinformatics software to predict the expression profile of miRNAs involved in LHPP regulation. We then established an early- and midstage ESCC diagnostic regression model in a testing cohort and performed external verification in a verification cohort.

Methods

Enrollment and Basic Data Collection for Early- and Midstage ESCC

A total of 137 patients with early- and midstage ESCC, treated from January 2016 to December 2016, were included in our study, with the approval of the Ethics Committee of Huaian Hospital (No. k16.0112) and Taizhou People's Hospital (No. 201601-002-1), in accordance to the Declaration of Helsinki. Informed oral consent was obtained from all individual participants included in the study. The tissue with ESCC and the adjacent healthy tissue (tumor-adjacent normal esophageal mucosa at a distance >2 cm from the edge of the cancerous tissue) were collected during an operation. The exclusion criteria for patients with ESCC were as follows: tumor history, tumor being at stage IV, patient declined to sign the informed consent form, history of radiotherapy or chemotherapy, and having incomplete clinical data for the patient. A total of 120 patients with ESCC were enrolled, including 75 patients from Huaian Hospital (testing cohort) and 45 patients from Taizhou People's Hospital (verification cohort). During the same period, 120 healthy participants were recruited for study inclusion. The flow diagram of the study is shown in **FIGURE 1**.

NGS Technology and Bioinformatics Analysis for miRNA Expression Profile Exploration

NGS was performed by Shanghai Kangcheng Biological Engineering. The Illumina-HiSeq 4000 sequencing platform (Illumina) was used for sequencing. The information on the NGS platform used in this study is shown in Supplementary Table 1.

Downloaded from https://academic.oup.com/labmed/article/54/4/411/6821144 by guest on 24 February 2025

FIGURE 2. The protein and mRNA levels of phospholysine phosphohistidine inorganic pyrophosphate phosphatase (LHPP) in early- and midstage esophageal squamous cell carcinoma (ESCC) are significantly decreased. A, Compared with paired adjacent healthy tissues, LHPP protein levels in tissues with early- and midstage ESCC were significantly decreased (×400). B, Real-time quantitative polymerase chain reaction amplification curves for LHPP and GAPDH. C, Compared with healthy control individuals, LHPP mRNA levels in patients with early- and midstage ESCC were significantly decreased in the testing cohort. D, Compared with healthy controls, LHPP mRNA levels in early- and midstage ESCC were significantly decreased in the verification cohort. The $2^{-\Delta\Delta CT}$ method was used in the present study. *P < .01 compared with healthy controls. NS, nonsignificant.

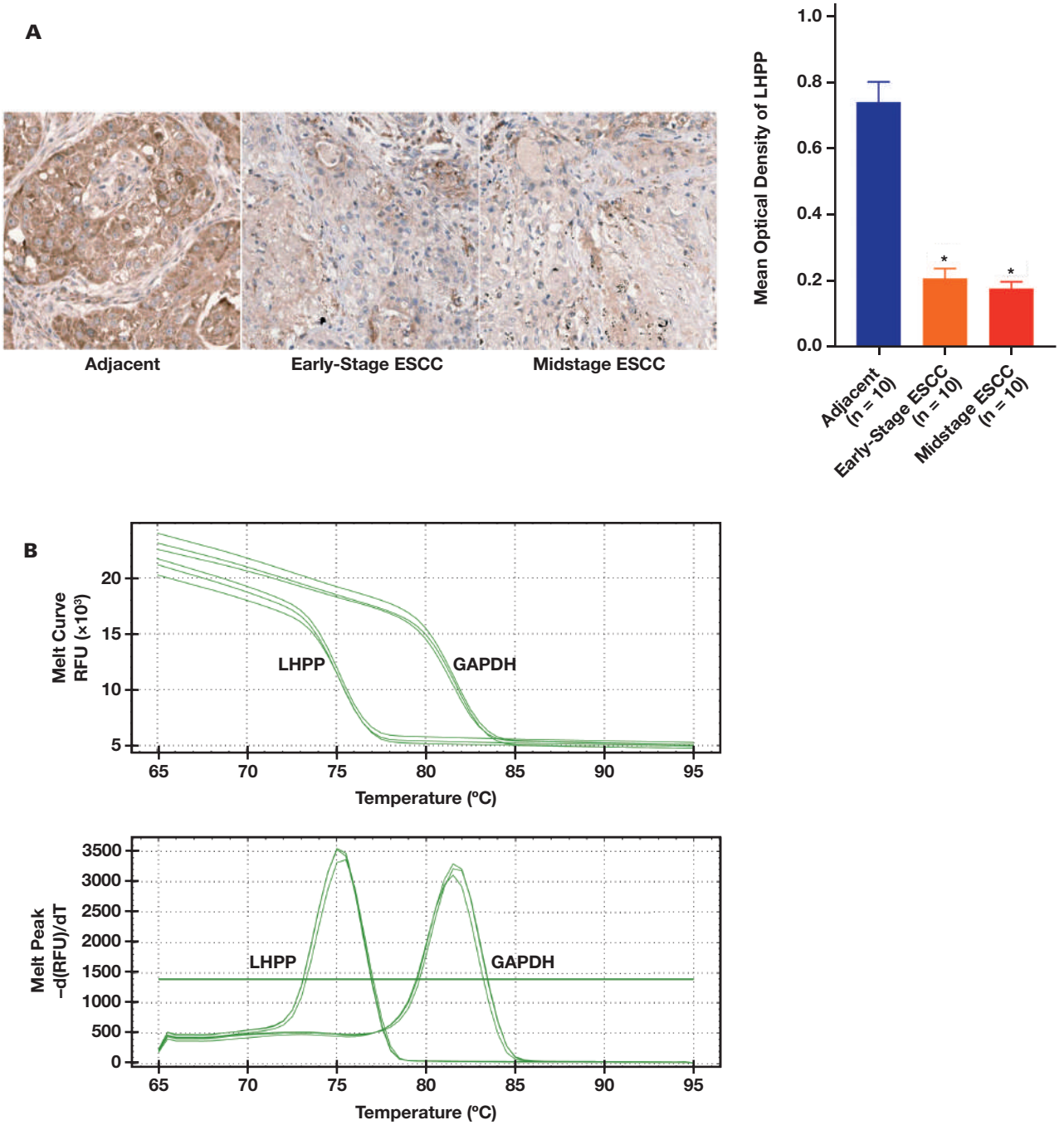

After the sequencing was completed, the original sequencing sequence was obtained, and bioinformatics analysis was then performed. The 2 important indicators (fold change and *P* value) in the volcano map can intuitively and reasonably screen miRNA genes that are differentially expressed between the 2 specimens. A *t* test was used to analyze the genes that were significantly differentially expressed between the 2 specimens. The abscissa of the volcano plot is log2 (fold change) and the ordinate is –log10 (*P* value). In this study, we also used the miRDB and TargetScan databases, and miRanda database (http://www.miranda.org/), to predict the regulatory miRNAs upstream of LHPP.

Downloaded from https://academic.oup.com/labmed/article/54/4/411/6821144 by guest on 24 February 2025

FIGURE 2. (cont)

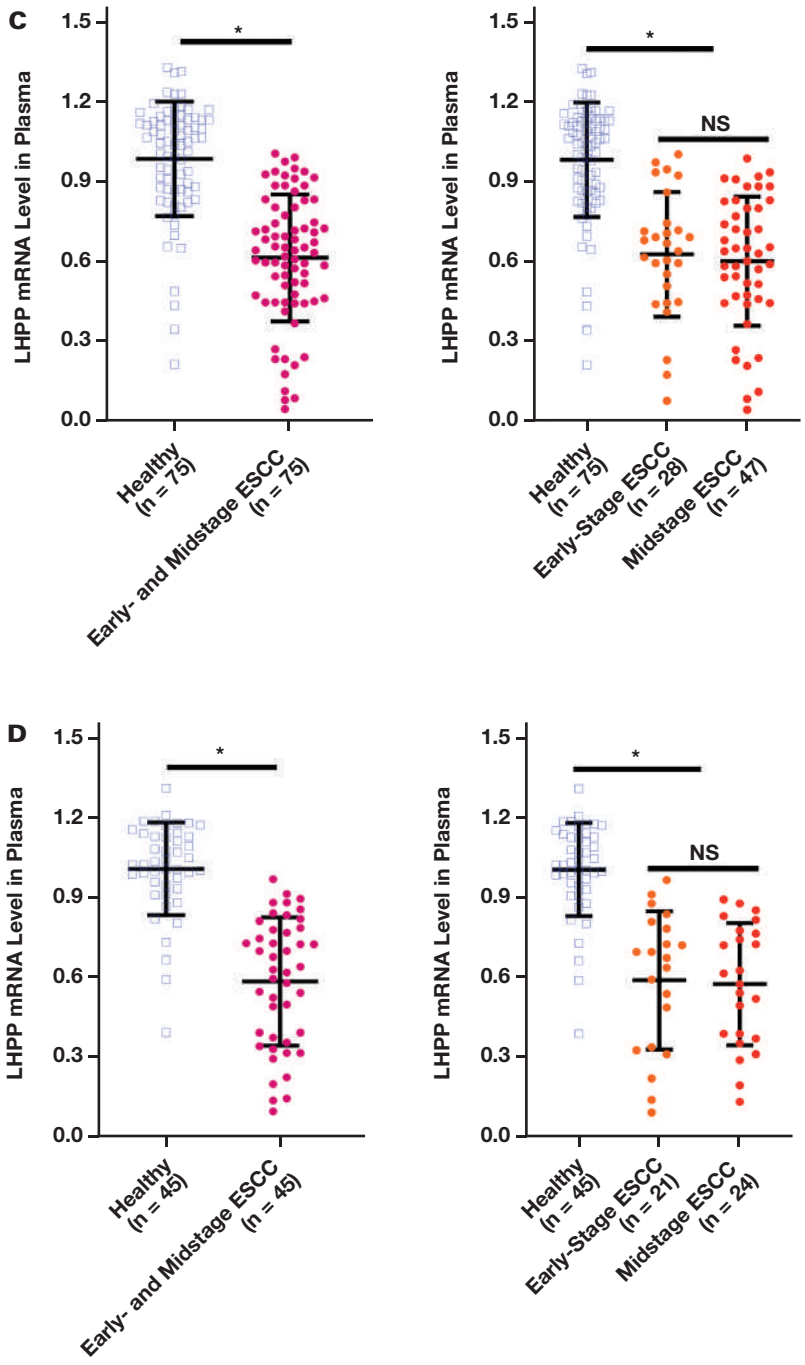

Cell Culture and Transfection

We purchased KYSE-30 (RRID: CVCL_1351; https://scicrunch.org/resources/data/source/SCR_013869-1/search?q=CVCL_1351&l=CVCL_1351) from the BeNa Culture Collection (BNCC) for in vitro research. KYSE-30 cells were inoculated in EMEM complete medium (BNCC338137, BNCC) mixed with FBS. miR-15b-5p, miR-424-5p, miR-497-5p, miR-363-5p, miR-195-5p mimics, and si-LHPP were obtained from Guangzhou Changyu Biotechnology.

Luciferase Reporter Assay

The 3′ UTR sequence or mutant sequence of LHPP was cloned into the pMIR-REPORT vector. The miRNA mimics or mimic controls were transfected into KYSE-30 cells, together with the reporter plasmid and pRL-SV40.

RNA Pull-Down Assay

RNA pull-down assays were performed, as described previously.[14] Total RNA extracts from ESCC cells were mixed with biotin-labeled-miRNA-15b-5p, or miRNA-424-5p, or miRNA-497-5p, or miRNA-363-5p, or miRNA-195-5p, incubated with Dynabeads M-280 Streptavidin (Invitrogen) at 4°C for 3 hours. Unbound RNA was washed away with 20 mmol/L Tris. Streptavidin Magnetic Beads were washed 3 times with washing buffer and then incubated with 50 μL elution buffer at 37°C for 15 minutes with stirring after incubation for 1.5 hours, with rotation at 4°C. The relative levels of LHPP protein contained in the pull-down complexes were analyzed using an ELISA kit for LHPP (item No. abx380698, Abbexa).

Downloaded from https://academic.oup.com/labmed/article/54/4/411/6821144 by guest on 24 February 2025

FIGURE 3. Next-generation sequencing (NGS) technology and bioinformatics technology were used to analyze the targeted regulatory miRNAs of phospholysine phosphohistidine inorganic pyrophosphate phosphatase (LHPP). NGS technology (A) and volcano map (B) of differentially expressed genes between tissues with early- and midstage esophageal squamous cell carcinoma (ESCC) and paired adjacent healthy tissues. In part B, the red nodes represent upregulation and the blue nodes represent downregulation. C, Venn diagrams were used to analyze the target miRNAs using the miRanda, miRDB, and TargetScan online prediction systems.

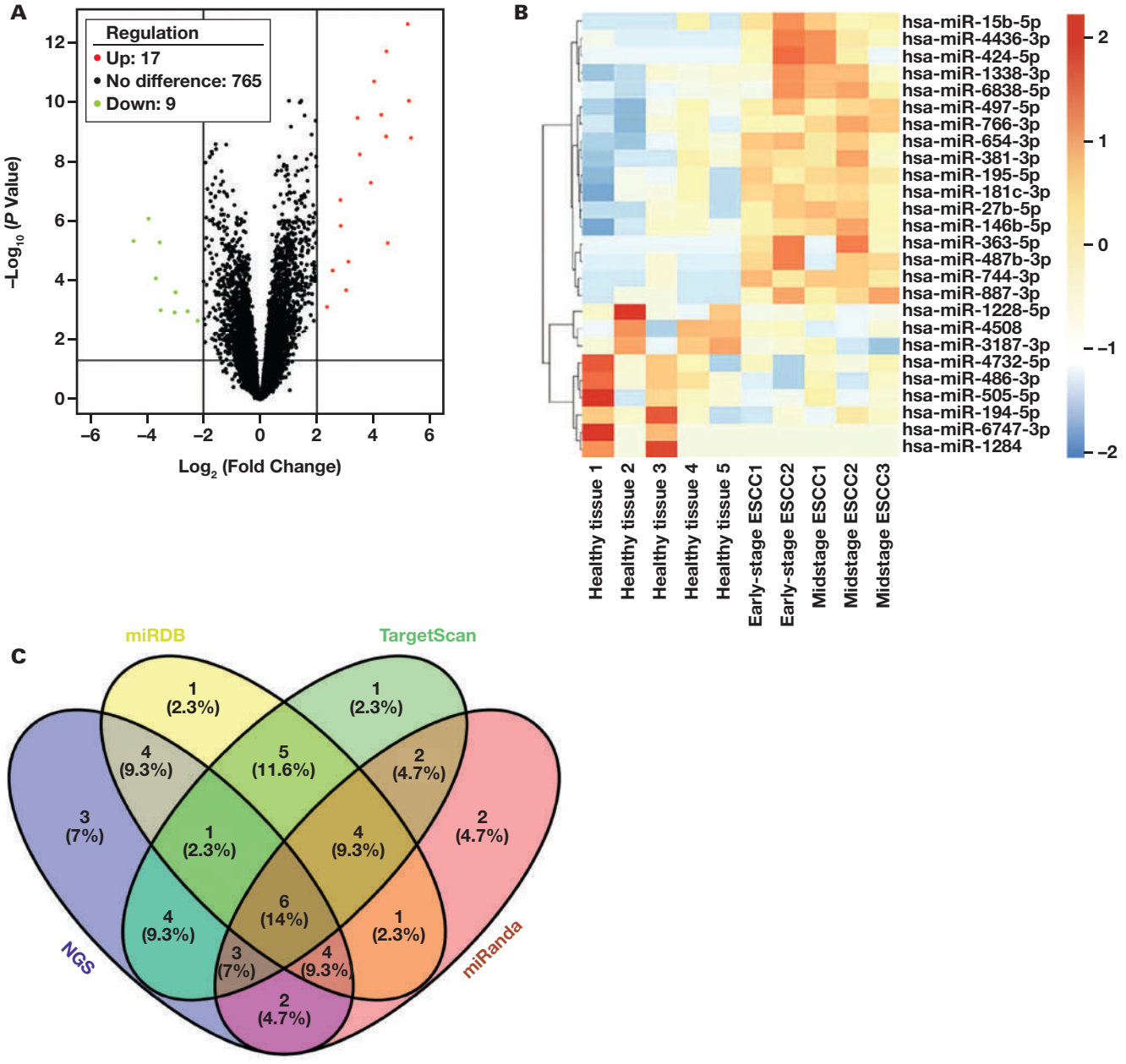

Immunohistochemical Staining

ESCC tissues were fixed with 4% formaldehyde for 1 to 24 hours, and then embedded in paraffin and made into sections. We placed the slices in a 65°C oven and baked them for 30 minutes to 1 hour, then soaked them in xylene for 3 minutes for dewaxing, and soaked them in ethanol of high to low concentration for 3 minutes for rehydration. Next, we soaked the slices in 0.01 mol/L citrate buffer at 95°C for 30 minutes for antigen retrieval. The endogenous peroxidase activity was soaked in hydrogen peroxide (3%) at room temperature for 10 minutes in the dark, and the sections were incubated with 5% bovine serum albumin for 1 hour at 37°C, to reduce nonspecific binding. Then, the sections were incubated overnight at 4°C with primary antibody for the detection of LHPP (ab116175; 1:200 dilution; Abcam). The tissues were then incubated with secondary antibody (ab205718;1:200 dilution; Abcam) at 37°C for another 30 minutes.

Real-Time Quantitative PCR (RT-qPCR) Assay

RT-qPCR was performed using the SYBR Green qPCR Kit (Thermo Fisher Scientific) on a StepOne Real-Time PCR System (Applied Biosystems). Glyceraldehyde-3-phosphate dehydrogenase (GAPDH) and U6 were used as control references for the mRNA and miRNA. Primers were purchased from Sangon Biotech. The primer sequences used are listed in **TABLE 1**.

Downloaded from https://academic.oup.com/labmed/article/54/4/411/6821144 by guest on 24 February 2025

FIGURE 4. **miR-15b-5p, miR-424-5p, miR-497-5p, miR-363-5p, and miR-195-5p regulate phospholysine phosphohistidine inorganic pyrophosphate phosphatase (LHPP) expression. Luciferase reporter gene and RNA pull-down assays were used to explore the relationships between LHPP and miR-15b-5p (A), miR-424-5p (B), miR-497-5P (C), miR-363-5p (D), miR-195-5p (E), and miR-6838-5p (F). **P* <.01; NS, nonsignificant; NC, negative control.**

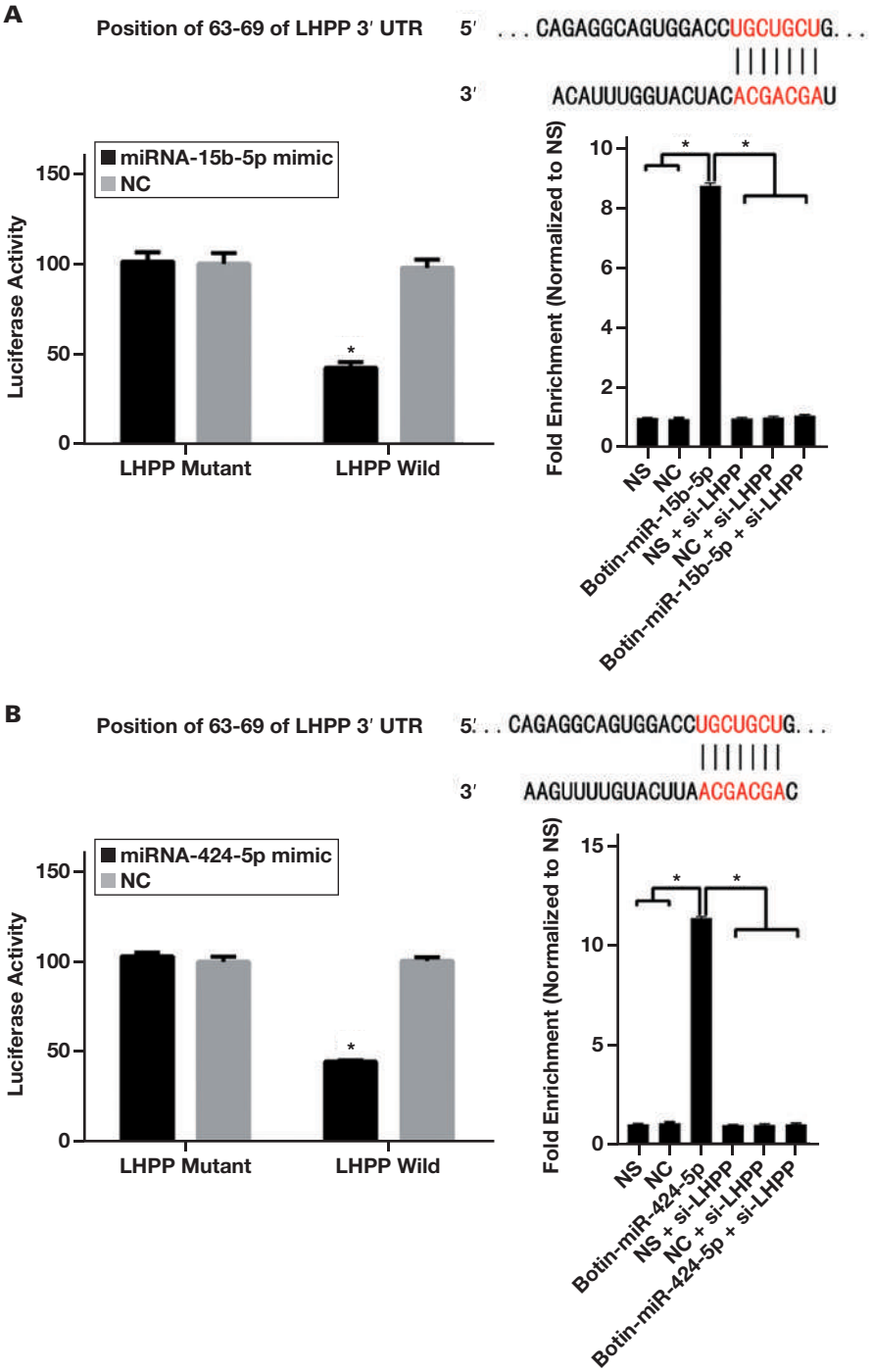

For relative quantification, the $2^{-\Delta\Delta CT}$ approach was applied. Three independent duplicates of each RT-qPCR experiment were carried out.

The Cancer Genome Atlas (TCGA) miRNA Dataset

The dataset TCGA-ESCA was used to find if the significant differentially expressed miRNAs (DEMs) were correlated with ESCC. The dataset TCGA-ESCA consists of 95 ESCC specimens with 19 normal esophageal mucosa specimens. We examined the significant DEMs expression and relationship with ESCC stages. The t test was applied to check expression level, and the χ^2 testing was used on different stages.

Statistics

We have created a Github page and uploaded all related scripts and supported data (https://github.com/tryyao/ESCC). SPSS software

Downloaded from https://academic.oup.com/labmed/article/54/4/411/6821144 by guest on 24 February 2025

FIGURE 4. (cont)

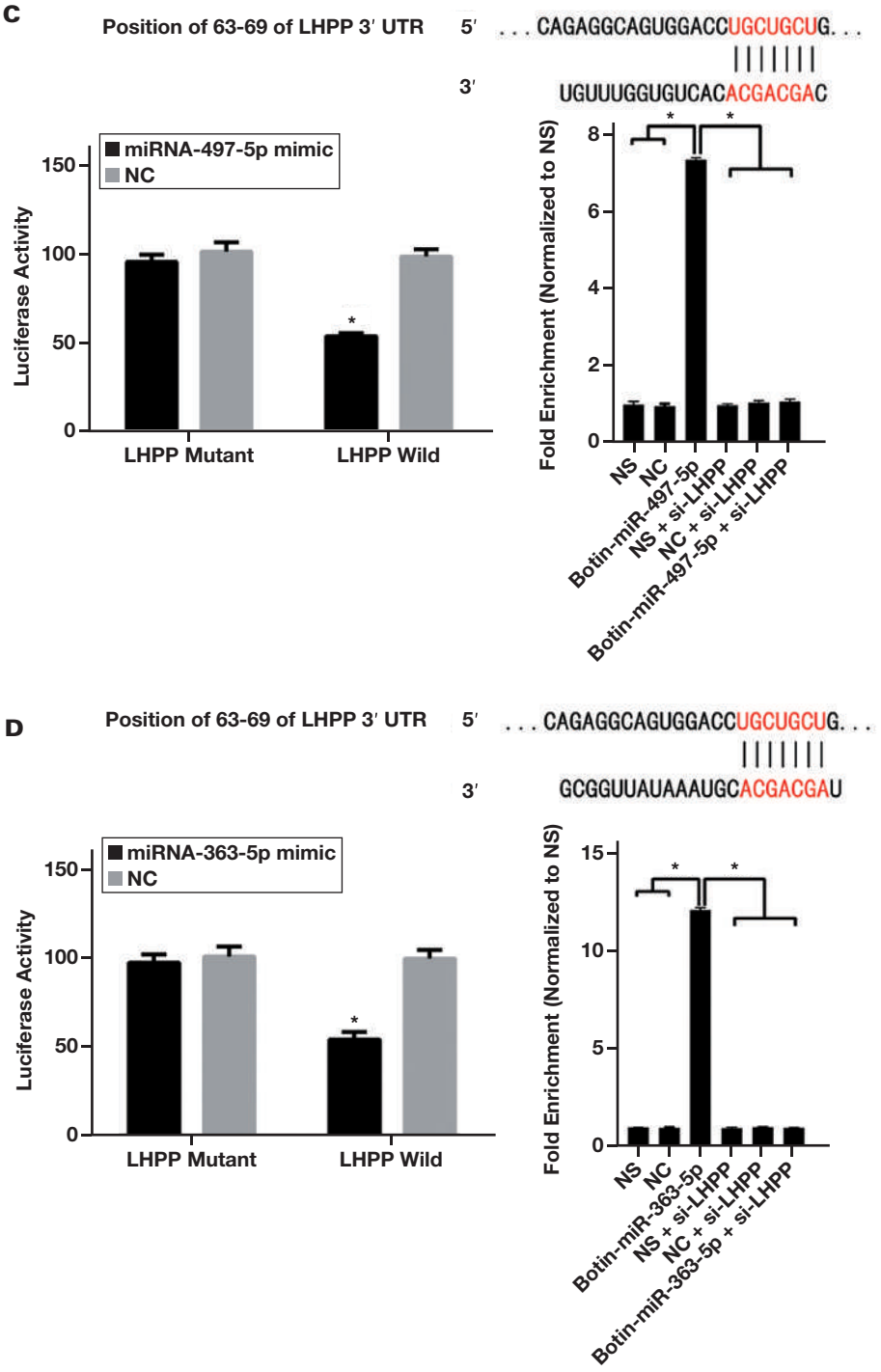

(version 18.0; IBM) was used for statistical analysis. The count data are expressed as a rate (%), and comparisons between groups were performed using the χ^2 test. The measurement data are expressed as mean (SD). F testing and *t* testing were used to compare multiple and 2 groups, respectively. The Spearman method was used for correlation test. The receiver operating characteristic (ROC) curve was used to compare the area under the curve (AUC) of each index to identify early- and midstage ESCC. The significance level was $\alpha = .05$.

Results

Flow Diagram of Early- and Midstage ESCC Diagnostic Regression Model Establishment

The flow diagram of the study is shown in **FIGURE 1**. According to the uniform inclusion and exclusion criteria, 120 patients with early- and midstage ESCC were included. These 120 patients were distributed into 2 cohorts for the model establishment and external verification.

Downloaded from https://academic.oup.com/labmed/article/54/4/411/6821144 by guest on 24 February 2025

FIGURE 4. (cont)

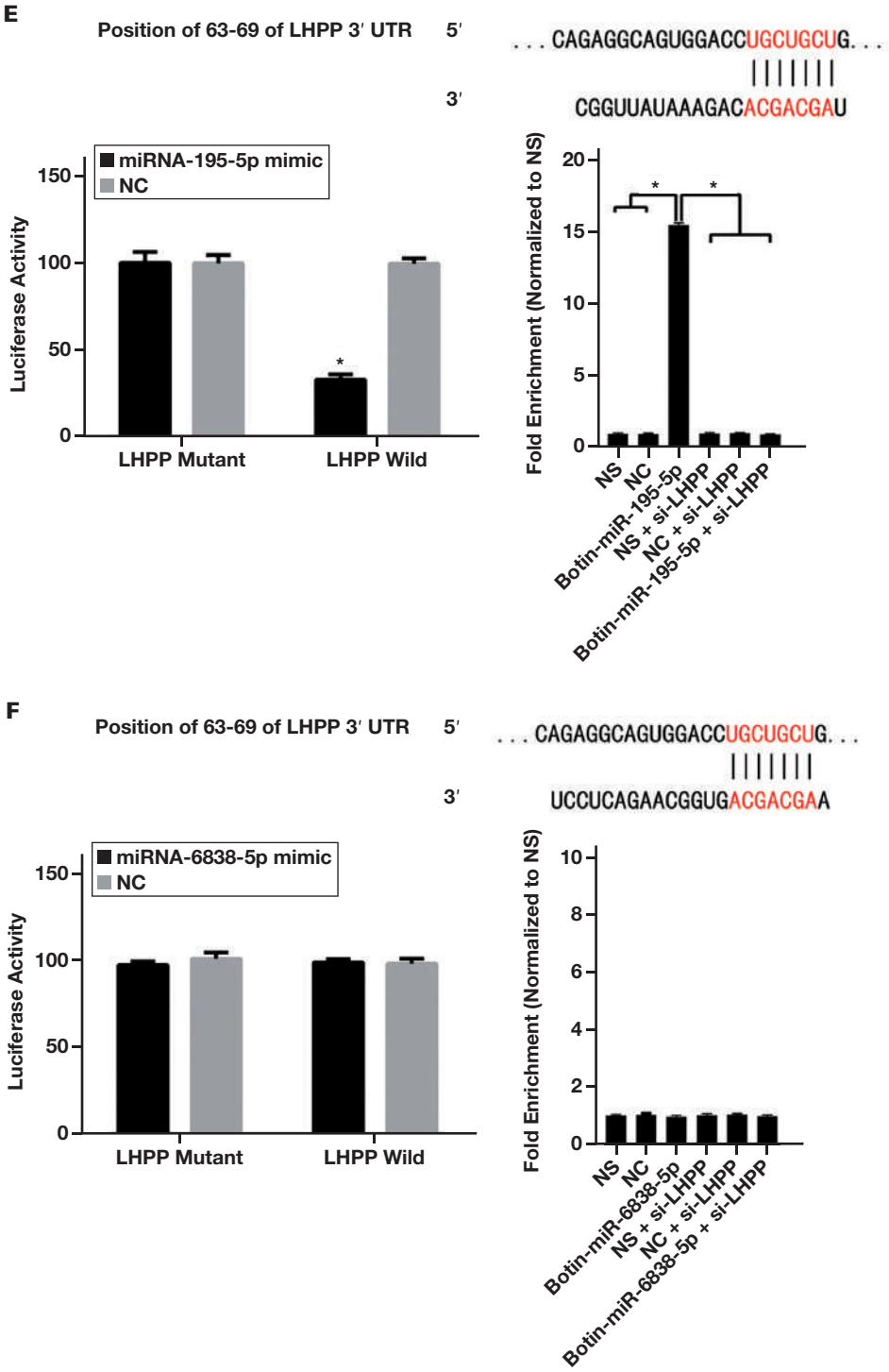

Expression of LHPP in the Early- and Midstage ESCC in the Testing Cohort and the Verification Cohort

Compared with paired adjacent healthy tissues, LHPP protein levels in tissues with early- and midstage ESCC were significantly decreased ($P < .01$; **FIGURE 2A**). Subsequently, we enrolled 120 patients with ESCC and 120 healthy control individuals (75 patients with ESCC and 75 healthy controls in the testing cohort; 45 patients with ESCC and 45 healthy controls in the verification cohort) and detected LHPP mRNA levels in the plasma (**FIGURE 2B**). Compared with healthy controls, LHPP mRNA levels in early- and midstage ESCC were significantly decreased in the testing cohort ($P < .01$; **FIGURE 2C**) and the verification cohort ($P < .01$; **FIGURE 2D**).

Involvement of miR-15b-5p, miR-424-5p, miR-497-5p, miR-363-5p, and miR-195-5p in the Regulation of LHPP in Tissues with Early- and Midstage ESCC

We used R package DESeq2 software (version 1.6.1), and the NGS technology results showed that there were 791 miRNA expression differences between tissues with early- and midstage ESCC and paired adjacent

Downloaded from https://academic.oup.com/labmed/article/54/4/411/6821144 by guest on 24 February 2025

FIGURE 5. Plasma miR-15b-5p, miR-424-5p, miR-497-5p, miR-363-5p, miR-195-5p, and miR-6838-5p levels in patients with early- and midstage esophageal squamous cell carcinoma (ESCC) in the testing cohort. Compared with healthy controls, the levels of plasma miR-15b-5p (A), miR-424-5p (B), miR-497-5p (C), miR-363-5p (D), and miR-195-5p (E) in patients with early- and midstage ESCC were significantly increased ($P < .01$), whereas there was no significant difference in the expression of miR-6838-5p (F). *$P < .05$; **$P < .01$; NS, nonsignificant.

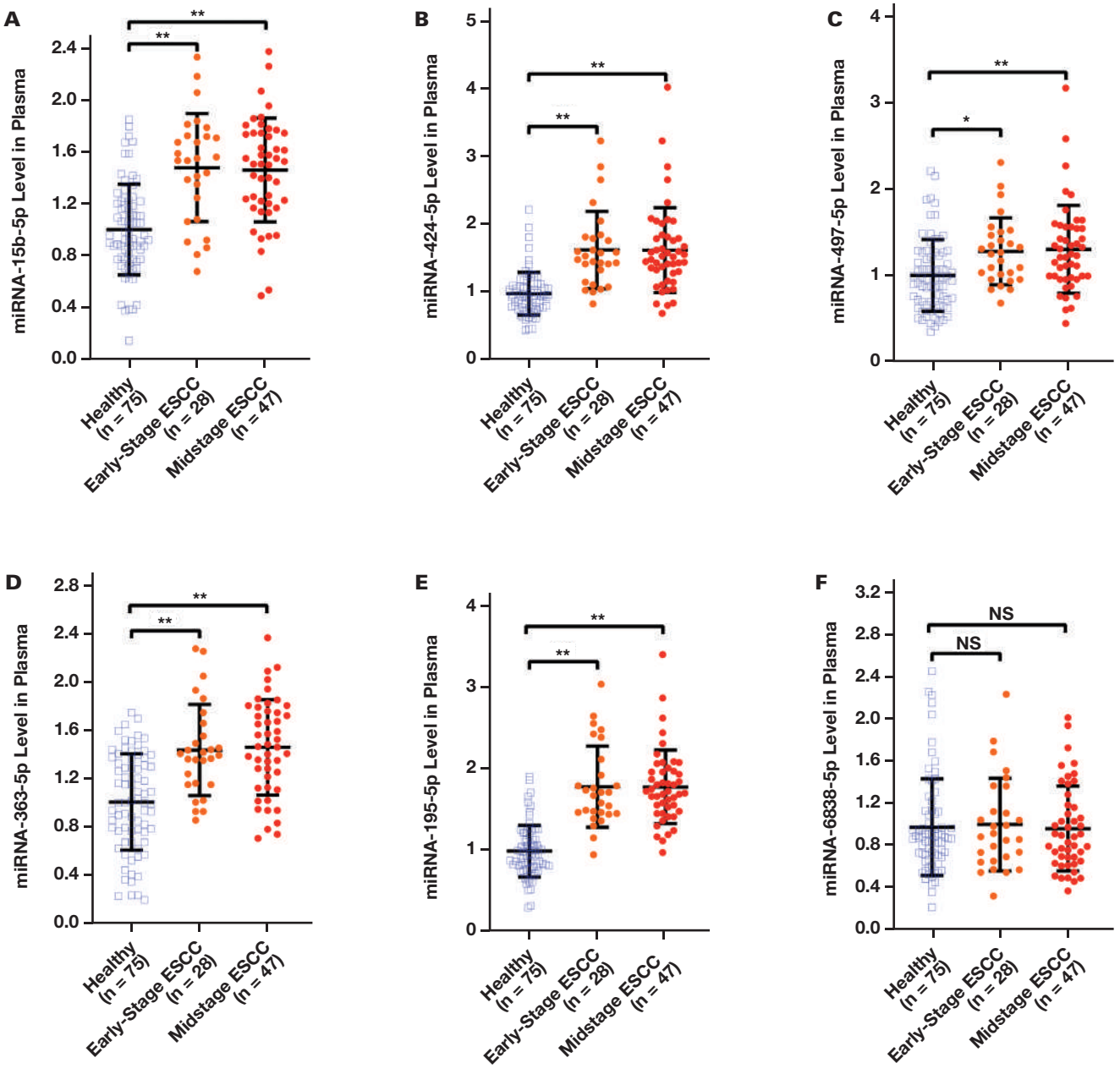

healthy tissues. Among them, there were 26 miRNAs with differences greater than 1.5-fold change and $P < .05$ (**FIGURE 3A**). A total of 17 miRNAs were highly expressed and 9 miRNAs were expressed at low levels in tissues with early- and midstage ESCC (**FIGURE 3B**). We then applied miRanda, miRDB, and TargetScan online prediction systems and determined the miRNA profiles predicted by each system with LHPP as the target protein (**FIGURE 3C**). Six miRNAs were predicted, namely, miR-15b-5p, miR-424-5p, miR-497-5p, miR-363-5p, miR-195-5p, and miR-6838-5p. Therefore, we selected these miRNAs for further research.

Next, we used the dual-luciferase reporter gene and RNA pull-down assays to verify the targeting relationships between LHPP and miR-15b-5p (**FIGURE 4A**), miR-424-5p (**FIGURE 4B**), miR-497-5p (**FIGURE 4C**), miR-363-5p (**FIGURE 4D**), miR-195-5p (**FIGURE 4E**), and miR-6838-5p (**FIGURE 4F**). Further, after comparing the expression level of miRNAs in the TCGA dataset, we found that 5 of the 6 significant DEMs were in accordance with the results in our study. However, the expression of miR-6838-5p was not significantly different between ESCC specimens and normal esophageal mucosa specimens. The relationship of miRNAs between the clinical TNM stages was also tested using χ^2 analysis. The results of the significant DEMs are shown in Supplementary Table 2. Therefore, we selected miR-15b-5p, miR-424-5p, miR-497-5p, miR-363-5p, and miR-195-5p as our test miRNAs.

Downloaded from https://academic.oup.com/labmed/article/54/4/411/6821144 by guest on 24 February 2025

FIGURE 6. **Plasma miR-15b-5p, miR-424-5p, miR-497-5p, miR-363-5p, miR-195-5p, and miR-6838-5p levels in patients with early- and midstage esophageal squamous cell carcinoma (ESCC) in the verification cohort. Compared with healthy controls, the levels of plasma miR-15b-5p (A), miR-424-5p (B), miR-497-5p (C), miR-363-5P (D), and miR-195-5p (E) in early- and midstage ESCC were significantly increased (*P* < .01), whereas there was no significant difference in the expression of miR-6838-5p (F). **P* < .05; ***P* < .01.**

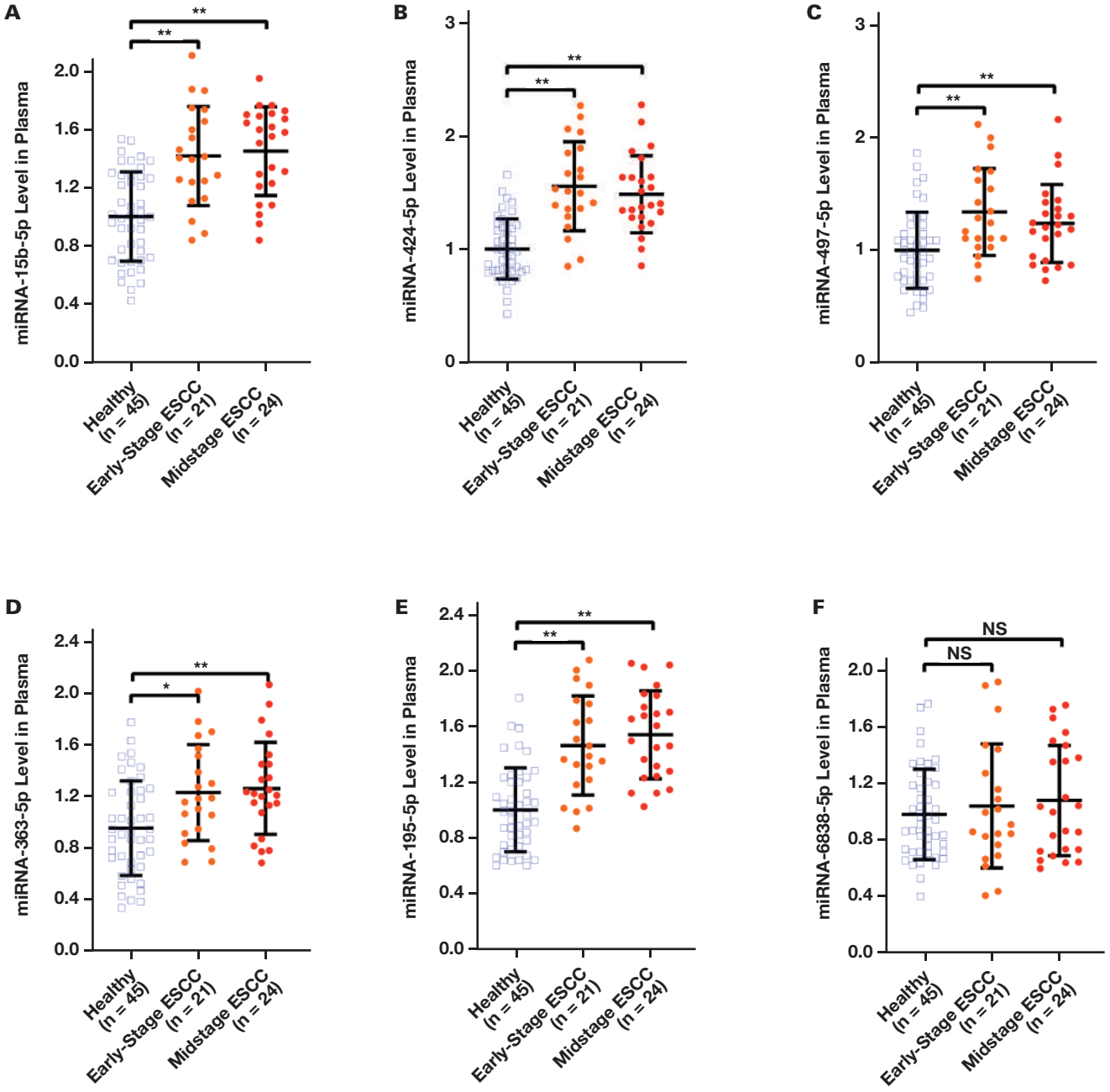

Levels of miR-15b-5p, miR-424-5p, miR-497-5p, miR-363-5p, miR-195-5p, and SCC in Early- and Midstage ESCC, in the Testing and Verification Cohorts

We then detected the expression levels of these 6 miRNAs in 75 patients with early- and midstage ESCC and 75 healthy controls in the testing cohort (**FIGURE 5**), and 45 patients with early- and midstage ESCCs and 45 healthy controls in the verification cohort (**FIGURE 6**). Compared with the healthy controls, the levels of plasma miR-15b-5p (**FIGURE 5A**, **FIGURE 6A**), miR-424-5p (**FIGURE 5B**, **FIGURE 6B**), miR-497-5p (**FIGURE 5C**, **FIGURE 6C**), miR-363-5p (**FIGURE 5D**, **FIGURE 6D**), miR-195-5p (**FIGURE 5E**, **FIGURE 6E**), and squamous cell carcinoma (SCC) (**TABLE 2**) in patients with early- and midstage ESCC were significantly increased ($P < .01$). No significant differences were observed in the expression of miR-6838-5p ($P = .58$, **FIGURE 5F**; $P = .21$, **FIGURE 6F**).

Establishment of an Early- and Midstage ESCC Diagnostic Regression Model

For the diagnosis of early- and midstage ESCC, ROC curve analysis showed that the AUC of miR-15b-5p, miR-424-5p, miR-497-5p,

Downloaded from https://academic.oup.com/labmed/article/54/4/411/6821144 by guest on 24 February 2025

TABLE 2. Clinicopathological Characteristics and Clinical Tumor Markers in the Test and Verification Cohorts

Variable	Test Cohort				Verification Cohort			
	Healthy	Early- and Midstage ESCC	χ^2/Z	*P* Value	Healthy	Early- and Midstage ESCC	χ^2/Z	*P* Value
Subjects, No.	75	75			45	45		
Age, median (IQR), y	63 (52–76)	65 (54–77)	1.035	.19	64 (51–74)	66 (53–78)	1.265	.20
Male, No. (%)	44 (58.7)	42 (56.0)	0.109	.74	28 (62.2)	31 (68.9)	0.443	.51
Smoking, No. (%)	37 (49.3)	41 (54.7)	0.427	.51	25 (55.6)	29 (64.4)	0.741	.39
Drinking, No. (%)	51 (68.0)	48 (64.0)	0.267	.60	32 (71.1)	35 (77.8)	0.526	.47
SCC, median (IQR), μg/L	0.98 (0.65–1.82)	3.66 (1.76–6.47)	6.845	<.001	1.13 (0.591.77)	3.75 (1.82–6.98)	7.638	<.001
CEA, median (IQR), U/mL	6.49 (5.48–8.19)	6.73 (5.98–8.54)	0.507	.42	6.24 (5.31–7.98)	6.32 (5.43–9.05)	0.426	.37
CA19-9, median (IQR), U/mL	27.64 (22.70–34.82)	28.47 (21.19–37.83)	0.876	.20	25.04 (19.87–31.18)	27.84 (20.70–32.76)	0.343	.21
Habit of eating preserved food, No. (%)	59 (78.7)	63 (84.0)	0.703	.40	39 (86.7)	38 (84.4)	0.090	.76

CEA, carcinoembryonic antigen; ESCC, esophageal squamous cell carcinoma; IQR, interquartile range; SCC, squamous cell carcinoma.

FIGURE 7. Establishment of early- and midstage esophageal squamous cell carcinoma diagnostic regression model. SCC indicates squamous cell carcinoma antigen.

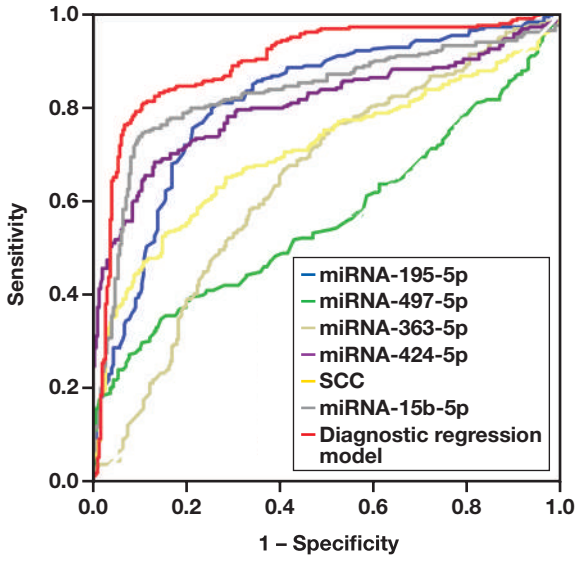

miR-363-5p, miR-195-5p, and SCC were 0.816, 0.778, 0.532, 0.637, 0.803 and 0.702, respectively (**FIGURE 7** and **TABLE 3**). Detailed information on diagnostic performance is listed in **TABLE 3**.

Each of the aforementioned variables was included in the multivariate logistic regression model. The final diagnostic regression model was Logit (P) = 3.370 – 0.125(miR-15b-5p) – 0.096(miR-424-5p) – 0.103(miR-497-5p) – 0.641(miR-363-5p) – 1.227(miR-195-5p) – 0.513(SCC). The identification value of this model was high, with an AUC of 0.851 (**FIGURE 7** and **TABLE 3**) and a probability of 0.725.

External Verification of the Early- and Midstage ESCC Diagnostic Regression Model

In the external validation group (**TABLE 2**), the probabilities of 42 (of 49) subjects were higher than 0.725, and the probabilities of 38 (of 41) subjects were lower than 0.725 (**FIGURE 8**). The sensitivity and specificity for early- and midstage ESCC were 85.7% and 92.7%, respectively.

Discussion

At present, the commonly used tumor detection methods, such as X-ray, ultrasound, positron emission tomography-computed tomography (PET-CT), and magnetic resonance imaging, still have limitations in clinical application owing to problems such as accuracy, resulting in delays in tumor detection. Radioactive detection methods, such as X-ray, CT, and PET-CT, are also not suitable for frequent detection in the general population. Additionally, the puncture method is time-consuming, complicated, and causes great harm to the body of the patient. In the past 10 years, early accurate tumor screening has developed rapidly, owing to its advantages of early diagnosis and treatment, noninvasiveness, accuracy, and dynamics. For patients, early and accurate tumor screening can not only relieve pain, improve prognosis, and increase the cure rate but can also greatly reduce the cost of treatment and the economic burden to the patient and society.

Researchers have found that LHPP has a significant tumor suppressor effect, and its potential tumor suppressor mechanism has been revealed in many cancers.[10–14] The Cancer Gene Atlas data showed that the median survival of patients with bladder cancer with low LHPP expression decreased by nearly 2 years in patients with high LHPP expression.[14] After downregulating the expression of LHPP, the protein histidine phosphorylation level in cancer cells increases significantly, which will trigger uncontrolled cancer cell proliferation.[14] However, LHPP expression in ESCC has not been reported. In the current study, we found, for the first time, that LHPP mRNA levels in tissues with early- and midstage ESCC were significantly lower in the test and validation cohorts, compared with adjacent healthy tissues.

Further, we explored LHPP-based miRNA signatures for the prediction of early- and midstage ESCC. We used NGS technology and 3 online prediction software to screen out 5 miRNAs that target and regulate LHPP, including miR-15b-5p, miR-424-5p, miR-497-5p, miR-363-5p, and miR-195-5p. These 5 miRNAs have also been found to function as oncogenes in clinical and basic research on various tumors.[15–18] Dong et al[15] demonstrated that miR-15b-5p levels are upregulated in

Downloaded from https://academic.oup.com/labmed/article/54/4/411/6821144 by guest on 24 February 2025

TABLE 3. Diagnostic Value of miR-15b-5p, miR-424-5p, miR-497-5p, miR-363-5p, miR-195-5p, and SCC for the Early- and Midstage ESCC in the Testing Cohort

Variable	AUC	95% CI	*P* Value	Sensitivity (%)	Specificity (%)
miR-15b-5p	0.816	0.765–0.983	<.001	75.9	91.7
miR-424-5p	0.778	0.688–0.862	<.001	69.1	89.3
miR-497-5p	0.532	0.468–0.593	.33	34.4	83.7
miR-363-5p	0.637	0.574–0.762	.002	74.1	43.9
miR-195-5p	0.803	0.713–0.879	<.001	85.3	60.9
SCC	0.702	0.593–0.814	<.001	54.5	83.2
Diagnostic regression model	0.851	0.815–0.910	<.001	81.6	91.4

AUC, area under the curve; CI, confidence interval; ESCC, esophageal squamous cell carcinoma; SCC, squamous cell carcinoma.

FIGURE 8. Scatter diagram of the predictive model in an external validation cohort. ESCC, esophageal squamous cell carcinoma.

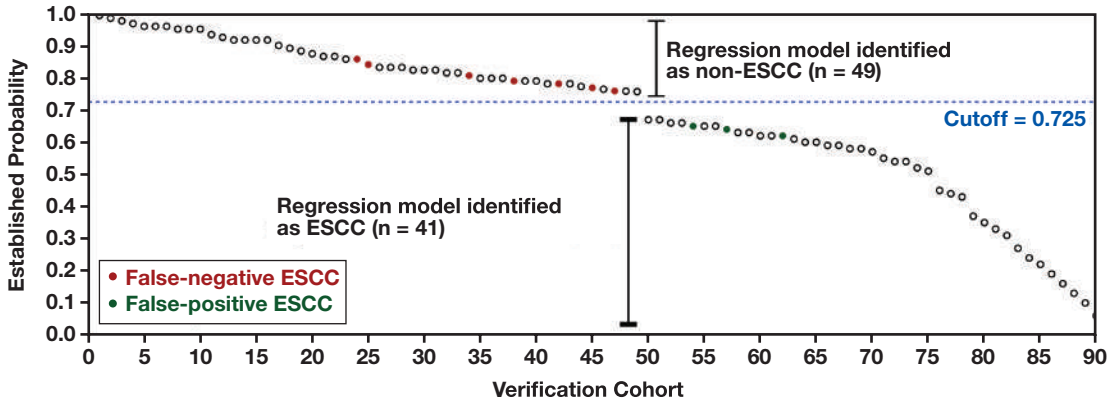

liver cancer tissues and cell lines. Dai et al[16] found through in vivo and in vitro experiments that miR-424-5p promotes colorectal cancer cell proliferation and metastasis. Also, they report that colorectal cancer cells secrete miR-424-5p into peripheral blood through exosomes.

Drahos et al[17] pointed out a trend of increased miR-424-5p levels in esophageal tissues with adenocarcinoma, which was contrary to our findings. The possible reasons include the following. First, all the patients we included in this study had ESCC, and we did not further explore the expression levels of miR-424-5p in different histological types. Second, individual differences among different races are another important factor. The study by Drahos et al[17] included an ethnic European population, whereas we included an ethnic Asian population. Bai et al[18] found that miR-497-5p promotes the epithelial-mesenchymal transition of colorectal cancer cells in vitro. Through the Kaplan-Meier test, Zhang et al[19] revealed that high expression of miR-363-5p was associated with poor overall survival of patients with hepatocellular carcinoma. The findings of previous studies[15–19] seem to suggest that miR-15b-5p, miR-424-5p, miR-497-5p, miR-363-5p, and miR-195-5p may promote the occurrence and development of tumors. Based on the aforementioned hypothesis, the differential value of these miRNAs in ESCC improves the noninvasive diagnostic ability of ESCC.

In this study, a total of 75 patients with ESCC and 75 healthy controls were included in the testing cohort. We found that the levels of miR-15b-5p, miR-424-5p, miR-497-5p, miR-363-5p, miR-195-5p, and SCC in the plasma of patients with ESCC were significantly higher than those in healthy controls. Our results are consistent with those of previous studies,[15–19] indicating that these markers may play a potential role in promoting ESCC.

miRNAs are involved in many processes in the cell cycle and affect the occurrence and development of tumors. They are present in the blood as nucleic acid–protein complexes that tolerate repeated freeze-thaw cycles and extreme pH environments and are therefore more stable than ctDNA.[7] For tumors with no typical clinical symptoms, nonspecific examination, and low early diagnosis rate (such as ESCC), detecting the expression level of specific miRNAs in peripheral blood can screen for a certain type of cancer, thereby avoiding invasive biopsy of tissue cells. This indicates that tumors can be detected even in the early stages of asymptomatic tumors, allowing us to intercept them earlier.

Combined detection of tumor markers is recommended by the updated National Academy of Clinical Biochemistry guidelines.[20] The accuracy of tumor detection can be significantly improved by combining several tumor markers with outstanding performance. For example,[21] although the classic CA125 marker has a sensitivity of 80% for the diagnosis of ovarian cancer, its positivity rate in the early stage is less than 50%, and its specificity is less than 60%. Another indicator of ovarian cancer, HE4, had significantly improved specificity, with a sensitivity of 67% when the specificity was 96%. The risk of ovarian malignancy algorithm (ROMA) index calculated by combining CA125 and HE4 had a sensitivity and specificity of 90.1% and 87.7%, respectively, for ovarian cancer.

Downloaded from https://academic.oup.com/labmed/article/54/4/411/6821144 by guest on 24 February 2025

In general, the combined detection of tumor markers enables their application of tumor markers to be optimized, and the detection sensitivity and accuracy are significantly improved. In this study, we used ROC analysis to analyze multiple combinations of the 6 markers we studied. The results showed that the specificity for predicting ESCC was 91.4% and the sensitivity was 81.6%. The aforementioned studies suggest that the combination of miR-15b-5p, miR-424-5p, miR-497-5p, miR-363-5p, miR-195-5p, and SCC in plasma with ESCC has clinical value for the evaluation of ESCC. In conclusion, we report that the combined detection of plasma miR-15b-5p, miR-424-5p, miR-497-5p, miR-363-5p, and miR-195-5p, as well as SCC in ESCC, has an early warning effect on the risk assessment of patients with early- and midstage ESCC.

Funding

This work was supported by the Ju Proiangsvincial Medical Youth Talent [QNRC2016508], Innovative Team of Jiangsu Province [CXTDA2017042], and the Scientific Research Project Contract of Jiangsu Provincial Health Commission [Z2020005]. Juan Yao was supported by grant No. 0000-0001-5396-4143 from Huaian Hospital of Huaian City, Huaian, China..

Conflict of Interest Disclosure

The authors have nothing to disclose.

REFERENCES

1. Kong P, Xu E, Bi Y, et al. Novel ESCC-related gene ZNF750 as potential prognostic biomarker and inhibits epithelial-mesenchymal transition through directly depressing SNAI1 promoter in ESCC. *Theranostics.* 2020;10(4):1798–1813.
2. Hu Z, Ke C, Shen Y, et al. Renal metastases from esophageal cancer and retroperitoneal lymphoma detected via chromosome duplications identified by fluorescence in situ hybridization in urine exfoliated cells: first 2 case reports. *Medicine (Baltimore).* 2021;100(10):e24010.
3. Codipilly DC, Qin Y, Dawsey SM, et al. Screening for esophageal squamous cell carcinoma: recent advances. *Gastrointest Endosc.* 2018;88(3):413–426.
4. Shin S, Jung Y, Uhm H, et al. Quantification of purified endogenous miRNAs with high sensitivity and specificity. *Nat Commun.* 2020;11:6033.
5. Luo D, Huang Z, Lv H, et al. Up-regulation of microRNA-21 indicates poor prognosis and promotes cell proliferation in esophageal squamous cell carcinoma via upregulation of lncRNA SNHG1. *Cancer Manag Res.* 2020;12:1–14.
6. Yang H, Su H, Hu N, et al. Integrated analysis of genome-wide miRNAs and targeted gene expression in esophageal squamous cell carcinoma (ESCC) and relation to prognosis. *BMC Cancer.* 2020;20:388.
7. Xian Q, Zhao R, Fu J. MicroRNA-527 induces proliferation and cell cycle in esophageal squamous cell carcinoma cells by repressing PH domain leucine-rich-repeats protein phosphatase 2. *Dose Response.* 2020;18(2):1559325820928687.
8. Zhang N, Liu JF. MicroRNA (MiR)-301a-3p regulates the proliferation of esophageal squamous cells via targeting PTEN. *Bioengineered.* 2020;11(1):972–983.
9. Hindupur SK, Colombi M, Fuhs SR, et al. The protein histidine phosphatase LHPP is a tumour suppressor. *Nature.* 2018;555(7698):678–682.
10. Hou B, Li W, Xia P, et al. *LHPP* suppresses colorectal cancer cell migration and invasion *in vitro* and *in vivo* by inhibiting Smad3 phosphorylation in the TGF-β pathway. *Cell Death Discov.* 2021;7:273.
11. Liao L, Duan D, Liu Y, Chen L. LHPP inhibits hepatocellular carcinoma cell growth and metastasis. *Cell Cycle.* 2020;19(14):1846–1854.
12. Wu F, Chen Y, Zhu J. LHPP suppresses proliferation, migration, and invasion and promotes apoptosis in pancreatic cancer. *Biosci Rep.* 2020;40(3):BSR20194142.
13. Lin J-X, Lian N-Z, Gao Y-X, et al. m6A methylation mediates LHPP acetylation as a tumour aerobic glycolysis suppressor to improve the prognosis of gastric cancer. *Cell Death Dis.* 2022;13:463.
14. Li Y, Zhang X, Zhou X, Zhang X. LHPP suppresses bladder cancer cell proliferation and growth via inactivating AKT/p65 signaling pathway. *Biosci Rep.* 2019;39(7):BSR20182270.
15. Dong Y, Zhang N, Zhao S, et al. miR-221-3p and miR-15b-5p promote cell proliferation and invasion by targeting Axin2 in liver cancer. *Oncol Lett.* 2019;18(6):6491–6500.
16. Dai W, Zhou J, Wang H, et al. miR-424-5p promotes the proliferation and metastasis of colorectal cancer by directly targeting SCN4B. *Pathol Res Pract.* 2020;216(1):152731.
17. Drahos J, Schwameis K, Orzolek LD, et al. MicroRNA profiles of Barrett's esophagus and esophageal adenocarcinoma: differences in glandular non-native epithelium. *Cancer Epidemiol Biomarkers Prev.* 2016;25(3):429–437.
18. Bai J, Xu J, Zhao J, Zhang R. lncRNA SNHG1 cooperated with miR-497/miR-195-5p to modify epithelial-mesenchymal transition underlying colorectal cancer exacerbation. *J Cell Physiol.* 2020;235(2):1453–1468.
19. Zhang J, Fan J, Zhou C, Qi Y. miR-363-5p as potential prognostic marker for hepatocellular carcinoma indicated by weighted co-expression network analysis of miRNAs and mRNA. *BMC Gastroenterol.* 2017;17:81.
20. Di Fiore R, Suleiman S, Ellul B, et al. GYNOCARE update: modern strategies to improve diagnosis and treatment of rare gynecologic tumors—current challenges and future directions. *Cancers (Basel).* 2021;13(3):493.
21. Wang H, Liu P, Xu H, Dai H. Early diagonosis [sic] of ovarian cancer: serum HE4, CA125 and ROMA model. *Am J Transl Res.* 2021;13(12):14141–14148.

Downloaded from https://academic.oup.com/labmed/article/54/4/411/6821144 by guest on 24 February 2025

The Continued Need for the Routine Assessment of Folate Status

Bremansu Osa-Andrews,[1] Melissa Sanchez, MIS, MT(ASCP),[2] Ibrahim A. Hashim[1,2,]*

Department of Pathology, [1]University of Texas Southwestern Medical Center, [2]Parkland Hospital System, Dallas, TX, USA. *To whom correspondence should be addressed: Ibrahim.Hashim@utsouthwestern.edu.

Keywords: folate, iron, anemias, hemoglobin, ferritin, vitamin B_{12}

Abbreviations: RBC, red blood cell; NHANES, National Health and Nutrition Examination Survey

Laboratory Medicine 2023;54:424-428; https://doi.org/10.1093/labmed/lmac148

ABSTRACT

Objective: The Choosing Wisely initiative recommended cessation of folate measurement, suggesting folate supplementation in macrocytic anemia. This study reviewed the need for continued blood folate testing at a large SafetyNet county teaching hospital.

Methods: Red blood cell (RBC) folate, vitamin B_{12}, iron, ferritin, and hemoglobin results were obtained for utilization review.

Results: Of the 593 RBC folate results, 69 (11.7%) were deficient and 30 (5%) had high values. Collectively, 369 (73.9%) had normal vitamin B_{12} levels, 342 (70%) had low hemoglobin, 184 (62.5) had normal and 57 (19.4%) had low ferritin, 122 (38.2%) had normal and 188 (59%) had low iron levels. A total of 41 (12%) had normal folate, low ferritin, low hemoglobin, and low iron, suggestive of iron deficiency anemia. There were 11 patients who exhibited low folate, low or normal ferritin, low hemoglobin, and low iron levels, suggesting combined folate and iron deficiency anemias.

Conclusion: This study highlights the need for institutions to assess the applicability of national recommendations to their local population.

Nearly 20 years after the US Food and Drug Administration mandated the fortification of all foods with folate, the Choosing Wisely organization of the American Society for Clinical Pathology in 2017 recommended the withdrawal of laboratory measurement of red blood cells (RBC) and serum folate, citing the progressive decline of folate deficiency.[1] This recommendation may have garnered support from National Health and Nutrition Examination Survey (NHANES) data, which indicate a substantial decrease in folate deficiency from 16% to 0.5% before and after fortification, respectively.[2] This NHANES report may not be representative of some patient demographics, which may have higher prevalence of folate deficiency than reported. Moreover, low dietary intake may represent only a partial component of the etiology of folate deficiency. Folate deficiency has been reported during pregnancy, in pediatric and geriatric patients where there is increased demand for folate, and in conditions such as hemolysis, leukemia, and exfoliative dermatitis, which are associated with rapid cellular proliferation. Jejunum disease and short bowel syndrome cause malabsorption, and bacterial overgrowth as well as drugs such as alcohol, anticonvulsants, and oral contraceptives have been shown to cause folate deficiency.[3] In populations with these conditions, supplementing folate without testing may not resolve the underlining conditions responsible for the folate deficiency. Diagnosis of folate deficiency anemia, one of two forms of megaloblastic macrocytic anemia (the other being vitamin deficiency anemia), requires low blood folate, hemoglobin, and macrocytosis (MCV >100 fL).[3] Nonmegaloblastic macrocytic anemia may occur due to hypothyroidism, liver disease, myelodysplastic syndrome, and certain drugs, and many patients with these conditions may have normal folate and vitamin B_{12} levels.[4] The Choosing Wisely organization further indicated that providers could commence folate supplementation treatment if macrocytic anemia is suspected without testing for folate status. However, peer-reviewed reports of elevated folate-related risks and resurgence of cancers[5] and other morbidities have multiplied.[6–8] Recent data from the National Institutes of Health revealed a strong association between oversupplementation of folate and vitamin B_{12} deficiency anemia masking with concomitantly serious clinical implications,[9,10] since folate is required to activate vitamin B_{12}. These situations underline the intricate role of folate in the diagnoses of macrocytic anemia and other folate-associated abnormalities.

The evidence provided above suggests the need for further investigation into the clinical utility of folate assessment. In this article, we lay out the argument for continued laboratory testing of RBC folate by laboratory institutions within the setting of accurate diagnosis and management of macrocytic anemia.

Materials and Methods

Laboratory findings for RBC folate, vitamin B_{12}, iron studies, ferritin, and hemoglobin of all patients being investigated for suspected anemia were obtained from 2020 to 2021 as part of a test utilization review effort

© The Author(s) 2023. Published by Oxford University Press on behalf of American Society for Clinical Pathology. All rights reserved. For permissions, please e-mail: journals.permissions@oup.com

Downloaded from https://academic.oup.com/labmed/article/54/4/424/6986983 by guest on 24 February 2025

at Parkland Memorial Hospital. The demographics of our patient population are 24.2% African American, 37.3% Hispanic, and 52% female; about 25,000 pregnant persons are seen annually. The population is unique in that 21.5% of those assessed for social determinants of health exhibited food insecurities. Over 38,000 patients present annually with gastrointestinal disorders, over 34,000 with eating disorders, and nearly 230,000 with clinical diagnosis of anemia; it is a population clearly at risk of folate deficiency. All measurements were performed in-house except RBC folate, which was sent to a reference laboratory. The reference laboratory where the RBC folate was determined used the quantitative chemiluminescent immunoassay method for testing using 1 mL whole blood sample in a lavender tube. Hemoglobin (a component of complete blood count profile) was measured using a Sysmex automated analyzer (Sysmex). Iron studies and ferritin were performed using cobas automated chemistry analyzers (Roche Diagnostics). Vitamin B_{12} was measured using the Vitamin B_{12} II binding assay using the cobas 8000 (e602) (Roche Diagnostics). The data used for this project were retrieved from Beaker EPIC in retrospect. The Excel and GraphPad Prism statistical software tools were used to filter and analyze the raw data, respectively. Of 593 patient results for RBC folate, 553 were analyzed for vitamin B_{12}, 489 for hemoglobin, 294 for ferritin, and 319 for iron. The cut-offs for RBC folate and vitamin B_{12} used were <366 ng/mL and <232 pg/mL, respectively. Considering the lack of well-defined reference ranges for RBC folate, elevated RBC for the purpose of this research was characterized as levels >1300 ng/mL (based on the Centers for Disease Control and Prevention microbiological assay reference range of 223–1100 ng/mL, given the difference in methodology)[11] and a postulated optimal RBC folate level of 1000 to1500 ng/mL by Knew Health.[12] Reference ranges used for statistical analysis were 13.2 to 16.9 g/dL (male) and 11.2 to 15.7 g/dL (female) for hemoglobin, 20 to 250 ng/mL (male) and 10 to 263 ng/mL (female) for ferritin, and 59 to 160 µg/dL (male) and 37 to 145 µg/dL (female) for iron. Institutional review board approval was obtained (study No. STU 2022-0262).

Results

A total of 593 RBC folate results of persons being investigated for diagnosis of suspected anemia were analyzed. A cut-off value of 366 ng/mL (in use by the reference laboratory) was used to define folate status. Of the total number of 593 patients, 69 (12%) had low RBC folate values, and 30 (5%) had elevated RBC folate values (**FIGURE 1**). Further, 494 patients had normal RBC folate levels, 83% (**FIGURE 1**) of all subjects tested for the vitamin. Of the 494 patients who showed normal RBC folate, 93 had anemia indicated by low hemoglobin. Of the 553 patients assessed using the cut-off of <232 pg/mL for vitamin B_{12}, 17 showed low values, 413 had normal levels, and 140 patients had high levels >2000 pg/mL (**FIGURE 1**). The hemoglobin results showed 342 with low values and 147 at normal levels of a total 489 patients tested for the analyte. We found that 342 of 489 patients were anemic with low hemoglobin levels, representing 70% of the population. Of 294 ferritin measurements, 57, 53, and 184 patients had low, high, and normal results, respectively. Of the 319 iron measurements taken, 188 patients showed low values, 9 had high values, and 122 showed normal results (**FIGURE 2**). Additional analysis indicated that 41 patients had normal folate, low ferritin, low hemoglobin, and low iron, representing 12.0% of the anemic group (**FIGURE 2**). There were 52 patients with normal folate, normal ferritin, low hemoglobin, and low iron, making up 15.2% of the anemia group. Interestingly, 4 patients had low folate levels with low ferritin, low hemoglobin, and low iron (1.2%) (**FIGURE 2**). A total of 8 patients showed low folate levels, normal ferritin, low hemoglobin, and low iron (2.3%) (**FIGURE 2**). There were 23 patients with low folate levels, low or normal ferritin, low hemoglobin, and normal iron. Additional results showed that 7 patients had low folate levels with normal ferritin, normal hemoglobin, and normal iron. Of the 30 patients who had high RBC folate, 14 (46.7%) were found to be anemic, representing 4.1% of the total anemic population (**FIGURE 2**). Altogether, 31.3% of the patients who had low hemoglobin also exhibited normal or high folate levels. Those patients would be most at risk of mistreatment (**FIGURE 2**). Three patients had low folate, low vitamin B_{12}, and low hemoglobin, whereas 2 patients had high folate, low vitamin B_{12}, and low hemoglobin levels (**FIGURE 2**). **TABLE 1** summarizes the ranges and median values of the results obtained. The upper limits of the analytical measuring range of RBC folate and vitamin B_{12} have been normalized as upper reference intervals to establish ranges.

Discussion

Following multiple reports of drastically diminished incidences of folate deficiency due to the FDA mandate to fortify all food with folate, the Choosing Wisely campaign recommended cessation of blood folate

FIGURE 1. Distribution of partial anemia indices. Uneven distribution of RBC folate, vitamin B_{12}, hemoglobin, ferritin, and iron in patients being investigated for anemia and presenting at a SafetyNet hospital.

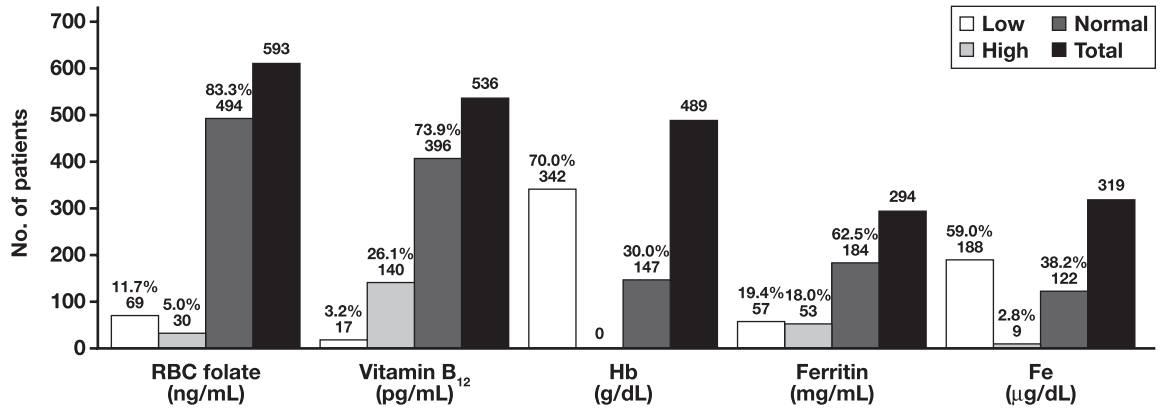

Downloaded from https://academic.oup.com/labmed/article/54/4/424/6986983 by guest on 24 February 2025

FIGURE 2. **Clinical utility of RBC folate measurement in the investigation of suspected anemia. Histograms showing the observed different permutations of RBC folate levels in the presence of low, normal, or high ferritin, hemoglobin, and iron. The anemic patients (n = 342) represent those with low hemoglobin levels.**

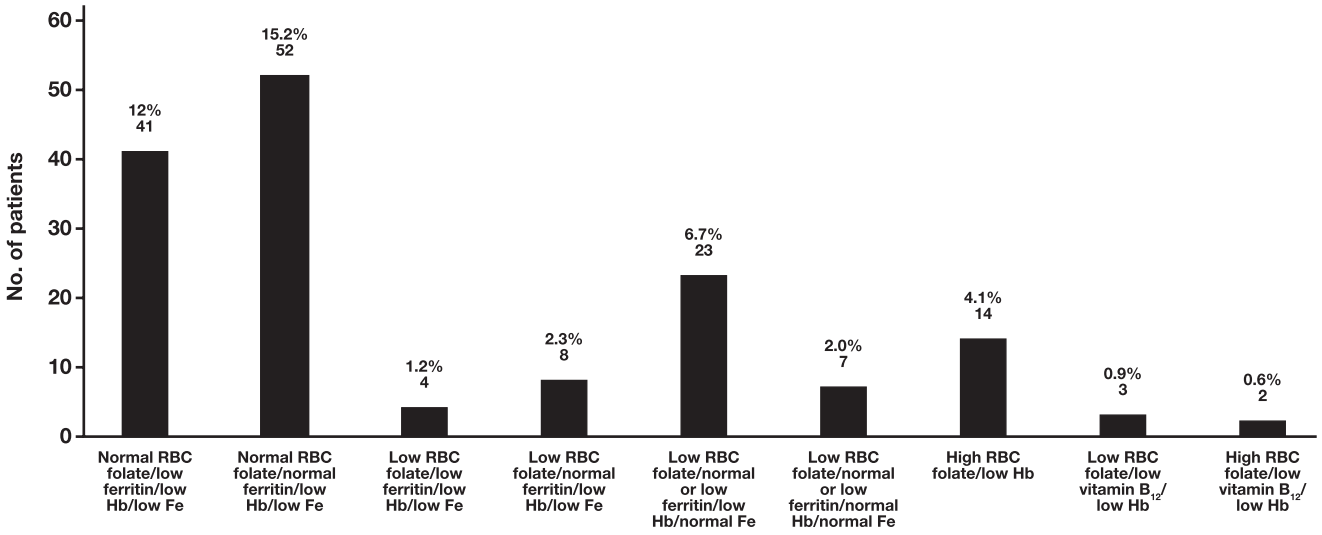

TABLE 1. **Summary of the Range and Median of Analyte Results**

	RBC Folate (ng/mL)	Vitamin B_{12} (pg/mL)	Hemoglobin (g/dL)	Ferritin (ng/mL)	Iron (μg/dL)
Range	96–1330	150–2000	5.2–18	2–13,798	9–462
Median	625	629	11.1	126.5	48

test orders. In this report, we investigated the continued need for blood folate measurement among our patient population and reasons that clinicians continue to order the test regardless of the aforementioned regulatory recommendation and examined the vital importance of blood folate testing before supplementation.

Although the notion that folate deficiency has markedly dwindled from a broader national perspective, it is not necessarily a reflection of specific local evidence. Moreover, decreased cases of folate deficiency may not be an adequate justification for the discontinuation of the assessment of folate status. Results based on our local patient population showed a 11.5% higher folate deficiency than the 0.5% reported in the 2005 NHANES postfortification data. Further, one of the articles on which the decision of the Choosing Wisely organization was based reported that only 4 out of 560 patients tested at the Health Sciences Center in Canada for blood folate had folate deficiency, representing 0.7% of all patients tested.[13] Data from our study not only shows a higher percentage of folate deficiency but does so based on a slightly higher sample size than the Shojania and von Kuster[13] report. Although folate deficiency can persist with or without anemia, the more clinically relevant folate index is that related to anemia. Folate deficiency anemia is generally considered to be low blood folate level with low hemoglobin and macrocytosis. Our results showed a higher percentage of folate deficiency–induced anemia, 35 of 593 patients, representing 6%, than earlier reports where no anemia cases attributable to low folate were found. The highest percentage of folate deficiency anemia in the Canadian study was 0.2%, recorded at the St Boniface General Hospital. The discrepancy between data from our study compared with the studies that informed the Choosing Wisely campaign's decision cannot be overemphasized.

Conventionally, folate deficiency has been a greater concern for clinicians and laboratory professionals than elevated blood folate levels. This observation is predominantly due to lack of clinically useful information regarding the consequences of increased blood levels of folate. Results from this study indicate that 5% of patients had elevated RBC folate levels, suggesting not just elevated folate but possibly folate toxicity. More concerning is that recent reports have revealed the association of elevated blood folate with higher risk of certain cancers, including lung, prostate, and small cell carcinomas. According to the Choosing Wisely campaign, clinicians may prescribe folate supplements in any cases of macrocytic anemia without the need to first evaluate folate status. However, this recommendation has the potential of exposing patients to elevated folate levels. Anemia is a multietiological condition that includes but is not limited to folate deficiency. Anemia is also known to be caused by vitamin B_{12} and iron deficiencies, both of which may present with a normal blood folate level. Normal RBC folate is useful to conclusively rule out folate deficiency anemia when found with low hemoglobin and when either ferritin or iron levels are reduced. Without folate assessment, misdiagnosis of folate deficiency anemia may escalate the risk of folate toxicity. Supplementing folate without testing in every case of macrocytic anemia diagnosis can elevate folate level, thereby compromising patient safety. In the current study, 16% of the 83% of patients who had normal folate were simultaneously diagnosed with anemia with a correspondent low hemoglobin. Persons in this group are at high risk for possible future folate spikes on folate supplementation prescription. It could be suggested that a segment of the 5% of patients who had elevated RBC folate may have been prescribed supplemental folate, or the possible abuse of folic acid supplements may be cited as the cause. However, patients exhibiting normal folate test results with the background

Downloaded from https://academic.oup.com/labmed/article/54/4/424/6986983 by guest on 24 February 2025

of anemia risk a similar hazard should providers comply with the folate supplementation without testing campaign. The risk to patients seems latent, untraceable, gradual, and long term since it correlates indirectly with the risk of cancer and not necessarily to the malignancy itself.[5–7] Also, there is a degree of ambiguity in some of the data implicating the relationship between high folate, when given with vitamin B_{12}, and risk of cancer. Nevertheless, it is reasonable not to trade patient safety for reduction in cost burden to patients.

Mean corpuscular volume >100 fL is a frequently used marker for macrocytic anemia, whereas folate (vitamin B_9) and vitamin B_{12} deficiencies are markers purposely for megaloblastic anemia. Measurement of homocysteine and methyl malonic acid distinctively distinguishes between vitamin B_{12} and vitamin B_9 deficiency megaloblastic anemia. The pathological consequences of folate deficiency and vitamin B_{12} deficiency anemias are similar and their distinctive management regimen are obvious. Supplementing folate without vitamin B_{12} usually treats the symptoms of anemia but not the neurological pathology. These facts demonstrate the importance of vitamin B_{12} testing and supplementation within the scope of anemia, especially if vitamin B_{12} deficiency is prevalent. However, our findings reveal a higher frequency of folate (12%) deficiency than vitamin B_{12} deficiency (3%) in a patient population presenting with anemia. This may suggest a higher incidence of folate-induced megaloblastic anemia than vitamin B_{12}-deficiency megaloblastic anemia. In contrast, the Choosing Wisely campaign has no documented reservation regarding vitamin B_{12} testing as it does folate testing. Deficiency of such nutritive analytes could be a function of food security within certain demographics and may vary from population to population. On the other hand, elevated folate causes vitamin B_{12} masking, which, although it can be resolved when diagnosed early, can go unnoticed without folate testing, leading to serious medical consequences.[14] Since folate is required for the activation of vitamin B_{12}, disproportionally high folate concentration can activate even small amounts of cobalamin, thereby concealing the underlining deficiency until neurological effects of vitamin B_{12} commence. In this study, only 17% of patients had low vitamin B_{12} levels. Two of those patients had high folate and low hemoglobin levels, the most at risk of high folate-mediated vitamin B_{12}-deficiency masking. Additionally, three patients had full-blown megaloblastic anemia with indices of low folate, low vitamin B_{12}, and low hemoglobin levels. Given our results, the operationalization and withdrawal of essential nutrient testing should be based on local population experience rather than generalized recommendation, albeit by a credible professional entity whose endorsement drew on alternative results.

Low RBC folate is an independent predictor of folate deficiency and folate deficiency anemia, improbable diagnoses to definitively obtain without the measurement of blood folate, demonstrating the continual need for the retention of the test. The alternative to RBC folate is serum folate, but RBC folate has some comparative advantages. Low serum folate reflects a transient deficiency whereas low RBC folate is a function of stored folate status over approximately 4 months. The nonspecific serum folate[15] may even be low in the presence of normal tissue folate storage, suggesting that low RBC folate indicates a higher risk of anemia does than serum folate. A single RBC folate measurement is therefore a reflection of the patient's stored folate level but, more than that, cumulative low folate results of a patient population are an indirect measure of the nutritive habits and economic status of the local demographic. However, RBC folate testing is not without inaccuracy. According to internal data from the Mayo Clinic, RBC folate testing is fraught with significant analytical variability and poor precision. The Mayo Proceedings stated that these drawbacks were the predominant informant in their withdrawal of the test, in addition to their comparative studies between serum and RBC folate that showed a strong correlation.[16] These pieces of information indicate that RBC and serum folate are generally comparable, barring methodological differences, strengths, and frailties. The Choosing Wisely campaign's recommendation for the abolishment of both tests suggests their rationale is not a function of the variability in the type of specimen but on the supposed clinical inexpediency of both tests. Data from the Mayo Clinic study[16] showed strong concordance between serum and RBC folate levels and support the use of RBC folate as the sole specimen type in this study.

Patients with combined folate and iron deficiency anemia do not necessarily show macrocytosis with a concomitantly lower value in the measurement of MCV. The one dependable way to distinguish such patients from other anemia variants is to measure blood folate. However, supplementation of folate without testing in this patient group will be unlikely to lead to clinical consequences. In the present data, only 3.5% of the anemic patient population exhibited this coexistence of folate and iron deficiency anemias, suggesting that it is an uncommon occurrence. Together with the group that had folate deficiency anemia without iron deficiency, only 9.4% of the anemic group would not have been affected by folate prescription without testing. This number is not comparable to the 31.3% of the population who had anemia in the setting of normal to high folate and whose safety might be compromised if folate were given without prior folate measurement. This normal folate anemic group could either have microcytic anemia, vitamin B_{12} deficiency anemia, or nonmegaloblastic macrocytic anemia, usually caused by hypothyroidism or liver disease. We have shown here that the conditions in which measurement of blood folate is not consequential are also rare. The more common anemic disorders pose realistic but silent risks if folate testing is disregarded. These data connote the necessity for institutions to conduct regionally based research as the major source of operationalization instead of implementing recommendations from regulatory entities without thorough considerations.

Conclusion

This study has shown the expediency of continuing blood folate measurement while creating awareness of the associated risks of supplementing folate without testing. Low RBC folate level is more prevalent than low vitamin B_{12} in a patient population presenting with anemia even in this era of folate fortification. Normal RBC folate is useful to assertively rule out folate deficiency anemia when hemoglobin and either ferritin or iron levels are decreased. Low RBC folate and hemoglobin levels consistent with folate deficiency anemia persist regardless of folate fortification. The RBC folate measurement remains clinically valuable and improves the diagnosis while reducing the incidence of misdiagnosis of folate deficiency anemia. Our study shows the importance for clinical laboratories to critically assess the applicability of recommendations by professional societies, particularly those referring to test utilization, to the population they serve and from which samples are being received. National recommendations may not be applicable to the local population. Assessment of folate status is useful to assess folate deficiency in patients with microcytic anemia. Higher than normal RBC folate values should be reevaluated for their association with the risk of certain cancers and appropriate intervention prescribed.

Downloaded from https://academic.oup.com/labmed/article/54/4/424/6986983 by guest on 24 February 2025

Acknowledgments

We thank Parkland Memorial Hospital for providing the opportunity of patients and chart reviews. Internal support was received from the Department of Pathology, University of Texas Southwestern Medical Center, Dallas, TX.

Conflict of Interest Disclosure

The authors have nothing to disclose.

REFERENCES

1. Joelson DW, Fiebig EW, Wu AH. Diminished need for folate measurements among indigent populations in the post folic acid supplementation era. *Arch Pathol Lab Med.* 2007;131(3):477–480. doi:10.5858/2007-131-477-DNFFMA.
2. Pfeiffer CM, Caudill SP, Gunter EW, Osterloh J, Sampson EJ. Biochemical indicators of B vitamin status in the US population after folic acid fortification: results from the National Health and Nutrition Examination Survey 1999-2000. *Am J Clin Nutr.* 2005;82(2):442–450. doi:10.1093/ajcn.82.2.442.
3. Bakerman S, Bakerman P, Strausbauch P. *ABC's of Interpretative Laboratory Data*. 5th ed. Scottsdale, AZ: Interpretative Laboratory Data Inc; 2014.
4. Nagao T, Hirokawa M. Diagnosis and treatment of macrocytic anemias in adults. *J Gen Fam Med.* 2017;18(5):200–204. doi:10.1002/jgf2.31.
5. Wallace K, Grau MV, Gui J, Barry E, Baron J. High red blood folate levels linked to silenced tumor-suppressors. https://www.mdanderson.org/newsroom/red-blood-folate-linked-to-tumor-suppressors.h00-158598468.html. Accessed June 13, 2022.
6. Figueiredo JC, Grau MV, Haile RW, et al. Folic acid and risk of prostate cancer: results from a randomized clinical trial. *J Natl Cancer Inst.* 2009;101(6):432–435. doi:10.1093/jnci/djp019.
7. Ebbing M, Bønaa KH, Nygård O, et al. Cancer incidence and mortality after treatment with folic acid and vitamin B12. *JAMA.* 2009;302(19):2119–2126. doi:10.1001/jama.2009.1622.
8. Patel KR, Sobczyńska-Malefora A. The adverse effects of an excessive folic acid intake. *Eur J Clin Nutr.* 2017;71(2):159–163. doi:10.1038/ejcn.2016.194.
9. Ankar A, Kumar A. Vitamin B12 deficiency. In: *StatPearls*. Treasure Island, FL: StatPearls Publishing LLC; 2021.
10. Hariz A, Bhattacharya PT. Megaloblastic anemia. In: *StatPearls*. Treasure Island, FL: StatPearls Publishing LLC; 2021.
11. Pirkle JL. CDC Laboratory Procedure Manual for Total Folate. https://www.cdc.gov/nchs/data/nhanes/nhanes_11_12/folate_g_met_rbc.pdf. Accessed June 13, 2022.
12. Rosenthal, J. Understanding your lab tests: vitamin B12 and RBC-folate levels (folic acid). https://knewhealth.com/understanding-your-lab-tests-vitamin-b12-and-rbc-folate/. Accessed June 13, 2022.
13. Shojania AM, von Kuster K. Ordering folate assays is no longer justified for investigation of anemias, in folic acid fortified countries. *BMC Res Notes.* 2010;3:22. doi:10.1186/1756-0500-3-22.
14. Mills JL, Molloy AM, Reynolds EH. Do the benefits of folic acid fortification outweigh the risk of masking vitamin B12 deficiency? *BMJ.* 2018;360:k724. doi:10.1136/bmj.k724.
15. Klee GG. Cobalamin and folate evaluation: measurement of methylmalonic acid and homocysteine vs vitamin B(12) and folate. *Clin Chem.* 2000;46(8 pt 2):1277–1283.
16. MayoClinicLabs Test Obsolete, Folate RBC #9199. https://www.mayocliniclabs.com/test-notifications/attachment.php?id=12188. Accessed December 29, 2021.

Downloaded from https://academic.oup.com/labmed/article/54/4/424/6986983 by guest on 24 February 2025

Reassessment of Critical Anti-D Antibody Titer in RhD Alloimmunized Antenatal Women

Bharat Singh, MD,[1] *Rajendra Chaudhary, MD,[1]* *Rahul Katharia, MD[1]*

[1]Department of Transfusion Medicine, Sanjay Gandhi Postgraduate Institute of Medical Sciences, Lucknow, India. *To whom correspondence should be addressed: bharatsgpgi@gmail.com.

Keywords: maternal alloimmunization, critical anti-D titer, hemolytic disease of the fetus and newborn, fetal ultrasound surveillance, fetal outcome, critical titer appropriateness

Abbreviations: CT, critical titer; IgG, immunoglobulin G; HDFN, hemolytic disease of the fetus and newborn; conventional tube technique; Doppler USG, Doppler ultrasound; IUT, intrauterine transfusion; DAT, direct antiglobulin test; ET, exchange transfusion; PT, phototherapy; PRBC, packed red blood cell

Laboratory Medicine 2023;54:429-433; https://doi.org/10.1093/labmed/lmac149

ABSTRACT

Objective: In the setting of RhD-alloimmunized pregnancy, laboratory variations in critical titer (CT) of anti-D antibody may result in needless referrals or a compromised fetal outcome.

Methods: RhD-alloimmunized pregnant women were included. Fetal outcome was categorized based on cord hemoglobin and interventions required. For 3 commonly used CTs of 8, 16, and 32, sensitivity and specificity as well as positive and negative predictive values were computed.

Results: When compared with CTs of 16 and 32, we detected 6.9% and 19.4% more cases of moderate-severe hemolytic disease of the fetus and newborn by using 8 as the CT. However, this leads to greater rate of unnecessary referral (12.1%, 10/82) than a CT of 16 (8.2%, 6/73) and 32 (4.9%, 3/61). A CT of 8 demonstrated 100% sensitivity, but 12.1% (10/82) of patients were referred needlessly.

Conclusion: Because of its 100% sensitivity, we advocate decreasing the CT to 8. However, this may lead to unwarranted referrals.

Hemolytic disease of the fetus and newborn (HDFN) is distinguished by the development of immunoglobulin G (IgG) antibodies in the mother against fetal erythrocyte antigens that cause hemolysis in the fetus by crossing the placenta. In antenatal women, the prevalence of alloimmunization against red cell antigens ranges from 0.89% to 5.98% worldwide and from 1.21% to 1.48% in India.[1–4] Maternal antibodies against Rh blood group system antigens are the most common cause of HDFN, with the D antigen accounting for more than 75% of these cases.[3,5] Although cases of anti-D–induced HDFN have been significantly reduced in the Western world, owing largely to an effective routine antenatal antibody screening program and the use of immunoprophylaxis, the complication remains common in countries such as India, resulting in significant perinatal morbidity.[6]

In addition to ABO/RhD typing, red cell antibody screening is performed during pregnancy to detect maternal red cell alloimmunization. Women with anti-D antibodies are also subjected to serial monitoring of maternal antibody titers to determine their risk of causing significant fetal hemolysis.[6] The conventional tube technique (CTT) of indirect Coomb's test is used routinely in many parts of the world, including India, to determine anti-D antibody titer. A low titer suggests that the infant will be unaffected or only mildly affected, whereas an increasing titer indicates a poor fetal outcome.[7]

Because of the use of Doppler ultrasound (Doppler USG) as the principal surveillance method and the need for specialized procedures like intrauterine transfusion (IUT), alloimmunized pregnancy management has gradually progressed beyond the purview of practice of a general obstetrician into the hands of a specialist in fetal medicine. The critical anti-D titer is used as a threshold for referring RhD-alloimmunized antenatal women for fetal Doppler assessment under the direction of a fetal medicine specialist. Critical titer (CT) is defined as the titer associated with significant risk of development of HDFN (fetal anemia, hydrops, etc). An ideal CT would reduce unnecessary referrals while also ensuring that women who are alloimmunized and in need of fetal therapy are not erroneously comforted and denied potentially life-saving fetal treatment. A referral was considered unnecessary when pregnancy was either unaffected or mildly affected by HDFN despite an anti-D titer level equal to or greater than the critical level.

Although the CT varies by laboratory, most centers use an anti-D titer of 8 to 32.[8] At our center, an anti-D titer of 1:8 is considered significant. In the United States, a CT of 16 is usually considered as an indicator for direct fetal monitoring.[9] Some, on the other hand, have questioned the safety of using a CT of 16 to guide clinical therapy.[10]

The middle cerebral artery peak systolic velocity in fetuses of antenatal women (referred with titers ≥CT) is measured with fetal Doppler USG to evaluate the presence of fetal anemia. When fetal middle cerebral

© The Author(s) 2022. Published by Oxford University Press on behalf of American Society for Clinical Pathology. All rights reserved. For permissions, please e-mail: journals.permissions@oup.com

Downloaded from https://academic.oup.com/labmed/article/54/4/429/6948049 by guest on 24 February 2025

artery Doppler examination reveals a peak systolic velocity of 1.5 times the median or higher, an intrauterine red cell transfusion is advised (indicates severe fetal anemia).[11]

Thus, the maternal anti-D antibody titer, which suggests the need for more intense fetal monitoring, becomes especially important. As a result, we decided to conduct a prospective analysis to reexamine the performance of 3 commonly used anti-D CTs (8, 16, and 32) in terms of referral decision adequacy.

Materials and Methods

This was a prospective study performed at a referral center in northern India. Data was collected between September 2015 and February 2018. Antenatal women sensitized with anti-D were incorporated in the study. We excluded women with blood group antibodies in addition to anti-D. Women with RhD antigen negative fetus/neonates and ABO incompatible pregnancies were also excluded. Thus, all of the children in the study were RhD positive.

Red cell antibody screening was done for all antenatal women who visited the hospital's obstetric unit. Many other required serological tests were performed, including antibody identification, manual antibody titration, red cell phenotyping of the fetus (before the first IUT), the father, and the mother, and a fetal/neonatal direct antiglobulin test (DAT), following departmental standard operating procedures. The DAT was performed on the fetal/neonatal pretransfusion sample (sample collected prior to any intrauterine/exchange/simple transfusion).

Clinical data were collected, including obstetric history, fetal outcome, and therapeutic interventions required. Various therapeutic interventions like IUT, exchange transfusion (ET), phototherapy (PT), and simple packed red blood cell (PRBC) transfusion were performed when required. PT and ET were used to manage neonatal hyperbilirubinemia whereas simple PRBC transfusion was used for neonatal anemia. The IUT was done when fetal hematocrit was <30% on fetal blood sampling. All live births were followed for 3 months to observe their survival. For the study, ethical clearance was obtained from the institutional ethics committee (IEC code: 2016-70-MD-90)

Categorization of HDFN Severity

In fetuses and neonates, HDFN was diagnosed using British Committee for Standards in Haematology standards.[12] The HDFN severity was categorized on the basis of cord hemoglobin level, therapeutic interventions required, and specific fetal medical conditions. Therapeutic interventions like IUT, ET, PT, and simple PRBC transfusion were considered for categorizing HDFN severity. Three categories, unaffected/mild, moderate, and severe HDFN, were considered for the purpose of the study as given in **TABLE 1**.

Identification and Titration of Antibodies

Red cell antibodies were screened in all antenatal women. The 3-cell screening panel (Diacell I, II, III; Biorad, DiaMed) was used for red cell antibody screening. For screen positive cases, an 11-cell identification panel (ID-DiaPanel; Biorad, DiaMed) was used to determine antibody specificity. Both the screening and identification of antibodies were performed in indirect antiglobulin phase using gel technology (ID-Card LISS/Coombs; Biorad, DiaMed). In RhD sensitized women, serial anti-D titration was done every 2 to 4 weeks during gestation. Titration was performed using the tube technique in the indirect antiglobulin phase. A pool of 3 group O R2R2 (DcE/DcE) red cells was used for titration. Serial doubling dilution of maternal serum was done. Subsequently, each dilution was incubated with a 5% suspension of pooled O R2R2 red cells in 1:1 ratio at 37°C for 1 hour. Post incubation, saline cell washing was done 3 times followed by the addition of antihuman globulin (Eryclone Anti Human Globulin; Tulip Diagnostics). Finally, centrifugation was performed using Megafuge-8 Small Benchtop Centrifuge (Thermo Scientific) at 1000 rpm for 1 minute and results recorded. Titration results are reported as the reciprocal of the highest serum dilution exhibiting a 1+ agglutination reaction (for example, 16 and not 1 in 16 or 1:16).

Statistical Analysis

The highest anti-D titer recorded throughout a pregnancy after testing a series of serum samples at different gestational ages was considered as single fixed titer for that pregnancy. Patient population was classified above (or equal to) or below a particular critical anti-D titer level using cumulative frequency based on the highest anti-D titer attained. The sensitivity, specificity, positive predictive value, and negative predictive value of 3 of the most regularly mentioned CTs (8, 16, and 32) were calculated to compare their diagnostic accuracy in terms of referral decision appropriateness.

Results

A total of 439 pregnant women were screened for irregular red cell antibodies. Of these, 194 (44.2%) were found to be RhD negative and the remaining 245 (55.8%) were RhD positive. All antenatal women had multiple pregnancies (from 2 to 7). Antibody screen was found to be positive in 32.3% (142/439) of antenatal women, with anti-D being the most prevalent antibody discovered. Incidentally, all the screen positive cases were RhD negative, whereas none of the RhD-positive women had red cell alloimmunization.

FIGURE 1 shows the distribution of antenatal women who tested positive for antibodies. Out of 142 women who tested positive for anti-D, 24 (17%) had additional antibodies (1 or more) in addition to anti-D, whereas the remaining 118 (83%) had anti-D alone. A total of

TABLE 1. Categorization of HDFN Severity in RhD-Alloimmunized Antenatal Women

Category	Evidence of Hemolysis[a]	Cord Hb[b] (g/dL)	Fetal/Neonatal Medical Condition or Intervention Required
Unaffected-mild	No	>12	No
Moderate	Yes	10–12	Exchange/simple PRBC transfusion/phototherapy
Severe	Yes	<10	Intrauterine transfusion/hydrops/intrauterine death

Hb, hemoglobin; HDFN, hemolytic disease of the fetus and newborn.
[a]Includes both clinical (pallor, icterus, hepatospleenomegaly, etc) and laboratory (Increased reticulocyte count, microspherocytosis, polychromasia, indirect hyperbilirubinemia) evidence of hemolysis.
[b]Fetal Hb level obtained by cordocentesis before first intrauterine transfusion or cord Hb at birth (where intrauterine transfusion was not performed).

Downloaded from https://academic.oup.com/labmed/article/54/4/429/6948049 by guest on 24 February 2025

FIGURE 1. Summary of RhD-sensitized antenatal cases and their fetal outcome. HDFN, hemolytic disease of the fetus and newborn.

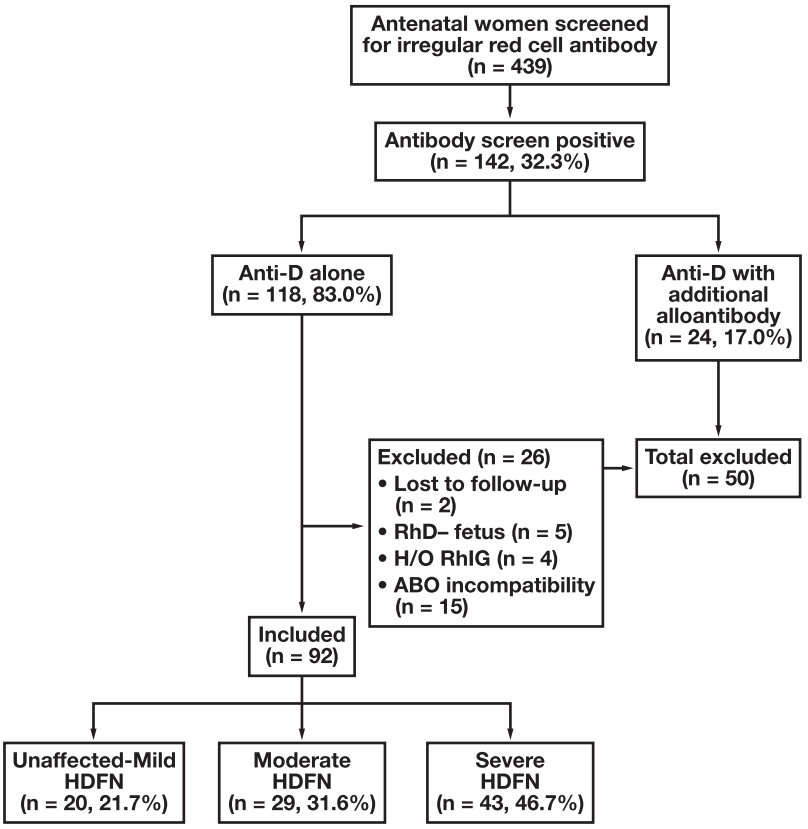

TABLE 2. Distribution of RhD Alloimmunized Cases Among Highest Anti-D Titer Levels Attained During Pregnancy

Highest Anti-D Levels Attained During Pregnancy	Unaffected-Mild HDFN	Moderate-Severe HDFN
<8 (n = 10)	10	0
8 (n = 9)	4	5
16 (n = 12)	3	9
32 (n = 14)	3	11
64 (n = 9)	0	9
>64 (n = 38)	0	38

HDFN, hemolytic disease of the fetus and newborn.

50 women were excluded for various reasons, including the presence of additional antibodies, having an RhD-negative fetus, and having an ABO incompatible pregnancy. In the end, 92 patients who had only anti-D were included in the statistical analysis. Twenty (21.7%) of the 92 cases studied were either unaffected or mildly affected, whereas 29 (31.6%) and 43 (46.7%) cases were moderately and severely affected, respectively. Four of the 43 moderately to severely affected fetuses died, 2 in the intrauterine phase and 2 in the first week after birth. The DAT was variable (positive/negative) in unaffected or mildly affected children but positive in all cases of moderately to severely affected children.

TABLE 2 shows the distribution of RhD-sensitized cases based on the highest anti-D titer acquired during pregnancy. At peak titer levels of 8 to 32, fetal outcome ranged from unaffected to severely affected. All pregnancies with titers of <8 were either unaffected or had minor HDFN manifestations, whereas titers of >32 were always associated with moderate-severe HDFN.

The comparison of the 3 commonly used anti-D titer levels is shown in **TABLE 3**. Cumulative frequency was used to split 92 antenatal cases and their fetal outcomes into 2 groups: those above and those below CT levels. False-negative cases (titer below critical level with affected fetus) increased in tandem with CT, whereas false-positive instances declined (titer above critical level with unaffected fetus). On the other end, when CT decreased, the number of false-negative instances decreased, and vice versa for false-positive cases.

The statistical performance of the 3 most widely referenced CTs is shown in **TABLE 4**. The sensitivity of using a CT of 8 for referral to fetal medicine experts was 100% (correctly detected all cases with moderate-severe HDFN), whereas the specificity was 50%. The specificity for detection of moderate-severe HDFN increased to 70% and 85%, respectively, when the CT was 16 and 32. However, 6.9% (05/72) and 19.4% (14/72) of moderate-severe HDFN cases were missed, respectively, in this setting (**TABLE 4**). At our center, the CT that necessitates a referral to a specialist is 8. When compared with CTs of 16 and 32, we could identify 6.9% and 19.4% additional cases of moderate-severe HDFN by adopting 8 as the CT. However, this resulted in a greater rate of unnecessary referrals (12.1%, 10/82) than CTs of 16 (8.2%, 6/73) and 32 (4.9%, 3/61), respectively.

TABLE 5 depicts the distribution of various therapeutic interventions required in RhD-alloimmunized women with the highest anti-D titers. As the anti-D titer increased, all therapeutic interventions

Downloaded from https://academic.oup.com/labmed/article/54/4/429/6948049 by guest on 24 February 2025

(IUT, ET, simple PRBC transfusion, PT) were required with increasing frequency.

Discussion

This study shows that anti-D titer as low as 8 may indicate moderate-to-severe HDFN whereas the fetus may not be affected at a titer of 32. This variation reflects the poor correlation between fetal outcome and anti-D titer, as shown by other authors.[13] Given the low correlation between anti-D titer and fetal outcomes, selecting the appropriate critical anti-D titer is challenging. Referral to a higher level of care based on lower CT reduces referral of false-positive cases while ensuring that no at-risk alloimmunized women are denied potentially life-saving fetal therapy.

According to the present study, a referral threshold titer of 16 or 32 would have failed to detect a significant number of moderate-to-severe cases (6.9% and 19.4%, respectively). This finding clearly highlights the need of change in CT referral level. Although a CT of 8 allowed all cases with moderate-severe HDFN to be identified, a larger proportion of cases (12.1%, 10/82) were referred needlessly when compared with CTs of 16 (8.2%, 6/73) and 32 (4.9%, 3/61). Given the purpose of the CT as a screening test (for subsequent referral), maintaining a high level of sensitivity is critical. Therefore, even with additional unnecessary referrals, decreasing CT to 8 seems prudent, considering the 100% sensitivity (zero undetected cases with moderate-severe anemia) and noninvasive nature of Doppler USG. However, this may add to the cost and workload.

Approximately 9% (30/339) of RhD-negative women were found to be immunized in a report by Varghese et al.[14] Extrapolating our findings to this study, 2 of 30 immunized cases would be missed (6.9% missing rate) when using 16 as the CT. If this rate were applied to a wider population, it could result in poor antenatal care.

Manual titration using CTT has been criticized due to concerns about inaccuracy, relatively low reproducibility, and the inherent subjectivity of the titer end point, despite its technical simplicity.[15] Interlaboratory differences in reporting titer levels may indeed be attributable to these shortcomings, resulting in either unnecessary referral or a delay in life-saving fetal care (IUT). Due to the unreliability of manual titration, lowering the CT to 8 would reduce false negatives and missed positives.

Our study had several strengths. The ABO incompatibility and additional alloantibody, which may promote fetal hemolysis, were eliminated. It is well known that anti-D titer fluctuates during the course of the pregnancy. Serial anti-D titrations were performed for each pregnancy to eliminate this confounder, and the highest anti-D titer recorded was used to correlate with final outcome. Antibody titration in all subjects was done by a single resident doctor to eliminate technical and subjective differences. Furthermore, to control intra- and interlaboratory variation, previous samples were tested in conjunction with the current samples, and external quality assessment services were used. Because this was a single-center study conducted between 2015 and 2018, the RhD-sensitized women's management strategies were consistent throughout the period. Standard procedures that have been widely published were used for both titration and ultrasonic surveillance.[16–18] As a result, we are confident in the study's findings.

TABLE 3. Comparison of Three Critical Anti-D Titer Levels to Evaluate Their Relative Ability to Predict Outcome of the RhD Alloimmunized Pregnancy

Critical Levels of Anti-D Antibody	Highest anti-D Level Attained during Pregnancy	Outcome of the RhD-Alloimmunized Pregnancy (n = 92)	
		Unaffected-Mild HDFN (n = 20)	Moderate-Severe HDFN (n = 72)
IAT titer-8	<8 (Cf = 10)	10 (TN[a])	00 (FN[b])
	≥8 (Cf = 82)	10 (FP[c])	72 (TP[d])
IAT titer-16	<16 (Cf = 19)	14 (TN[a])	05 (FN[b])
	≥16 (Cf = 73)	06 (FP[c])	67 (TP[d])
IAT titer-32	<32 (Cf = 31)	17 (TN[a])	14 (FN[b])
	≥32 (Cf = 61)	03 (FP[c])	58 (TP[d])

Cf, cumulative frequency; HDFN, hemolytic disease of the fetus and newborn.
[a]TN (true negative): Fetal outcome correctly predicted as unaffected-mild HDFN where anti-D antibody level was less than critical level.
[b]FN (false negative): Fetal outcome incorrectly predicted as unaffected-mild HDFN where anti-D antibody level was less than critical level.
[c]FP (false positive): Fetal outcome incorrectly predicted as moderate-severe HDFN where anti-D antibody level was more or equal to critical level.
[d]TP (true positive): Fetal outcome correctly predicted as moderate-severe HDFN where anti-D antibody level was more or equal to critical level.

TABLE 4. Evaluation of Measures of Diagnostic Accuracy for Three Commonly Used Critical Titer Levels

Predictive Value	Critical Titer 8	Critical Titer 16	Critical Titer 32
Sensitivity	100%	93.0%	80.5%
Specificity	50.0%	70.0%	85.0%
Positive predictive value	87.8%	91.7%	95.0%
Negative predictive value	100%	73.6%	54.8%

TABLE 5. Interventions Required in Management of RhD-Alloimmunized Pregnancy

Number of RhD-Alloimmunized Pregnancy (Highest Anti-D Levels Attained during Pregnancy)	No. of Fetuses Received IUT	No. of Pregnancies Received ET	No. of Pregnancies Receiving Simple PRBC Transfusion	No. of Pregnancies Where Neonate Received PT	No. of Pregnancies with Untreated Fetus/Neonate
10 (<8)	0	0	0	0	10
9 (8)	0	0	2	5	4
12 (16)	0	2	3	7	4
14 (32)	2	5	5	11	0
9 (64)	3	6	4	9	0
38 (>64)	24	19	15	36	0

ET, exchange transfusion; IUT, intrauterine transfusion; PT, phototherapy.

Downloaded from https://academic.oup.com/labmed/article/54/4/429/6948049 by guest on 24 February 2025

There are some possible limitations of this study. The sample size at each CT level was insufficient to determine the CT level with confidence. It is also important to know that our facility is a tertiary care hospital. As a result, the patient group may be at a higher risk of developing a severe disease or developing complicating consequences than a general population.

Conclusion

The sensitivity of a critical anti-D titer of 16 and 32 for appropriate referral for USG surveillance is insufficient. Because fetal Doppler USG is noninvasive, adopting 8 as the CT (100% sensitivity) appears sensible even when leading to unneeded referrals. However, these unwarranted referrals may increase expense and workload. More multicenter studies with a larger sample size are required to confirm our findings.

Acknowledgments

We thank the people from the Departments of Maternal and Reproductive Health and Neonatology for helping us finalize this study.

Conflict of Interest Disclosure

The authors have nothing to disclose.

REFERENCES

1. Gunduz E, Akay OM, Teke HU, et al. Incidence of red-cell alloimmunization due to non-anti D antibodies during pregnancy: an experience from Turkey. *Transfus Apher Sci*. 2010;43:261–263. doi: 10.1016/j.transci.2010.09.011
2. Foudoulaki-Paparizos L, Valsami S, Bournas N, et al. Alloimmunisation during pregnancy in Greece: need for nation wide HDFN prevention programme. *Transfus Med.* 2013;23:254–259. doi: 10.1111/tme.12063
3. Pahuja S, Gupta SK, Pujani M, et al. The prevalence of irregular erythrocyte antibodies among antenatal women in Delhi. *Blood Tranfusion.* 2011;9:388–393. doi: 10.2450/2011.0050-10
4. Devi SA, Alwar VA, Sitalakshmi S, Rameshkumar K, Mhaskar R. Red blood cell antibody screening in pregnancy. *Asian J Transfus Sci*. 2011;5(1):56.
5. Suresh B, Sreedhar Babu KV, Arun R, et al. Prevalence of "unexpected antibodies" in the antenatal women attending the Government Maternity Hospital, Tirupati. *J Clin Sci Res.* 2015;4:22–30. doi: 10.15380/2277-5706.JCSR.13.034
6. Basu S, Kaur R, Kaur G. Hemolytic disease of the fetus and newborn: current trends and perspectives. *Asian J Transfus Sci.* 2011;5(1):3–7.
7. Fasano RM, Hendrickson JE, Luban NC. Alloimmunehemolytic disease of the fetus and newborn. In: Kaushansky K, Lichtman MA, Prchal JT, et al. eds. *Williams Hematology*, Vol. 9e. New York, NY: McGraw Hill; 2015. https://accessmedicine.mhmedical.com/content.aspx?bookid=1581&sectionid=94305868.
8. Van Buren NL. Perinatal transfusion medicine. In: Shaz BH, Hillyer CD, Gil MR, eds. *Transfusion Medicine and Hemostasis*. 3rd ed. Elsevier; 2019: 301–312.
9. Judd WJ, Luban NLC, Ness PM, et al. Prenatal and perinatal immunohematology: recommendations for serologic management of the fetus, newborn infant and obstetric patient. *Transfusion*. 1990;30(2):175–183.
10. Van Dijk BA, Dooren MC, Overbeeke MA. Red cell antibodies in pregnancy: there is no "critical titer". *Transfus Med.* 1995;5(3):199–202.
11. Mari G. Middle cerebral artery peak systolic velocity. *J Ultrasound Med.* 2005;24(5):697–702.
12. British Committee for Standards in Haematology (BCSH); White J, Qureshi H, Massey E, et al. Guideline for blood grouping and red cell antibody testing in pregnancy. *Transfus Med.* 2016;26(4):246–263.
13. Velkova E. Correlation between the amount of anti-D antibodies and IgG subclasses with severity of hemolytic disease of fetus and newborn. *Maced J Med Sci.* 2015;3(2):293–297.
14. Varghese J, Chacko MP, Rajaiah M, et al. Red cell alloimmunization among antenatal women attending a tertiary care hospital in south India. *Indian J Med Res.* 2013;138(1):68–71.
15. Engelfriet CP, Reesink HW, Bowman JM, et al. Laboratory procedure for prediction of the severity of hemolytic disease of new born. *Vox Sang.* 1995;69:61–69. doi: 10.1159/000462793
16. The Management of Women with Red Cell Antibodies during Pregnancy. Royal College of Obstetricians & Gynecologists. Green-top Guideline No. 65, May 2014. https://www.rcog.org.uk/guidance/browse-all-guidance/green-top-guidelines/the-management-of-women-with-red-cell-antibodies-during-pregnancy-green-top-guideline-no-65/. Accessed November 17, 2022.
17. Gupte SC, Bhatia HM. Correlation of Rh(D) antibody titer and obstetric history with severity of Rh(D) HDN of the newborn. *Ind J Haematol*. 1985;3(1):76–80.
18. Mari G, Deter RL, Carpenter RL, et al. Noninvasive diagnosis by Doppler ultrasonography of fetal anemia due to maternal red-cell alloimmunization. *N Engl J Med.* 2000;342(1):9–14.

Downloaded from https://academic.oup.com/labmed/article/54/4/429/6948049 by guest on 24 February 2025

CASE STUDY

Type 1 von Willebrand Disease in a Pediatric Patient Caused by a Novel Heterozygous Deletion of Exons 1 to 6 of the von Willebrand Factor Gene: A Case Report

Ivana Lapić, MSc,[1,] Margareta Radić Antolic, MSc,[1] Dunja Rogić, PhD,[1,2] Sara Dejanović Bekić, MD,[3] Désirée Coen Herak, PhD,[1] Ernest Bilić, PhD,[3] Renata Zadro, PhD[4]*

[1]Department of Laboratory Diagnostics, University Hospital Center Zagreb, Zagreb, Croatia, [2]Faculty of Pharmacy and Biochemistry, University of Zagreb, Zagreb, Croatia, [3]Referral Center for Pediatrics Hematology and Oncology, Department of Pediatrics, University Hospital Center Zagreb, Zagreb, Croatia, [4]Medical Biochemistry Laboratory, St Catherine Specialty Hospital, Zagreb, Croatia. *To whom correspondence should be addressed: ilapic@kbc-zagreb.hr.

Keywords: von Willebrand disease, bleeding, von Willebrand factor, coagulation testing, next-generation sequencing, multiplex ligation-dependent probe amplification

Abbreviations: VWD, von Willebrand disease; VWF, von Willebrand factor; NGS, next-generation sequencing; MLPA, multiplex ligation-dependent probe amplification; GPIb, glycoprotein Ib; FVIII, coagulation factor VIII; VWF:Ag, von Willebrand factor antigen; VWF:GPIbM, von Willebrand factor gain-of-function mutant glycoprotein-Ib binding activity; VWF:CB: von Willebrand factor collagen-binding activity

Laboratory Medicine 2023;54:434-438; https://doi.org/10.1093/labmed/lmac138

ABSTRACT

A 6-year-old boy was referred to a hematologist due to excessive mucocutaneous bleeding. Diagnostic assessment for von Willebrand disease (VWD) was indicated and included both coagulation and genetic testing. Laboratory testing revealed proportionally decreased von Willebrand factor (VWF) glycoprotein Ib-binding activity (23.6%) compared to VWF antigen (24.7%), similarly decreased VWF collagen-binding activity (24.2%), and normally distributed VWF multimers, with decreased intensity of all fractions. Diagnosis of type 1 VWD was established. Genetic analysis by means of next-generation sequencing (NGS) of VWF and coagulation factor VIII genes did not identify any causative mutations. Additionally, multiplex ligation-dependent probe amplification (MLPA) of VWF gene exons revealed a heterozygous deletion of exons 1 to 6, which is reported in type 1 VWD for the first time. Application of MLPA was crucial for revealing the genetic basis of type 1 VWD in this case, which would have remained undetected if only NGS was used.

von Willebrand disease (VWD) is the most common inherited bleeding disorder caused by quantitative or qualitative changes of von Willebrand factor (VWF), a large multimeric glycoprotein with 2 crucial roles in hemostasis. It mediates platelet adhesion and aggregation at the site of vascular injury through interaction with the platelet receptor glycoprotein Ib (GPIb), as well as transports and stabilizes coagulation factor VIII (FVIII) in circulation.[1] The gene encoding VWF is located on the short arm of chromosome 12, spans 178 kilobases of genomic sequence, and consists of 52 exons.[2]

Type 1 is the most frequent form of VWD, affecting up to 80% of all persons with VWD, and is characterized by variable degrees of quantitative deficiencies involving structurally and functionally normal VWF.[1,3,4] The majority of patients present with mild mucocutaneous bleeding symptoms, including epistaxis, easy bruising, and prolonged bleeding following minor injuries, whereas severe bleeding symptoms are rare and related to cases with significantly reduced VWF levels.[4,5] Key laboratory findings in type 1 VWD comprise proportionally reduced VWF activity and antigen levels (VWF:Ag), resulting in a ratio of the 2 above 0.7. The VWF multimers are normally distributed, with equally decreased intensity of all fractions.[1]

Type 1 VWD shows an autosomal dominant inheritance pattern, and its genetic basis is largely heterogeneous. To date, around 140 different mutations associated with type 1 VWD have been identified throughout the whole VWF gene.[6] Missense mutations are found to be the most common genetic cause, accounting for about 70% of cases, whereas splice, transcriptional, nonsense, and frameshift mutations constitute the remainder.[7] Reduced levels of VWF in type 1 VWD are a consequence of altered molecular processing mechanisms that either result in increased clearance or decreased cellular secretion of VWF.[7] However, phenotypic presentation of type 1 VWD can be largely variable, even among members of the same family or unrelated patients with the same mutations, due to their incomplete penetrance and variable expressivity.[8] Genetic characterization of patients with type 1 VWD requires analysis of the entire VWF gene coding region, which became possible with the introduction of next-generation sequencing (NGS) capable of reliably detecting point and small frameshift mutations.[9] In addition, a minority of type 1 VWD cases are reportedly caused by large heterozygous deletions and duplications. To correctly detect and identify those cases, gene dosage analysis, particularly multiplex ligation-dependent probe amplification (MLPA), should be used.[2,9,10]

© The Author(s) 2022. Published by Oxford University Press on behalf of American Society for Clinical Pathology. All rights reserved. For permissions, please e-mail: journals.permissions@oup.com

Downloaded from https://academic.oup.com/labmed/article/54/4/434/6873308 by guest on 24 February 2025

Here, we present a case of a pediatric patient with bleeding symptoms and coagulation testing results indicative of type 1 VWD, in whom MLPA analysis was crucial for identification of the underlying genetic cause.

Materials and Methods

Patient Presentation and Blood Sampling

A 6-year-old boy without a known family history of bleeding disorders was referred to a hematologist at the Department of Pediatrics Hematology and Oncology, University Hospital Center Zagreb, Zagreb, Croatia, due to recurrent episodes of epistaxis, prolonged bleeding following trivial injuries, and excessive bruising after minor trauma. Laboratory testing for VWD was indicated and included both coagulation and genetic analyses. For this purpose, two 2.7 mL 3.2% trisodium citrate and one 2 mL EDTA vacutainers (Becton Dickinson) were drawn. The study was approved by the University Hospital Center Zagreb Ethics Committee (8.1-19/293-2, 02/21 AG), and the patient's mother gave written informed consent for anonymous publication of medical data.

Coagulation Testing

Capacity of primary hemostasis was determined from whole blood samples, within 2 hours from blood draw, on the platelet function analyzer-200 (PFA-200) using dedicated cartridges coated with platelet agonists collagen and both epinephrine and adenosine-diphosphate.

For other coagulation assays, platelet-poor plasma was obtained by double centrifugation for 15 minutes at 2000*g*. Prothrombin time was determined using the recombinant thromboplastin Dade Innovin and activated partial thromboplastin time with Dade Actin FS and calcium chloride on the Sysmex CS-5100 coagulation analyzer. The VWF activity was measured on an Atellica COAG 360 analyzer by means of the automated immunoturbidimetric assay INNOVANCE VWF Ac that uses microparticles coated with GPIb containing 2 gain-of-function mutations that enhance VWF binding (VWF:GPIbM), thus reflecting the GPIb-binding activity of VWF. The VWF:Ag was determined using the automated immunoturbidimetric assay VWF Ag, and FVIII activity was measured by a 1-stage clotting assay, using FVIII-deficient plasma and Dade Actin FS, on the Atellica COAG 360 coagulation analyzer. All respective reagents and analyzers are produced by Siemens Healthcare, and all analyses were performed following the original manufacturer's protocols.

The VWF collagen-binding activity (VWF:CB) was measured using the enzyme-linked immunosorbent assay Technozym vWF:CBA (Technoclone) that reflects the ability of VWF to bind human collagen type III. The ratios VWF:GPIbM/VWF:Ag and VWF:CB/VWF:Ag were calculated.

Multimeric analysis was performed by agarose gel electrophoresis with direct immunofixation using the Hydragel 5 von Willebrand multimers assay kit on the Hydrasys 2 Scan instrument (Sebia). The results were interpreted in relation to the multimeric profile of normal plasma with values of VWF:Ag ~ 100%, as recommended by the manufacturer.

Genetic Analyses

Genomic DNA was isolated from EDTA whole blood using the automated magnetic bead-based method on the MagNA Pure Compact instrument (Roche Diagnostics).

Genetic analysis included NGS of all 52 exons, intronic flanking regions, and the promoter of the VWF gene as well as all 26 exons and the promoter of the FVIII gene. The DNA samples were prepared for sequencing using the Illumina DNA Prep with Enrichment kit (Illumina), strictly following the manufacturer's protocol.[11] The NGS was performed on Miseq (Illumina) using the 300-cycle Miseq reagent kit v2 with 150 bp paired end reads. Sequencing raw data were uploaded in the form of FASTQ files in the BaseSpace Variant Interpreter software (Illumina), where alignment to the hg19 reference genome was carried out.

For detection of large duplications or deletions within the VWF gene, MLPA analysis using the SALSA MLPA reagent kit and probe sets dedicated for VWF gene analysis SALSA MLPA Probemix VWF P011 and P012 (MRC Holland) was performed according to the manufacturer's protocol. Amplification products were identified on the ABI-3130xl Genetic Analyzer (Applied Biosystems), and DNA dosage was estimated using Coffalyser.Net software (MRC Holland). Interpretation of results was based on the evaluation of changes in probe signal intensity in relation to reference samples; specifically, a decrease or increase in probes signal intensity compared to reference samples indicates a deletion or duplication, respectively.

Results

Results of coagulation testing are presented in **TABLE 1** and indicated partial quantitative deficiency of VWF. Multimeric analysis showed

TABLE 1. Results of Coagulation Testing

Assay	Result	Reference Interval
PT (ratio)	1.01	>.70
aPTT (s)	32.6	20.0–30.0
VWF:GPIbM (%)	23.6	50.0–187.0
VWF:Ag (%)	24.7	50.0–160.0
VWF:GPIbM/ VWF:Ag (ratio)	0.96	N/A
FVIII (%)	54.0	50.0–149.0
VWF:CB (%)	24.2	40.0–250.0

aPTT, activated partial thromboplastin time; FVIII, coagulation factor VIII activity; N/A, not applicable; PT, prothrombin time; VWF:Ag, von Willebrand factor antigen; VWF:CB, von Willebrand factor collagen-binding activity; VWF:GPIbM, von Willebrand factor gain-of-function mutant glycoprotein-Ib binding activity.

FIGURE 1. Results of multimers analysis showing a normal multimer distribution with proportional decrease of all multimer fractions. The gray line represents the patient's multimer distribution, while the black line represents normal pooled plasma sample. LMWM, low-molecular-weight multimers; IMWM, intermediate-molecular-weight multimers; HMWM, high-molecular-weight multimers.

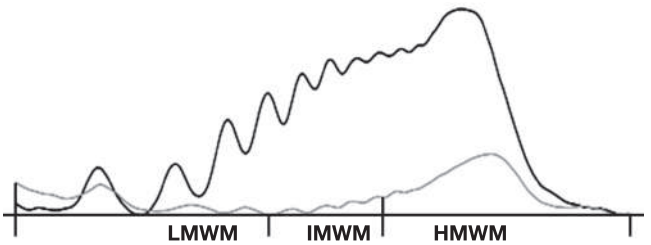

Downloaded from https://academic.oup.com/labmed/article/54/4/434/6873308 by guest on 24 February 2025

proportional reduction of all VWF multimer fractions compared to normal plasma, as shown in **FIGURE 1**. Based on these results, diagnosis of type 1 VWD was established.

For identification of the genetic cause of VWD in this patient, first NGS analysis was performed. No disease-associated genetic variants were identified either within the VWF or the FVIII gene. Additional analysis using MLPA revealed the presence of only 1 copy of exons 1 to 6 of the VWF gene, as shown in **FIGURE 2A** and **2B**. A ratio of 0.5 between signals of the analyzed probes for the respective exons in the patient's sample and reference samples was obtained, thus indicating a deletion in the heterozygous state. For comparison, **FIGURE 2C** and **2D** show results for a control sample with 2 copies of all analyzed exons, with all ratios being ~1.

Discussion

The presented case represents a rare occurrence of a large frameshift mutation associated with type 1 VWD phenotype in a pediatric patient. To the best of our knowledge, this is the first report of a type 1 VWD caused by the heterozygous deletion of exons 1 to 6 within the VWF gene.[2,6]

The obtained coagulation testing results that included proportionally reduced VWF:GPIbM, VWF:Ag, and VWF:CB, with values below 30%, as

FIGURE 2. Results of multiplex ligation-dependent probe amplification showing the presence of 1 copy of exons 2, 5, and 6 using SALSA Probemix P011 VWF (A) and exons 1, 3, and 4 with SALSA Probemix P012 VWF (B). A ratio of 0.5 between signals of the analyzed probes for the respective exons in the patient's sample and reference samples was obtained, as indicated by squared frames. For comparison, results of analysis of a control sample with 2 copies of exons analyzed with SALSA Probemix P011 VWF (C) and with SALSA Probemix P012 VWF (D) are shown. The obtained ratio for all exons in the control sample is ~1.

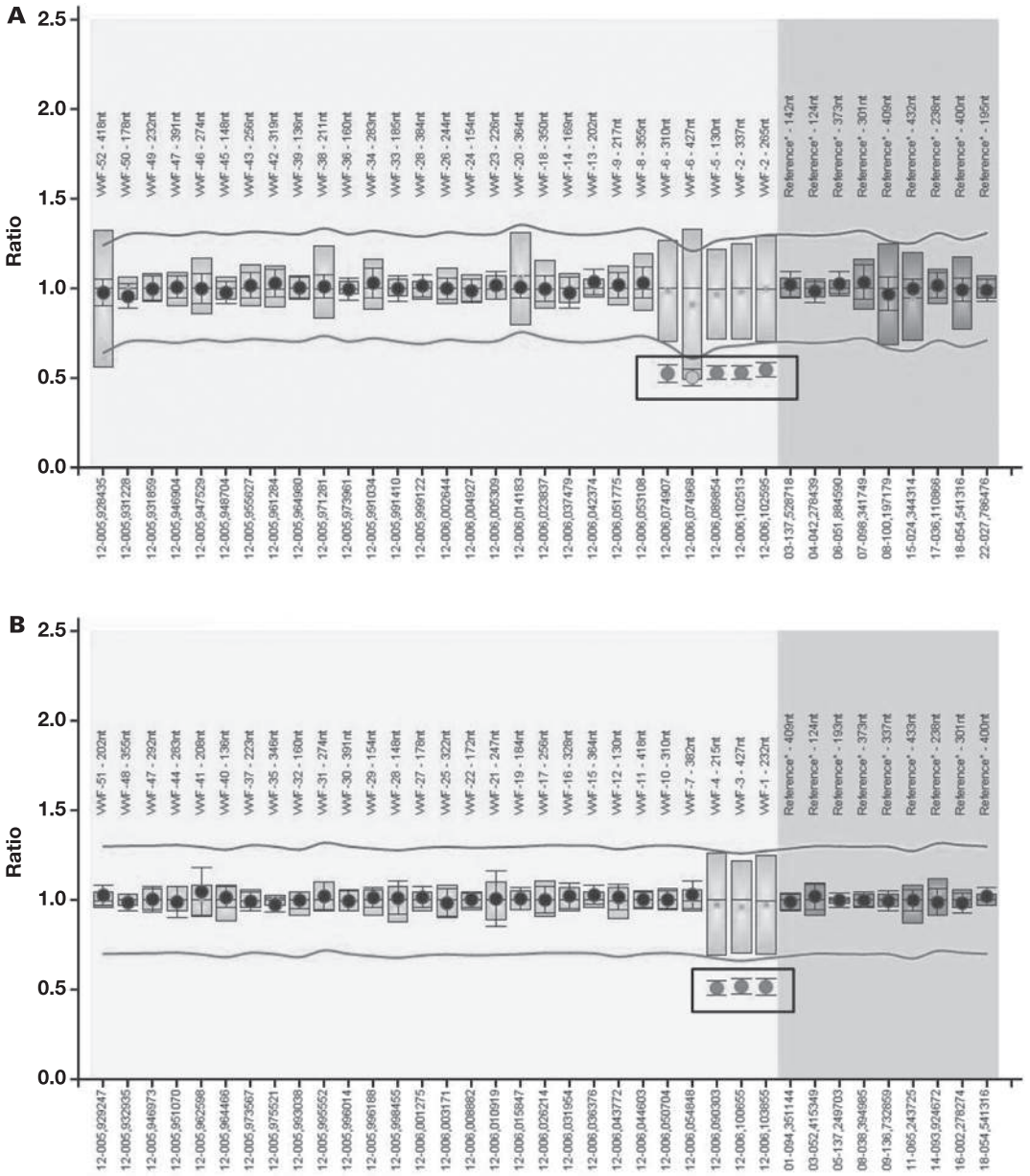

Downloaded from https://academic.oup.com/labmed/article/54/4/434/6873308 by guest on 24 February 2025

FIGURE 2. (cont)

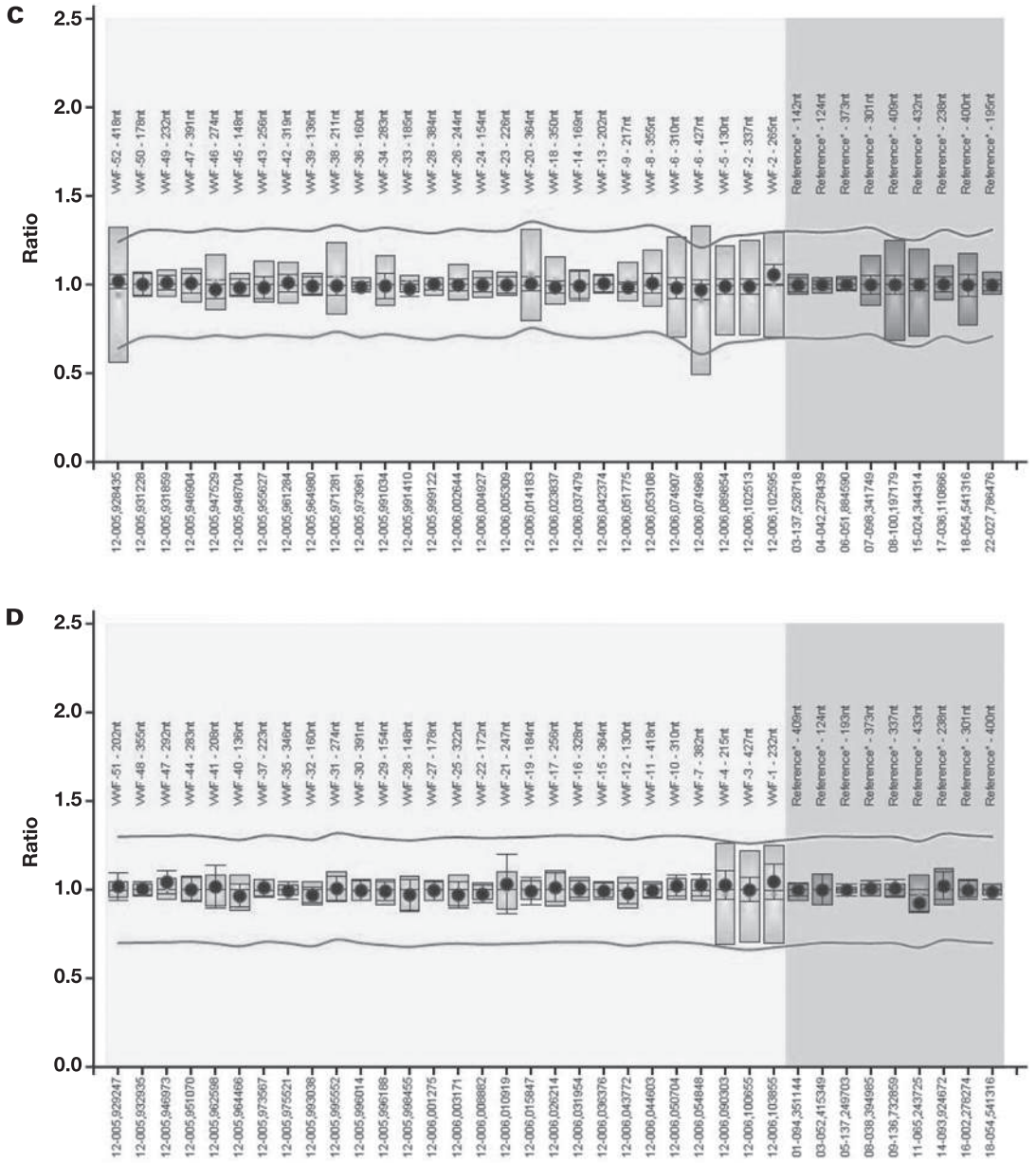

well as normal multimeric distribution characterized by decreased intensity of all fractions, indicated quantitative deficiency of VWF and, together with mild mucocutaneous bleeding symptoms, fulfilled the diagnostic criteria for type 1 VWD.[12] Rather unexpectedly, the initial genetic analysis by means of NGS failed to identify the causative mutation. It is known that only about 65% of patients with type 1 VWD have an underlying mutation in the VWF gene, the incidence of which increases with decreased levels of VWF.[13] In this case, the levels of VWF below 30% clearly indicated that the observed deficiency of VWF must be caused by a genetic alteration that NGS failed to detect due to inherent method limitations. Therefore, we speculated that a quantitative change of 1 or more exons could be the cause of type 1 VWD phenotype in this case. For this purpose, MLPA analysis was performed and indeed revealed that the patient is a heterozygous carrier of a deletion spanning exons 1 to 6 of the VWF gene. The NGS is a polymerase chain reaction–based technique that could not detect this genomic abnormality due to the presence of 1 copy of the affected gene region that was regularly amplified and sequenced, consequently masking the absence of the second allele.[9,14] In contrast, MLPA is a molecular technique based on amplification of probes hybridized to targeted gene regions. A decrease in respective exon copy numbers allowed reliable detection of the large heterozygous deletions involving exons 1 to 6.[9,14,15]

Most studies dealing with MLPA have predominantly included patients with type 3 VWD, and it is presumed that the incidence of large deletions in type 1 VWD is likely to be underestimated due to limited studies in this group of patients.[16] In patients with type 1 VWD, heterozygous deletions of exons 3, 4 to 5, 26 to 34, 32 to 34, and 33 to 34 have been identified so far.[2] Deletion of exons 4 to 5 has been extensively studied by Sutherland et al,[10] who reported that homozygotes invariably present with unmeasurably low VWF levels and severe bleeding symptoms, thus usually ending up classified as type 3 VWD. In heterozygotes,

Downloaded from https://academic.oup.com/labmed/article/54/4/434/6873308 by guest on 24 February 2025

mild-to-moderate clinical and laboratory phenotypes characteristic for type 1 VWD were recorded. There was similar patient presentation in our case, which could be expected since the heterozygous deletion of exons 1 to 6 also affects the initial part of the VWF gene responsible for encoding part of the D1 domain within the VWF propeptide, hence causing decreased secretion and defective multimerization of the mutant VWF and resulting in type 1 VWD phenotype.[10,17] However, when such heterozygous deletion is part of a compound heterozygous genotype, as in the case described by Yadegari et al[14] where heterozygous deletion of exons 1 to 5 was combined with a missense mutation, the patient's phenotype is compatible with type 3 VWD. In fact, up to 80% of patients with type 3 VWD have a null allele mutation, which is either autosomal recessive and homozygous, or compound heterozygous, thus resulting in undetectably low VWF levels and severe bleeding phenotype.[8] A similarly severe phenotype can be found in the minority of patients with type 1 VWD caused either by fully penetrant dominant mutations or more rarely, a recessive genotype. However, severe type 1 VWD cases differ from type 3 VWD by the presence of low but still detectable VWF levels.[18] Differentiation of severe type 1 VWD from type 3 VWD is important for choosing the appropriate treatment approach as patients with severe type 1 VWD might be responsive to desmopressin, whereas the only therapeutic option for patients with type 3 VWD are plasma-derived VWF/FVIII concentrates due to the lack of endogenous VWF.[19] This clearly emphasizes the complexity of the genetic basis of VWD and the importance of the detection of the underlying genetic cause, which can be properly elucidated only through the use of adequate molecular techniques. The choice of the most suitable molecular diagnostic approach should be based on detailed evaluation of clinical symptoms and coagulation testing results as well as family history data, if available.

In conclusion, in this case, the addition of MLPA analysis to the molecular diagnostic algorithm of VWD was crucial for revealing the genetic basis of type 1 VWD, which would have remained undetected if only NGS was used. Therefore, in patients with clear clinical and laboratory evidence of type 1 VWD in whom causative mutations are not detected using sequencing methods, large heterozygous deletions of 1 or more exons should be considered as a possible cause of VWD and therefore MLPA should be applied for their detection. Proper genetic characterization of VWD might be especially important in pediatric patients such as this one for whom no positive family history of bleeding disorders is known. Such elaborate mutational analysis in the setting of type 1 VWD not only unequivocally confirms the diagnosis but also elucidates the underlying pathophysiological mechanism of the disorder, reveals recurrence risks in family members, and provides differential diagnosis from other mild bleeding disorders with overlapping clinical symptoms but different etiology,[8] hence providing the basis for proper future therapeutic management as well as genetic counselling.

Conflict of Interest Disclosure

The authors have nothing to disclose.

REFERENCES

1. Sadler JE, Budde U, Eikenboom JC, et al. Update on the pathophysiology and classification of von Willebrand disease: a report of the Subcommittee on von Willebrand Factor. *J Thromb Haemost.* 2006;4(10):2103–2114. doi:10.1111/j.1538-7836.2006.02146.x.
2. Cartwright A, Webster SJ, de Jong A, et al. Characterization of large in-frame von Willebrand factor deletions highlights differing pathogenic mechanisms. *Blood Adv.* 2020;4(13):2979–2990. doi:10.1182/bloodadvances.2018027813.
3. Leebeek FWG, Eikenbiim JCJ. Von Willebrand's disease. *N Engl J Med.* 2016;375(21):2067–2080.
4. Ng C, Motto DG, Di Paola J. Diagnostic approach to von Willebrand disease. *Blood.* 2015;125(13):2029–2037. doi:10.1182/blood-2014-08-528398.
5. Tosetto A, Rodeghiero F, Castaman G, et al. A quantitative analysis of bleeding symptoms in type 1 von Willebrand disease: results from a multicenter European study (MCMDM-1 VWD). *J Thromb Haemost.* 2006;4(4):766–773. doi:10.1111/j.1538-7836.2006.01847.x.
6. The European Association for Haemophilia and Allied Disorders. Von Willebrand factor variant database. http://www.vWF.group.shef.ac.uk/, Accessed June 22, 2022.
7. Goodeve AC. The genetic basis of von Willebrand disease. *Blood Rev.* 2010;24(3):123–134. doi:10.1016/j.blre.2010.03.003.
8. Atiq F, Boender J, van Heerde WL, et al. Importance of genotyping in von Willebrand disease to elucidate pathogenic mechanisms and variability in phenotype. *HemaSphere.* 2022;6(6):e718. doi:10.1097/HS9.0000000000000718.
9. Baronciani L, Goodeve A, Peyvandi F. Molecular diagnosis of von Willebrand disease. *Haemophilia.* 2017;23(2):188–197. doi:10.1111/hae.13175.
10. Sutherland MS, Cumming AM, Bowman M, et al. A novel deletion mutation is recurrent in von Willebrand disease types 1 and 3. *Blood.* 2009;114:1091–1098. doi:10.1182/blood-2008-08-173278.
11. Illumina DNA Prep with enrichment. (Document #1000000048041, v06), San Diego, CA: Illumina; April 2021.
12. James PD, Connell NT, Ameer B, et al. ASH ISTH NHF WFH 2021 guidelines on the diagnosis of von Willebrand disease. *Blood Adv.* 2021;5(1):280–300. doi:10.1182/bloodadvances.2020003265.
13. Lillicrap D. von Willebrand disease: advances in pathogenetic understanding, diagnosis, and therapy. *Hematology Am Soc Hematol Educ Program.* 2013;2013:254–260. doi:10.1182/asheducation-2013.1.254.
14. Yadegari H, Driesen J, Hass M, Budde U, Pavlova A, Oldenburg J. Large deletions identified in patients with von Willebrand disease using multiple ligation-dependent probe amplification. *J Thromb Haemost.* 2011;9(5):1083–1086. doi:10.1111/j.1538-7836.2011.04260.x.
15. Acquila M, Bottini F, DI Duca M, et al. Multiplex ligation-dependent probe amplification to detect a large deletion within the von Willebrand gene. *Haemophilia.* 2009;15(6):1346–1348.
16. Hampshire DJ, Goodeve AC. The molecular basis of von Willebrand disease: the under investigated, the unexpected and the overlooked. *Haematologica.* 2011;96(6):798–800. doi:10.3324/haematol.2011.046623.
17. Haberichter SL. von Willebrand factor propeptide: biology and clinical utility. *Blood.* 2015;126(15):1753–1761. doi:10.1182/blood-2015-04-512731.
18. Michiels JJ, Berneman Z, Gadisseur A, et al. Characterization of recessive severe type 1 and 3 von Willebrand Disease (VWD), asymptomatic heterozygous carriers versus bloodgroup O-related von Willebrand factor deficiency, and dominant type 1 VWD. *Clin Appl Thromb Hemost.* 2006;12(3):277–295. doi:10.1177/1076029606291401.
19. Leebeek FWG, Atiq F. How I manage severe von Willebrand disease. *Br J Haematol.* 2019;187(4):418–430. doi:10.1111/bjh.16186.

Downloaded from https://academic.oup.com/labmed/article/54/4/434/6873308 by guest on 24 February 2025

A Novel Homozygous Pathogenic Variant in *CYP11B1* in a Female Iranian Patient with 11B Hydroxylase Deficiency

Marziyeh Hoseinzadeh, MSc,[1] Newsha Molavi, MSc,[1] Mahnaz Norouzi, PhD,[1] Shahrzad Aghaei, PhD,[2] Mehrdad Zeinalian, MD, PhD,[1] Mahin Hashemipour, MD,[3] Mohammad Amin Tabatabaiefar, PhD[1,4,5]*

[1]Department of Genetics and Molecular Biology, School of Medicine, Isfahan University of Medical Sciences, Isfahan, Iran, [2]Department of Molecular Medicine, School of Advanced Technologies, Sahrekord University of Medical Sciences, Shahrekord, Iran, [3]Metabolic Liver Disease Research Center, Isfahan University of Medical Sciences, Isfahan, Iran, [4]Department of Pediatrics, School of Medicine, Isfahan University of Medical Sciences, Isfahan, Iran, [5]Pediatric Inherited Diseases Research Center, Research Institute for Primordial Prevention of Noncommunicable Disease, Isfahan University of Medical Sciences, Isfahan, Iran. *To whom correspondence should be addressed: tabatabaiefar@med.mui.ac.ir, tabatabaiefar@gmail.com.

Keywords: congenital adrenal hyperplasia (CAH), *CYP11B1* gene, 11β-hydroxylase deficiency (11βOHD), sequence analysis, homozygous, molecular docking

Abbreviations: CAH, congenital adrenal hyperplasia; 11βOHD, 11β-hydroxylase deficiency; 21-OHD, steroid 21-hydroxylase deficiency; ACTH, adrenocorticotropic hormone; DOC, deoxycorticosterone; HGMD, Human Gene Mutation Database; PCR, polymerase chain reaction; 3D, 3-dimensional; 17-OHP, serum 17-hydroxyprogesterone; ACMG, American College of Medical Genetics and Genomics; PDB, Protein Data Bank

Laboratory Medicine 2023;54:439-446; https://doi.org/10.1093/labmed/lmac141

ABSTRACT

Objective: Congenital adrenal hyperplasia (CAH) addresses a number of autosomal recessive disorders characterized by the enzyme defects in steroid hormones biosynthesis. The second common form of CAH is caused by mutations in the *CYP11B1* gene. Here, we reveal a novel mutation in the *CYP11B1* gene related to the 11βOHD phenotype.

Methods and Results: Sequence analysis of the *CYP11B1* gene in a 19-year-old Iranian woman with the 11βOHD phenotype was performed. In silico analysis and molecular docking were done. A novel missense homozygous variant c.1351C > T (p.L451F) in the *CYP11B1* gene was identified in the patient and, according to American College of Medical Genetics and Genomics criteria, was categorized as likely pathogenic. Protein docking showed destructive effects of the variant on the CYP11B1 protein-ligand interactions.

Conclusion: This study broadens the *CYP11B1* mutation spectrum and introduces the novel p.L451F likely pathogenic variant leading to destructive effects on protein-ligand interactions. Our results provide reliable information for genetic counseling and molecular diagnostics of CAH.

Congenital adrenal hyperplasia (CAH) is a group of genetic disorders associated with endocrine system dysfunction. CAH is inherited in an autosomal recessive manner and consists of various clinical phenotypes related to the aberrant function of specific genes. These include genes involved in cortisol biosynthesis pathways in the adrenal glands.[1–3] Pathogenic mutations of the *CYP21A2* gene account for more than 90% of CAH cases, leading to steroid 21-hydroxylase deficiency (21-OHD; OMIM: 201910).[2] The second common cause is related to 11β-hydroxylase deficiency (11βOHD; OMIM: 202010), due to *CYP11B1* gene mutations, which account for 5% to 8% of all cases.[4–7] The 11βOHD is characterized by a reduction in cortisol synthesis leading to an elevated plasma level of adrenocorticotropic hormone (ACTH) and accumulation of the steroid intermediates.[8] The 11βOHD is classified as a classic and nonclassic disease on the basis of phenotypic severity.[9] Androgen overproduction in classic 11βOHD is the main reason for virilization of external genitalia in females and peripheral precocious puberty in males.[9–14] Patients with nonclassic 11βOHD represent moderate clinical features with no abnormal manifestations at birth.[15] Hyperandrogenism can be observed in patients with 11βOHD at any age from infancy to early adulthood and, even later in life in some persons.[9]

The 11β-hydroxylase (*CYP11B1*, EC 1.14.15.4) is a P450 type I mitochondrial enzyme that catalyzes the hydroxylation of 11-deoxycortisol and deoxycorticosterone (DOC) to cortisol and corticosterone, respectively.[16] An 11β-hydroxylase dysfunction contributes to excessive steroid hormone intermediates production that shunts androgen synthesis pathways, resulting in 11βOHD presentation.[10] Overproduction of DOC, a less potent mineralocorticoid, activates mineralocorticoid receptors, referring to salt retention and hypertension. Hypertension is introduced as a differentiating clinical feature of 11βOHD from 21-OHD, observed in two-thirds of all cases.[9]

The 11β-hydroxylase encoding gene, *CYP11B1*, is located on chromosome 8q21 and contains 9 exons. To date, more than 100 different

© The Author(s) 2022. Published by Oxford University Press on behalf of American Society for Clinical Pathology.
All rights reserved. For permissions, please e-mail: journals.permissions@oup.com

Downloaded from https://academic.oup.com/labmed/article/54/4/439/6885678 by guest on 24 February 2025

pathogenic and likely pathogenic mutations have been reported in the *CYP11B1* gene based on the Human Gene Mutation Database (HGMD) and ClinVar database (www.hgmd.org, https://www.ncbi.nlm.nih.gov/clinvar/). These mutations, including frameshift, missense, nonsense, and splice site variants, have mainly been reported from exons 2, 6, 7, and 8, which are the hot spot regions of *CYP11B1*.[17–20]

The human genome encodes another 11β-hydroxylase isoenzyme, aldosterone synthase (P450c11Aldo), through the *CYP11B2* gene located 40 kb downstream of *CYP11B1*.[9,18] The *CYP11B2* and *CYP11B1* genes contain highly homologous sequences, with about 93% homology in the coding region and about 90% in introns, that cause a major challenge for routinely used molecular genetic diagnostic methods.[21,22] Indeed, homologous regions introduce complexity to discriminate calls from these sequences, hence different diagnostic approaches need to be refined to identify variants in *CYP11B2* and *CYP11B1* genes in homologous regions.[13,21]

Polymerase chain reaction (PCR)-based sequencing detection methods for entire gene regions are the most-used molecular genetic testing for *CYP11B1* mutation detection. The location and high rate of homology between these 2 genes increase the rate of misalignments that would result in reporting false variant calls due to the paucity of primers that would amplify *CYP11B1* without amplifying the highly homologous *CYP11B2*. However, PCR-based diagnoses have been refined with time, and gene fragments can be amplified while avoiding simultaneous amplification of homologous sequences, enabling direct DNA sequence analysis.[4,23] Although routine methods can reliably detect point mutations and small indel, they do not easily detect intragenic/intergenic deletion or the chimeric *CYP11B2/CYP11B1* gene, which are important causes of 11βOHD.[23,24]

Regarding the location and the presence of homologous sequences between *CYP11B1* and *CYP11B2* genes, genetic recombination and crossing over during meiotic reduction do occur. The chimeric *CYP11B2/CYP11B1* gene has been confirmed to be an actual cause of 11βOHD, mostly occurring in introns 2 and 6 of *CYP11B2*.[24–26] Because other molecular diagnosis tools such as multiplex ligation-dependent probe amplification have not been widely used in genetic laboratories, sequence analysis may be complicated by failure to identify the chimeric *CYP11B2/CYP11B1* gene, resulting in misdiagnosis. Therefore, to identify the genetic etiology in patients with signs of 11βOHD, it is crucial to consider alternative assays to sequence analysis for critical genes.[23,27]

The present study was launched by exploiting the combined strategy of phenotype-directed genotyping and hotspot exon prioritization to clarify the molecular basis of 11βOHD. We identified a novel likely pathogenic variant (*CYP11B1*:c.1351C > T) consistent with 11βOHD by using *CYP11B1* gene-specific primers. Proper bioinformatic tools and three-dimensional (3D) protein structure models predicted the destructive molecular consequences of this mutation on the human CYP11B1 protein.

Materials and Methods

Patient History

A family with an affected person was chosen for the study. The patient was a 19-year-old woman diagnosed with ambiguous genitalia at birth, and the standard 46, XX karyotype had confirmed the female genotype for her. She was diagnosed with characteristic 11βOHD based on typical hypertension, significant external genital virilization, and an elevated level of serum 17-hydroxyprogesterone (17-OHP). Her genital abnormality included clitoral enlargement, fusion of the labial folds, and a single opening of the urogenital sinus. At age 2, when she was admitted to the hospital due to hypertension and hypokalemia, a surgical operation was performed to correct the genital ambiguity. The patient received 2 years of regular treatments with amlodipine, prednisolone, spironolactone, and hydrocortisone. The review boards of Isfahan University of Medical Sciences approved this study (No.IR.MUI.MED.RE.1397.147), and written informed consent was obtained from the subject.

DNA Extraction, PCR Amplification, and Sanger Sequencing

The subject and family members underwent sampling of 5 mL peripheral blood in EDTA-containing complete blood count tubes. The DNA isolation was performed using a standard extraction protocol.[20] Quality control was completed using 1.2 % agarose gel. The *CYP11B1* gene primers (**TABLE 1**) were designed using Primer3 v.0.4.0 (http://bioinfo.ut.ee/primer3-0.4.0/) online web-based software and were blasted in NCBI primer blast for monitoring specificity and affinity. Nine exons and the flanking introns of the *CYP11B1* gene were specifically amplified in 7 fragments without amplification of homologous *CYP11B2* sequences. The PCR amplification was performed under the following conditions: 1 μL DNA (about 70 mg), 1 μL of each of the primers, 12.5 μL of 2X Master Mix (Ampliqon), 9.5 μL ddH2O; and the standard cycling condition for each applicant regarding its product size. The PCR products were sequenced (at first for hot spot exons of *CYP11B1* gene) bi-directionally on an automated Genetic Analyzer ABI 3130 (Applied Biosystems 3130), after quality control on the 1.2% agarose gel.

Nucleotide Sequence Analysis

The sequences were aligned to the reference sequence GenBank NM_000497 and NP_000488, using SeqMan software version 5.00 (DNASTAR) for coding variant calling. The National Heart, Lung, and Blood Institute Exome Sequencing Project (http://evs.gs.washington.edu/EVS/), Genome Aggregation Database (http://gnomad.broadinstitute.org**),** Genome Aggregation Database (gnomAD, https://gnomad.broadinstitute.org/), Iranome (http://www.iranome.ir/), and

TABLE 1. The Details of the Primers Used in This Study

Primer Sequence (3→5)	Primer Type	Product Size (bp)	Exon
TTTCCCCTGTCTACGCTCATGCACC	F	672	1
TCTTGCTGACTGCCCGGAACCTCTT	R		
GAAGTTAAGAGGTTCCGGGCAGT	F	479	2
GCAGACACGACCCCACGGA	R		
GAGGTGGTGCCAGACTTGGGGT	F	1098	3,4
CCTCAGACTTTGGTGCTGGGAGA	R		
GAAGTGCTGTCGCCCAACGCT	F	1025	5
GTGGGCGCCGTGTGACATTGG	R		
AGGACTCAGGGAAAGGGGTTTGG	F	927	6
ACCCAGAGAGTAGAGGAACACGC	R		
GTCCTTCTGCGCTCGGGGCTGCTT	F	677	7,8
ACCGGCTCTGCCCAGTCCAGGAAAC	R		
TGGACTGGGCAGAGCCGGTACTGGG	F	777	9
AGCCTGGAGCCAGCACTGGGAGGGA	R		

Downloaded from https://academic.oup.com/labmed/article/54/4/439/6885678 by guest on 24 February 2025

LOVD (www.lovd.nl) were investigated to identify the consequence of variants. Bioinformatics predictive tools, including Polyphen-2, SIFT, PROVEAN, Mutation Taster, PANTHER, and FATHMM, were applied to examine the novel variant pathogenicity. Variant nomenclature and interpretation were made according to the HGMD (www.hgmd.org) and American College of Medical Genetics and Genomics (ACMG) (www.acmg.net) rules, respectively.

Sequence Alignment and Molecular Modeling

Multiple sequence alignment was performed to compare the human CYP11B1 protein sequence with human CYP11B2, as well as rat, mouse, pig, bovine, and sheep CYP11B1 protein sequences, using CLUSTALW online software. The HEME ligand structure-data file was received from the ChEBI database (https://www.ebi.ac.uk/chebi/) and was converted to a Protein Data Bank (PDB) file using the online Simplified Molecular Input Line Entry System translator and a structure file generator (https://cactus.nci.nih.gov/translate/). The wild-type protein structure of the *CYP11B1* gene was taken from the Research Collaboratory for Structural Bioinformatics PDB (https://www.rcsb.org/).

The p. L451F mutation was applied in proteins using Discovery Studio software version 2017. The mutated protein 3D structure in the PDB file was taken from the swissmodel.expasy.org. After preparing ligand and macromolecules, docking parameters were set up, then AutoDock V. 4.2[21] was run for evaluating protein–ligand interaction, and the estimation of the binding energy of the ligand in the normal and mutant protein. Ultimately, the results were displayed in Context v0.98.6 software.

Results

Clinical Characteristics

The proband was 19 years old (46, XX). At birth, she was diagnosed with classical 11βOHD according to typical presentations of hypertension and severe external genitalia virilization. The 17-OHP and ACTH levels were also increased to 19 ng/mL (normal range for females: 0.9–2.28 ng/mL) and 360.7 pg/mL (normal range: 7.2–63.3 pg/mL), respectively. Genital examination showed severe external genitalia virilization featuring clitoromegaly, labial fusion, and urogenital sinus. She was subjected to genital correction surgery when she was taken to the hospital for hypertension (14/97 mm Hg) and hypokalemia (serum K+: 3.2 mEq/L, normal range: 3.5–5.5 mEq/L) at the age of 2 years. At the time of clinical examination, she had a weight of 61 kg, a height of 160 cm, and a body mass index of 23.8 kg/m^2. All family members, including both parents and her sister, were apparently healthy. Due to experiencing a growth spurt in her childhood, she could not reach the expected average height (165.3–180.5 cm) in adolescence, which was expected from her parental height. She experienced precocious puberty, and menarche had occurred spontaneously at the age of 11 years. At the time of the investigation, she presented with genital melanoderma, mild hirsutism, and secondary amenorrhea with no evidence of deepening voice or appearance of acne. Due to an effective response to medical interventions, normal sodium (serum NA+: 145 mEq/L, normal range: 135–145) and potassium (serum K+: 3.6–5.2 mmol/L, normal range: 3.5–5.5 nmol/L) levels were achieved, and her blood pressure was reduced to within the normal range (130/80 mm Hg). At the time of investigation, laboratory examination results showed 17OHP to be 7.37 ng/mL (normal range: 0.9–2.28 ng/mL) and serum ACTH was 83.3 pg/mL (normal range: 7.2–63.3 pg/mL).

CYP11B1 Mutational Analysis

Sequence analysis of *CYP11B1* exons led to the identification of a novel missense variant (c.1351C > T), which causes leucine-to-phenylalanine substitution (p. L451F). The variant, C to T transition, located in exon 8, was inherited in a homozygous manner in the proband (**FIGURE 1**). The variant was found to be co-segregating with the phenotype; both parents were heterozygous for the mutation, and her sister was normal homozygous. The variant was not found in the NCBI dbSNP human build 147, 1000 Genomes Project, Genome Aggregation Database, the NHLBI GO Exome Sequencing Project, HGMD, or the ClinVar database. Accessed information showed novelty and probable evidence for the damaging effect of the variant in the protein based on in silico predictive tools (**TABLE 2**). The sequence alignment against the reference sequence showed specific *CYP11B1* gene amplification without the production of *CYP11B2* amplicon.

Protein Docking

Multiple sequence alignment of the CYP11B1 protein from different species showed conservation of the L451 residue in human, rat, mouse, pig, bovine, and sheep (**FIGURE 2A**). The native and p.L451F mutant 3D spatial models, which are shown in **FIGURE 2**, indicated a larger size of F451 compared to L451 in the heme-binding peptide (**FIGURE 2B**). The ligand-binding energy of heme estimated –5.53 kcal/mol in the normal and –2.51 kcal/mol in the mutant protein. The comparison of the results suggested that the L451F variant in the CYP11B1 protein affects its structure and reduced the tendency of the ligand to the protein (**FIGURE 2**).

Discussion

Congenital adrenal hyperplasia, the most common etiology of adrenal insufficiency, is caused by the impairment of enzymatic activity in cortisol biosynthesis pathways from cholesterol.[28,29] A variety of symptoms characterize the clinical picture of CAH, depending on a specific enzyme defect that impairs cortisol production.[20] In particular, deleterious mutations in the *CYP11B1* gene cause inefficient adrenal 11ß-hydroxylase enzyme activity, resulting in decreased cortisol output encountered in 11βOHD.[30] The 11βOHD is the second most common form of CAH associated with androgen excess representations such as genital ambiguity, precocious puberty, and hypertension.[7,31] Hypertension, as a distinct clinical feature of 11βOHD, occurs in approximately two-thirds of cases.[7,9,29,32] To date, over 100 different *CYP11B1* pathogenic variants have been reported to affect the functional properties of the 11β-hydroxylase enzyme to varying degrees.[33] The majority of these variants are missense and nonsense mutations, but they also include deletions and insertions, splicing, and regulatory and complex rearrangements. Notably, all *CYP11B1* mutations, found in encoding regions of the *CYP11B1* gene, tend to cluster in exons 2, 6, 7, and 8.[3,34–37] Although in vitro studies have considered activity less than 5% for 11β-hydroxylase to be compatible with classic 11βOHD, the precise genotype-phenotype correlations of 11βOHD have not been completely defined.[19,35] Furthermore, 11βOHD diagnosis using common procedures, including next-generation sequencing and Sanger

Downloaded from https://academic.oup.com/labmed/article/54/4/439/6885678 by guest on 24 February 2025

FIGURE 1. **Mutational analysis of the *CYP11B1* gene. A, Location of L451F mutation in the *CYP11B1* gene. B, Family pedigree indicating autosomal recessive inheritance of congenital adrenal hyperplasia. The affected female has a homozygous variant and her parents were heterozygous (C). The electropherograms of this family representing the heterozygous state of the father and mother and the homozygous state of the patient for L451F variant. The unaffected daughter is a wild-type homozygote.**

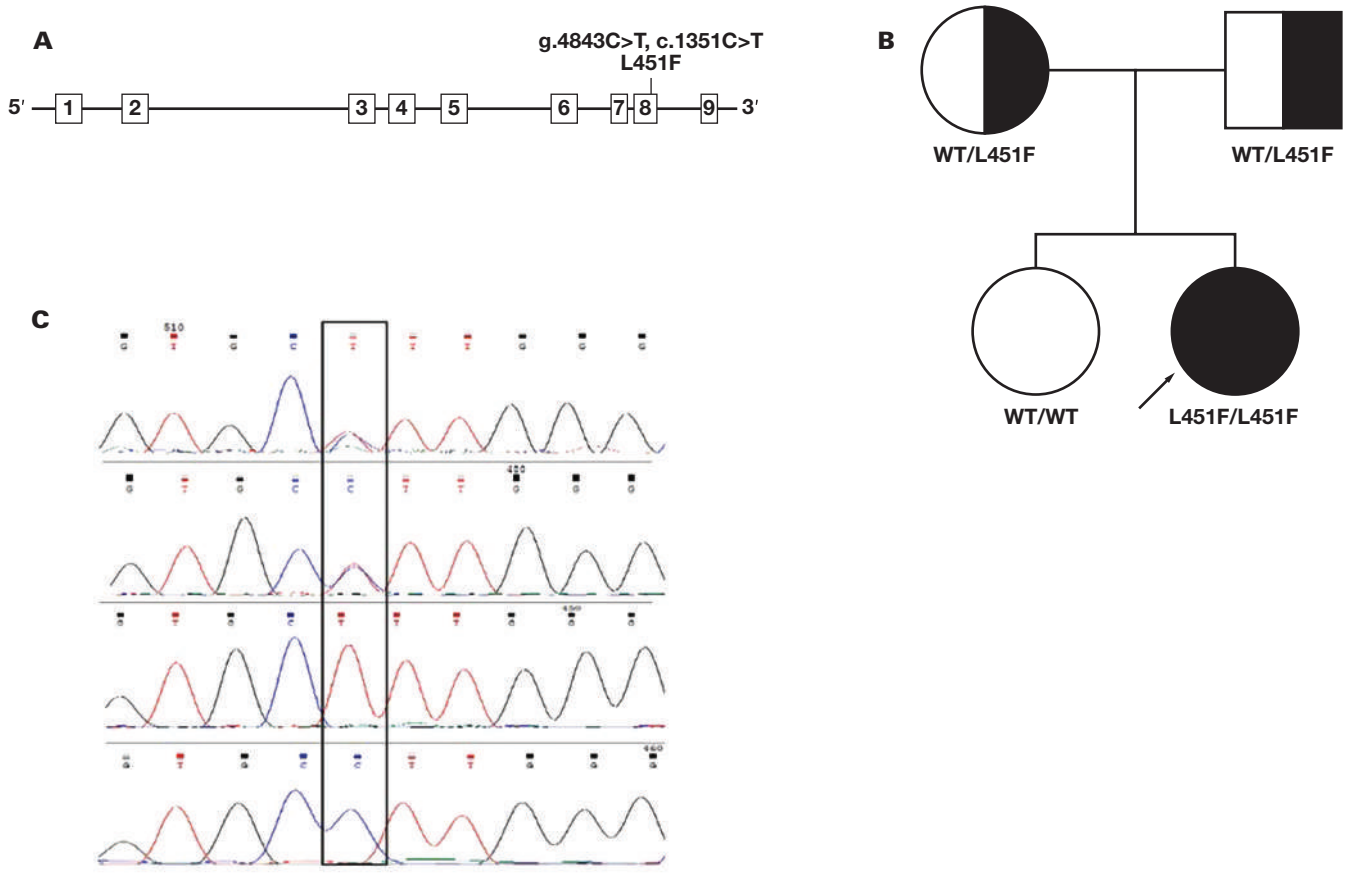

TABLE 2. **In Silico Pathogenicity Analysis**

Tool	Score	Prediction
MutationTaster2	NA	Disease-causing
PROVEAN	−2.99	Deleterious
SIFT	0.003	Damaging
Polyphen	0.998	Probably damaging

sequencing, encounters technical challenges due to the presence of homologous sequences and pseudogenes. These limitations are overcome through several approaches consisting of long-read sequencing (target enrichment) without the need for PCR amplification,[22,38] or amplification using allele-specific primers with long-range PCR or conventional PCR, followed by DNA sequencing of smaller fragments.[39]

We used a protocol involving the amplification of the *CYP11B1* gene in 7 overlapping fragments. Using specific primers designed to attach to the mismatch at the 3′ end, we prevented the amplification of the homologous gene, *CYP11B2*. By applying this strategy, a novel missense variant (c.1351C > T; p.L451F) in the *CYP11B1* gene was identified in an Iranian woman suspected of 11βOHD presenting with severe external genitalia virilization accompanied by hypertension. This variant has been reported neither in the literature nor in the public databases, including ClinVar, HGMD, LOVD, dbSNP, and gnomAD. Moreover, cosegregation analysis demonstrated the variant to be heterozygous in parents and homozygous in the patient. Furthermore, in silico analysis by using computational predicting tools supported the damaging effect of the variant (c.1351C > T) located at the mutational hotspot (HGMD; www.hgmd.org).[40-42] Therefore, all of the evidence supported by the patient's phenotype that was highly specific to the disease with a single genetic etiology led us to classify this variant as probably pathogenic, according to the ACMG-Association for Molecular Pathology variant interpretation guideline.[43]

The 11β-hydroxylase cytochrome P-450 enzyme, consisting of 503 amino acid residues, uses heme as a prosthetic group to catalyze redox reactions.[44,45] It has been demonstrated that amino acid substitutions in the heme-binding domain in this protein reduce enzyme activity partially or completely.[20,30] Previous studies demonstrated a high degree of conservation in the peptide surrounded heme-binding domain in all eukaryotic P450 enzymes.[20,44] In particular, the Cys450 residue, the fifth ligand of the heme iron atom, is completely conserved in all cytochrome P450 enzymes.[46,47] A missense variant in the *CYP11B1* gene surrounding the heme-binding peptide, Arg448His substitution, was the first reported mutation described in patients with classic 11βOHD. So far, 6 missense pathogenic and probable pathogenic variants have been reported adjacent to the Cys450 codon of the *CYP11B1* gene, suggesting that substitutions at these positions are poorly tolerated (**TABLE 3**).[3,34,48] Nevertheless,

Downloaded from https://academic.oup.com/labmed/article/54/4/439/6885678 by guest on 24 February 2025

FIGURE 2. **A 3D molecular model of *CYP11B1*. A, Location of L451 residue and heme in *CYP11B1* protein structure. Model of wild type *CYP11B1* (B) and mutant L451F (C) in the heme-binding environment. The larger size of F451 compared with L451 is clear. The binding energy in normal (D) and mutant (E) protein, obtained from Autodock software.**

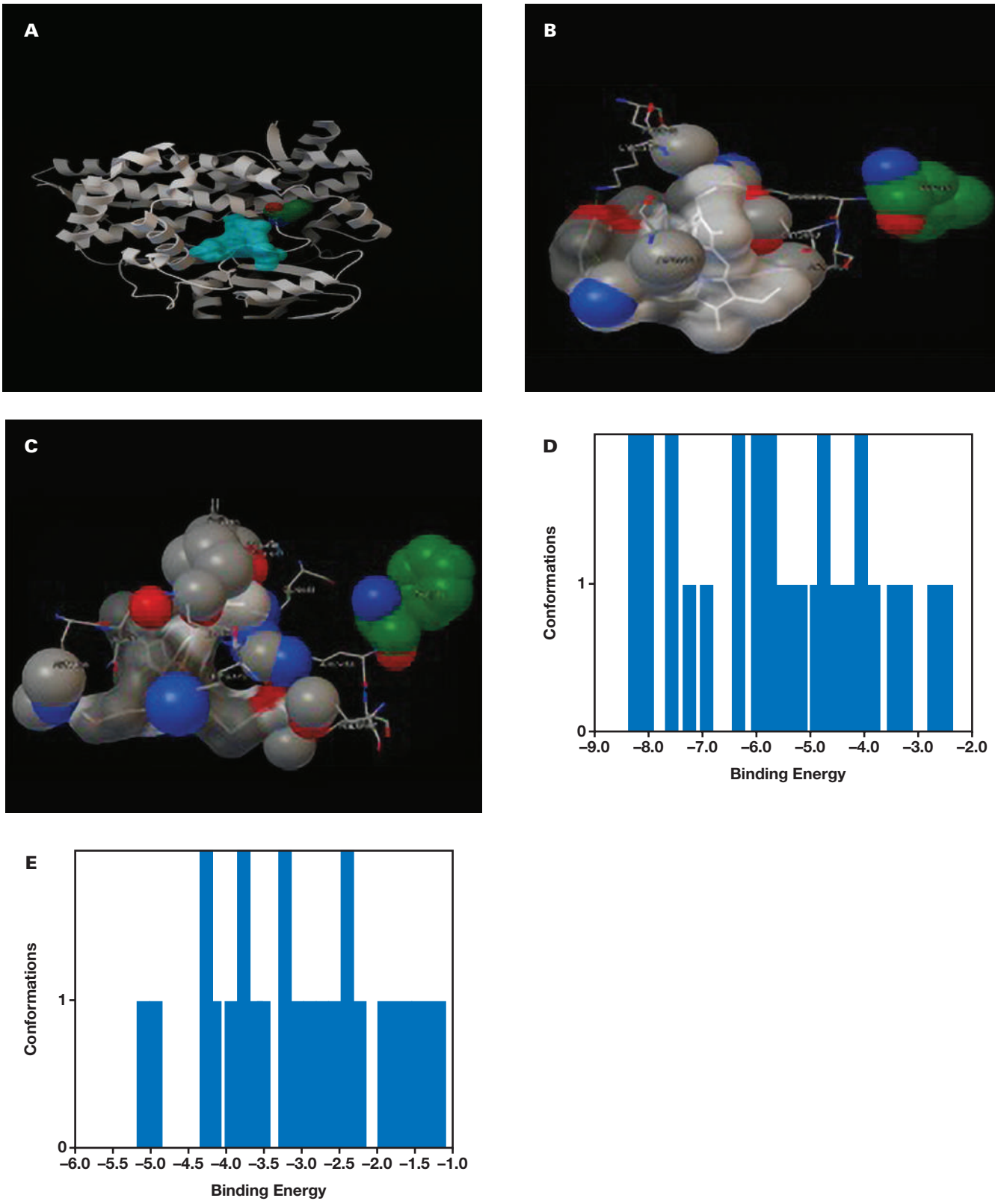

the association of 11βOHD disease with an exact amino acid change in leucine 451 has not been demonstrated previously. As we have shown with multiple sequence alignment (**FIGURE 3**), leucine 451 is a highly conserved residue in human, rat, mouse, pig, bovine, and sheep, located in a helix, where ligand binds to the protein.[3,34,49,50] A leucine 451 to phenylalanine substitution has been created in the helix, which is the core of

Downloaded from https://academic.oup.com/labmed/article/54/4/439/6885678 by guest on 24 February 2025

TABLE 3. Pathogenic/Likely Pathogenic Variants around L451 Location in *CYP11B1* Gene

Variant	Codon Number	Exon Number	Phenotype	Clinical Significance	Reference
p.Gly444Asp	444	8	Steroid-11β-hydroxylase deficiency	Pathogenic/Likely pathogenic	Motaghedi et al[31]
p.Arg448His	448	8	Steroid-11β-hydroxylase deficiency	Pathogenic/Likely pathogenic	White et al[46]
p.Arg453Gln	453	8	Adrenal hyperplasia	Pathogenic	Krone et al[41]
p.Arg454Cys	454	8	Steroid-11β-hydroxylase deficiency	Pathogenic	Ye et al[48]
p.Arg454His	454	8	Steroid-11β-hydroxylase deficiency	Likely pathogenic	Wang et al[42]
p.Leu461Pro	461	8	NA	Pathogenic	Chang et al[37]

FIGURE 3. Multiple protein sequence alignment of *CYP11B1* of human, rat, mouse, pig, bovine, sheep, and *CYP11B2* of human using CLUSTALW online site; 451 residues (leucine) in the specified box are conserved in all cases and the underlined amino acids in the *CYP11B1* sequence are related to the helix of the heme binding region.

the 11β-hydroxylase enzyme, and where the ligand binds to the protein[34]; therefore, this substitution could possibly alter the stability and affinity of this binding. Moreover, the same amino acid change in the corresponding position (L451F) has been reported as a pathogenic mutation in the homologous gene, *CYP11B2*, which causes aldosterone synthase deficiency.[51] Altogether, these data are suggestive of a critical structural and functional role for L451 in 11β-hydroxylase enzyme. For further evaluation, we used the AutoDock (V. 4.2) software to create a computational model of the mutant p. L451 protein. Estimated ligand-binding energy in the normal and mutant protein compared with the wild-type model of CYP11B1 as a template that demonstrates the destructive effects of L451F substitution on protein structure and ligand affinity (**FIGURE 2**).

Conclusions

In conclusion, a precise genetic diagnosis is essential to optimize patient management and treatment outcomes in patients suffering from CAH. In our patient, the identified homozygous *CYP11B1* gene variant was classified as a probable pathogenic consistent with clinical findings of the 11βOHD phenotype. This novel variant was located in a mutational hot spot in the vicinity of the heme-binding domain, which was predicted to disrupt enzyme activity using molecular docking. Further functional and structural studies may provide more support to this variant pathogenicity. Analysis of this new mutation and other known mutations should be applied to high-risk families and consanguineous marriages for early diagnosis and neonatal screening followed by proper biochemical and molecular tests for diagnosis and treatment of 11βOHD. Furthermore, the cost-effective approach we used in this study can be used to establish 11βOHD molecular diagnostics strategies in our country (Iran).

Acknowledgments

We thank all individuals who participated in this study.

Funding

This work was supported by the Isfahan University of Medical Science (grant numbers 397356, 397111, and 197060).

Conflict of Interest Disclosure

The authors have nothing to disclose.

REFERENCES

1. Ellaithi M, de LaPiscina IM, de La Hoz AB, et al. Simple virilizing congenital adrenal hyperplasia: a case report of sudanese 46, XY DSD male with G293D variant in CYP21A2. *Open Pediatr Med J.* 2019;9:7–11. doi:10.2174/1874309901909010007.
2. Wu C, Zhou Q, Wan L, et al. Novel homozygous p. R454C mutation in the CYP11B1 gene leads to 11β-hydroxylase deficiency in a Chinese patient. *Fertil Steril.* 2011;95(3):1122.e3-6–. doi:10.1016/j.fertnstert.2010.09.035.
3. Nimkarn S, New MI. Steroid 11β-hydroxylase deficiency congenital adrenal hyperplasia. 2008;19:96-9. *Trends Endocrinol Metab.* 2008;19(3):96–99. doi:10.1016/j.tem.2008.01.002.
4. Kandemir N, Yilmaz DY, Gonc EN, et al. Novel and prevalent CYP11B1 gene mutations in Turkish patients with 11-β hydroxylase deficiency. *J Steroid Biochem Mol Biol.* 2017;165:(pt A)57–63. doi:10.1016/j.jsbmb.2016.03.006.
5. New MI, White PC. Genetic disorders of steroid hormone synthesis and metabolism. *Baillieres Clin Endocrinol Metab.* 1995;9(3):525–554. doi:10.1016/s0950-351x(95)80587-7.
6. Nguyen H-H, Eiden-Plach A, Hannemann F, et al. Phenotypic, metabolic, and molecular genetic characterization of six patients with congenital adrenal hyperplasia caused by novel mutations in the CYP11B1 gene. *Biochem Mol Biol.* 2016;155 (pt A):126–134. doi:10.1016/j.jsbmb.2015.10.011.
7. White PC, Curnow KM, Pascoe L. Disorders of steroid 11β-hydroxylase isozymes. *Endocr Rev.* 1994;15(4):421–438. doi:10.1210/edrv-15-4-421.
8. Riedl S, Nguyen H-H, Clausmeyer S, Schulze E, Waldhauser F, Bernhardt R. A homozygous L299P mutation in the CYP11B1 gene leads to complete virilization in 46, XX individuals with 11-beta-hydroxylase deficiency. *Horm Res.* 2008;70(3):145–149. doi:10.1159/000137659.
9. Bulsari K, Falhammar H. Clinical perspectives in congenital adrenal hyperplasia due to 11β-hydroxylase deficiency. *Endocrine.* 2017;55(1):19–36. doi:10.1007/s12020-016-1189-x.
10. Alqahtani MA, Shati AA, Zou M, et al. A novel mutation in the CYP11B1 gene causes steroid 11β-hydroxylase deficient congenital adrenal hyperplasia with reversible cardiomyopathy. *Int J Endocrinol.* 2015;2015:595164. doi:10.1155/2015/595164.
11. Rösler A, Leiberman E, Cohen T. High frequency of congenital adrenal hyperplasia (classic 11β-hydroxylase deficiency) among Jews from Morocco. *Am J Med Genet.* 1992;42(6):827–834. doi:10.1002/ajmg.1320420617.
12. Oberman AS, Flatau E, Luboshitzky R. Bilateral testicular adrenal rests in a patient with 11-hydroxylase deficient congenital

Downloaded from https://academic.oup.com/labmed/article/54/4/439/6885678 by guest on 24 February 2025

adrenal hyperplasia. *J Urol.* 1993;149(2):350–352. doi:10.1016/s0022-5347(17)36079-2.

13. Charfeddine IB, Riepe FG, Kahloul N, et al. Two novel CYP11B1 mutations in congenital adrenal hyperplasia due to steroid 11β hydroxylase deficiency in a Tunisian family. *Gen Comp Endocrinol.* 2012;175(3):514–518. doi:10.1016/j.ygcen.2011.12.017.
14. Joehrer K, Geley S, Strasser-Wozak EM, et al. CYP11B1 mutations causing non-classic adrenal hyperplasia due to 11β-hydroxylase deficiency. *Hum Mol Genet.* 1997;6(11):1829–1834. doi:10.1093/hmg/6.11.1829.
15. Zhang M, Liu Y, Sun S, et al. A prevalent and three novel mutations in CYP11B1 gene identified in Chinese patients with 11-beta hydroxylase deficiency. *J Steroid Biochem Mol Biol.* 2013;133:25–29. doi:10.1016/j.jsbmb.2012.08.011.
16. Turcu AF, Nanba AT, Auchus RJ. The rise, fall, and resurrection of 11-oxygenated androgens in human physiology and disease. *Horm Res Paediatr.* 2018;89(5):284–291. doi:10.1159/000486036.
17. Stenson PD, Ball E, Howells K, Phillips A, Mort M, Cooper DN. Human gene mutation database: towards a comprehensive central mutation database. *J Med Genet.* 2008;45(2):124–126. doi:10.1136/jmg.2007.055210.
18. Abbaszadegan MR, Hassani S, Vakili R, et al. Two novel mutations in CYP11B1 and modeling the consequent alterations of the translated protein in classic congenital adrenal hyperplasia patients. *Endocrine.* 2013;44(1):212–219. doi:10.1007/s12020-012-9861-2.
19. Parajes S, Loidi L, Reisch N, et al. Functional consequences of seven novel mutations in the CYP11B1 gene: four mutations associated with nonclassic and three mutations causing classic 11β-hydroxylase deficiency. *J Clin Endocrinol Metab.* 2010;95(2):779–788. doi:10.1210/jc.2009-0651.
20. Menabo S, Polat S, Baldazzi L, et al. Congenital adrenal hyperplasia due to 11-beta-hydroxylase deficiency: functional consequences of four CYP11B1 mutations. *Eur J Hum Genet.* 2014;22(5):610–616. doi:10.1038/ejhg.2013.197.
21. Mandelker D, Schmidt RJ, Ankala A, et al. Navigating highly homologous genes in a molecular diagnostic setting: a resource for clinical next-generation sequencing. *Genet Med.* 2016;18(12):1282–1289. doi:10.1038/gim.2016.58.
22. Cheetham SW, Faulkner GJ, Dinger ME. Overcoming challenges and dogmas to understand the functions of pseudogenes. *Nat Rev Genet.* 2020;21(3):191–201. doi:10.1038/s41576-019-0196-1.
23. Xie H, Yin H, Ye X, et al. Detection of small CYP11B1 deletions and one founder chimeric CYP11B2/CYP11B1 gene in 11β-hydroxylase deficiency. *Front Endocrinol.* 2022;24(13):882863. doi:10.3389/fendo.2022.882863.
24. Kuribayashi I, Nomoto S, Massa G, et al. Steroid 11-beta-hydroxylase deficiency caused by compound heterozygosity for a novel mutation, p. G314R, in one CYP11B1 allele, and a chimeric CYP11B2/CYP11B1 in the other allele. *Horm Res.* 2005;63(6):284–293. doi:10.1159/000087074.
25. Krone N, Arlt W. Genetics of congenital adrenal hyperplasia. *Best Pract Res Clin Endocrinol Metab.* 2009;23(2):181–192. doi:10.1016/j.beem.2008.10.014.
26. Portrat S, Mulatero P, Curnow KM, Chaussain J-L, Morel Y, Pascoe L. Deletion hybrid genes, due to unequal crossing over between CYP11B1 (11β-hydroxylase) and CYP11B2 (aldosterone synthase) cause steroid 11β-hydroxylase deficiency and congenital adrenal hyperplasia. *J Clin Endocrinol Metab.* 2001;86(7):3197–3201. doi:10.1210/jcem.86.7.7671.
27. MacKenzie SM, Davies E, Alvarez-Madrazo S. Analysis of the aldosterone synthase (CYP11B2) and 11β-hydroxylase (CYP11B1) genes. *Methods Mol Biol.* 2017;1527:139–150. doi:10.1007/978-1-4939-6625-7_11.
28. Sumińska M, Bogusz-Górna K, Wegner D, Fichna M. Non-classic disorder of adrenal steroidogenesis and clinical dilemmas in 21-hydroxylase deficiency combined with backdoor androgen pathway: mini-review and case report. *Int J Mol Sci .* 2020;21(13):4622. doi:10.3390/ijms21134622.
29. Zhou Q, Wang D, Wang C, et al. Clinical and molecular analysis of four patients with 11β-hydroxylase deficiency. *Front Pediatr.* 2020;24(8):410. doi:10.3389/fped.2020.00410. eCollection 2020.
30. Shammas C, Byrou S, Phelan MM, et al. Genetic screening of non-classic CAH females with hyperandrogenemia identifies a novel CYP11B1 gene mutation. *Hormones.* 2016;15(2):235–242. doi:10.14310/horm.2002.1651.
31. Motaghedi R, Betensky B, Slowinska B, et al. Update on the prenatal diagnosis and treatment of congenital adrenal hyperplasia due to 11β-hydroxylase deficiency. *J Pediatr Endocrinol Metab.* 2005;18(2):133–142. doi:10.1515/jpem.2005.18.2.133.
32. Peter M, Dubuis J-M, Sippell W. Disorders of the aldosterone synthase and steroid 11β-hydroxylase deficiencies. *Horm Res Paediatr.* 1999;51(5):211–222.
33. Yuan X, Lu L, Chen S, et al. A Chinese patient with 11β-hydroxylase deficiency due to novel compound heterozygous mutation in CYP11B1 gene: a case report. *BMC Endocr Disord.* 2018;18(1):68. doi:10.1186/s12902-018-0295-6.
34. Chabraoui L, Abid F, Menassa R, Gaouzi A, El Hessni A, Morel Y. Three novel CYP11B1 mutations in congenital adrenal hyperplasia due to steroid 11beta-hydroxylase deficiency in a Moroccan population. *Horm Res Paediatr.* 2010;74(3):182–189. doi:10.1159/000281417.
35. Gu C, Tan H, Yang J, Lu Y, Ma Y. Congenital adrenal hyperplasia due to 11-hydroxylase deficiency—compound heterozygous mutations of a prevalent and two novel CYP11B1 mutations. *Gene.* 2017;30(626):89–94. doi:10.1016/j.gene.2017.05.029.
36. Matallana-Rhoades AM, Corredor-Castro JD, Bonilla-Escobar FJ, Mecias-Cruz BV, Beldjena LM. Congenital adrenal hyperplasia due to 11-beta-hydroxylase deficiency: description of a new mutation, R384X. *Colomb Méd.* 2016;47(3):172–175. PMID: 27821898.
37. Chang S-H, Lee H-H, Wang P-J, Chen J-H, Chu S-Y. Congenital adrenal hyperplasia with 11β-hydroxylase deficiency. *J Formos Med Assoc.* 2004;103(11):860–864. PMID: 15549155.
38. Gulilat M, Lamb T, Teft WA, et al. Targeted next generation sequencing as a tool for precision medicine. *BMC Med Genomics.* 2019;12(1):81.
39. Lee H-H. Mutational analysis of CYP21A2 gene and CYP21A1P pseudogene: long-range PCR on genomic DNA. *Methods Mol Biol.* 2014;1167:275–287. doi:10.1007/978-1-4939-0835-6_19.
40. Geley S, Kapelari K, Jöhrer K, et al. CYP11B1 mutations causing congenital adrenal hyperplasia due to 11 beta-hydroxylase deficiency. *J Clin Endocrinol Metab.* 1996;81(8):2896–2901. doi:10.1210/jcem.81.8.8768848.
41. Krone N, Grötzinger J, Holterhus P-M, Sippell WG, Schwarz H-P, Riepe FG. Congenital adrenal hyperplasia due to 11-hydroxylase deficiency–insights from two novel CYP11B1 mutations (p. M92X, p. R453Q). *Horm Res Paediatr.* 2009;72(5):281–286.
42. Wang X, Nie M, Lu L, Tong A, Chen S, Lu Z. Identification of seven novel CYP11B1 gene mutations in Chinese patients with 11β-hydroxylase deficiency. *Steroids.* 2015;100:11–16. doi:10.1016/j.steroids.2015.04.003.
43. Richards S, Aziz N, Bale S, et al. Standards and guidelines for the interpretation of sequence variants: a joint consensus recommendation of the American College of Medical Genetics and Genomics and the Association for Molecular Pathology. *Genet Med.* 2015;17(5):405–424. doi:10.1038/gim.2015.30.
44. Belkina N, Lisurek M, Ivanov A, Bernhardt R. Modelling of three-dimensional structures of cytochromes P450 11B1 and 11B2. *J Inorg Biochem.* 2001;87:197–207. doi:10.1016/s0162-0134(01)00331-2.
45. Kawamoto T, Mitsuuchi Y, Ohnishi T, et al. Cloning and expression of a cDNA for human cytochrome P-450aldo as related to primary aldosteronism. *Biochem Biophys Res Commun.* 1990;173(1):309–316. doi:10.1016/s0006-291x(05)81058-7.
46. White PC, Dupont J, New MI, Leiberman E, Hochberg Z, Rösler A. A mutation in CYP11B1 (Arg-448----His) associated with steroid 11

Downloaded from https://academic.oup.com/labmed/article/54/4/439/6885678 by guest on 24 February 2025

beta-hydroxylase deficiency in Jews of Moroccan origin. *J Clin Invest.* 1991;87(5):1664–1667. doi:10.1172/JCI115182.

47. Peter M. Congenital adrenal hyperplasia: 11beta-hydroxylase deficiency. *Semin Reprod Med.* 2002;20(3):249–254. doi:10.1055/s-2002-35389.
48. Z-q YE, Zhang M-n, Zhang H-j, Jiang J-j, X-y LI, Zhang K-q. A novel missense mutation, GGC (Arg454)→ TGC (Cys), ofCYP11B1gene identified in a Chinese family with steroid 11β-hydroxylase deficiency. *Chin Med J.* 2010;123:1264–1268. PMID: 20529578.
49. Doss CGP, Rajith B, Chakraboty C, et al. In silico profiling and structural insights of missense mutations in RET protein kinase domain by molecular dynamics and docking approach. *Mol Biosyst.* 2014;10(3):421–436. doi:10.1039/c3mb70427k.
50. Riahi A, Messaoudi A, Mrad R, Fourati A, Chabouni-Bouhamed H, Kharrat M. Molecular characterization, homology modeling and docking studies of the R2787H missense variation in BRCA2 gene: association with breast cancer. *J Theor Biol.* 2016;403:188–196. doi:10.1016/j.jtbi.2016.05.013.
51. Nguyen HH, Nguyen TH, Vu CD, Nguyen KT, Le BV, Nguyen TL. Novel homozygous p. Y395X mutation in the CYP11B1 gene found in a Vietnamese patient with 11β-hydroxylase deficiency. *Gene.* 2012;509:295–297. doi:10.1016/j.gene.2012.08.009.

Downloaded from https://academic.oup.com/labmed/article/54/4/439/6885678 by guest on 24 February 2025

SCIENCE

Imbalance of Circulating Monocyte Subsets in Subjects with Newly Emerged and Recurrent Hospital-Acquired Pneumonia

Yu-jia Jin, BS,[1,3] Yu Shen, BS,[2,3] Yi-fan Jin, BS,[1,3] Jia-wei Zhai, BS,[1] Yao-xin Zhang, MS,[1] Pan-pan Xu, BS,[1] Cheng Chen, PhD,[1] Qiu-xia Qu, PhD[2,#]

[1]Department of Respiratory and Critical Medicine, First Affiliated Hospital of Soochow University, Suzhou, 215000, China, [2]Jiangsu Key Laboratory of Clinical Immunology, Soochow University, Suzhou, 215000, China. [#]To whom correspondence should be addressed. quqiuxia81@163.com. [3]Yu-jia Jin, Yu Shen, and Yi-fan Jin contributed equally and were regarded as co-first authors.

Keywords: monocyte, HAP, PD-L1, pathogen, immunity, recurrent

Abbreviations: HAP, hospital-acquired pneumonia; NC, nonclassical; ITM, intermediate; CL, classical; PD-L1, programmed death ligand 1; ICU, intensive care unit; COPD, chronic obstructive pulmonary disease; SOFA, sequential organ failure assessment; PCT, procalcitonin; ATS/ERS, American Thoracic Society/European Respiratory Society; new-HAP, newly emerged HAP; re-HAP, recurrent HAP; FSC, forward scatter; SSC, side scatter; K.p, Klebsiella pneumonia; PD-1, programmed cell death receptor-1.

Laboratory Medicine 2023;54:e100–e107; https://doi.org/10.1093/labmed/lmac133

ABSTRACT

Objective: Hospital-acquired pneumonia (HAP) is one of the most common diseases in the intensive care unit, where the development of disease is closely related with the host immune response. Monocytes play an important role in both innate and adaptive immune system. We aimed to investigate the changes of circulating monocyte subsets in subjects with HAP to explore its value in monitoring HAP.

Methods: In total, 60 HAP patients and 18 healthy individuals were enrolled in this study. Human monocyte subsets are classified into 3 groups: nonclassical (NC), intermediate (ITM), and classical (CL). Also, programmed death ligand 1 (PD-L1) expression on circulating monocyte subsets was measured by flow cytometry.

Results: Data showed that the ratio of NC, ITM, and CL among monocytes was comparable between HAP patients and healthy controls ($P > .05$). There was a remarkable imbalance of NC and CL in newly emerged HAP compared to healthy controls ($P < .05$), subsequently reaching normalization in recurrent HAP ($P > .05$). Furthermore, although PD-L1 was seemly constitutively expressed by NC, ITM, and CL groups regardless of disease status, it was noted that PD-L1 was dominantly expressed in the CL group ($P < .05$).

Conclusion: Given distinct PD-L1 expression, a shift of CL/NC in newly emerged HAP would constitute an inhibitory anti-pathogen immune response. Normalization of circulating monocyte subsets on recurrence of HAP might be the consequence of immune memory of bacterial infection.

Bacterial pneumonia is mainly caused by microbial components that transfer from the upper to the lower respiratory tract. Various innate immune cells move to the first line in defense against pathogens when the lower respiratory tract is exposed to the microorganisms.[1]

Monocytes play an important role in both the innate and adaptive immune systems, which are highly skilled in immune defense, inflammation, and tissue remodeling.[2] Recently, human monocyte subsets have been classified into three types: nonclassical (NC) (CD14-CD16+), intermediate (ITM) (CD14 + CD16+) and classical (CL) (CD14 + CD16-).[3] Changes in monocyte counts have been observed in chronic obstructive pulmonary disease (COPD) and have proven to be associated with unfavorable outcome.[4,5] It has also been demonstrated that ITM monocytes are correlated with disease progression in idiopathic pulmonary fibrosis, and absolute circulating counts of NC and CL are greatly increased in Gram-negative sepsis.[3]

Hospital-acquired pneumonia (HAP) is one of the most common intensive care unit (ICU)-acquired infections.[6] Intubation and mechanical ventilation are widely used to rescue patients in ICU, where bacterial colonization is often found and pathogens interfere with normal host defense mechanisms through persistent activation of the immune response.[1] Currently, little is known about monocyte subsets during bacterial infections for patients with HAP. Here, we aimed to investigate the

© The Author(s) 2022. Published by Oxford University Press on behalf of American Society for Clinical Pathology. All rights reserved. For permissions, please e-mail: journals.permissions@oup.com

Downloaded from https://academic.oup.com/labmed/article/54/4/e100/6758541 by guest on 24 February 2025

changes of circulating monocyte subsets in subjects with HAP to explore its value in the monitoring to HAP.

Materials and Methods

Study Participants

A total of 60 patients diagnosed with HAP from August 2019 to November 2021 in the First Affiliated Hospital of Soochow University and 18 healthy individuals were enrolled in this study. Diagnosis of HAP was established according to the American Thoracic Society/European Respiratory Society (ATS/ERS) standards. Patients with HAP who had comorbidities of COPD, progressive malignant diseases, and autoimmune diseases were excluded from the study. The study was approved by the Ethics Committee of the Institute of the First Affiliated Hospital of Soochow University (2019-070).

Data Collection

The clinical data of all patients was collected from an electronic medical record and included the following: subject characteristics (age, gender, and underlying diseases), clinic status, and therapeutic response. The sequential organ failure assessment (SOFA) score was calculated according to the worst laboratory examinations before inclusion. The sputum or bronchoalveolar lavage fluid samples were collected from patients for microbiological examination. Procalcitonin (PCT) was measured using B.R.A.H.M.S. PCT automated immunoassays.

Study Design

The subjects with HAP were divided into different cohorts, including well-controlled/progressive, SOFA < 3 or ≥ 3 scores, non-Enterobacter/Enterobacter infection, PCT < 2/ or ≥ 2 (ng/mL) and newly emerged/recurrent HAP.

Definition

Newly emerged HAP (new-HAP) was required to meet the following criteria: (i) ATS/ERS standards of HAP[7] and (ii) a new episode of pneumonia. Recurrent HAP (re-HAP) was required to meet the following criteria: (i) ATS/ERS standards of HAP and (ii) recurrence defined as a discrete episode of pneumonia separated by at least a 1-month asymptomatic interval, a radiographic clearing of the acute infiltrate, or both.[8]

Progressive HAP was defined as clinical deterioration such as respiratory failure requiring mechanical ventilation or septic shock after 72 hours of treatment.[9]

Flow Cytometry Analysis

A total of 5 mL of peripheral blood sample from each subject was collected into an anti-coagulant tube. Peripheral blood mononuclear cells strained with anti-CD56-PECF594 (clone 5.1H11), anti-CD14-PE (clone 63D3), anti-CD16-FITC (clone 3G8), anti-PD-L1-PC7 (clone 29E_2A3) were incubated for 30 min at room temperature in the dark. Antibodies were purchased from Biolegend (USA). Monocytes were first gated by forward scatter (FSC) and side scatter (SSC); CD56 + cells were then gated out. Monocyte subsets were further identified by CD14 + and CD16 + staining.[4,10] All data were analyzed using Flowjo 10 software. The populations of NC, ITM, and CL as a percentage of total monocytes were calculated from the plot. The expression of programmed death ligand 1 (PD-L1) was assessed by plotting it versus the given NC, ITM, and CL monocyte. A fluorescence activated cell sorter Calibur flow cytometer was used for analyzing the samples.

Statistical Analysis

Statistical analysis were performed using SPSS 25.0. The ratios of NC, ITM, and CL in this study were expressed as medians (25th to 75th percentile range), which were not normally distributed. The Mann-Whitney U test was used for analyzing all data. Spearman's correlation analysis was used to assess the correlation between PCT value and ratio of monocyte subsets. A *P*-value of less than .05 was considered statistically significant.

Results

Patient Characteristics

The baseline subject characteristics are summarized in **TABLE 1**. From August 2019 to November 2021, a total of 60 patients were included in our study, including 44 men and 16 women, with ages ranging from 21 to 92 years. Patients had underlying diseases including cerebral stroke (n = 33), cardiac disease (n = 18), and diabetes (n = 14). A total of 18 healthy volunteers were recruited as controls.

Circulating Monocyte Subsets Between HAP Patients and Healthy Controls

In humans, NC and ITM monocytes emerged from matured CL, which displayed dynamical differentiation in the monocyte pool.[11] In this study, NC, ITM, and CL were identified according to the different expression of CD14 and CD16 (**FIGURE 1**). First, we compared circulating monocyte subsets between patients with HAP and healthy controls. As shown in **FIGURE 2A**, the ratios of 3 monocyte subsets defined by CD14 and CD16 antibody staining did not show significant difference between these 2 groups ($P > .05$).

Circulating Monocyte Subsets and Clinic Severity

Study patients were divided into well-controlled (n = 26) and progressive (n = 34) groups according to prior clinic therapeutic response. As shown in **FIGURE 2B**, the ratios of the 3 circulating monocyte subsets were compared between these 2 cohorts. Although the ratio of ITM was higher in the well-controlled cohort than that in the progressive

TABLE 1. Subject Characteristics

Characteristic	n = 60
Age (years)	21–92
≥65	43
<65	17
Gender	
male	44
female	16
Underlying diseases	
Diabetes	14
Cerebral stroke	33
Cardiac disease	18

Downloaded from https://academic.oup.com/labmed/article/54/4/e100/6758541 by guest on 24 February 2025

FIGURE 1. The gating strategy of monocyte subsets in flow cytometry. Monocytes were gated on an FSC/SSC dot plot (A). Gating out of CD56 + cells (B) and CD14-CD16- cells (C), NC, ITM, and CL were identified on a CD14/CD16 dot plot (D). Representative dot plots and density plots are shown. FSC, forward scatter; SSC, side scatter; NC, nonclassical; ITM, intermediate; CL, classical.

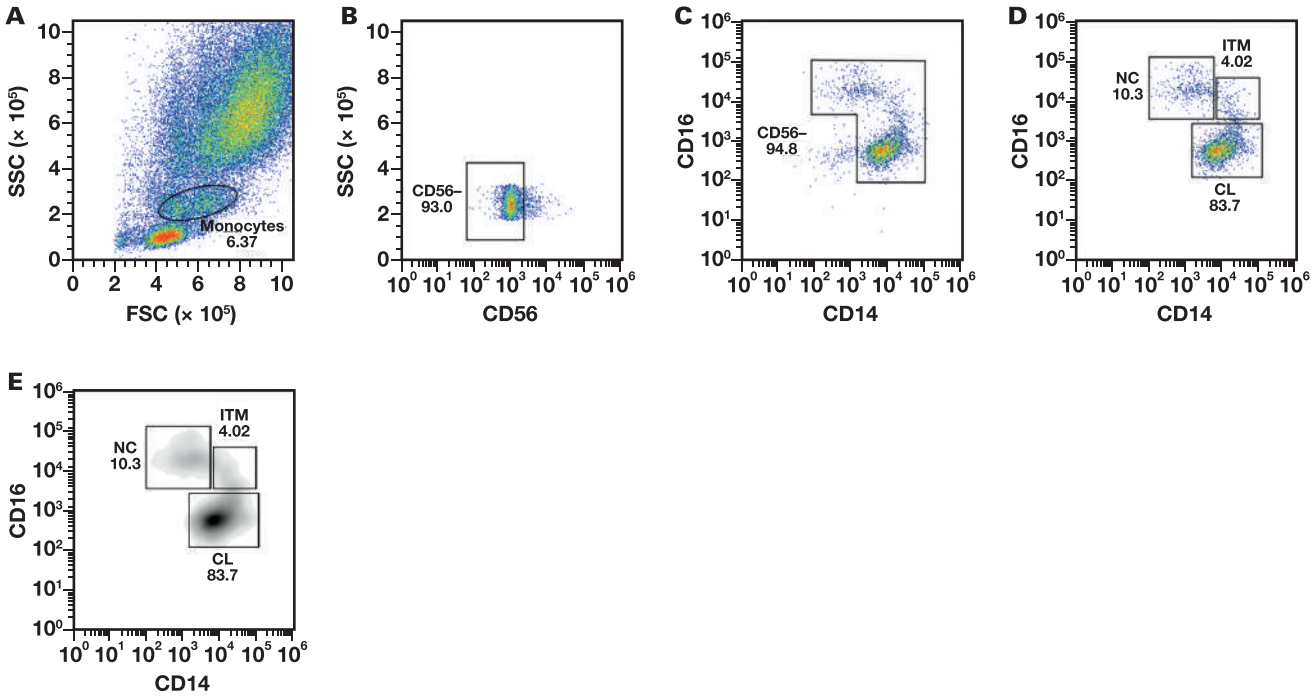

group, (4.96% [2.75, 9.13] vs 3.23% [1.67, 5.85], $P < .05$), no significant differences in the ratio of NC and CL between the 2 cohorts were observed ($P > .05$).

The SOFA scores were used to assess the severity of disease. We divided patients into < 3 and ≥ 3 groups according to their SOFA score. As shown in **FIGURE 2C**, no significant differences in the ratios of NC, ITM and CL among monocytes were observed between the 2 groups ($P > .05$).

Circulating Monocyte Subsets and Infectious Pathogen

We then investigated whether there was imbalance of circulating monocyte subsets correlating to specific infectious pathogens. A total of 53 pathogenic bacteria were detected in 60 subjects with HAP, of which 22 cases were Enterobacter infection, including *Klebsiella pneumoniae* (K.p) (n = 17), *Escherichia coli* (n = 3), *Proteus mirabilis* (n = 1), and *Serratia marcescens* (n = 1). The remaining 31 cases were non-Enterobacter, including *Acinetobacter baumannii* (n = 12), *Pseudomonas maltophilia* (n = 3), *Pseudomonas aeruginosa* (n = 7), *Pseudomonas cepacia* (n = 1), *Candida albicans* (n = 7), and *Elizabethkingia meningosepticum* (n = 1). As shown in **FIGURE 2D**, ratios of circulating NC, ITM, and CL among monocytes did not achieve statistical significance between the Enterobacter and non-Enterobacter groups ($P > .05$).

Circulating Monocyte Subsets and PCT Levels

Procalcitonin has proven to be a highly sensitive and specific biomarker to diagnose serious bacterial infections and inform clinicians of disease severity.[12,13] We expanded the investigation to include circulating monocyte subsets and PCT values. First, patients were divided by PCT value into < 2 (n = 14) and ≥ 2 (n = 44) (ng/mL) groups. As shown in **FIGURE 3A**, the ratios of NC, ITM, and CL among monocyte between these 2 subgroups were not statistically significant ($P > .05$).

The correlations between PCT value and the ratio of NC, ITM, and CL were determined using a Spearman's correlation analysis. As shown in **FIGURE 3B**, the result indicated only a weak correlation between the ratio of CL and PCT level ($r_s = -0.282$, $P = .032$), with no statistical difference between PCT value and ratio of NC and ITM ($P > .05$).

Imbalance of Monocyte Subsets in New-HAP

As mentioned, we did not find that imbalance of monocyte subsets was associated with disease severity and infectious pathogens. We analyzed the peripheral blood monocyte counts among healthy controls, new-HAP, and re-HAP groups. As shown in **FIGURE 4**, the peripheral blood monocyte counts did not achieve statistical significance among them (10^9/L, 0.415 [0.358, 0.468] vs 0.525 [0.340, 0.733] vs 0.545 [0.298, 0.800], respectively, $P > .05$. We then hypothesized that the imbalance of monocyte subsets may be related to immunologic memory of infection. Therefore, 36 and 24 patients were defined as new-HAP and re-HAP, respectively.

As shown in **FIGURE 4**, a significantly decrease in NC 12.9% [7.81, 17.73]) was observed in new-HAP compared to healthy controls (21.95% [16.43, 28.95], $P < .05$). Similarly, a significant increase was found in new-HAP (81.05% [70.18, 85.68]) compared to healthy (71.90% [66.23, 76.63]) with respect to the ratio of CL ($P < .05$). As a result, the new-HAP group showed lower NC/CL than healthy controls (0.16 [0.09, 0.26] vs 0.31 [0.22, 0.43], $P < .05$). No significant difference was observed in the ratio of ITM between these 2 groups.

Notably, the ratio of NC (25.40% [13.85, 41.78]), the ratio of CL (70.05% [52.53, 77.25]), and that of NC/CL (0.38 [0.19, 0.80]) for

Downloaded from https://academic.oup.com/labmed/article/54/4/e100/6758541 by guest on 24 February 2025

FIGURE 2. Comparison of NC, ITM, and CL between HAP patients and healthy controls (A), well-controlled and progressive groups (B), SOFA < 3 and SOFA ≥ 3 groups (C), non-Enterobacter and Enterobacter groups (D). Results are presented as medians with interquartile range. Levels were compared by Mann-Whitney U test. HAP, hospital-acquired pneumonia; NC, nonclassical; ITM, intermediate; CL, classical; SOFA, sequential organ failure assessment.

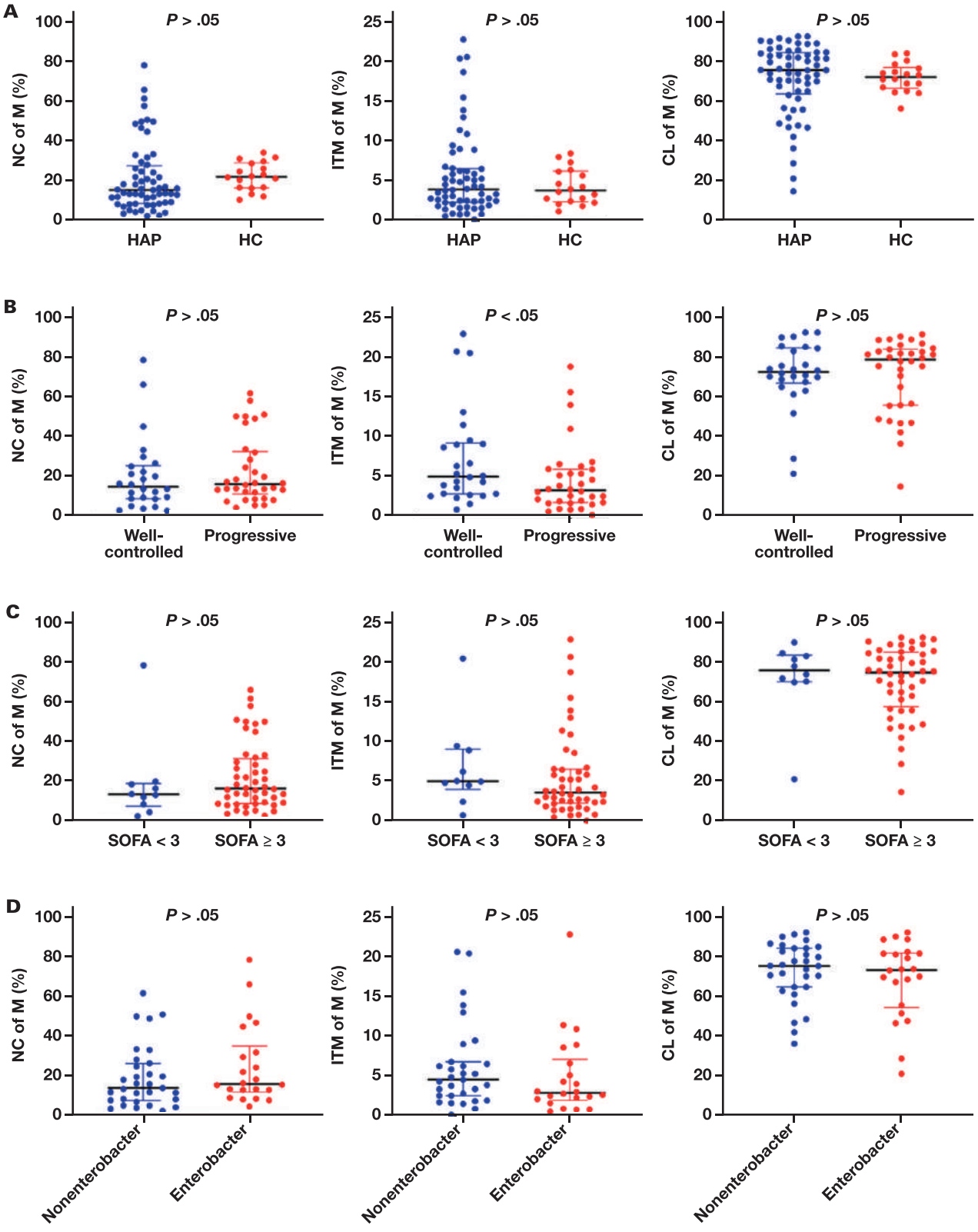

Downloaded from https://academic.oup.com/labmed/article/54/4/e100/6758541 by guest on 24 February 2025

FIGURE 3. **Association between monocyte subsets and PCT level in HAP patients. Levels of NC, ITM, and CL in HAP patients were compared between PCT < 2 and PCT ≥ 2 (ng/mL) groups (A). Scatterplot of monocyte subsets vs PCT value was analyzed by Spearman's correlation analysis (B). HAP, hospital-acquired pneumonia; NC, nonclassical; ITM, intermediate; CL, classical; PCT, procalcitonin.**

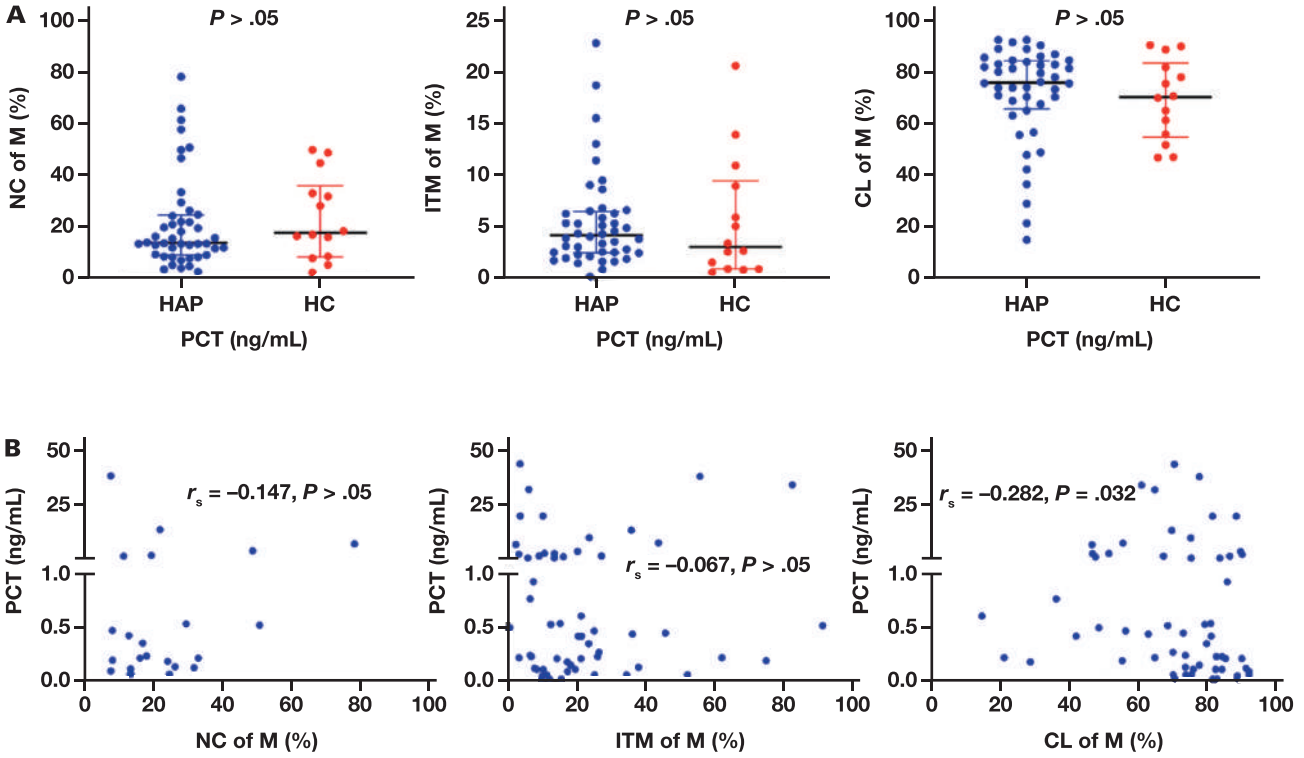

re-HAP patients returned to healthy control levels ($P > .05$ for each). The re-HAP group also showed distinct differences in the ratio of NC, CL, and NC/CL compared to the new-HAP group ($P < .05$ for each).

Accordingly, results indicated that an imbalance of monocyte subsets was correlated with acute and chronic bacterial infection.

Expression of PD-L1 in Circulating Monocyte Subsets

The programmed cell death receptor-1 (PD-1) and PD-L1 pathway, as a new therapeutic target, mediates suppression of T-cell activation and escape of host immune surveillance.[14] Therefore, the expression of PD-L1 on the subset of monocytes was investigated (**FIGURE 5**). As shown in **FIGURE 6A**, ITM from patients with HAP expressed higher PD-L1 than that of healthy (75.60% [51.18, 90.63] vs 46.65% [33.90, 70.13], $P < .05$), whereas NC and CL from both the HAP group and healthy controls showed a comparable level of PD-L1 ($P > .05$).

Additionally, PD-L1 expression in NC, ITM, and CL monocytes were comparable between the re-HAP and new-HAP cohorts ($P > .05$) (**FIGURE 6B**). This indicates that PD-L1 expression on monocytes was constitutive rather than inducible, which represented that no difference of that existed between two groups.

Finally, we analyzed the expression of PD-L1 among the 3 monocyte subsets from patients with HAP. As shown in **FIGURE 6C**, the PD-L1 significantly increased in the ITM group (75.60% [51.18–90.63]) compared with the NC (25.85% [15.98–42.50], $P < .05$) and CL groups (54.20% [33.73–74.43], $P < .05$), whereas CL expressed more PD-L1 than NC ($P < .05$). This suggests that PD-L1 was differently expressed by individual monocyte subsets, which provides regulation of anti-pathogen immune response.

Discussion

The HAPs are considered to be in close relationship with immune-mediated responses. Human monocytes are heterogeneous cells and can be subdivided into 3 subsets according to the differential expression of CD14 and CD16, which have been identified as specialized functions. Classical monocytes engage in proinflammatory and antimicrobial responses. Nonclassical monocytes, known as patrolling monocytes, specialize in phagocytosis, trans-endothelial migration and antiviral responses. Intermediate monocytes, transiting from classical to nonclassical monocytes, are involved in both a patrolling function and anti-inflammatory effects.[2,4]

In this study, the ratios of NC, ITM, and CL did not show significant difference between patients with HAP and healthy controls. We then evaluated the expression of monocyte subsets in patients with HAP between well-controlled and progressive cohorts. The NC and CL did not differ between these 2 groups, which was consistent with a study that found no significant difference between severe and nonsevere groups for NC and CL in children at admission with *Mycoplasma pneumoniae* pneumonia.[15] Our results also showed that the ratio of ITM increased in the well-controlled group. In contrast, Passos et al[16] found that ITM monocytes increased soon after Leishmania infection and may contribute to the development of the disease. Wang et al[15] found that ITM were comparable between severe and nonsevere groups. These results suggest that further experiments need to be done to explore whether ITM monocytes are concerned with disease severity.

In our study, human monocyte subsets from peripheral blood were investigated between non-Enterobacter and Enterobacter groups. Experiments have demonstrated that the lungs of K.p.-infected mice show monocyte-involved immune response.[17] In contrast, the

Downloaded from https://academic.oup.com/labmed/article/54/4/e100/6758541 by guest on 24 February 2025

FIGURE 4. **Comparison of monocyte counts, NC, ITM, CL, and NC/CL among healthy, new-HAP and re-HAP groups. The new-HAP cohort showed the imbalance of NC/CL compared to that of healthy controls and re-HAP ($P < .05$ for each). The Mann-Whitney U test was used for analyzing data. HAP, hospital-acquired pneumonia; new-HAP, newly emerged HAP; re-HAP, recurrent HAP; NC, nonclassical; ITM, intermediate; CL, classical.**

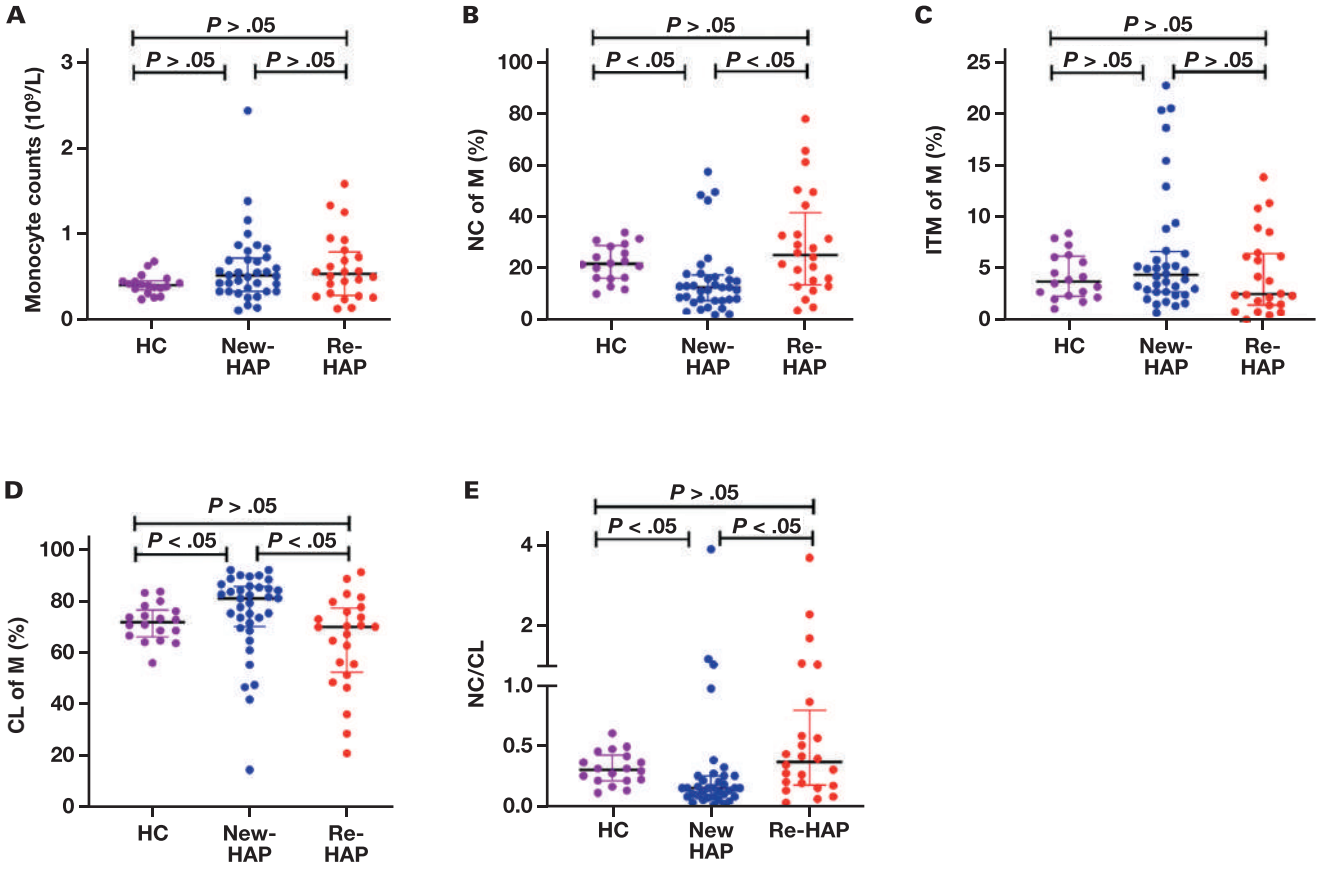

imbalance of human NC, ITM, and CL were not observed between these 2 groups in our study. We speculate that monocyte subsets are nonspecific and pathogens may colonize in the lungs instead of in the peripheral blood.

Our reports that new-HAP patients had a lower level of NC and a higher level of CL monocytes than re-HAP patients and the healthy controls. It was suggested that the activation of the circulating monocyte subsets could play an important role in the newly emerged HAP. This is consistent with data showing that decreased NC monocyte subsets are observed in severe acute SARS-CoV-2 infection.[18] Interestingly, our results indicate that the ratio of monocyte subsets for re-HAP patients tended to return to normal. Yao et al[19] found a new paradigm of immunological memory formation, where memory macrophage were triggered with the help of effector CD8 T-cells in early response to virus. Memory alveolar macrophages were found in a low-rate proliferation status independently of monocytes to maintain itself unless they encounter viral infection. It has also been demonstrated that trained monocytes can exhibit an effective response in defense of microbial components.[20] It has been suggested that increased ratio of CL may facilitate immune escape for new-HAP patients. Also, the distribution of NC and CL showed normalization for re-HAP patients, which indicates specific adaptive immune response like immunological memory instead of nonspecific innate immune response was involved during this period.

Finally, to ascertain functional implications of PD-L1 expression on monocyte subsets, NC, ITM, and CL PD-L1 expression were analyzed in our study. Both PD-1 and PD-L1 are co-inhibitory receptor molecules, mediating the exhausting of T-cell immunity in chronic infectious diseases and tumors.[21,22] Previous studies showed that PD-L1 expression in monocytes was related to increased mortality and hospital-acquired infections. Patients with high levels of PD-L1 expression in monocytes should receive more attention, as they are considered immunosuppressed and may be vulnerable to potential harmful effects.[21] In our study, PD-L1 expression was significantly higher in the ITM monocyte subset than in NC and CL, consistent with a study in advanced melanoma patients.[23] Our study also showed that PD-L1 + expression on CL monocyte was significantly higher than NC monocyte. This led to the speculation that PD-L1 was constitutively expressed in the monocyte. The decreased ratio of PD-L1 + CL in the re-HAP group might be the consequence of immune memory of bacterial infection and constitute a protective anti-pathogen immune response.

Limitations of this study should be noted. First, the number of patients with HAP and healthy controls was limited. Second, dynamic changes in the levels of monocyte subsets and functions of PD-L1 expressed in monocyte subsets remain targets for future studies. Further experiments could be performed to enhance the understanding of monocyte subsets.

In conclusion, our study highlighted the imbalance of circulating monocyte subsets in patients with HAP, which were correlated with immunological memory response. The PD-L1 was differently expressed

Downloaded from https://academic.oup.com/labmed/article/54/4/e100/6758541 by guest on 24 February 2025

FIGURE 5. **The PD-L1 was analyzed in defined NC, ITM, and CL by flow cytometry. The representative dot plots of staining for PD-L1 was shown. PD-L1, programmed death ligand 1; NC, nonclassical; ITM, intermediate; CL, classical.**

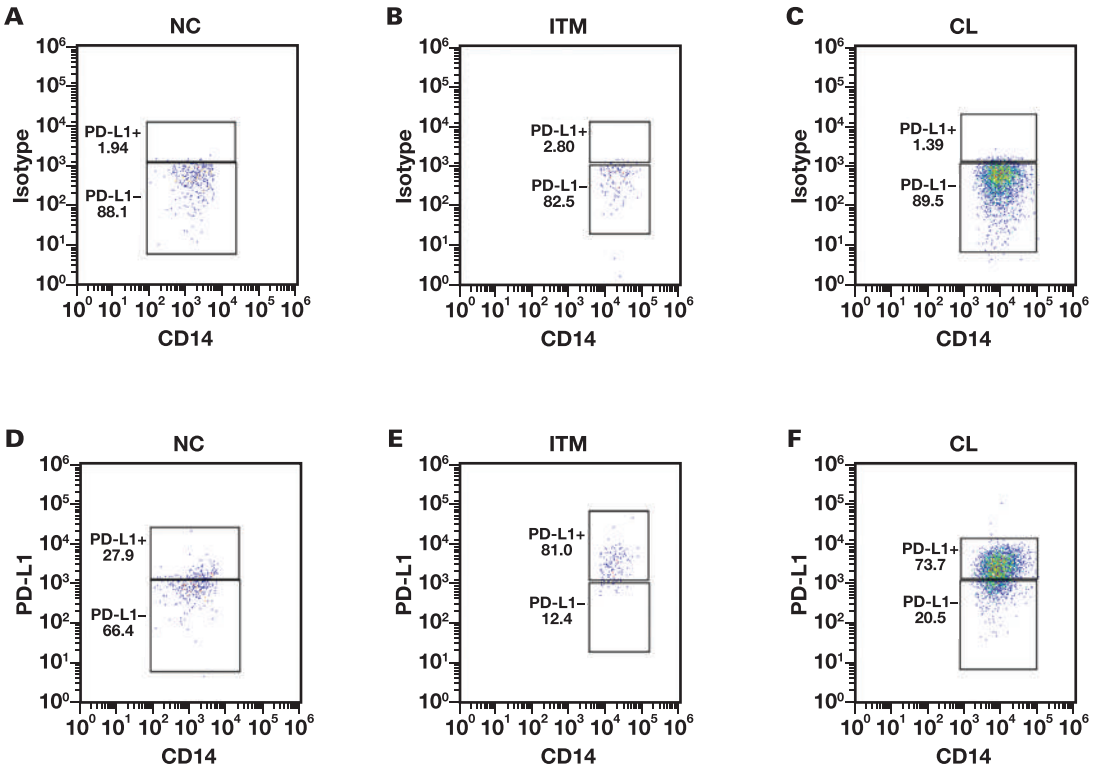

FIGURE 6. **Analysis of circulating PD-L1 + monocyte subsets in healthy and HAP patients. A, comparison of PD-L1 + monocyte subsets between HAP patients and healthy controls. B, comparison of PD-L1 + monocyte subsets between new-HAP and re-HAP cohorts. C, comparison of PD-L1 + population among NC, ITM, and CL in HAP patients. PD-L1, programmed death ligand 1; NC, nonclassical; ITM, intermediate; CL, classical.**

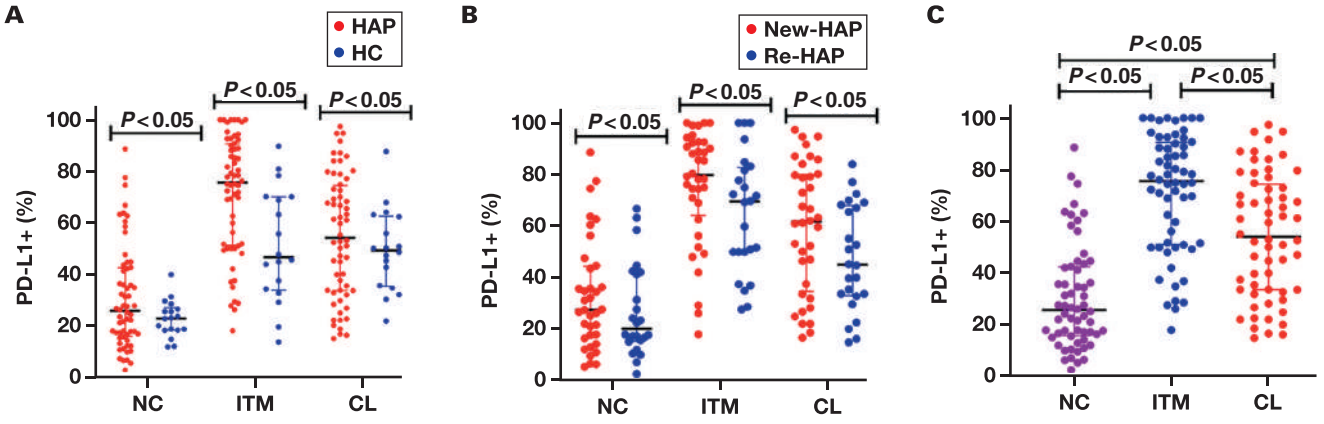

by monocyte subset, mediating the regulation of anti-pathogen immune response.

Ethics Approval and Consent to Participate

This study was approved by the Institutional Review Boards of The First Affiliated Hospital of Soochow University (2019-070).
Informed consent was obtained from all participants.

Conflict of Interest

The authors declare that they have no competing interests.

Author Contributions

QQX and CC conceived the idea and designed and supervised the study. JYJ, SY, and JYF performed the experiment and drafted the manuscript. ZJW, ZYX, and XPP collected data. JYJ analyzed data and performed statistical analysis. All authors reviewed and approved the final version of the manuscript.

Financial Disclosures

This work was supported by Technology Research and Development Funding of Suzhou city SKY2021034 (to CC). The funders had no role in the study design, data collection and analysis, decision to publish, or preparation of the manuscript.

Downloaded from https://academic.oup.com/labmed/article/54/4/e100/6758541 by guest on 24 February 2025

REFERENCES

1. Torres A, Cilloniz C, Niederman MS, et al. Pneumonia. *Nat Rev Dis Primers.* 2021;7(1):25. doi:10.1038/s41572-021-00259-0.
2. Kratofil RM, Kubes P, Deniset JF. Monocyte conversion during inflammation and injury. *Arterioscler Thromb Vasc Biol.* 2017;37(1):35–42. doi:10.1161/ATVBAHA.116.308198.
3. Gainaru G, Papadopoulos A, Tsangaris I, Lada M, Giamarellos-Bourboulis EJ, Pistiki A. Increases in inflammatory and CD14dim/CD16pos/CD45pos patrolling monocytes in sepsis: correlation with final outcome. *Crit Care.* 2018;22(1):56–56. doi:10.1186/s13054-018-1977-1.
4. Kapellos TS, Bonaguro L, Gemünd I, et al. Human monocyte subsets and phenotypes in major chronic inflammatory diseases. *Front Immunol.* 2019;10:2035. doi:10.3389/fimmu.2019.02035.
5. Moore BB, et al., Inflammatory leukocyte phenotypes correlate with disease progression in idiopathic pulmonary fibrosis. *Front Med.* 2014;1(56). doi:10.3389/fmed.2014.00056.
6. Martin-Loeches I, Rodriguez AH, Torres A. New guidelines for hospital-acquired pneumonia/ventilator-associated pneumonia: USA vs. Europe. *Curr Opin Crit Care.* 2018;24(5):347–352. doi:10.1097/MCC.0000000000000535.
7. Shen Y, Qu Q-X, Jin M-N, Chen C. Investigating the role of circulating CXCR5-expressing CD8+ T-cells as a biomarker for bacterial infection in subjects with pneumonia. *Respir Res.* 2019;20(1):54. doi:10.1186/s12931-019-1011-4.
8. Dang TT, Majumdar SR, Marrie TJ, Eurich DT. Recurrent pneumonia: a review with focus on clinical epidemiology and modifiable risk factors in elderly patients. *Drugs Aging.* 2015;32(1):13–19. doi:10.1007/s40266-014-0229-6.
9. Low DE, Mazzulli T, Marrie T. Progressive and nonresolving pneumonia. *Curr Opin Pulm Med.* 2005;11(3):247–252. doi:10.1097/01.mcp.0000158727.20783.70.
10. Ong S, Teng K, Newell E, et al. A novel, five-marker alternative to CD16-CD14 gating to identify the three human monocyte subsets. *Front Immunol.* 2019;10:1761–1761. doi:10.3389/fimmu.2019.01761.
11. Patel AA, Zhang Y, Fullerton JN, et al. The fate and lifespan of human monocyte subsets in steady state and systemic inflammation. *J Exp Med.* 2017;214(7):1913–1923. doi:10.1084/jem.20170355.
12. Lucas G, Bartolf A, Kroll N, et al. Procalcitonin (PCT) level in the emergency department identifies a high-risk cohort for all patients treated for possible sepsis. *eJIFCC* 2021;32(1):20–26.
13. Hu L, Shi Q, Shi M, Liu R, Wang C. Diagnostic value of PCT and CRP for detecting serious bacterial infections in patients with fever of unknown origin: a systematic review and meta-analysis. *Appl Immunohistochem Mol Morphol.* 2017;25(8):e61–e69. doi:10.1097/PAI.0000000000000552.
14. Chen S, Crabill GA, Pritchard TS, et al. Mechanisms regulating PD-L1 expression on tumor and immune cells. *J ImmunoTher Cancer.* 2019;7(1):305. doi:10.1186/s40425-019-0770-2.
15. Wang Z, Yang L, Ye J, Wang Y, Liu Y. Monocyte subsets study in children with *Mycoplasma pneumoniae* pneumonia. *Immunol Res.* 2019;67(4-5):373–381. doi:10.1007/s12026-019-09096-6.
16. Passos S, Carvalho LP, Costa RS, et al. Intermediate monocytes contribute to pathologic immune response in *Leishmania braziliensis* infections. *J Infect Dis.* 2015;211(2):274–282. doi:10.1093/infdis/jiu439.
17. Xiong H, Keith JW, Samilo DW, Carter RA, Leiner IM, Pamer EG. Innate lymphocyte/Ly6Chi monocyte crosstalk promotes *Klebsiella pneumoniae* clearance. *Cell.* 2016;165(3):679–689. doi:10.1016/j.cell.2016.03.017.
18. Gatti A, Radrizzani D, Viganò P, Mazzone A, Brando B. Decrease of non-classical and intermediate monocyte subsets in severe acute SARS-CoV-2 infection. *Cytometry A.* 2020;97(9):887–890. doi:10.1002/cyto.a.24188.
19. Yao Y, Jeyanathan M, Haddadi S, et al. Induction of autonomous memory alveolar macrophages requires T cell help and is critical to trained immunity. *Cell.* 2018;175(6):1634–1650.e17. doi:10.1016/j.cell.2018.09.042.
20. Quintin J, Saeed S, Martens JHA, et al. Candida albicans infection affords protection against reinfection via functional reprogramming of monocytes. *Cell Host Microbe.* 2012;12(2):223–232. doi:10.1016/j.chom.2012.06.006.
21. Shao R, Fang Y, Yu H, Zhao L, Jiang Z, Li C-S. Monocyte programmed death ligand-1 expression after 3-4 days of sepsis is associated with risk stratification and mortality in septic patients: a prospective cohort study. *Crit Care.* 2016;20(1):124. doi:10.1186/s13054-016-1301-x.
22. Xia L, Liu Y, Wang Y. PD-1/PD-L1 blockade therapy in advanced non-small-cell lung cancer: current status and future directions. *Oncologist (Dayton, Ohio)* 2019;24(S1):S31–S41.
23. Pico de Coaña Y, Wolodarski M, van der Haar Àvila I, Nakajima T, Rentouli S, Lundqvist A, Masucci G, Hansson J, Kiessling R. PD-1 checkpoint blockade in advanced melanoma patients: NK cells, monocytic subsets and host PD-L1 expression as predictive biomarker candidates. *Oncoimmunology.* 2020;9(1):1786888. doi:10.1080/2162402X.2020.1786888.

Downloaded from https://academic.oup.com/labmed/article/54/4/e100/6758541 by guest on 24 February 2025

CASE STUDY

A Case of Fatal *Clostridium perfringens* Sepsis with Massive Hemolysis in the Setting of a Coincidental Platelet Transfusion

Frank A. Boyd, MD,[1,] Mandy F. O'Leary, MD,[2] Kaaron Benson, MD,[2] Aliyah Baluch, MD[3]*

[1]Department of Pathology & Cell Biology, University of South Florida Morsani College of Medicine, Tampa, FL, USA, [2]Department of Pathology, H. Lee Moffitt Cancer Center and Research Institute, Tampa, FL, USA, [3]Division of Infectious Diseases, H. Lee Moffitt Cancer Center and Research Institute, Tampa, FL, USA.
*To whom correspondence should be addressed. faboyd@usf.edu

Abbreviations: AHTR, acute hemolytic transfusion reaction; AML, acute myeloid leukemia; DAT, direct antiglobulin test; IV, intravenous; ICU, intensive care unit; RBC, red blood cell; PRT, pathogen-reduced technology; TRALI, transfusion-related acute lung injury; TACO, transfusion-associated circulatory overload; TTI, transfusion-transmitted infection.

Laboratory Medicine 2023;54:e108–e110; https://doi.org/10.1093/labmed/lmac135

ABSTRACT

A 62-year-old woman with acute myeloid leukemia (AML) died of shock and massive hemolysis shortly after receiving two platelet transfusions at a routine clinic visit. Subsequent investigation into what was initially believed to be an acute hemolytic transfusion reaction secondary to platelet transfusions revealed that the patient died of *Clostridium perfringens* sepsis leading to massive hemolysis. Further investigation ruled out bacterially-contaminated platelets since a patient blood sample from 2 days prior had *Clostridium* species. The unusual findings and management considerations for this oncology patient are reviewed and compared with previously reported cases of *C. perfringens* transfusion-transmitted infections. Oncology patients may be especially susceptible to unusual presentations involving unusual pathogens.

Patient History

We present the case of a 62-year-old woman with acute myeloid leukemia (AML), 100 days posthaploidentical hematopoietic stem cell transplant. Her posttransplant course was complicated by grade IV cutaneous graft-versus-host disease and recurrent bacterial, fungal, and viral infections. The patient presented for a routine clinic visit as well as platelet transfusion prior to a port placement. Two days prior, she had another clinic visit due to diarrhea; however, her physical exam was benign.

Approximately 1 hour after the second platelet transfusion in the clinic, the patient became hypoxic with SpO_2 of 80% to 90%, lethargic, and tachypneic. Initially she was afebrile during assessment. Due to concern for a possible acute hemolytic transfusion reaction (AHTR), the patient was given 100 mg of hydrocortisone, intravenous (IV) fluids, and oxygen. The patient rapidly developed a fever of 39.4°C and became hypotensive and tachycardic. Blood cultures were drawn, and the patient was transferred to the intensive care unit (ICU). After transfer to the ICU, the patient was started on empiric IV antibiotics. Initially in the ICU, the patient was fully alert, oriented, and normotensive but soon developed slurred speech, shock, tachypnea, and cyanosis. She was started on norepinephrine bitartrate (Levophed) and was intubated. Shortly after intubation the patient went into asystole, and despite recovering circulation twice, the patient died approximately 6 hours after the initial event in clinic.

Clinical and Laboratory Information

The patient was blood group B, and the transfused platelets were both group O. There was no evidence of a clerical error. Pretransfusion direct antiglobulin test (DAT) was negative, but posttransfusion DAT was + 1 for both polyspecific antisera and monospecific immunoglobulin G. However, the eluate was negative for both anti-B and anti-AB. Both units of platelets had anti-A and anti-B titers performed, and all titers were 32 or less. Gross examination of the centrifuged pretransfusion sample showed slightly pink-tinged yellow plasma, but the posttransfusion sample was a dark red consistent with massive hemolysis (**FIGURE 1A**). The final complete blood count, which was completed postmortem, showed a hemoglobin of 4.9 g/dL (initially 7.8 g/dL). Urinalysis was consistent with hemoglobinuria, which was not present on the prior urinalysis (4 + blood on dipstick but few red blood cells [RBCs] on microscopic exam).

The initial platelet transfusion bag was unable to be located. Prior to transport to our institution, the initial platelet bag had been cultured by the blood center and showed no growth. The second bag of platelets, a pathogen-reduced technology (PRT) platelet, was returned to the blood bank; no organisms were seen after Gram stain, and there was no growth found on culturing the bag. Each of the 2 platelet bags were part of a paired platelet donation, and the 2 corresponding units were transfused to other patients without adverse events. The patient's blood cultures taken after her platelet transfusions grew *Clostridium perfringens*. During investigation, a blood sample held from the patient's clinic visit 2 days prior to death was recovered, and an acridine orange stain showed box-shaped bacilli consistent with *Clostridium perfringens,* as was seen in

© The Author(s) 2022. Published by Oxford University Press on behalf of American Society for Clinical Pathology. All rights reserved. For permissions, please e-mail: journals.permissions@oup.com

Downloaded from https://academic.oup.com/labmed/article/54/4/e108/6758539 by guest on 24 February 2025

FIGURE 1. Pre-transfusion (left) and post-transfusion (right) centrifuged blood samples (1A). *Clostridium sp.* showing rods clustered on an acridine orange stain (1B).

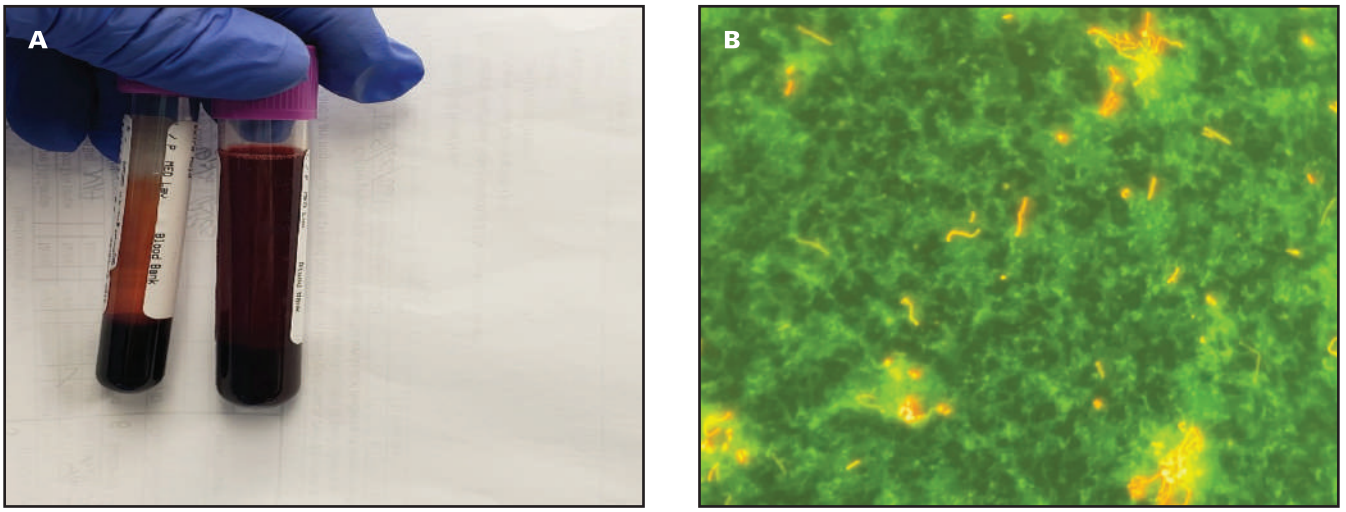

the patient's blood cultures (**FIGURE 1B**). An autopsy was requested by the primary team but was declined by the patient's family.

Discussion

Clostridium species bacteremias are among several opportunistic infections that affect patients with hematologic malignancies. *Clostridium perfringens* makes up 77% of nonpolymicrobial Clostridial infections.[1] Various strains of *C. perfringens* produce alpha-toxin, which contains phospholipase C and sphingomyelinase. These enzymes in sufficient concentrations in the blood cause degradation of RBC membranes, which can lead to massive intravascular hemolysis, a complication seen in 7% to 15% of *C. perfringens* bacteremias.[2,3]

Acute hemolytic transfusion reactions are medical emergencies that typically are secondary to ABO group incompatibility and are most often the result of a clerical error.[4] Hemolysis resulting from AHTRs is a result of interactions between either donor antibodies and recipient RBC antigens or donor RBC antigens with recipient antibodies. The former interaction is less common but was in our differential and should be considered in other cases with a similar clinical presentation shortly after transfusion with products such as platelets or fresh frozen plasma. Although AHTRs caused by non-ABO recipient antibodies against donor RBCs are uncommon, non-ABO antibodies in the donor plasma are typically of an insignificant titer.[5] Affected patients most commonly present with fever and chills but may also develop flank pain, hypotension, and dyspnea.[4,5]

Transfusion-related acute lung injury (TRALI) and transfusion-associated circulatory overload (TACO) are also relevant consideration in a patient who becomes hypoxic within 6 hours of transfusion. Both TRALI and TACO can result in shock but hypotension and fever are more closely associated with TRALI. The risk of both these entities may be increased in patients with hematologic malignancies.[6]

Allergic transfusion reactions typically present with a milder clinical picture than as seen in this case but should be considered in patients with a reaction in a similar timeframe as this case. Allergic reactions may present with only urticaria but can range to anaphylaxis in severity.[7] Another important differential diagnosis, especially if the patient develops fever with hypotension, nausea, or emesis, is a transfusion-transmitted infection (TTI).[4] The risk of a TTI is increased with platelet products compared to RBC products due to platelet storage at room temperature in contrast to refrigeration of RBC units.[8]

One of the most striking aspects of this case is that the patient's *Clostridium* bacteremia remained subclinical for at least 48 hours until her sudden decompensation. Her only clinical symptom was diarrhea, and she had serial benign abdominal exams. This is likely due to her high net state of immunosuppression; this patient with AML and only 100 days posttransplant was taking 30 mg prednisone, ruxolitinib (Jakafi), sirolimus, and mycophenolate mofetil. After her transfer to the ICU, the patient was started on vancomycin and cefepime for empiric coverage, and if she had not had a benign abdominal exam, piperacillin/tazobactam (Zosyn) would have been administered for anaerobic coverage per institutional protocols.

Clostridium perfringens is present in the normal microbiota of roughly half of healthy North Americans. These normal strains are all type A genotype and subsequently carry *plc*, which codes for alpha-toxin, the etiology of the massive hemolysis it may cause.[9] Given our patient's immunosuppressed state, the likely source for her *C. perfringens* bacteremia was spread from the intestine; an autopsy would have likely borne this out.

Serum lactate levels may identify patients at high risk for sepsis. However, during the patient's clinical course, this assay was not ordered stat, and so when it was completed and found to be above the "sepsis threshold" of > 2.0 mmol/L (3.0 mmol/L), she had already died. Had her abdominal exam in the clinic provided any suggestion of infection, abdominal imaging may have had clues to support empiric coverage for anaerobes.

Given the timing of our patient's platelet transfusions, it is important to contrast her case to bacterial TTIs. As stated before, due to the nonrefrigerated storage of platelet products, bacterial TTIs are more common after platelet transfusion (1/5000) than RBC transfusion (1/38,500), making platelet transfusions the most frequent infectious transfusion risk.[8,10] Transfusion-transmitted infections from platelet products are most commonly due to coagulase-negative staphylococci, but fatal TTIs are more commonly due to Gram negative species. Of the 60 deaths from platelet TTIs reported to the Food and Drug

Downloaded from https://academic.oup.com/labmed/article/54/4/e108/6758539 by guest on 24 February 2025

Administration from 1995 to 2004, 62% were Gram negative.[11] Platelet product contamination with *C. perfringens* is very uncommon, with only a few reported cases in the literature.[12–14] Among these 4 cases, 3 were fatal, and each patient had a variable onset of symptoms ranging from during the transfusion to a few hours after. Two of the 4 cases describe intravascular hemolysis.[12,14]

Pathogen reduction technology is an approach that significantly reduces platelet TTI risk. One of the most common methods of PRT is a technique using amotosalen and ultraviolet light. The first platelet product this patient received was cultured traditionally, whereas the second bag had undergone PRT and, therefore, no culture was needed, but one was performed posttransfusion from a few drops of the now empty bag. As PRT becomes more widely adopted, there is opportunity to see further reduction in the rates of platelet product TTIs. Further investigation of the efficacy of PRT is needed in the oncologic and immunocompromised patient population.

REFERENCES

1. Bodey GP, Rodriguez S, Fainstein V, Elting LS. Clostridial bacteremia in cancer patients. A 12-year experience. *Cancer.* 1991;67(7):1928–1942. doi:10.1002/1097-0142(19910401)67:7<1928::aid-cncr2820670718>3.0.co;2-9.
2. Sakurai J, Nagahama M, Oda M. *Clostridium perfringens* alpha-toxin: characterization and mode of action. *J Biochem.* 2004;136(5):569–574. doi:10.1093/jb/mvh161.
3. Simon TG, Bradley J, Jones A, et al. Massive intravascular hemolysis from Clostridium perfringens septicemia: a review. *J Intensive Care Med.* 2014;29(6):327–333.
4. Delaney M, Wendel S, Bercovitz RS, et al. Transfusion reactions: prevention, diagnosis and treatment. *Lancet.* 2016;388(10061):2825–2836. doi:10.1016/s0140-6736(15)01313-6.
5. Strobel E. Hemolytic transfusion reactions. *Transfus Med Hemother.* 2008;35(5):346–353. doi:10.1159/000154811.
6. Roubinian N. TACO and TRALI: biology, risk factors, and prevention strategies. *Hematol 2014 Am Soc Hematol Educ Prog.* 2018;(1):585–594.
7. Hirayama F. Current understanding of allergic transfusion reactions: incidence, pathogenesis, laboratory tests, prevention and treatment. *Br J Haematol.* 2013;160(4):434–444. doi:10.1111/bjh.12150.
8. Bihl F, Castelli D, Marincola F, et al. Transfusion-transmitted infections. *J Transl Med.* 2007;5(1):25.
9. Carman RJ, Sayeed S, Li J, et al. *Clostridium perfringens* toxin genotypes in the feces of healthy North Americans. *Anaerobe.* 2008;14(2):102–108. doi:10.1016/j.anaerobe.2008.01.003.
10. Hillyer CD, Josephson CD, Blajchman MA, et al. Bacterial contamination of blood components: risks, strategies, and regulation: joint ASH and AABB educational session in transfusion medicine. *ASH Educ Prog.* 2003;(1):575–589.
11. Palavecino EL, Yomtovian RA, Jacobs MR. Bacterial contamination of platelets. *Transfus Apher Sci.* 2010;42(1):71–82. doi:10.1016/j.transci.2009.10.009.
12. McDonald CP, Hartley S, Orchard K, et al. Fatal *Clostridium perfringens* sepsis from a pooled platelet transfusion. *Transfus Med.* 1998;8(1):19–22.
13. Eder AF, Meena-Leist CE, Hapip CA, et al. *Clostridium perfringens* in apheresis platelets: an unusual contaminant underscores the importance of clinical vigilance for septic transfusion reactions (CME). *Transfusion.* 2014;54(3pt2):857–862.
14. Horth R, Jones JM, Kim JJ, et al. Fatal sepsis associated with bacterial contamination of platelets—Utah and California, August 2017. *Morb Mortal Wkly Rep.* 2018;67(25):718.

Downloaded from https://academic.oup.com/labmed/article/54/4/e108/6758539 by guest on 24 February 2025

CASE STUDY

Falsely Elevated Estradiol Results in a 62-Year-Old Male Patient

Gergely Talaber, MD, PhD,[1,] Tomas Meisel, MD,[2] Thord Rosen, MD, PhD[3]*

[1]Unilabs AB, Department of Clinical Chemistry, Skaraborg Hospital, Skövde, Sweden, [2]Sjövalla Klint Health Care, Mölndal, Sweden, [3]Sahlgrenska University Hospital, Department of Medicine, Section of Endocrinology, Diabetes and Metabolism, Gothenburg, Sweden. *To whom correspondence should be addressed. gergely.talaber@unilabs.com

Keywords: interference, estradiol, immunoassay, aromatase inhibitor, heterophile antibodies, macro-estradiol

Abbreviations: LC-MS/MS, liquid chromatography-tandem mass spectrometry; RF, rheumatoid factor; PEG, polyethylene glycol; SHBG, sex hormone-binding globulin; PSA, prostate-specific antigen, LH, luteinizing hormone, FSH, follicle-stimulating hormone; hCG, human chorionic gonadotropin; TSH, thyroid stimulating hormone.

Laboratory Medicine 2023;54:e111–e114; https://doi.org/10.1093/labmed/lmac136

ABSTRACT

Falsely increased estradiol levels can lead to unnecessary tests and therapeutic interventions. Here, we present a case of a 62-year-old man with falsely elevated estradiol, which led to subsequent follow-up testing and prescriptions. Alternative immunoassay testing, in conjunction with Scantibodies' blocking reagents, polyethylene glycol precipitation, and liquid chromatography-tandem mass spectrometry confirmation demonstrated that the falsely elevated estradiol was due to the presence of macro-estradiol. This report emphasizes the importance of recognizing analytical interferences in immunoassays to appropriately manage subsequent testing and patient care.

Clinical History

A 62-year-old male patient presented with general fatigue and decreased libido at a urology clinic in December 2016. His testosterone level was estimated to be low (5.6–6.4 nmol/L, analyzed on Beckman Dxl), and his testes were found to be normal on palpation. Clinical hypogonadism was diagnosed, and with continuous testosterone medication (Tostrex), his general well-being, including sexual function, was greatly improved, with serum testosterone levels of around 20 nmol/L, hematocrit 44%, and prostate-specific antigen (PSA) within normal ranges.

The patient is a former factory worker with a family history of cardiovascular disease. He is a nonsmoker, has no problems with alcohol or drugs, and exercises regularly. At the age of 27 (1986), low lumbar disc herniation with neurological deficits was diagnosed. He underwent surgery in 1993 and 1995 due to constant intense back pain, but unfortunately, the operations gave no pain relief; therefore, he is still in need of regular treatment with opioid (Tramadol). Hypertension (170/100) and hyperlipidemia, diagnosed in 2010, are now under control with a beta-blocker (Metoprolol) and a statin (Atorvastatin). In 2018, an acute myocardial infarction was successfully treated through cardiac bypass surgery.

Due to his hypogonadism, in 2020, the patient was referred from the urology clinic to a private healthcare center. At his first visit, a serum test for estradiol was taken, being a routine test at this center for all new patients prior to the introduction of testosterone therapy. The patient's estradiol level, never analyzed before, was highly elevated (1106 pmol/L), approximately 10 times the cutoff (<150 pmol/L) for men of the same age (**TABLE 1**). His blood count and hemoglobin level were within the reference range (not shown). Due to suspicion of extreme aromatization, the aromatase inhibitor anastrozole (Arimidex) was prescribed and testosterone therapy was briefly interrupted. However, the anastrazole rendered only a slight decrease in the estradiol levels. Due to the highly elevated estradiol, the patient was followed up with more estradiol sampling, which gave approximately the same results (**TABLE 1**).

During later follow-up visits and sampling over the course of some months, additional hormones/parameters were analyzed (**TABLE 1**; all parameters were analyzed on a Siemens ADVIA Centaur in the same laboratory). The laboratory parameters were in alignment with the clinical picture of testosterone substitution, such as low luteinizing hormone (LH) (0.8 IU/mL, reference range 1.5-9.3 for men of the same age), and somewhat low sex hormone-binding globulin (SHBG) (18 nmol/L, reference range 22–113 nmol/L). A thorough review of the patient's clinical status concluded that there were no clinical signs whatsoever of high estradiol, thus raising the suspicion that a laboratory error was causing falsely elevated estradiol. Consequently, the aromatase inhibitor anastrozole was withdrawn.

A laboratory consultation was initiated to confirm analytical interference. The sample, after being analyzed on a Siemens ADVIA Centaur, was sent to external laboratories using another immunoassay, Abbott Alinity and a QTRAP 5500 Liquid Chromatography-Tandem Mass Spectrometry (LC-MS/MS), respectively. The obtained estradiol results are summarized in **TABLE 2**. Abbott Alinity and LC-MS/MS showed results that were not in line with the high level measured on the Siemens ADVIA Centaur, indicating that there was analytical interference with the Siemens ADVIA Centaur method but not with the other 2 methods (**TABLE 2**).

To explore the nature of the interference, a new sample was obtained and the estradiol levels were still high (2214 pmol/L, Siemens ADVIA

© The Author(s) 2022. Published by Oxford University Press on behalf of American Society for Clinical Pathology. All rights reserved. For permissions, please e-mail: journals.permissions@oup.com

Downloaded from https://academic.oup.com/labmed/article/54/4/e111/6758537 by guest on 24 February 2025

TABLE 1. Hormone Levels and Related Parameters during the Patient's Initial Visit and Estradiol Results during Later Follow Ups (Visit Number Indicated in the Table) Analyzed on Siemens ADVIA Centaur.

Hormone	Visit	Result	Reference Range
Estradiol	1	1106 pmol/L*	<150 pmol/L
	2	1007 pmol/L*	
	3	913 pmol/L*	
	4	1342 pmol/L*	
	5	1054 pmol/L*	
	6	1145 pmol/L*	
	7	956 pmol/L*	
	8	843 pmol/L*	
	9	918 pmol/L*	
	10	2214 pmol/L*	
Prolactin		135 mIU/L	60–260 mIU/L
SHBG		18 nmol/L*	22–113 nmol/L
FSH		3.6 IU/L	1.4–18 IU/L
LH		0.8 IU/L*	1.5–9.3 IU/L
HCG		<0.6 IU/L	<3 IU/L
Testosterone		1.7 nmol/L*	3–27 nmol/L
Total PSA		2.4 µg/L	<3 µg/L

FSH, follicle-stimulating hormone; HCG, human chorionic gonadotropin; LH, luteinizing hormone; PSA, prostate-specific antigen; SHBG, sex hormone-binding globulin
** Indicates results outside reference range.*

Centaur). Rheumatoid factor (RF) (Siemens ADVIA XPT Chemistry) was measured, and to exclude monoclonal immunoglobulins, serum electrophoresis (Sebia Capillarys 3) with subsequent immunofixation (Sebia Hydragel IF 2/4 and Hydrasys) was performed. The RF was below the cut-off (<25 IU/mL), and electrophoresis together with immunfixation showed no trace of monoclonal immunoglobulins, thus excluding RF and paraprotein as analytical interferences. Next, to verify the presence of heterophile antibodies, Scantibodies' Heterophilic Blocking Reagent was added to the sample. The estradiol level was almost identical (2184 pmol/L) (**TABLE 2**) following the sample rerun after incubation with Scantibodies' reagent, thus ruling out heterophile antibodies as interfering substances. Furthermore, the patient had no history of therapy with monoclonal antibodies or immunoglobulins and denied contact with domestic animals.

Next, to eliminate a possible hormone-immunoglobulin complex, polyethylene glycol 6000 (PEG) precipitation was performed, and the estradiol result after PEG was 321.8 pmol/L after rerunning the sample on the Siemens ADVIA Centaur (**TABLE 2**). The sample was split again and sent to the same 2 external laboratories for analysis. The results obtained with Abbott Alinity (353 pmol/L) and LC-MS/MS (337 pmol/L) were in line with those of the PEG precipitated sample, indicating the presence of a larger hormone-immunoglobulin complex in the sample. This finally explained the falsely high estradiol result and corresponded more consistently to the clinical picture.

It was noted in the patient's record that estradiol should no longer be included as a follow-up test during visits.

Discussion

Analytical interferences in immunoassays have an estimated frequency of 0.05% to 6%,[1,2] depending on the interference and the analyte. In most cases, the causes of interference behind false results are unknown among clinicians. Thus, when not discovered early, they can lead to improper patient care. In this case report, we present a male patient case with falsely elevated estradiol, in which the suspicion of analytical interference was raised at a later stage, after several follow-ups with the same high estradiol results and ineffective medication with aromatase inhibitor. Then, the clinician contacted the laboratory and an investigation regarding analytical interference was carried out by the laboratory.

TABLE 2. Summary and Comparison of Estradiol Measurements of New Sample after Sample Split, Incubation with Scantibodies Treatment and PEG-precipitation together with Reference Ranges.

Estradiol Method	Result (pmol/L)				Reference Range
	Sample Split 1	Sample Split 2			(pmol/L)
Siemens ADVIA Centaur	Untreated	Untreated	Scantibodies	PEG	<150
	918*	2214*	2184*	321,8*	
Abbott Alinity	<70	353*			<161
QTRAP 5500 LC-MSMS	29*	337*			37-–147

** Indicates results outside reference range. PEG, polyethylene glycol.*

Clinical laboratories have knowledge about interference and strategies for verifying the interference and reporting the correct results to the clinician. To verify the presence of an analytical interference, a sample can be analyzed using different immunoassays[2] or other non-immunoassay methods. In our case, similar estradiol results were obtained with Abbott Alinity (one-step, delayed immunoassay) and LC-MS/MS as a nonimmunoassay alternative for analyzing estradiol,[3] but not with Siemens ADVIA Centaur (competitive immunoassay). This indicates that there was analytical interference with Siemens ADVIA Centaur but not with Abbott Alinity or LC-MS/MS.

To the best of our knowledge, 10 cases have been described[4–13] with falsely elevated estradiol due to analytical interference. All the cases were female patients, and 7 of them were due to heterophile antibodies.[14] Besides heterophile antibodies, monoclonal antibody production[9] and aromatase inhibitors[4,5] were also reported as agents interfering with estradiol immunoassays. Heterophile antibodies and monoclonal immunoglobulins,[15] as well as RF,[16] were ruled out in our case study as interferences. Aromatase inhibitor therapy was introduced as a consequence of the high estradiol level and suspected high aromatase activity, which resulted in only a marginal decrease in serum estradiol levels. It was therefore discontinued, as the patient's serum estradiol levels were still consistently high after repeated measurements, thus ruling out the role of drugs as an interference. It is well known that aromatase inhibitor medication might cause general fatigue and muscle pain in male patients, which is addressed by an interruption of the medication. However, our patient never displayed any side effects.

Besides the interferences discussed above, hormone-immunoglobulin/macro complexes can also affect immunoassays by causing falsely high levels, often with no clinical relevance. Prolactin,[17] TSH,[18] and plasma enzymes such as alkaline phosphatase[19] and lactate dehydrogenase[20] can build up macro complexes, mostly by binding to immunoglobulins. The most widely known macro complex in clinical practice is macroprolactin, routinely screened by many clinical laboratories using PEG precipitation.[21] The PEG precipitation is a widely used, simple procedure for removing larger protein-immunoglobulin

Downloaded from https://academic.oup.com/labmed/article/54/4/e111/6758537 by guest on 24 February 2025

complexes from the sample.[22] In our case study, the Siemens ADVIA Centaur estradiol result after PEG precipitation was almost identical to those of the other methods, indicating that a larger immunoglobulin-hormone complex, macro-estradiol, was present in the sample, causing the falsely high estradiol. Therefore, unusually high hormone levels, especially when they do not match the clinical picture and patient history, must be interpreted cautiously by the clinician. Similar to macroprolactin, reporting the correct post-PEG precipitation result, with the help of alternative immunoassays, has crucial importance in determining patient management.

Finally, the few cases presented in the literature concerning falsely elevated estradiol levels are related to female patients. To our knowledge, this is the first male case described with falsely high estradiol, and that is uniquely explained by a macro-hormone complex. It is important to stress that, when observing laboratory results with an unexpected pattern, the ordering clinician should question early on that the results may be incorrect, with the suspicion of analytical interference as the cause. Neglecting to do this could lead to erroneous medical decisions regarding therapy and interventions, including unnecessary repeated sampling.

Conflict of interest

The authors declare no conflicts of interest.

REFERENCES

1. Sturgeon CM, Viljoen A. Analytical error and interference in immunoassay: minimizing risk. *Ann Clin Biochem.* 2011;48(Pt 5):418–432. doi:10.1258/acb.2011.011073.
2. Tate J, Ward G. Interferences in immunoassay. *Clin Biochem Rev.* 2004;25(2):105–120.
3. Hoofnagle AN, Wener MH. The fundamental flaws of immunoassays and potential solutions using tandem mass spectrometry. *J Immunol Methods.* 2009;347(1–2):3–11.
4. Owen LJ, Monaghan PJ, Armstrong A, et al. Oestradiol measurement during fulvestrant treatment for breast cancer. *Br J Cancer.* 2019;120(4):404–406. doi:10.1038/s41416-019-0378-9.
5. Mandic S, Kratzsch J, Mandic D, et al. Falsely elevated serum oestradiol due to exemestane therapy. *Ann Clin Biochem.* 2017;54(3):402–405. doi:10.1177/0004563216674031.
6. Atkins P, Mattman A, Thompson D. Falsely elevated serum estradiol due to heterophile antibody interference: a case report. *Arch Endocrinol Metab*. 2021;65(2):237–241. doi:10.20945/2359-3997000000324. Online ahead of print.
7. Gordon DL, Holmes E, Kovacs EJ, Brooks MH. A spurious markedly increased serum estradiol level due to an IgA lambda. *Endocr Pract.* 1999;5(2):80–83. doi:10.4158/EP.5.2.80.
8. Langlois F, Moramarco J, He G, Carr BR. Falsely elevated steroid hormones in a postmenopausal woman due to laboratory interference. *J Endocr Soc.* 2017;1(8):1062–1066. doi:10.1210/js.2017-00191.
9. Kairemo KJ, Kahn JA, Taipale PJ. Monoclonal gammopathy may disturb oestradiol measurement in the treatment and monitoring of in-vitro fertilization: case report. *Hum Reprod.* 1999;14(11):2724–2726. doi:10.1093/humrep/14.11.2724.
10. Maharjan AS, Wyness SP, Ray JA, Willcox TL, Seiter JD, Genzen JR. Detection and characterization of estradiol (E2) and unconjugated estriol (uE3) immunoassay interference due to anti-bovine alkaline phosphatase (ALP) antibodies. *Pract Lab Med.* 2019;17:e00131. doi:10.1016/j.plabm.2019.e00131.
11. Check JH, Ubelacker L, Lauer CC. Falsely elevated steroidal assay levels related to heterophile antibodies against various animal species. *Gynecol Obstet Invest.* 1995;40:139–140. doi:10.1159/000292323.
12. Anckaert E, Platteau P, Schiettecatte J, Devroey P, Van Steirteghem A, Smitz J. Spuriously elevated serum estradiol concentrations measured by an automated immunoassay rarely cause unnecessary cancellation of in vitro fertilization cycles. *Fertil Steril.* 2006;85:1822.e5–1822.e8.
13. Zhang J, Xu L, Qiao L. Falsely elevated serum estradiol in woman of reproductive age led to unnecessary intervention and delayed fertility opportunity: a case report and literature review. *BMC Womens Health.* 2022;22(1):232.
14. Bolstad N, Warren DJ, Nustad K. Heterophilic antibody interference in immunometric assays. *Best Pract Res Clin Endocrinol Metab.* 2013;27(5):647–661. doi:10.1016/j.beem.2013.05.011.
15. Dalal BI, Brigden ML. Factitious biochemical measurements resulting from hematologic conditions. *Am J Clin Pathol.* 2009;131(2):195–204. doi:10.1309/AJCPY9RP5QYTYFWC.
16. Xu L, Wang X, Ma R, et al. False decrease of HBsAg S/CO values in serum with high-concentration rheumatoid factors. *Clin Biochem.* 2013;46(9):799–804. doi:10.1016/j.clinbiochem.2013.03.013.
17. Barth JH, Lippiatt CM, Gibbons SG, Desborough RA. Observational studies on macroprolactin in a routine clinical laboratory. *Clin Chem Lab Med.* 2018;56(8):1259–1262. doi:10.1515/cclm-2018-0074.
18. Larsen CB, Petersen ERB, Overgaard M, Bonnema SJ. Macro-TSH: a diagnostic challenge. *Eur Thyroid J.* 2021;10(1):93–97. doi:10.1159/000509184.
19. Cervinski MA, Lee HK, Martin IW, Gavrilov DK. A macro-enzyme cause of an isolated increase of alkaline phosphatase. *Clin Chim Acta.* 2015;440:169–171. doi:10.1016/j.cca.2014.11.017.
20. Fillee C, Van Hoof V, Larnbert M. Increase of serum lactate dehydrogenase caused by a macroenzyme. A case report. *Acta Clin Belg.* 2011;66(1):63–65. doi:10.2143/ACB.66.1.2062519.
21. Beltran L, Fahie-Wilson MN, McKenna TJ, Kavanagh L, Smith TP. Serum total prolactin and monomeric prolactin reference intervals determined by precipitation with polyethylene glycol: evaluation and validation on common immunoassay platforms. *Clin Chem.* 2008;54(10):1673–1681. doi:10.1373/clinchem.2008.105312.
22. Fahie-Wilson M, Halsall D. Polyethylene glycol precipitation: proceed with care. *Ann Clin Biochem.* 2008;45(Pt 3):233–235. doi:10.1258/acb.2008.007262.

Downloaded from https://academic.oup.com/labmed/article/54/4/e111/6758537 by guest on 24 February 2025

SPECIAL REPORT

Looking into the Laboratory Staffing Issues that Affected Ambulatory Care Clinical Laboratory Operations during the COVID-19 Pandemic

Faisal M Huq Ronny, MD, PhD, FASCP, FCAP[1,2,*] *Tshering Sherpa, BS, CLT*[2] *Tenzin Choesang, MA, CLT, MB(ASCP)*[CM 2] *Shana Ahmad, MBA, MLS(ASCP)*[CM1]

[1]Laboratory Services, Gouverneur DTC, Gotham Health New York City Health and Hospitals Corporation, New York, NY, USA, [2]Laboratory Services, Gotham Health New York City Health and Hospitals Corporation, New York, NY, USA. *To whom correspondence should be addressed. huqronf@nychhc.org

Keywords: ambulatory care clinics, clinical laboratory operations, COVID-19 pandemic, point of care testing, staffing issues, effects on test quality and numbers

Abbreviations: POCT, point of care tests; PPM, provider-performed microscopy; LSL, limited-service laboratory licenses

Laboratory Medicine 2023;54:e114–e116; https://doi.org/10.1093/labmed/lmac139

ABSTRACT

Objective: Our New York City Municipal Public Health System-based multisite ambulatory and school-based Gotham Health clinics offer waived point-of-care tests and provider-performed microscopy to the local communities. Our Gotham Health laboratory service conducts system-wide centralized implementation, monitoring, and oversight of the POCT operations. Laboratory staffing has always been an issue for us as there is a decades-long shortage of laboratory staff, primarily licensed medical technologists and technicians, in New York, like many other states. Our clinical laboratory operations team struggled to hire qualified people even before the COVID-19 pandemic onset. It has faced more significant challenges with the emergence of SARS-CoV-2 pandemic cases in New York City and across the country since mid-March 2020.

Methods: As staffing continues to be a struggle, it directly affected the POCT performances and a system-wide reduction in the test numbers during the pandemic. We investigated to identify the factors that made staffing more challenging.

Results: The impact on our POCT started after laboratory staff relocated to the acute care hospital laboratories to provide testing support during the pandemic's peak. That caused significant delays or complete cessation of POCT operations in the clinics due to a lack of oversight support. We also experienced the risk of more vacated positions where staff already feel overworked, overwhelmed, and emotionally drained, causing professional burnout. The significant challenges identified are noncompliance with vaccine mandates resulting in job dismissal and voluntary resignations in exchange for higher-paying laboratories. Finally, the other challenges identified were frequent sick calls due to mental fatigue, retirement of seasoned staff, and inability to attract qualified technologists to meet the demands of increasing test-ordering patterns.

Conclusions: Determining the factors that culminated in the staffing issues becoming more challenging during the COVID-19 pandemic in our ambulatory care clinic laboratory operations will help us in future crisis planning and mitigation.

Originally, Gotham Health ambulatory care clinics were operated under different New York City owned acute care hospital clinical laboratory limited-service laboratory (LSL) licenses. Gotham sites across New York City's 5 boroughs include ambulatory care clinics and school-based clinics that offer waived point-of-care tests (POCTs) and provider-performed microscopy to local communities and send out tests to the reference laboratories.

A wide range of variability existed among the clinics concerning regulatory compliance, test performance, quality control, and training. To decrease adverse effects due to variability in POCT procedures, standardization and quality improvement of POCT across Gotham Health ambulatory care clinics were implemented. Laboratory services executed a plan for system-wide LSL transfer from acute care hospitals to ambulatory care laboratory service for centralized implementation, monitoring, and oversight of POCT operations. Thus, having around 50 clinics system-wide, our qualified laboratory personnel update and provide standard operating procedures, perform quality assurance and validation of new tests/devices, provide competency assessments, and help clinical staff maintain compliance with state and regulatory agencies.[1] With standardization, the clinical teams who perform POCTs get expeditious training and troubleshooting, and the providers get the results

© The Author(s) 2022. Published by Oxford University Press on behalf of American Society for Clinical Pathology. All rights reserved. For permissions, please e-mail: journals.permissions@oup.com

Downloaded from https://academic.oup.com/labmed/article/54/4/e114/6772484 by guest on 24 February 2025

of the POCTs they order much faster and more efficiently. Overall, after the successful implementation of the ambulatory care laboratory operations, the quality metrics get improved markedly.

Across the nation, clinical laboratories are severely understaffed, and the trend has been an ongoing issue for over 2 decades. Licensure states such as New York incur further complications due to the qualifications a candidate must acquire before seeking employment.[2] Gotham Health's' clinical laboratory operations team, which had already been struggling to hire enough people before the COVID-19 pandemic onset, is facing more considerable challenges. The group's difficulties went from a simmer to a rolling boil with the emergence of SARS-CoV-2 pandemic cases in New York City in early 2020.

On March 20, 2020, the Governor of New York issued an executive order requiring all nonessential businesses to be closed and limiting any concentration of individuals outside their homes to prevent the spread of SARS-CoV-2.[3] For most of the Gotham Health clinical laboratory operations team, which conducts the monitoring and oversight of the POCT, closure and social distancing requirements in response to the COVID-19 pandemic resulted in the suspension of POCT operations system-wide. For ambulatory site clinics that enlist drawing stations and specimen processing, the service is essential and uninterrupted. Since staffing continued to struggle, it directly affected the POC test performances and caused a system-wide reduction in the test numbers.

Materials and Methods

As the laboratory staffing issue directly affected POCT performances and a system-wide reduction in test numbers and that was accentuated during the pandemic, our study data were collected using qualitative interviews and employee feedback to identify the factors that made staffing issues more challenging in our Gotham health ambulatory care clinics. We obtained the POCT numbers from our POC middleware Teclor and also verified the numbers through our Laboratory Information System, Cerner.

Results and Discussion

The spread of SARS-CoV-2 among the public, health care workers, and laboratory staff pushed the acute care hospital clinical laboratories to the breaking point. In addition, during the COVID-19 pandemic's peak, a severe staff shortage started in the acute care hospital clinical laboratories due to skyrocketed admissions and in-house testing. In response to the request from the acute care hospital laboratories, most of our Gotham Health laboratory technical staffs were temporarily relocated. The impact on our POCTs started after the laboratory staff relocated to the acute care hospital laboratories to provide testing support during the pandemic's peak. That caused significant delays or complete cessation of POCT operations in the clinics due to a lack of oversight support. There was also increased risk of increased vacated positions where staff already feel overworked, overwhelmed, and emotionally drained, causing professional burnout. The other significant challenges identified are noncompliance with vaccine mandates resulting in job dismissal and voluntary resignations in exchange for higher-paying laboratories, frequent sick calls due to mental fatigue, the retirement of seasoned staff, and the inability to attract qualified technologists to meet the demands of increasing test ordering patterns and laboratory supply shortages affecting staffs.

Staffing Challenges and POCT Impact

The relocation of Gotham Health laboratory staff to the acute care hospital clinical laboratories during the pandemic caused staff disappointment due to changing shifts and work hours (regular hours for Gotham Health staff is, 8 AM–4 PM), changes in job type (POCT monitoring versus bench testing), and job relocation (ambulatory care clinics versus acute care hospital clinical laboratories that were overwhelmed with admitted SARS-CoV-2 patients) and health safety issues similar to those of any frontline healthcare worker.

The citywide introduction of COVID-19 testing also created more hardship for our Gotham Health laboratory staff. Difficulties included fundamental tasks performed by limited staffing of a pandemic magnitude (Pandemic magnitude was meant here as the perceived or real level of threat of a pandemic), monitoring sample collection and specimen processing, and manual result entries to individual patient charts, which imposed a vast challenge regarding the enormous volume of specimen processing. Interfacing of results was not an option during the onset of the pandemic. Due to this vast and unprecedented workload, the transferred laboratory personnel were pulled back from the acute care hospital clinical laboratories, trained, and deployed to the abovementioned tasks. Even after the manual test ordering and resulting interface with the referral laboratories (partial), the immense workload remained persistent for months due to exceedingly large backlogs and ongoing test volume. Furthermore, the orientation and training of nursing staff at many testing sites to access COVID-19 specimens in the laboratory information system also harnessed (harnessed was meant here as being engaged, tied up or occupied with) the POCT oversight staff. Not only the laboratory staff issues but also reduced number of outpatient visits, telecommuting by providers in the clinics, nursing staff shortage, and absence due to illness and fatigue were the other issues that affected the total POCT numbers in our ambulatory clinics.

Recruitment and Retention Issues

At this stage, one of our POCT Coordinators resigned due to a schedule conflict, creating a confounding vacuum. As well as this unexpected vacancy and resulting added workload, our laboratory operations grappled with frequent sick calls (due to COVID-19) and increasing complaints of professional burnout from the overworked, overwhelmed, and emotionally drained staff. Recruitment efforts for a new laboratory technician were initiated. Advertising and recruitment took a few months to identify and onboard a qualified candidate due to the pandemic slowing human resources processes, the relative sparsity of interested and eligible candidates, and increasing vacancies in the other clinical laboratories. Meanwhile, one of the laboratory technicians received an offer from a higher-paying private laboratory, and another laboratory technologist nearing retirement stepped down due to health issues and stress due to increasing workload.

Backfills were submitted to fill the increasing vacancies for Gotham Health. Posted vacancies were advertised for as much as 2 weeks with no qualifying responses from potential candidates. At the request of laboratory operations, team vacancies were published as "until filled" to allow laboratory administrators to attend to priority laboratory workflow tasks while awaiting resumes of qualified candidates for review. Unfortunately, due to the comparative low pay offered (in comparison to the private hospitals and laboratories), shortages across the nation, and New York State licensure requirements, resumes for review were few or none.

Downloaded from https://academic.oup.com/labmed/article/54/4/e114/6772484 by guest on 24 February 2025

The New York State SARS-CoV-2 Testing Consortium survey, conducted in May 2021, showed the average of open positions at member institutions had climbed to 12% and qualified candidates for posted positions were scarce.[4] Our difficulties in hiring qualified candidates were consistent with the survey findings. As the Covid-19 pandemic slowed the overall process of recruitment, applicant scarcity made it worse. We mitigated the issue by hiring temporary laboratory technicians.

Not only recruitment but also workforce retention became challenging. Laboratory management tactics such as daily staff huddles, prospective monthly scheduling, and staff appreciation were used to somewhat enhance the work–life quality of staff. However, unfilled positions remained a significant issue with overall and diffuse impact.

Supply Shortages

Another important factor that affected our staff was the shortages of laboratory supplies during the pandemic. The qualitative analysis of recent survey responses nationally showed that laboratory supply shortages affected not only timely acquisition of laboratory reagents and supplies but also the job satisfaction and wellbeing of laboratory personnel.[5] Gotham Health faced these hurdles; that is, shortages of supplies of blood collection tubes, reagents, needles, media, COVID-19 test kits, and personal protective equipment consumed critical time to validate alternative supplies, make procedure changes, and training, which led to testing and reporting delays. Eventually, shortages disrupted laboratory routine workflow, leading to stress and burnout. Furthermore, outsourcing tests to reference laboratories and borrowing supplies from other ambulatory clinics were required due to insufficient laboratory materials to complete tests on time, adding additional stress on the laboratory staffs.

Strategies were examined and executed to combat supply shortages and prevent the cessation of daily workflow for Gotham. Processes were executed: changes in vendors, borrowing from and loaning to other acute care hospital and ambulatory care clinic laboratories, use of alternative test supplies due to the extended backorder of essential supplies needed for specimen collection, decreased par levels in inventory, and continuous communication between vendors and providers, administration, and laboratory staff. Although little could be done to mitigate staff workload and stress, having supplies available for daily workflow was essential to the continuity of patient care.

The COVID-19 pandemic experience revealed a much-needed conversation about the staffing challenges that laboratories have long experienced. The experience has also identified work–life balance challenges and burnout among laboratory staff, as it profoundly affects our ambulatory care laboratory workforce and may accentuate future hurdles in clinical laboratory operations.

REFERENCES

1. Sherpa T, Choesang T, Ahmad S, Huq Ronny FM. Ensuring standardization, quality management and improvement of point-of-care testing in the municipal public health system based ambulatory care and school health clinics in New York City. *Am J Clin Pathol.* 2021;156(Suppl 1):S114.
2. Clinical Laboratory Technologist & Clinical Laboratory Technician License Requirements: NYS Department of Education, Office of the Professions, Title 8, Article 165 of New York's Education Law and Subparts 79-13 and Subparts79-15 of the Regulations of the Commissioner of Education.
3. Executive Order No 202. Declaring a Disaster Emergency in the State of New York;2020.
4. Crawford JM, Aguero-Rosenfeld ME, Aifantis I, et al. The New York State SARS-CoV-2 Testing Consortium: regional communication in response to the COVID-19 pandemic. *Acad Pathol.* 2021;8:23742895211006818. doi:10.1177/23742895211006818.
5. Hilborne LH, Garcia E, Kundu I. Laboratory supply chain shortage effects on laboratory workforce and effective test utilization: critical values. *Am Soc Clin Pathol.* 2022. https://criticalvalues.org/news/all/2022/05/10/laboratory-supply-chain-shortage-effects-on-laboratory-workforce-and-effective-test-utilization

Downloaded from https://academic.oup.com/labmed/article/54/4/e114/6772484 by guest on 24 February 2025

On labmedicine.com

Several articles featuring practical information are now available on labmedicine.com.

This month, the website features a paper by Talaber et al about elevated estradiol results in a male patient. In “A Case of Fatal *Clostridium perfringens* Sepsis with Massive Hemolysis in the Setting of a Coincidental Platelet Transfusion,” Boyd et al discuss the case of a woman with AML who died of shock and hemolysis after receiving platelets. In “Looking into the Laboratory Staffing Issues that Affected Ambulatory Care Clinical Laboratory Operations during the COVID-19 Pandemic,” Ronny et al discuss staffing during the height of the COVID-19 pandemic.

Check out these articles and more on labmedicine.com.

Lablogatory

Recent contributions to the blog for medical laboratory professionals include case studies as well as posts on forensic pathology and laboratory safety. To see why over half a million readers visit Lablogatory each year, visit labmedicineblog.com.

Downloaded from https://academic.oup.com/labmed/article/54/4/337/7216959 by guest on 24 February 2025

Published by Oxford University Press on behalf of American Society for Clinical Pathology, 2023.

REGISTER BY AUGUST 31ST TO SAVE UP TO 28%!

ASCP 2023 will leave you energized and equipped with new skills, knowledge, and connections that allow you to make an immediate impact in your lab.

ascp.org/2023

"Great education, amazing speakers."

"Informative, insightful, inspirational!"

- 2022 attendees

ASCP 2023 ANNUAL MEETING

OCTOBER 18-20 | LONG BEACH, CA

Engage · Educate · Empower

Downloaded from https://academic.oup.com/labmed/article/54/4/337/7216908 by guest on 24 February 2025